

Utah State University

DigitalCommons@USU

---

All Graduate Theses and Dissertations

Graduate Studies

---

5-2013

## Bioactivities of Milk Polar Lipids in Influencing Intestinal Barrier Integrity, Systemic Inflammation, and Lipid Metabolism

Albert Lihong Zhou  
*Utah State University*

Follow this and additional works at: <https://digitalcommons.usu.edu/etd>



Part of the [Food Chemistry Commons](#), and the [Nutrition Commons](#)

---

### Recommended Citation

Zhou, Albert Lihong, "Bioactivities of Milk Polar Lipids in Influencing Intestinal Barrier Integrity, Systemic Inflammation, and Lipid Metabolism" (2013). *All Graduate Theses and Dissertations*. 1517.  
<https://digitalcommons.usu.edu/etd/1517>

This Dissertation is brought to you for free and open access by the Graduate Studies at DigitalCommons@USU. It has been accepted for inclusion in All Graduate Theses and Dissertations by an authorized administrator of DigitalCommons@USU. For more information, please contact [digitalcommons@usu.edu](mailto:digitalcommons@usu.edu).



BIOACTIVITIES OF MILK POLAR LIPIDS IN INFLUENCING INTESTINAL  
BARRIER INTEGRITY, SYSTEMIC INFLAMMATION, AND LIPID METABOLISM

by

Albert Lihong Zhou

A dissertation submitted in partial fulfillment  
of the requirements for the degree

of

DOCTOR OF PHILOSOPHY

in

Nutrition and Food Sciences

Approved:

---

Dr. Robert E. Ward  
Major Professor

---

Dr. Korry J. Hintze  
Committee Member

---

Dr. Ilka Nemere  
Committee Member

---

Dr. Michael Lefevre  
Committee Member

---

Dr. David A. York  
Committee Member

---

Dr. Mark R. McLellan  
Vice President for Research and  
Dean of the School of Graduate Studies

UTAH STATE UNIVERSITY  
Logan, Utah

2013

Copyright © Albert Lihong Zhou 2013  
All Rights Reserved

**ABSTRACT**

Bioactivities of Milk Polar Lipids in Influencing Intestinal Barrier Integrity, Systemic Inflammation, and Lipid Metabolism

by

Albert Lihong Zhou, Doctor of Philosophy

Utah State University, 2013

Major Professor: Dr. Robert E. Ward  
Department: Nutrition, Dietetics and Food Sciences

Milk polar lipids reduce cholesterol, protect against bacterial infection, reduce inflammation, and help maintain gut integrity. Four rodent models were used to test the hypotheses that dietary milk polar lipids may increase intestinal barrier integrity, reduce systemic inflammation, and affect lipid metabolism during obesity and inflammatory stresses.

The dietary lipids and the polar lipids supplementation affected lipid partitioning, gene expression, and the liver pathology in a rat model (Chapter 2). In an obese mouse model (Chapter 3), the phospholipids increased gut permeability and systemic inflammation, decreased the liver mass and the liver lipids, and increased the plasma lipids; the gangliosides did not affect gut permeability, systemic inflammation, and lipid

metabolism. In a lipopolysaccharide (LPS) stressed mouse model (Chapter 4), the phospholipids decreased the liver mass and the polar lipids in the intestinal mucosa, and increased gut permeability and the plasma LPS level; the gangliosides did not affect gut permeability and systemic inflammation, and had little effect on lipid metabolism. In a diet-induced obesity (DIO) mouse model (Chapter 5), the phospholipids increased the body fat, the plasma LPS level and the gut permeability, increased the polar lipids level in the liver, and decreased the polar lipids level in the intestinal mucosa; the phospholipids did not affect the systemic inflammatory cytokines; the gangliosides increased the expression of the tight junction protein zonula occludens-1 in the colon mucosa, did not affect the plasma inflammatory cytokines, and had little effect on lipid metabolism. There were dynamic changes in plasma cytokines, gut permeability, and lipid metabolism in the LPS-stressed and the DIO models.

In summary, the milk polar lipids affected lipid partitioning and relevant gene expression in rats. The milk phospholipids increased gut permeability in all three mouse models. The phospholipids increased the plasma LPS level and reduced liver mass and liver lipids in genetic obesity and during the LPS stress. The phospholipids increased the body fat in the diet-induced obesity model. The milk gangliosides did not significantly affect gut permeability, systemic inflammation, and lipid metabolism in all three mouse models. Milk phospholipids as dietary supplements may have undesirable effects on gut permeability, systemic inflammation, and lipid metabolism during obesity and inflammatory responses.

**PUBLIC ABSTRACT**

Bioactivities of Milk Polar Lipids in Influencing Intestinal Barrier Integrity, Systemic inflammation, and lipid Metabolism

by

Albert Lihong Zhou, Doctor of Philosophy

Utah State University, 2013

The purpose of lactation is for nutrient provision and also importantly for protection from various environmental stressors. Milk polar lipids reduce cholesterol, protect against bacterial infection, reduce inflammation and help maintain gut integrity. Dynamic interactions within dietary fat, lipid metabolism, gut permeability and inflammatory cytokines remain unclear in the context of obesity and systemic inflammation. A rat model and three mouse models were developed to test the hypotheses that dietary milk polar lipids may affect lipid metabolism and intestinal integrity and may protect against systemic inflammation in the context of stressful diet, systemic inflammation, and obesity.

The milk polar lipids isolates had complex effects on lipid metabolism and associated gene expression in the rat model. There were complex dynamics in lipid metabolism, gut permeability and systemic inflammation at different time points in all mouse models. The milk phospholipids increased gut permeability in genetic and diet-induced obesity and during the lipopolysaccharide (LPS) -induced inflammation. The phospholipids increased the plasma LPS level in genetic obesity and during the LPS stress. The phospholipids

reduced liver mass and liver lipids in genetic obesity and during the LPS-induced inflammation. The phospholipids increased the body fat in the diet-induced obesity model. The milk gangliosides did not significantly affect gut permeability, systemic inflammation, and lipid metabolism in all three mouse models.

Current estimate by the Centers for Disease Control is that about 1/3 Americans are obese (body mass index,  $BMI \geq 30$ ) and 1/3 Americans are overweight ( $25 \leq BMI < 30$ ). More than 25% of Americans today have a fatty liver which could lead to further health problems. The data from this dissertation shed light on the complicated interrelationships between gut permeability, systemic inflammation, and lipid metabolism in obesity. The results contribute to our understanding of the bioactivities of milk polar lipids and provide scientific evidence for the role of milk polar lipids rich materials in affecting biological functions. The study of the influence of milk polar lipids on gut barrier integrity adds new information on understanding the mechanisms of gut leakiness and recovery. The investigation of the impact of milk polar lipids on lipid metabolism reveals new perspectives for the development of diet-induced obesity.

## ACKNOWLEDGMENTS

This dissertation is dedicated to all of those who encouraged me to explore science and supported me in completing my graduate studies.

I want to express my deepest gratitude to my major professor, Dr. Robert E. Ward, for giving me an opportunity and plenty of flexibility to carry out my dissertation project and providing continuous support and guidance throughout the course.

I want to gratefully thank all my other committee members for their great service. Dr. Michael Lefevre and Dr. David York provided constructive criticism and thoughtful comments on my dissertation proposal. Dr. Lefevre let me use his lab equipment and gave me great suggestions on network analysis. Dr. York provided great insights on a manuscript prepared from one chapter of my dissertation and gave me insightful feedback and detailed comments on the whole dissertation draft. Dr. Korry Hintze gave me free access to his lab and provided great feedback on several chapters of my dissertation draft. Dr. Ilka Nemere let me use her equipment and always welcomed my walk-in questions.

My sincere appreciation goes to the whole Ward Lab. Special acknowledgment goes to previous undergraduate students Philip Bassett, Thiel Lehman, and Brent Pickett in the lab who helped with harvesting animal samples and with whom I had a good time in discussing science and learning mentoring.



Many thanks to the financial support providers for the studies. The rat study (Chapter 2) was supported by both a seed grant from the Center for Integrated Biosystems at Utah State University and by the Utah Agricultural Experiment Station. The rest of the studies were supported by the Western Dairy Center.

I am very grateful to the many opportunities at local and national conferences for me to present the data collected for my dissertation. And I am honored to receive and really appreciate the several awards from the American Oil Chemists' Society.

I want to thank all departmental staff for their wonderful support. Special gratitude goes to Department Head Dr. Charles Carpenter for his willingness to answer my questions at any time. I am thankful to many nice people I met in the NDFS Department and on campus.

Additionally, I want to thank Issac Wong for his help with animal procedures. I am grateful to Dr. Aaron Olsen, Kent Udy, and the staff at the Lab Animal Research Center for assistance with animal studies. Many thanks to Nancie Hergert for her technical assistance with the cytokine assay. Thanks to Patti Champine and Ninglin Yin for help with equipment usage at the Center for Integrated Biosystems. Thanks to Dr. Jeff Broadbent's lab and Dr. Chris Davies's lab for allowing me to use their equipment. Thanks to Dallin Snow for preparing RNA samples for the microarray analysis (Chapter 2).

Finally, I want to thank my mom, dad, and younger brother for their understanding of my situation and sharing my happy and hard moments. I gratefully dedicate this dissertation to my beloved grandmother, Yongnian Tan. She encouraged me to be brave and self-confident in exploring adventures and I am very regretful that I wasn't at her side when she left us.

我要感谢人生当中影响和鼓励我从事科学和艺术探索的所有老师和朋友，特别要感谢何盛耕老师、刘忠武老师、张铁梅老师和赵家祥老师。何盛耕老师的平易近人、高超的英语水平和对科学的热爱深深地启迪了我。何老师还给了我很多很好的职业发展方面的建议，使我终身受益。刘忠武老师给我树立了很好的榜样。刘老师激发了我对科学研究的热情。张铁梅老师给了我一个进入科研领域的机会。赵家祥老师在音乐方面对我产生了很大的影响。赵老师使我更正式地把音乐作为自己的毕生兴趣爱好。我十分感激音乐为我带来了许多快乐并给我很多灵感。最后，我要感谢我的家人，感激父母一直对我人生当中的任何决定和新的探索表示理解和积极支持，感谢弟弟为我分担了照顾父母的责任。

Albert Lihong Zhou/周立红

## CONTENTS

ABSTRACT .....	iii
PUBLIC ABSTRACT .....	v
ACKNOWLEDGMENTS .....	vii
LIST OF TABLES .....	xiii
LIST OF FIGURES .....	xiv
LIST OF SYMBOLS AND ABBREVIATIONS .....	xvii
 CHAPTER	
1. INTRODUCTION .....	1
Milk Fat Globule Membrane .....	1
Isolation of MFGM Polar Lipids .....	2
Biological Properties of MFGM Polar Lipids .....	3
Physiology and Pathophysiology of Intestinal Barrier Integrity .....	5
Adipose Tissue, Obesity and Inflammation .....	6
High Fat Diet, Intestinal Barrier Integrity, Endotoxemia, Systemic Inflammation and Obesity .....	8
Rationale for Animal Models and Diets Selections .....	11
Dissertation Outline .....	13
References .....	17
2. DIETARY FAT COMPOSITION INFLUENCES TISSUE LIPID PROFILE AND GENE EXPRESSION IN FISCHER-344 RATS .....	31
Abstract .....	31
Introduction .....	32
Materials and Methods .....	35
Results .....	42
Discussion .....	46
References .....	54
3. DIETARY MILK POLAR LIPIDS AFFECT LIPID METABOLISM, GUT PERMEABILITY AND SYSTEMIC INFLAMMATION IN C57BL/6J OB/OB MICE .....	70
Abstract .....	70
Introduction .....	71

	Materials and Methods .....	74
	Results .....	83
	Discussion .....	87
	Summary .....	94
	References .....	96
4.	DIETARY MILK POLAR LIPIDS AFFECT GUT BARRIER INTEGRITY AND LIPID METABOLISM IN C57BL/6J MICE DURING SYSTEMIC INFLAMMATION INDUCED BY ESCHERICHIA COLI LIPOPOLYSACCHARIDE.....	117
	Abstract .....	117
	Introduction .....	118
	Materials and Methods .....	121
	Results .....	124
	Discussion .....	128
	Summary .....	138
	References .....	139
5.	DIETARY MILK POLAR LIPIDS PROMOTE BODY FAT ACCUMULATION AND AFFECT GUT PERMEABILITY, SYSTEMIC INFLAMMATION, AND LIPID METABOLISM IN C57BL/6J MICE FED A MODERATELY HIGH-FAT DIET.....	160
	Abstract .....	160
	Introduction .....	161
	Materials and Methods .....	164
	Results .....	166
	Discussion .....	171
	Summary .....	180
	References .....	182
6.	SUMMARY AND FUTURE DIRECTIONS.....	202
	Rat Model with High Sucrose Diet .....	203
	Genetic Obesity Model with High Fat Diet .....	204
	LPS-induced Systemic Inflammation Model .....	209
	Diet-induced Obesity Model .....	213
	Effects of Dietary Polar Lipids across Different Rodent Models .....	219
	Future Directions.....	223
	References .....	225
	APPENDIX.....	234
	CORRELATION COEFFICIENT NETWORK ANALYSIS.....	233
	REPRINT PERMISSIONS .....	250

CURRICULUM VITAE..... 255

## LIST OF TABLES

Table	Page
1.1 Major components of MFGM in bovine milk.....	29
2.1 Composition of dietary treatments.....	59
2.2 Metabolic pathways significantly affected across all three diet combinations.....	60
2.3 Differentially expressed genes by ANOVA in liver.....	61
2.4 %20:3n-9 in highly unsaturated fatty acids (HUFA).....	61
3.1 Diets composition.....	104
3.2 Mouse primers sequences.....	105
3.3 Effects of milk polar lipids on plasma levels of MCP-1, TNF- $\alpha$ , insulin, glucose, and homeostasis model assessment of insulin resistance (HOMA-IR) in ob/ob mice.....	106
3.4 Diabetes associated parameters measured in mice GO3 and PO4.....	106
4.1 Effects of milk polar lipids on plasma levels of leptin, MCP-1 and TNF- $\alpha$ .....	147
5.1 Food intake.....	189
5.2 Food intake and energy stored as body fat.....	189
5.3 Effects of milk polar lipids on liver and adipose tissue mass.....	190
5.4 Effects of milk polar lipids on plasma levels of MCP-1 and TNF- $\alpha$ .....	190
A1 Number of Pearson correlation coefficients.....	244
A2 Number of Pearson correlation coefficients.....	244

## LIST OF FIGURES

Figure	Page
1.1	Complex links between dietary lipids, leaky gut, endotoxemia, obesity, NAFLD and metabolic inflammation .....30
2.1	Fatty acid profile of experimental diets .....62
2.2	Effect of experimental diets on food intake (a), total weight gain (b) and body fat composition (c).....63
2.3	Red blood cell (RBC) fatty acids .....64
2.4	Fatty acid profile of skeletal muscle .....65
2.5	Fatty acid profile of visceral adipose tissue.....66
2.6	Fatty acid profile of liver tissue .....67
2.7	Quantitation of lipid classes from plasma, visceral adipose and liver .....68
2.8	Liver histological slides .....68
2.9	Hepatic Oil Red O Staining (A) and hepatic DGAT activity (B) .....69
3.1	Effects of polar lipids on food intake, weight gain and fat depots .....107
3.2	Effects of milk polar lipids on body fat and body weight.....108
3.3	Effects of milk polar lipids on liver mass and tissue lipid profile .....109
3.4	Effects of milk polar lipids on gene expression.....110
3.5	Effects of milk polar lipids on plasma lipid profile .....111
3.6	Effects of milk polar lipids on gut permeability .....112
3.7	Effects of milk polar lipids on plasma cytokines.....113
3.8a-c	Body fat plotted against fat-free mass.....114
3.8d-f	Body fat plotted against fat-free mass.....115
3.9	Summary of major findings in Chapter 3 .....116

4.1	Dietary milk polar lipids did not significantly affect food intake.....	147
4.2	Effects of the polar lipids on body weight and body fat content .....	148
4.4	Effects of milk polar lipids on PL and GG content in intestinal mucosa .....	150
4.5	Effects of milk polar lipids on plasma lipid profile .....	151
4.6	Effects of milk polar lipids on gut permeability .....	152
4.7	Effects of milk polar lipids on gut permeability .....	153
4.8	Effects of milk polar lipids on plasma cytokines.....	154
4.9a	Body fat plotted against fat-free mass.....	155
4.9b-d	Body fat plotted against fat-free mass .....	156
4.9e-g	Body fat plotted against fat-free mass .....	157
4.9h-j	Body fat plotted against fat-free mass .....	158
4.10	Summary of major findings in Chapter 4 .....	159
5.1	Effects of the polar lipids on body weight and body fat content .....	191
5.2	Effects of milk polar lipids on tissue lipid profile .....	192
5.3	Effects of milk polar lipids on plasma lipid profile .....	193
5.4	Effects of milk polar lipids on gut permeability .....	194
5.5	Effects of the polar lipids on plasma LPS and cytokines.....	195
5.6	Effects of milk polar lipids on fasting glucose and HOMA-IR .....	196
5.7a	Body fat plotted against fat-free mass.....	197
5.7b-d	Body fat plotted against fat-free mass .....	198
5.7e-g	Body fat plotted against fat-free mass .....	199
5.8	Comparison between lean and obese mice .....	200
5.9	Summary of major findings in Chapter 5 .....	201



6.1	Most of the hypothesized effects of the polar lipids were not supported .....	232
6.2	Stress-induced dysfunction of the subcutaneous white adipose tissue .....	233
A1a	Visual legend – node color mapping.....	245
A1b	Visual legend – node shape mapping.....	246
A1c	Visual legend – color, line width and line style of edge mapping .....	247
A2	Correlations ( $p < 0.05$ ) involve the following parameters measured at the end of the LPS study .....	248
A3	Correlations ( $p < 0.05$ ) involve the following parameters measured at the end of the DIO study.....	249

**LIST OF SYMBOLS AND ABBREVIATIONS**

<i>Acaa2</i>	Acetyl-Coenzyme A acyltransferase 2 (mitochondrial 3-oxoacyl-Coenzyme A thiolase)
<i>Acacb</i>	Acetyl-Coenzyme A carboxylase beta
<i>Acat2</i>	Acetyl-Coenzyme A acetyltransferase 2
ACF	Aberrant crypt foci
<i>Acox3</i>	Acyl-Coenzyme A oxidase 3, pristanoyl
<i>Actb</i>	Actin, beta
AMF	Anhydrous milk fat
ANOVA	Analysis of variance
AUC	Area under the curve
BHT	Butylated hydroxytoluene
BMI	Body mass index
BSA	Bovine serum albumin
CE	Cholesteryl esters
CHD	Coronary heart disease
CO	Control (chapter 3-5)
CO	Corn oil (chapter 2)
<i>Cpt2</i>	Carnitine palmitoyltransferase 2
Ct	Cycle threshold
<i>Cyp7a1</i>	Cytochrome P450, family 7, subfamily a, polypeptide 1
DG	Diglyceride(s)

DIO	Diet-induced obesity
DST	Differential sugar absorption test
ELISA	Enzyme-linked immunosorbent assay
<i>Elovl5</i>	ELOVL family member 5, elongation of long chain fatty acids
FAME	Fatty acid methyl ester(s)
FFA	Free fatty acid(s)
FITC	Fluorescein isothiocyanate
<i>Gapdh</i>	Glyceraldehyde-3-phosphate dehydrogenase
GC	Gas chromatography
GC-MS	Gas chromatography–mass spectrometry
GD3	5-acetyl-alpha-neuraminic acid(2-8)5-acetyl-alpha-neuraminic acid (2-3)beta-D-galactopyranose(1-4)beta-D-glucopyranose(1-1)ceramide
GG	Ganglioside(s)
GM3	5-acetyl-alpha-neuraminic acid(2-3)beta-D-galactopyranose(1-4) beta-D-glucopyranose(1-1)Ceramide
HDL	High density lipoprotein
<i>Hmgcr</i>	3-hydroxy-3-methylglutaryl-Coenzyme A reductase
HOMA-IR	Homeostasis model assessment of insulin resistance
HPTLC	High performance thin layer chromatography
HUFA	Highly unsaturated fatty acid(s)
IBD	Inflammatory bowel disease
IFN- $\gamma$	Interferon $\gamma$
IL-6	Interneukin-6

JAM	Junctional adhesion molecule
LBP	Lipopolysaccharide-binding protein
LCSFA	Long-chain saturated fatty acids
<i>Ldlr</i>	Low density lipoprotein receptor
LPC	Lysophosphatidylcholine
LPS	Lipopolysaccharide
MCP-1	Monocyte chemotactic protein-1
<i>Me1</i>	Malic enzyme 1, NADP(+)-dependent, cytosolic
MFGM	Milk fat globule membrane
MRI	Magnetic resonance imaging
MW	Molecular weight
NAFLD	Non-alcoholic fatty liver disease
NASH	Nonalcoholic steatohepatitis
NHANES	National Health and Nutrition Examination Survey
OxLDL	Oxidized low-density lipoprotein
PAI-1	Plasminogen activator inhibitor-1
PC	phosphatidylcholine
PE	Phosphatidylethanolamine
PI	Phosphatidylinositol
PL	Phospholipid(s)
<i>Ppia</i>	Peptidylprolyl isomerase A
PS	phosphatidylserine
PUFA	Polyunsaturated fatty acids

RBC	Red blood cell(s)
RT-qPCR	Real-time reverse transcription polymerase chain reaction
<i>Scarb1</i>	Scavenger receptor class B, member 1
<i>Scd1</i>	Stearoyl-Coenzyme A desaturase 1
<i>Slc27a5</i>	Solute carrier family 27 (fatty acid transporter), member 5
SM	Sphingomyelin
TBS	Tris-buffered saline
TG	Triglyceride(s)
TJ	Tight junction
TLC	Thin layer chromatography
TNF- $\alpha$	Tumor necrosis factor- $\alpha$
ZO	Zonula occludens

# CHAPTER 1

## INTRODUCTION

Milk provides the primary source of nutrition for young mammals. Interestingly, comparative evolutionary biology suggests that the origins of lactation are not exclusively for nutrient provision, but rather protection from various environmental stressors (1). In modern society, especially the western world, milk and other dairy products are common food items among all age groups. Despite their wide applications, milk and other dairy products have not been assessed extensively for their potential protective effects against environmental stresses. The early lactation milk, colostrum, carries the mother's antibodies to the baby thereby reducing the risk of many diseases in the infant. Rich in nutrients, milk provides protection for the gut and enhances the immune system of the newborn (2, 3). The composition of milk results from selective pressure to promote the health of infants through nutrient provision and protection against environmental insults. Among the nutrients in milk, lipids are important in delivering energy and providing substrates for metabolism. One fraction of the lipids, milk fat globule membrane (MFGM) polar lipids including phospholipids (PL) and gangliosides (GG), may have important roles in biological functions such as maintaining gastrointestinal barrier integrity and affecting systemic inflammation, and lipid metabolism.

### **Milk Fat Globule Membrane**

MFGM is a biological membrane synthesized and secreted by the mammary epithelial cells. Surrounding a triglyceride (TG) core, MFGM forms a 4-

10-nm multilayer membrane composed primarily of cholesterol, proteins, and polar lipids (4). MFGM contains approximately 60% proteins and 40% lipids (Table 1.1) (5-7).

Recent proteomic and lipidomic characterizations (8-11) have shown that MFGM is the most diverse fraction of milk. Although there are a lot of minor components in MFGM, xanthine oxidase, periodic acid/schiff 6/7, adipophilin, and butyrophilin are the most abundant MFGM-associated proteins (12), and polar lipids are the major lipids secondary to TG in MFGM. Polar lipids include phospholipids and sphingolipids. The major phospholipids include phosphatidylethanolamine (PE), phosphatidylcholine (PC), phosphatidylserine (PS), and phosphatidylinositol (PI). The major sphingolipids are glucosylceramide, lactosylceramide, and sphingomyelin (6, 13).

### **Isolation of MFGM Polar Lipids**

Milk polar lipids are mainly situated in the MFGM. Mechanical treatments, such as heating (14), homogenization (15), aeration, and agitation (16), have been used to release MFGM from the fat globules into the corresponding serum phase. Phase inversion, such as churning, releases MFGM from the fat globules into the serum fraction (i.e., buttermilk and butter serum). Once MFGM is disrupted and released into the serum, it needs to be separated from the other components of milk. Larger amounts of MFGM can be produced as a byproduct from buttermilk or cheese whey during butter or cheese making processes. Tangential filtration is one of the most common techniques for the isolation of MFGM from whey, the byproduct of cheese and casein manufacturing (17). The isolating procedures can be easily carried out in industrial settings. MFGM polar lipids can be harvested from dried milk cream through ethanol extraction. The resulting

lipid extract can be further processed to obtain GG enriched concentrates and PL enriched concentrates.

### **Biological Properties of MFGM Polar Lipids**

Forming a lipid tri-layer, MFGM stabilizes milk fat globules in the milk serum and protects them from enzymatic attack by lipases (16, 18) so that milk fats can be passed from mothers to babies for utilization. Both lipid and protein fractions of MFGM have been found to have health-promoting effects (19). Due to its unique lipid profile, relative polar lipids enrichment and widespread availability, MFGM has been suggested as a nutraceutical (20). One type of polar lipids isolated from MFGM, sphingolipids, have very specific nutritional benefits. Sphingolipids are hydrolyzed in the gastrointestinal tract into ceramide, sphingosine, sphingosine 1-phosphate, and other metabolites, all of which can modulate cell growth, differentiation, and apoptosis (21). Studies have been conducted to investigate the physiological properties of MFGM sphingolipids, which have been shown to reduce the uptake of cholesterol (22, 23), protect against bacterial infections in the gut (24-26), reduce inflammatory response (27-30), and inhibit the development of preneoplastic lesions in rodent models of colon cancer (31-33).

Sphingomyelin, one subfraction of sphingolipids, plays an important role in gut maturation during the suckling period in rats (34). Recent work shows that sphingomyelin content in intestinal cell membranes may regulate cholesterol absorption (35). Another subfraction of sphingolipids, dairy GG inhibits degradation of gut occludin tight junction (TJ) protein during lipopolysaccharide (LPS)-induced acute inflammation (36). Dietary GG affect intestinal immune system maturation in mice during weaning



(37). Dietary GG can be absorbed in the small intestine and distributed to different tissues. Dietary GG alters GG levels in the intestinal mucosa, plasma and brain (38).

Dietary supplemented PL may enrich PL in circulating lipoproteins and enhance their endotoxin-neutralizing capabilities (39). High-density lipoprotein (HDL) has the highest percentage of PL among the lipoproteins. MFGM PL may increase plasma HDL level, which neutralizes endotoxins in the blood (40, 41). Oral time-release capsules of PC ameliorate gastrointestinal symptoms and facilitate recovery in patients with chronic ulcerative colitis (42, 43). Some of this protection by PC may be partially due to its anti-inflammatory property on human intestinal cells (44). As a constitutively developing tissue, the gut epithelium is the most vigorously self-renewing tissue of adult mammals (45) and is constantly differentiating from stem cells in a progenitor pool throughout the life of the organism (46). As an essential component of cell membrane, polar lipids may be actively involved in the process of gut epithelium regeneration and barrier maintenance.

Being digested and incorporated into tissues, MFGM polar lipids and their metabolites may be actively involved in lipid metabolism. The effects of dietary PL on hepatic lipid metabolism have been studied in rats and dietary PL reduced liver TG and cholesterol (47). A MFGM isolate increases PL and TG levels in plasma in rat (Chapter 2, 48). The isolate lowers TG and total lipids levels in adipose tissue. It also reduces free fatty acids (FFA), cholesterol esters (CE) and total lipids in the liver. PL-rich MFGM extract reduces hepatomegaly, hepatic steatosis and hyperlipidemia in mice fed a high-fat

diet (49). The extract also positively regulates genes associated with fatty acid synthesis and cholesterol metabolism. A methionine and choline-deficient diet reduces PC biosynthesis, which results in reduced very-low-density lipoprotein (VLDL) secretion (50). The decrease of VLDL secretion is one of the many factors contributing to the pathogenesis of hepatic steatosis and non-alcoholic steatohepatitis (NASH). High dietary sucrose results in hepatic steatosis (51) and dietary PC may relieve the condition. The beneficial effects of MFGM could be partially due to the choline contributed by PC when the diets were high in sucrose in most of the aforementioned studies.

### **Physiology and Pathophysiology of Intestinal Barrier Integrity**

The mammalian intestinal epithelium, composed of a single layer of epithelial cells, carries out the primary functions of digestion and absorption of nutrients and forms a barrier against luminal pathogens (52). The intestinal barrier has several components which can be divided into extrinsic barriers and intrinsic barriers (53). The extrinsic barrier, also known as "unstirred layer," stabilizes the microenvironment adjacent to epithelial cell apical membranes. The intrinsic barrier has two components: the epithelial cells (transcellular pathway) and the spaces around these cells (paracellular pathway) (54). The major permeability route across the epithelium is located within the paracellular pathway (55), which has two components: the TJ and the subjunctional paracellular space (54). The TJ is the main determinant of intestinal barrier integrity. TJ are formed by specific interactions of a wide spectrum of proteins (56). Occludin (57), claudins (58), and junctional adhesion molecule (JAM) (59) are the important ones. The cytoplasmic domains of these proteins interact extensively with scaffolding and regulatory proteins such as zonula occludens (ZO)-1, ZO-2, ZO-3 (56). TJ are dynamically regulated in both

health and disease by many mechanisms (60). Compromised function of intestinal TJ has been implicated in the pathogenesis of several intestinal disorders such as inflammatory bowel disease (IBD) and celiac disease (61).

Several studies have shown that gastrointestinal surface hydrophobic properties decrease under pathological conditions. Maintenance of the PC in the hydrophobic surface may play an important role in health and prevention of disease (62). In the ileal and colonic mucus from patients suffering from ulcerative colitis, the concentration of PC was significantly lower compared with that of healthy controls (63). The PL concentration and species composition of the intestinal mucus barrier are significantly altered in patients with ulcerative colitis. The alterations in PL may be important for the pathogenesis of diseases associated with disruption of intestinal barrier integrity. The enzymatic breakdown of intestinal PL has been linked to a higher rate of intestinal permeability in Caco-2 cells (64).

### **Adipose Tissue, Obesity and Inflammation**

Excess energy can be reversibly stored as lipids in adipocytes (65). Excess TG accumulation in adipose tissue results in hypertrophy and hyperplasia (66). Adipogenesis, proliferation and differentiation of preadipocytes into new adipocytes, results in hyperplasia (67). Hypertrophy and hyperplasia of adipocytes contribute to excessive adipose tissue growth, which eventually leads to obesity (68). Adipocyte function can be impaired by excessive fat accumulation in the cell. Cellular lipid loading may initiate inflammation and lipid mediators could play important roles in this process since they are precursors to inflammatory signaling molecules (69). In obesity, the hypoxic adipose

tissue may release proinflammatory cytokines that may initiate systemic inflammation (70-72).

Adipose tissue contains many different types of cells, including adipocytes, fibroblasts, leukocytes, and macrophages. These cells may jointly produce proinflammatory cytokines, such as tumor necrosis factor- $\alpha$  (TNF- $\alpha$ ), and interleukin-6 (IL-6) (69). The close location of adipocytes with immune cells facilitates continuous dynamic interactions between immune and metabolic responses (73). Macrophages and T lymphocytes are the main components of the innate immune system in adipose tissue (74-77). Monocytes are recruited to adipose tissue and become macrophages through interaction with dysfunctional adipocytes during obesity in animal models (78). Preadipocytes can be converted into macrophages in a macrophage environment (79). Macrophages contribute to local proinflammatory environment in adipose tissue and also influence systemic inflammation especially in chronic inflammatory states (80).

Adipocytes might be both the source and target of proinflammatory signals since adipocytes express receptors for several proinflammatory molecules such as TNF- $\alpha$  and IL-6 (75). Local inflammatory effectors in adipose tissue can act on adipocytes in a paracrine manner and exacerbate inflammation and adipocyte dysfunction (74, 75, 81). Systemic inflammatory effectors may affect adipose tissue in a similar manner. Adipose tissue in a lean body has the potential to develop inflammation upon systemic inflammatory stimulation. It is not clear yet which original factor(s) triggers inflammation in adipose tissue. Endotoxemia caused by periodontal gram-negative

pathogens in patients with severe periodontitis might lead these people to obesity (82). It is possible that proinflammatory signals resulting from systemic metabolic inflammation may trigger an inflammatory response in adipose tissue and therefore cause adipocyte dysfunction and subsequent obesity development. Proinflammatory signals resulting from metabolic endotoxemia caused by dietary fat and associated bile release might be one of the initiating factors for inflammation in adipose tissue during the development of diet-induced obesity (DIO). Then in the context of DIO, systemic metabolic inflammation and subsequent inflammation in adipose tissue may precede obesity development, which is still lack of supporting evidence.

### **High Fat Diet, Intestinal Barrier Integrity, Endotoxemia, Systemic Inflammation and Obesity**

A link between high fat diets and endotoxemia has been suggested. A chronic high fat diet could increase endotoxin absorption during the digestion of dispersed dietary lipids. The resultant metabolic endotoxemia leads to low-grade metabolic inflammation (83). One study found that high fat diet increases intestinal permeability in rats primarily through excessive dietary fat and increased luminal bile juice levels instead of obesity and metabolic disorders (84). A recent study revealed that chylomicrons could be postprandial carriers for LPS and the digestion of emulsified dietary lipids can enhance intestinal endotoxin absorption in healthy young men (85). The increased endotoxemia upon high-fat diet might be contributed by enhanced endotoxin absorption through the small intestine instead of the large intestine (84, 86).

Current evidence suggests that high fat diets may decrease gut barrier integrity and/or increase endotoxin absorption, which may lead to systemic inflammation independent of obesity. Obesity may also decrease intestinal barrier integrity. Increased intestinal permeability has been observed in obese animals (86, 87). As animals become more obese, their intestines become larger with an increased surface area due to a larger amount of intestinal mucosa needed to absorb the surplus of ingested nutrients (88). This increased surface area has been shown to be caused by intestinal hyperplasia (89). The TJ proteins may not be increased accordingly and distributed properly, which could lead to the decrease of barrier integrity (88). Leptin-deficient C57BL/6J ob/ob (ob/ob) mice were shown to have an abnormal distribution of TJ proteins within the intestinal mucosa that causes compromised intestinal barrier integrity leading to portal endotoxemia (90). The genetic obesity model of ob/ob mice have been reported to have increased intestinal permeability when fed a standard chow diet (90). Plasma levels of lipopolysaccharide-binding protein (LBP), a marker of endotoxemia, were increased in ob/ob mice and mice with DIO compared with lean mice (91). The systemic inflammatory state in obesity is associated with endotoxemia resulting from increased gut barrier permeability (92).

Obesity may potentiate systemic inflammation and the proinflammatory cytokines can reach the gut through the circulation and result in local inflammation. Intestinal inflammation leads to an increase of mucosal permeability and bacterial translocation. In obese subjects, inflammatory cytokine levels stay high. These cytokines may alter structure and localization of TJ and thereby cause malfunction of the intestinal barrier (93,

94). For example, TNF- $\alpha$ , interferon (IFN)- $\gamma$ , IL-4 and IL-13 have been shown to increase barrier permeability *in vitro* (95) by altering TJ morphology and distribution (96). Therefore, obesity, systemic inflammation and increased intestinal permeability may generate a self-perpetuating vicious cycle (Figure 1.1) (97).

In summary, current evidence suggests that during the development of high-fat DIO, increased gut barrier permeability, endotoxemia, systemic inflammation and obesity may occur in sequential steps. It is also possible that in the context of high-fat DIO, obesity develops before any other aforementioned conditions. Once obesity is developed, the adipose tissue may release proinflammatory cytokines that may initiate systemic inflammation. The inflammatory state may increase gut barrier permeability, which could lead to endotoxemia and worsen the condition of inflammation (Figure 1.1). Therefore, increased gut barrier permeability, endotoxemia, systemic inflammation and DIO are complexly interrelated events. Lipid metabolism could be an important linkage among these events. Diet supplemented with the buttermilk MFGM isolate was effective in promoting mucosal integrity against LPS stress in mice (98). The effects of MFGM polar lipids on intestinal barrier integrity could have an influence on endotoxemia and systemic inflammation. MFGM polar lipids could also influence systemic lipid metabolism and may interfere with the development of DIO. Dietary supplementation of MFGM polar lipids in the context of preexisting obesity and during the development of DIO may facilitate the understanding of the interrelationships among intestinal barrier integrity, endotoxemia, systemic inflammation and obesity.

## **Rationale for Animal Models and Diets Selections**

The main endpoints of the project are gut permeability, systemic inflammation, and lipid metabolism in the context of obesity. The C57BL/6J ob/ob (ob/ob) and wild type mice were used. The reason to use ob/ob mice was that these mice have preexisting obesity and its complications such as increased gut permeability and systemic inflammation. Since these mice are leptin deficient, caution should be taken in interpreting the data. By using these mice, MFGM polar lipids can be tested to see if they have any beneficial effects on gut permeability and systemic inflammation, which may result from obesity and may be sustained and/or exacerbated by fat intake. For wild type mice, it took time for them to develop obesity even when they were fed a high fat diet. High fat diet feeding has been shown to increase gut permeability and induce subsequent metabolic inflammation. Wild type mice were used to determine if MFGM polar lipids can prevent the increase of gut permeability and systemic inflammation during the development of obesity. Data from this study may shed some light on how the supplements may affect the complicated causal relationships among gut permeability, systemic inflammation and DIO.

Diets based on AIN-93G rodent diet were used. Part of the fat source in experimental diets was provided by MFGM polar lipids. The fat provided 34% energy (16.8% by weight). This amount of fat is considered high compared with 16% (energy) fat in regular mice chow diet. High fat diets with 30% or more fat as energy have successfully induced obesity in C57BL/6J mice (99). Data from National Health and Nutrition Examination Survey (NHANES 2007-2008) indicates that the mean amount of fat consumed per



individual American is 34% by energy. Using diets with 34% (energy) fat emulated real dietary practices in America. Current estimates by Centers for Disease Control is that about 1/3 Americans are obese ( $BMI \geq 30$ ) and 1/3 Americans are overweight ( $25 \leq BMI < 30$ ). So it could be common practice to have diets with 34% (energy) fat in the background of obesity or overweight.

When the same diets were used in both animal models, these two experiments could be compared to generate hypotheses. The DIO model had at least two stressors, high dietary fat and DIO. Dietary fat was a constant stressor while DIO was added on later. The effects of the milk polar lipids on the stresses caused by dietary fat (and maybe also bile) were tested during the early part of the experiment. Once the animals developed obesity, the effects of the milk polar lipids on complications of DIO were also tested. The results from the ob/ob model were negative and the results from the DIO model were positive for the early part but negative for the latter part, meaning that the milk polar lipids prevented the detrimental effects of dietary fat but could not ameliorate the complications of obesity. The milk polar lipids did not ameliorate complications in ob/ob mice and did not improve complications of DIO, meaning that the lack of beneficial effects of milk polar lipids on obesity complications may not be leptin-dependent.

The LPS injection is widely used in mice for modeling the acute and chronic systemic inflammation. The subcutaneous injection of LPS induces endotoxemia and intestinal stress in mice (100, 101). The intraperitoneal injection of LPS increases the level of the plasma inflammatory cytokines (102). Six percent of the subcutaneously injected LPS is

still retained at the injection site 32 days after the injection (103). The subcutaneous LPS injection induces both the acute and chronic inflammatory responses. The LPS injection will increase gut leakiness, endotoxemia and systemic inflammation. The combination of the high fat diet and the LPS injection should increase the severity of gut leakiness, endotoxemia and systemic inflammation (Figure 1.1) and should make it easier to detect the potential beneficial effects of the polar lipids on these endpoints. The mouse model of the LPS stress and the high fat diet is a great platform for studying the effects of the milk polar lipids on gut permeability and systemic inflammation.

### **Dissertation Outline**

During this dissertation research, I explored the effects of milk polar lipids on gut permeability, systemic inflammation, and lipid metabolism during inflammation and obesity. The following hypotheses were tested (Figure 1.1): 1) Dietary milk polar lipids will reduce liver lipid levels and affect the expression of genes associated with fatty acid synthesis and cholesterol regulation in the liver in both C57BL/6J ob/ob and wild type mice fed a diet with 34% fat by energy; 2) Dietary milk polar lipids will reduce intestinal permeability and systemic inflammation in C57BL/6J ob/ob mice fed a diet with 34% fat by energy; 3) Dietary milk polar lipids will improve intestinal barrier integrity, lipid metabolism and systemic inflammation during acute and chronic systemic inflammation induced by LPS injected subcutaneously; 4) Dietary milk polar lipids will prevent gut permeability increase and subsequent systemic inflammation during the development of DIO in C57BL/6J wild type mice fed a diet with 34% fat by energy.

To begin with, I tried to explore the effects of dietary milk polar lipids isolate on lipid metabolism and gene expression in a rat model. I obtained the lipid profiles of liver, gonadal adipose and skeletal muscle samples from a previous rat study on the effects of milk polar lipids isolate on the development of aberrant crypt foci in the colon. I also analyzed microarray gene expression data of those tissue samples. The results are reported in Chapter 2. The milk polar lipids reduced liver lipid levels and the reduction of liver lipids coincided with the increase of lipids in the plasma. The effects of the milk polar lipids on tissue gene expression were complex in the rats.

To test the aforementioned hypotheses, I used three mouse models, a genetic obesity model, a LPS-induced inflammation model, and a diet-induced obesity model. The first hypothesis was tested in all three models. I analyzed the liver samples from all three mouse studies. As reported in Chapters 3, 4, and 5, the milk polar lipids reduced the liver lipid level and slightly affected gene expression associated with the liver lipid metabolism in all three mouse models.

To test the second hypothesis, I used the ob/ob mouse model. The ob/ob mice were fed moderately high-fat diets. As reported in Chapter 3, the milk polar lipids did not prevent the increase of gut permeability. The milk phospholipids increased the colon permeability and the plasma IL-6 level, decreased the liver mass and the liver cholesteryl ester level, and increased the plasma levels of FFA, DG, SM, and PL. The milk gangliosides decreased ZO-1 and increased occludin in the colon mucosa but had little effect on gut permeability, systemic inflammation, and lipid metabolism.

To test the third hypothesis, I used a LPS-induced inflammation model. Lean C57BL/6J mice were injected subcutaneously with LPS. The effects of the milk polar lipids were tested during acute and chronic inflammation induced by the injected LPS. As reported in Chapter 4, the subcutaneous injection of the LPS at 5 mg/kg body weight successfully induced leaky gut and acute and chronic systemic inflammation. The milk phospholipids decreased occludin expression in jejunum mucosa and increased ZO-1 & occludin in colon mucosa; increased plasma LPS; decreased liver mass, muscle TG, liver expression of *Acacb* & *Hmgcr* and plasma CE; decreased PC & PE in ileum mucosa and PE & GG in colon mucosa. The milk gangliosides decreased adipose PE, PC & SM, hepatic FFA & PI; increased liver expression of *Acaa2*. LPS stress in combination with high fat diets increased gut permeability and plasma proinflammatory cytokine levels. LPS stress reduced plasma insulin level, blocked the accumulation of body fat, and increased plasma IL-6 level. The experimental feeding increased plasma LPS but did not raise plasma cytokine levels.

To test the last hypothesis, I used a diet-induced obesity model. C57BL/6J lean mice were fed the AIN93G based diets with 34% fat by energy. As reported in Chapter 5, the milk phospholipids promoted body fat accumulation and increased obesity; increased gut permeability and plasma LPS; decreased occludin in jejunum mucosa; increased liver PE, PC & SM and plasma TG; decreased plasma FFA & PC; decreased PC & SM in colon mucosa. The milk gangliosides decreased adipose SM, plasma FFA & PC; increased liver PE & SM; increased ZO-1 in colon mucosa. The experimental feeding increased body fat and plasma CE; increased colon permeability and plasma levels of LPS, leptin, resistin,

insulin and glucose; decreased insulin sensitivity as indicated by the increased HOMA-IR; increased plasma IL-6 before the establishment of DIO; decreased permeability of the small intestine.

In addition to testing the aforementioned hypotheses, I also tried to explore the dynamic changes of gut permeability, systemic inflammation, and lipid metabolism during genetic obesity, the LPS-induced inflammatory response, and diet-induced obesity. The endpoints were measured at multiple time points. Often times the measurements did not stay in one direction. The repeated measurements also indicated that dietary supplementations had different effects at different time points.

In this dissertation, I demonstrated that repeated measurements are important for monitoring the dynamic changes of biological endpoints and evaluating the effects of dietary supplementations. The milk polar lipids in general did not have strong positive effects on gut permeability and systemic inflammation during obesity and the acute and chronic inflammatory responses. The milk polar lipids tended to have more positive effects when the animals were under more stressful conditions such as preexisting obesity and the LPS-induced inflammation. Several of the unexpected findings are quite interesting. The milk phospholipids promoted body fat accumulation in C57BL/6J lean mice. The milk polar lipids decreased the polar lipid levels in the intestinal mucosa and sometimes in the liver and the skeletal muscle. The LPS absorbed through the gut did not induce strong systemic inflammation while the LPS injected subcutaneously stimulated much stronger inflammation. As described in Chapter 6, many hypotheses can be

generated from the data collected in this dissertation. Further studies are needed to test those hypotheses and reveal the mechanisms for the observed new findings.

## References

1. Blackburn DG. Lactation: historical patterns and potential for manipulation. *J Dairy Sci* 1993;76:3195-212.
2. Armogida SA, Yannaras NM, Melton AL, Srivastava MD. Identification and quantification of innate immune system mediators in human breast milk. *Allergy Asthma Proc* 2004;25:297-304.
3. Hanson LA, Winberg J. Breast milk and defence against infection in the newborn. *Arch Dis Child* 1972;47:845-8.
4. Mcpherson AV, Dash MC, Kitchen BJ. Isolation of bovine-milk fat globule-membrane material from cream without prior removal of caseins and whey proteins. *J Dairy Res* 1984;51:113-21.
5. Fox PF, and P. L. H. McSweeney. *Dairy Chemistry and Biochemistry*. Blackie Academic & Professional: London, UK, 1998.
6. Keenan TW, I. H. Mather, and D. P. Dylewski. Physical equilibria: Lipid phase. In: Wong NP, (ed). *Fundamentals of Dairy Chemistry*. Aspen Publishers, Inc.: Gaithersburg, MD: 1999. pp 511–83.
7. Keenan TW, Patton S. *The Structure of Milk: Implications for Sampling and Storage A. The Milk Lipid Globular Membrane*. Academic Press: San Diego, 1995.

8. Affolter M, Grass L, Vanrobaeys F, Casado B, Kussmann M. Qualitative and quantitative profiling of the bovine milk fat globule membrane proteome. *J Proteomics* 2009.
9. Cavaletto M, Giuffrida MG, Conti A. The proteomic approach to analysis of human milk fat globule membrane. *Clin Chim Acta* 2004;347:41-8.
10. Cavaletto M, Giuffrida MG, Conti A. Milk fat globule membrane components - A proteomic approach. *Adv Exp Med Biol* 2008;606:129-41.
11. Cavaletto M, Giuffrida MG, Fortunato D, et al. A proteomic approach to evaluate the butyrophilin gene family expression in human milk fat globule membrane. *Proteomics* 2002;2:850-6.
12. Mather IH. A review and proposed nomenclature for major proteins of the milk-fat globule membrane. *J Dairy Sci* 2000;83:203-47.
13. Deeth HC. The role of phospholipids in the stability of milk fat globules. *Aust J Dairy Technol* 1997;52:44-6.
14. Kim HHY, Jimenezflores R. heat-induced interactions between the proteins of milk-fat globule-membrane and skim milk. *J Dairy Sci* 1995;78:24-35.
15. CanoRuiz ME, Richter RL. Effect of homogenization pressure on the milk fat globule membrane proteins. *J Dairy Sci* 1997;80:2732-9.
16. Evers JM. The milkfat globule membrane - compositional and structural changes post secretion by the mammary secretory cell. *Int Dairy J* 2004;14:661-74.
17. Rombaut R, Dejonckheere V, Dewettinck K. Filtration of milk fat globule membrane fragments from acid buttermilk cheese whey. *J Dairy Sci* 2007;90:1662-73.

18. Danthine S, Blecker C, Paquot M, Innocente N, Deroanne C. Progress in milk fat globule membrane research: a review. *Lait* 2000;80:209-22.
19. Dewettinck K, Rombaut R, Thienpont N, Le TT, Messens K, Van Camp J. Nutritional and technological aspects of milk fat globule membrane material. *Int Dairy J* 2008;18:436-57.
20. Spitsberg VL. Bovine milk fat globule membrane as a potential nutraceutical. *J Dairy Sci* 2005;88:2289-94.
21. Schmelz EM, Dillehay DL, Webb SK, Reiter A, Adams J, Merrill AH, Jr. Sphingomyelin consumption suppresses aberrant colonic crypt foci and increases the proportion of adenomas versus adenocarcinomas in CF1 mice treated with 1,2-dimethylhydrazine: implications for dietary sphingolipids and colon carcinogenesis. *Cancer Res* 1996;56:4936-41.
22. Eckhardt ERM, Wang DQH, Donovan JM, Carey MC. Dietary sphingomyelin suppresses intestinal cholesterol absorption by decreasing thermodynamic activity of cholesterol monomers. *Gastroenterology* 2002;122:948-56.
23. Noh SK, Koo SI. Milk sphingomyelin is more effective than egg sphingomyelin in inhibiting intestinal absorption of cholesterol and fat in rats. *J Nutr* 2004;134:2611-6.
24. Pfeuffer M, Schrezenmeir J. Dietary sphingolipids: metabolism and potential health implications. *Kieler Milchw Forsch* 2001;53:31-42.
25. Vesper H, Schmelz EM, Nikolova-Karakashian MN, Dillehay DL, Lynch DV, Merrill AH. Sphingolipids in food and the emerging importance of sphingolipids to nutrition. *J Nutr* 1999;129:1239-50.



26. Clare DA, Zheng Z, Hassan HM, Swaisgood HE, Catignani GL. Antimicrobial properties of milkfat globule membrane fractions. *J Food Prot* 2008;71:126-33.
27. Dalbeth N, Gracey E, Pool B, et al. Identification of dairy fractions with anti-inflammatory properties in models of acute gout. *Ann Rheum Dis* 2010;69:766-9.
28. El Alwani M, Wu BX, Obeid LM, Hannun YA. Bioactive sphingolipids in the modulation of the inflammatory response. *Pharmacol Ther* 2006;112:171-83.
29. Park EJ, Suh M, Thomson B, et al. Dietary ganglioside inhibits acute inflammatory signals in intestinal mucosa and blood induced by systemic inflammation of Escherichia coli lipopolysaccharide. *Shock* 2007;28:112-7.
30. Park EJ, Suh M, Thomson B, Thomson AB, Ramanujam KS, Clandinin MT. Dietary ganglioside decreases cholesterol content, caveolin expression and inflammatory mediators in rat intestinal microdomains. *Glycobiology* 2005;15:935-42.
31. Duan RD. Anticancer compounds and sphingolipid metabolism in the colon. *In Vivo* 2005;19:293-300.
32. Schmelz EM. Sphingolipids in the chemoprevention of colon cancer. *Front Biosci* 2004;9:2632-9.
33. Snow DR, Jimenez-Flores R, Ward RE, et al. Dietary milk fat globule membrane reduces the incidence of aberrant crypt foci in Fischer-344 rats. *J Agric Food Chem* 2010;58:2157-63.
34. Motouri M, Matsuyama H, Yamamura J, et al. Milk sphingomyelin accelerates enzymatic and morphological maturation of the intestine in artificially reared rats. *J Pediatr Gastroenterol Nutr* 2003;36:241-7.

35. Chen H, Born E, Mathur SN, Johlin FC, Jr., Field FJ. Sphingomyelin content of intestinal cell membranes regulates cholesterol absorption. Evidence for pancreatic and intestinal cell sphingomyelinase activity. *Biochem J* 1992;286 (Pt 3):771-7.
36. Park EJ, Thomson AB, Clandinin MT. Protection of intestinal occludin tight junction protein by dietary gangliosides in lipopolysaccharide-induced acute inflammation. *J Pediatr Gastroenterol Nutr* 2010;50:321-8.
37. Vazquez E, Gil A, Rueda R. Dietary gangliosides positively modulate the percentages of Th1 and Th2 lymphocyte subsets in small intestine of mice at weaning. *Biofactors* 2001;15:1-9.
38. Park EJ, Suh M, Ramanujam K, Steiner K, Begg D, Clandinin MT. Diet-induced changes in membrane gangliosides in rat intestinal mucosa, plasma and brain. *J Pediatr Gastroenterol Nutr* 2005;40:487-95.
39. Gordon BR, Parker TS, Levine DM, et al. Neutralization of endotoxin by a phospholipid emulsion in healthy volunteers. *J Infect Dis* 2005;191:1515-22.
40. Hubsch AP, Powell FS, Lerch PG, Doran JE. A reconstituted, apolipoprotein A-I containing lipoprotein reduces tumor necrosis factor release and attenuates shock in endotoxemic rabbits. *Circ Shock* 1993;40:14-23.
41. Parker TS, Levine DM, Chang JC, Laxer J, Coffin CC, Rubin AL. Reconstituted high-density lipoprotein neutralizes gram-negative bacterial lipopolysaccharides in human whole blood. *Infect Immun* 1995;63:253-8.

42. Stremmel W, Merle U, Zahn A, Autschbach F, Hinz U, Ehehalt R. Retarded release phosphatidylcholine benefits patients with chronic active ulcerative colitis. *Gut* 2005;54:966-71.
43. Stremmel W, Ehehalt R, Autschbach F, Karner M. Phosphatidylcholine for steroid-refractory chronic ulcerative colitis: a randomized trial. *Ann Intern Med* 2007;147:603-10.
44. Treede I, Braun A, Sparla R, et al. Anti-inflammatory effects of phosphatidylcholine. *J Biol Chem* 2007;282:27155-64.
45. Heath JP. Epithelial cell migration in the intestine. *Cell Biol Int* 1996;20:139-46.
46. de Santa Barbara P, van den Brink GR, Roberts DJ. Development and differentiation of the intestinal epithelium. *Cell Mol Life Sci* 2003;60:1322-32.
47. Cohn JS, Wat E, Kamili A, Tandy S. Dietary phospholipids, hepatic lipid metabolism and cardiovascular disease. *Curr Opin Lipidol* 2008;19:257-62.
48. Zhou AL, Hintze KJ, Jimenez-Flores R, Ward RE. Dietary fat composition influences tissue lipid profile and gene expression in Fischer-344 rats. *Lipids* 2012;DOI: 10.1007/s11745-012-3729-3.
49. Wat E, Tandy S, Kapera E, et al. Dietary phospholipid-rich dairy milk extract reduces hepatomegaly, hepatic steatosis and hyperlipidemia in mice fed a high-fat diet. *Atherosclerosis* 2009;205:144-50.
50. Rinella ME, Elias MS, Smolak RR, Fu T, Borensztajn J, Green RM. Mechanisms of hepatic steatosis in mice fed a lipogenic methionine choline-deficient diet. *J Lipid Res* 2008;49:1068-76.

51. Bacon BR, Park CH, Fowell EM, McLaren CE. Hepatic steatosis in rats fed diets with varying concentrations of sucrose. *Fundam Appl Toxicol* 1984;4:819-26.
52. van der Flier LG, Clevers H. Stem cells, self-renewal, and differentiation in the intestinal epithelium. *Annu Rev Physiol* 2009;71:241-60.
53. Madara JL, Nash S, Moore R, Atisook K. Structure and function of the intestinal epithelial barrier in health and disease. *Monogr Pathol* 1990:306-24.
54. Powell DW. Barrier function of epithelia. *Am J Physiol* 1981;241:G275-88.
55. Frizzell RA, Schultz SG. Ionic conductances of extracellular shunt pathway in rabbit ileum. Influence of shunt on transmural sodium transport and electrical potential differences. *J Gen Physiol* 1972;59:318-46.
56. Gonzalez-Mariscal L, Betanzos A, Nava P, Jaramillo BE. Tight junction proteins. *Prog Biophys Mol Biol* 2003;81:1-44.
57. Furuse M, Hirase T, Itoh M, et al. Occludin - a novel integral membrane-protein localizing at tight junctions. *J Cell Biol* 1993;123:1777-88.
58. Furuse M, Fujita K, Hiiragi T, Fujimoto K, Tsukita S. Claudin-1 and -2: Novel integral membrane proteins localizing at tight junctions with no sequence similarity to occludin. *J Cell Biol* 1998;141:1539-50.
59. Martin-Padura I, Lostaglio S, Schneemann M, et al. Junctional adhesion molecule, a novel member of the immunoglobulin superfamily that distributes at intercellular junctions and modulates monocyte transmigration. *J Cell Biol* 1998;142:117-27.
60. Barrett KE. New ways of thinking about (and teaching about) intestinal epithelial function. *Adv Physiol Educ* 2008;32:25-34.

61. Grootjans J, Thuijls G, Verdam F, Derikx JP, Lenaerts K, Buurman WA. Non-invasive assessment of barrier integrity and function of the human gut. *World J Gastrointest Surg* 2010;2:61-9.
62. Dial EJ, Zayat M, Lopez-Storey M, Tran D, Lichtenberger L. Oral phosphatidylcholine preserves the gastrointestinal mucosal barrier during LPS-induced inflammation. *Shock* 2008;30:729-33.
63. Braun A, Treede I, Gotthardt D, et al. Alterations of phospholipid concentration and species composition of the intestinal mucus barrier in ulcerative colitis: a clue to pathogenesis. *Inflamm Bowel Dis* 2009;15:1705-20.
64. Tazuke Y, Drongowski RA, Teitelbaum DH, Coran AG. Interleukin-6 changes tight junction permeability and intracellular phospholipid content in a human enterocyte cell culture model. *Pediatr Surg Int* 2003;19:321-5.
65. Singh R, Kaushik S, Wang Y, et al. Autophagy regulates lipid metabolism. *Nature* 2009;458:1131-5.
66. Duncan RE, Ahmadian M, Jaworski K, Sarkadi-Nagy E, Sul HS. Regulation of lipolysis in adipocytes. *Annu Rev Nutr* 2007;27:79-101.
67. Pages C, Simon MF, Valet P, Saulnier-Blache JS. Lysophosphatidic acid synthesis and release. *Prostag Oth Lipid M* 2001;64:1-10.
68. Jaworski K, Ahmadian M, Duncan RE, et al. AdPLA ablation increases lipolysis and prevents obesity induced by high-fat feeding or leptin deficiency. *Nat Med* 2009;15:159-68.
69. Iyer A, Fairlie DP, Prins JB, Hammock BD, Brown L. Inflammatory lipid mediators in adipocyte function and obesity. *Nat Rev Endocrinol* 2010;6:71-82.

70. Trayhurn P, Wang B, Wood IS. Hypoxia in adipose tissue: a basis for the dysregulation of tissue function in obesity? *Br J Nutr* 2008;100:227-35.
71. Wang B, Wood IS, Trayhurn P. Dysregulation of the expression and secretion of inflammation-related adipokines by hypoxia in human adipocytes. *Pflugers Arch* 2007;455:479-92.
72. Ye J. Emerging role of adipose tissue hypoxia in obesity and insulin resistance. *Int J Obes (Lond)* 2009;33:54-66.
73. Hotamisligil GS. Inflammation and metabolic disorders. *Nature* 2006;444:860-7.
74. Bastard JP, Maachi M, Lagathu C, et al. Recent advances in the relationship between obesity, inflammation, and insulin resistance. *Eur Cytokine Netw* 2006;17:4-12.
75. Weisberg SP, McCann D, Desai M, Rosenbaum M, Leibel RL, Ferrante AW. Obesity is associated with macrophage accumulation in adipose tissue. *J Clin Invest* 2003;112:1796-808.
76. Cinti S. The adipose organ. *Prostaglandins Leukot Essent Fatty Acids* 2005;73:9-15.
77. Winer S, Chan Y, Paltser G, et al. Normalization of obesity-associated insulin resistance through immunotherapy. *Nature Medicine* 2009;15:921-U126.
78. Olefsky JM, Glass CK. Macrophages, inflammation, and insulin resistance. *Annu Rev Physiol* 2010;72:219-46.
79. Charriere G, Cousin B, Arnaud E, et al. Preadipocyte conversion to macrophage. Evidence of plasticity. *J Biol Chem* 2003;278:9850-5.

80. Nawrocki AR, Scherer PE. The adipocyte as a drug discovery target. *Drug Discov Today* 2005;10:1219-30.
81. Van Gaal LF, Mertens IL, De Block CE. Mechanisms linking obesity with cardiovascular disease. *Nature* 2006;444:875-80.
82. Saito T, Hayashida H, Furugen R. Comment on: Cani et al. (2007) Metabolic endotoxemia initiates obesity and insulin resistance: *Diabetes* 56:1761-1772. *Diabetes* 2007;56:e20; author reply e1.
83. Laugerette F, Vors C, Peretti N, Michalski MC. Complex links between dietary lipids, endogenous endotoxins and metabolic inflammation. *Biochimie* 2010.
84. Suzuki T, Hara H. Dietary fat and bile juice, but not obesity, are responsible for the increase in small intestinal permeability induced through the suppression of tight junction protein expression in LETO and OLETF rats. *Nutr Metab (Lond)* 2010;7:19.
85. Laugerette F, Vors C, Geloën A, et al. Emulsified lipids increase endotoxemia: possible role in early postprandial low-grade inflammation. *J Nutr Biochem* 2010.
86. Cani PD, Bibiloni R, Knauf C, et al. Changes in gut microbiota control metabolic endotoxemia-induced inflammation in high-fat diet-induced obesity and diabetes in mice. *Diabetes* 2008;57:1470-81.
87. Cani PD, Amar J, Iglesias MA, et al. Metabolic endotoxemia initiates obesity and insulin resistance. *Diabetes* 2007;56:1761-72.
88. Ferraris RP, Vinnakota RR. Intestinal nutrient transport in genetically obese mice. *Am J Clin Nutr* 1995;62:540-6.

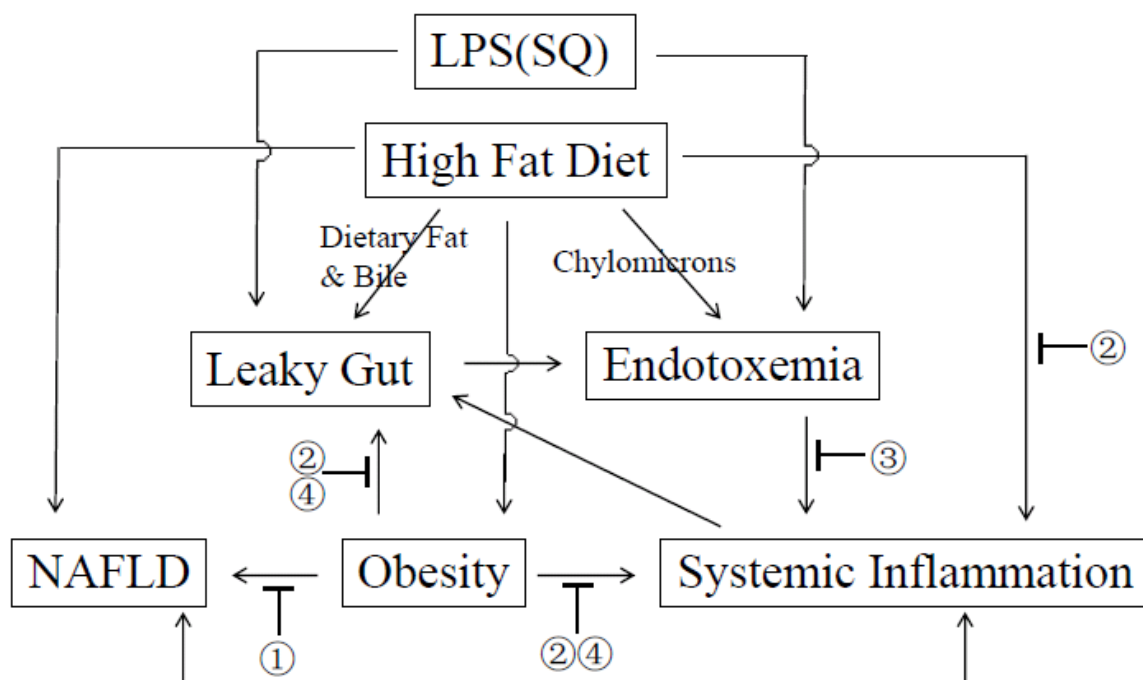
89. Morton AP, Hanson PJ. Monosaccharide transport by the small intestine of lean and genetically obese (ob/ob) mice. *Q J Exp Physiol* 1984;69:117-26.
90. Brun P, Castagliuolo I, Di Leo V, et al. Increased intestinal permeability in obese mice: new evidence in the pathogenesis of nonalcoholic steatohepatitis. *Am J Physiol Gastrointest Liver Physiol* 2007;292:G518-25.
91. Naito E, Yoshida Y, Makino K, et al. Beneficial effect of oral administration of *Lactobacillus casei* strain Shirota on insulin resistance in diet-induced obesity mice. *J Appl Microbiol* 2010.
92. Kahn SE, Hull RL, Utzschneider KM. Mechanisms linking obesity to insulin resistance and type 2 diabetes. *Nature* 2006;444:840-6.
93. Bruewer M, Luegering A, Kucharzik T, et al. Proinflammatory cytokines disrupt epithelial barrier function by apoptosis-independent mechanisms. *J Immunol* 2003;171:6164-72.
94. Das UN. Is obesity an inflammatory condition? *Nutrition* 2001;17:953-66.
95. Ceponis PJ, Botelho F, Richards CD, McKay DM. Interleukins 4 and 13 increase intestinal epithelial permeability by a phosphatidylinositol 3-kinase pathway. Lack of evidence for STAT 6 involvement. *J Biol Chem* 2000;275:29132-7.
96. Ma DL, Forsythe P, Bienenstock J. Live *Lactobacillus reuteri* is essential for the inhibitory effect on tumor necrosis factor alpha-induced interleukin-8 expression. *Infection and Immunity* 2004;72:5308-14.
97. Iacono A, Raso GM, Canani RB, Calignano A, Meli R. Probiotics as an emerging therapeutic strategy to treat NAFLD: focus on molecular and biochemical mechanisms. *J Nutr Biochem* 2011.



98. Snow DR, Ward RE, Olsen A, Jimenez-Flores R, Hintze KJ. Membrane-rich milk fat diet provides protection against gastrointestinal leakiness in mice treated with lipopolysaccharide. *J Dairy Sci* 2011;94:2201-12.
99. Takahashi M, Ikemoto S, Ezaki O. Effect of the fat/carbohydrate ratio in the diet on obesity and oral glucose tolerance in C57BL/6J mice. *J Nutr Sci Vitaminol (Tokyo)* 1999;45:583-93.
100. Mathan VI, Penny GR, Mathan MM, Rowley D. Bacterial lipopolysaccharide-induced intestinal microvascular lesions leading to acute diarrhea. *J Clin Invest* 1988;82:1714-21.
101. Wang Q, Wang JJ, Fischer JE, Hasselgren PO. Mucosal production of complement C3 and serum amyloid A is differentially regulated in different parts of the gastrointestinal tract during endotoxemia in mice. *J Gastrointest Surg* 1998;2:537-46.
102. Nandi D, Mishra MK, Basu A, Bishayi B. Protective effects of interleukin-6 in lipopolysaccharide (LPS)-induced experimental endotoxemia are linked to alteration in hepatic anti-oxidant enzymes and endogenous cytokines. *Immunobiology* 2010;215(6):443-51.
103. Yokochi T, Inoue Y, Yokoo J, Kimura Y, Kato N. Retention of Bacterial Lipopolysaccharide at the Site of Subcutaneous Injection. *Infection and Immunity* 1989;57:1786-91.

**Table 1.1** Major components of MFGM in bovine milk (adapted from Ref (7)).

<b>Lipids</b>	<b>%</b>
Triglycerides	62
Diglycerides	9
Monoglycerides	Trace
Sterols	0.2-2
Sterol esters	0.1-0.3
Free fatty acids	0.6-6
Hydrocarbons (squalene and phytene derivatives)	1.2
Phospholipids	26-31
<b>Polar lipids</b>	<b>%</b>
Sphingomyelin	22
Phosphatidylcholine	36
Phosphatidylethanolamine	27
Phosphatidylinositol	11
Phosphatidylserine	4
Lysophosphatidylcholine	2
<b>Proteins</b>	
Mucin 1	
Xanthine oxidoreductase	
PAS III	
CD 36	
Butyrophilin	
PAS 6/7	
Adipophilin	
Fatty acid binding protein	



**Figure 1.1** Complex links between dietary lipids, leaky gut, endotoxemia, obesity, NAFLD and metabolic inflammation and the effect of the LPS injection. T shaped arrows indicate the hypothesized effects of polar lipids on NAFLD (①), leaky gut (②, ④), endotoxemia (③), and systemic inflammation (②, ③, ④). Milk polar lipids decrease gut permeability and NAFLD and therefore decrease endotoxemia and metabolic inflammation in mice during the high fat diet feeding and during the LPS stress in combination with the high fat diet. SQ: subcutaneous injection. NAFLD: nonalcoholic fatty liver disease. LPS: lipopolysaccharide.

## CHAPTER 2

### DIETARY FAT COMPOSITION INFLUENCES TISSUE LIPID PROFILE AND GENE EXPRESSION IN FISCHER-344 RATS

#### Abstract

The AIN-76A diet causes fatty liver in rodents when fed for long periods of time. The aim of this study was to utilize fatty acid analysis and transcriptomics to investigate the effects of different fat sources in the AIN-76A diet on tissue lipid profiles and gene expression in male, weanling Fischer-344 rats. Animals were fed isocaloric diets that differed only in the fat source: 1) corn oil (CO) 2) anhydrous milk fat (AMF) and 3) AMF supplemented with 10% phospholipids from the milk fat globule membrane (AMF-MFGM). There were no differences in food intake, body weight, growth rate or body fat composition among the groups, and the fatty acid compositions of red blood cells (RBCs), plasma, muscle and visceral adipose tissues reflected the dietary fat sources. Modifying the fat source resulted in 293 genes differentially regulated in skeletal muscle, 1,124 in adipose and 831 in liver as determined by analysis of variance (ANOVA). While tissue fatty acid profiles mostly reflected the diet, there were several quantitative differences in lipid classes in the liver and plasma. The AMF diet resulted in the highest level of hepatic triglycerides, but the lowest level in plasma. The CO diet decreased DGAT expression and activity and resulted in significant accumulation of hepatic unesterified fatty acids, a potential trigger for steatohepatitis. These results indicate that the fatty acid composition and presence of polar lipids in the AIN-76A diets have significant effects on lipid partitioning, gene expression, and potentially the development of liver pathology.

Reprinted with modifications from Zhou AL, Hintze KJ, Jimenez-Flores R, and Ward RE. Dietary Fat Composition Influences Tissue Lipid Profile and Gene Expression in Fischer-344 Rats. *Lipids*. 2012. 47(12):1119-30. doi: 10.1007/s11745-012-3729-3. Robert Ward and Korry Hintze raised the rat, collected the tissue samples and obtained the microarray raw data. Albert Lihong Zhou did the lipid profiling of the diets and the tissues, carried out the RT-PCR, histology and enzyme assay, processed the microarray data, carried out data analyses and statistical analyses, interpreted all of the data and prepared the first draft of the manuscript. Robert Ward revised the manuscript. Korry Hintze provided the reagents for the RT-PCR experiment. The only contribution to this work from Rafael Jimenez-Flores was to provide the testing material, the MFGM isolate.

## **Introduction**

The AIN-76 diet is a purified rodent diet that was developed in the late 1970's by an ad hoc committee formed by the American Institute of Nutrition (AIN) (1). One rationale for developing this diet was to provide researchers with a nutritionally adequate diet that would allow for standardizing studies between laboratories. Not long after this diet was developed several groups reported undesirable physiological effects linked to the diet, such as hemorrhagic deaths (2), nephrocalcinosis (3) and fatty liver (4). An amended formulation of the diet (AIN-76A) was developed in 1980 with an increased vitamin K content to address the hemorrhagic effect (5). In 1993 two revised diets were formulated to replace the AIN-76A, a version for growing animals (AIN-93G) and a maintenance formula for mature animals (AIN-93M). These revised diets contained a higher calcium:phosphorous ratio (from 0.75 to 1.3) to prevent the nephrocalcinosis found in female rats consuming the AIN-76A diet (1). In addition, the carbohydrate composition was changed from 50% sucrose and 15% cornstarch in the AIN-76A formula to ~40% cornstarch, 15% dextrinized cornstarch and 10% sucrose in the AIN-93G diet. This change represents a 5-fold decrease in the fructose content of the diet and is not

associated with the accumulation of hepatic lipids caused by long term feeding of the high sucrose levels (6). Despite the availability of the improved rodent diets, the AIN-76A remains popular in specific research fields, such as in studies investigating the effects of diet on colon cancer using the aberrant crypt foci model (ACF). In fact, in a database maintained to compare the efficacy of diet modulation on the incidence of ACF, the overwhelming majority of studies have utilized the AIN-76A (7) .

The propensity of the AIN-76A diet to result in accumulation of hepatic lipids is potentially of interest to human nutrition, as it is estimated that between 20% and 30% of adults in Western countries have nonalcoholic fatty liver disease (NAFLD) and this level rises to between 70% and 90% in obese individuals and those with diabetes (8). To test the hypothesis that high levels of dietary fructose are responsible for the accumulation of hepatic lipids, Bacon et al. tested the effects of modifying the sucrose content of the AIN-76A diet in a three week feeding study in rats (9). According to the results, diets containing greater than 25% sucrose resulted in significantly higher hepatic triglycerides (TG) than ones with less than 20% sucrose or chow.

We recently conducted an aberrant crypt foci (ACF) study utilizing the AIN-76A diet to investigate the potential chemopreventive effects of a complex milk fat fraction (10). In the study we used three diets with different fat compositions: 1) corn oil (CO), 2) anhydrous milk fat (AMF), and 3) anhydrous milk fat supplemented with milk fat globule membrane (AMF-MFGM). CO diet is the standard fat source for the AIN-76A diet, and for the AMF diet, the 5% mass of fat was replaced with AMF. Formulation of the

AMF-MFGM diet was achieved by utilizing an isolate of MFGM (providing 10% phospholipids of total fat) that was isolated from cream, and which also contained protein, carbohydrate and minerals in addition to the fat. The details of the diet formulation have been reported previously (10) and are shown in Table 2.1.

MFGM is derived from the apical surface of mammary epithelial cells and surrounds the fat droplets in milk (11). It is composed primarily of TG, proteins, and phospholipids (PL) (12). The composition of the polar lipids of MFGM can vary according to the method of isolation, but the major constituents are phosphatidylcholine (~32%), phosphatidylethanolamine (32%), sphingomyelin (~24%), phosphatidylinositol (~4%), phosphatidylserine (~3%) and gangliosides (~3%) (13). A large amount of this material is produced in the US each year as a byproduct of butter production, and is available as a food ingredient. Due to its unique lipid profile and membrane protein profile, MFGM has been suggested as a potentially bioactive food ingredient with novel nutritional functionalities (14). Despite this supposition, few studies have been conducted *in vivo* with either animal models or humans to evaluate the potential of this material as a bioactive ingredient.

The goal of this study was to investigate lipid metabolism in rats fed a diet known to induce hepatic stress. Our approach involved subjecting lipid metabolizing tissues to two different, yet comprehensive analytical techniques (lipid and gene expression profiling) to understand how the dietary fats affected lipid metabolism.

## **Materials and Methods**

### **Animals and diets**

Eleven animals used in this study were among a group of sixty-three male, weanling Fischer-344 rats (Charles River Laboratories) used in another study (10). They were randomly assigned to one of three isocaloric dietary treatments that differed only in the fat source (10). After a 7 day acclimation period on standard chow diets, the rats were individually housed in a room controlled for temperature, humidity, and light cycle and were given free access to experimental diets and deionized water. Food intake and body weight were measured weekly. All experimental protocols involving animals were approved by the Utah State University Institutional Animal Care and Use Committee.

Animals were fed experimental diets for twelve weeks. After MRI analysis of body composition (EchoMRI-900™), rats were sacrificed by cardiac puncture following ketamine/xylazine anesthesia. The liver, the gonadal adipose tissue, and the skeletal muscle and the blood samples were collected, flash frozen in liquid nitrogen, and stored at -80 °C until the time of analysis.

### **Lipid extraction**

Tissue samples were removed from the freezer and a sample of tissue was cut into small pieces with a razor and placed in a mortar with liquid nitrogen and ground to obtain a fine homogenous powder. About 200 mg of the tissue powder from each sample was weighed and put into a glass tube with screw cap. Surrogate standards, including sphingomyelin, phosphatidylcholine, phosphatidylserine, phosphatidylethanolamine,



diglycerides (DG), free fatty acids (FFA), TG, and Cholesteryl esters (CE), were prepared in chloroform. 100  $\mu$ l surrogate standards for different lipid classes were added to each sample and weights were recorded. Lipids were extracted by the method of Folch et al. (15) with slight modifications. Samples were mixed with 5 ml chloroform/methanol (2:1 with butylated hydroxytoluene, BHT). The whole mixture was sonicated and then agitated for 15-20 minutes in an orbital shaker at room temperature. The mixture was washed with 0.2 volumes (1 ml for 5 ml solvent mixture) of 0.9% NaCl solution and vortexed for 20 seconds. Subsequently, the mixture was centrifuged at  $1,500 \times g$  for 10 minutes to separate the two phases. The lower chloroform phase containing lipids was collected and evaporated under a nitrogen stream and then reconstituted in a small volume of hexane with BHT in a 4ml amber vial and stored at  $-80\text{ }^{\circ}\text{C}$  until further analysis.

### **Separation and recovery of different lipid classes**

Individual lipid classes of the extracted lipid were separated using thin layer chromatography (TLC). Extracted lipid from each tissue was diluted by hexane with BHT such that 20  $\mu$ l of solution contained around 2.5 mg of lipid. Aliquots of 20  $\mu$ l were spotted on a  $20 \times 20$  cm silica gel 60  $\text{\AA}$  analytical plate (500  $\mu$ m layer) (Whatman Inc., Florham Park, NJ). Lipid class standards were also spotted for detecting target bands. Total lipid classes were separated by developing the plate in a solvent system containing hexane, diethyl ether, and formic acid in the ratio of 80:20:2 (v/v). The TLC plate was then sprayed with 0.05% primulin in acetone:water (8:2 v/v). Individual lipid bands on the TLC plate were detected under a hand-held UV lamp and the margins were marked with a pencil. Target lipid class bands were scraped from the TLC plate using a small

razor blade and collected into glass tubes with screwed caps. Recovered lipid classes from total lipid TLC plate were: PL, DG, FFA, TG, and CE.

### **Fatty acid methyl esters**

Recovered lipid classes were transesterified into fatty acid methyl esters (FAMES) using the method of Curtis et al. (16) with slight modifications. In each tube, 0.8 ml hexane and 1.2 ml 10% (v/v) acetyl chloride in methanol were added. Tubes were capped, vortexed for 20 seconds and placed in 100 °C oven for 40 minutes. Upon completion of incubation period, samples were removed and allowed to cool down to room temperature. Then 2 ml 6% sodium carbonate solution and 0.4 ml hexane were added into each tube. On subsequent vortexing and centrifuging of tubes two distinct phases were obtained. The top organic layer was removed and transferred to gas chromatography (GC) vials. Solvent was evaporated under a nitrogen stream and fatty acid methyl esters were collected in 100 µl of hexane with BHT and transferred to GC vial inserts. The samples were subsequently analyzed by GC using a GC2010 (Shimadzu Scientific Instruments, Columbia, MD).

### **GC data analysis**

For each GC run, standard curves were generated using commercially available FAME standards (Nu-Chek Prep, Elysian, MN). To establish the linearity of the detector response, a three point calibration was generated with every sample set. The calibration standard, GLC-463, contained 42 fatty acids representing most of the common species found in mammalian tissues and dairy products. Chromatograms of sample FAMES were compared with those of FAME standards to identify target fatty acids. The peak area for

each fatty acid was then normalized to the peak area and concentration of the corresponding surrogate standard. Next, the molar concentration of the analytes was calculated and then converted to moles of the corresponding lipid classes through molecular weight calculations. The molar concentration of lipid classes was normalized to tissue sample weights to obtain concentrations ( $\mu\text{mole/g}$  tissue) in each tissue. Lastly, the mole percentage of each fatty acid species was calculated.

### **Gene expression analysis**

Total RNA was extracted from liver, muscle, and adipose tissue as previously described (10). Tissue samples were homogenized in Trizol with a tissue homogenizer. Total RNA was extracted using the RNAqueous kit (Ambion) according to the manufacturer's protocol. Frozen total RNA was sent to Genome Quebec for analysis. Microarray data were generated by Genome Quebec using the Illumina platform (Illumina, Inc., San Diego, CA). Data were analyzed using FlexArray 1.6, a custom statistical software program developed by Genome Quebec (17). The expression data were filtered to remove feature ids that have not been detected. Next, a background adjustment and normalization were carried out using the Lumi algorithm (based on lumi Bioconductor package) in FlexArray 1.6. Background correction was carried out by using negative controls. Variance was stabilized by the Variance-Stabilizing Transformation (VST) method and subsequently a robust spline normalization was conducted. Analysis of variance (ANOVA) was conducted to evaluate significant diet effects on gene expression across treatment groups. The Cyber-T algorithm was employed to identify differentially regulated genes (CT gene lists) among tissues between treatment groups from ANOVA gene lists (18) followed by the Benjamini-Hochberg False Discovery Rate

multiple testing correction (19). The CT gene lists were then subjected to KEGG pathway analysis using ArrayTrack v.3.5.0 (NCTR/FDA) (20).

### **Real time PCR**

Total RNA was extracted from liver samples using the RNeasy Mini-Kit (Qiagen, Valencia, CA). RNA quality was checked and the concentration measured by NanoDrop 1000 (Thermo Fisher, Waltham, MA). One microgram RNA was converted to cDNA using high capacity cDNA reverse transcription kit (Life Technologies, Carlsbad, CA). Validated and predesigned TaqMan primers and probes (Life Technologies) were used to quantify cytochrome P450, family 8, subfamily b, polypeptide 1 (*Cyp8b1*, ID: Rn00579921\_s1), 1-acylglycerol-3-phosphate O-acyltransferase 2 (*Agpat2*, ID: Rn01438505\_m1), and angiotensin-like 4 (*Angptl4*, ID: Rn01528817\_m1). Actin, beta (*Actb*, ID: ID Rn00667869\_m1) was used as an endogenous control. Real-time PCR amplifications were carried out in a DNA Engine Opticon® 2 Two-Color Real-Time PCR Detection System (Biorad, Hercules, CA). PCR results were analyzed with the Opticon Monitor 3 Software (Biorad). The comparative Ct method was used to quantify gene expression.  $\Delta$ Ct was obtained by normalizing to actin, beta.  $\Delta\Delta$ Ct was determined by the arithmetic formula described by López-Parra et al. (21). Symmetrical raw fold change was obtained by comparing  $\Delta\Delta$ Ct values of two groups compared.

### **Liver fat analysis by histology**

Cryostat sections of 6  $\mu$ m thickness were made from liver samples taken out of -80 °C freezer. The tissue sections were brought to room temperature on glass slides. The slides were dipped a few times in 60% triethyl phosphate and then stained in 0.5% Oil

Red O (in 60% triethyl phosphate) for 15 minutes. After being rinsed in water for 2 minutes, the slides were counterstained in Harris modified method hematoxylin stain (Thermo Fisher, Waltham, MA) for 2 minutes. The slides were placed in saturated lithium carbonate solution for 10 seconds, rinsed in water for 5 minutes, and held in water. The slides were mounted with warm glycerin jelly and observed with light microscopy. Color images were captured with a digital camera attached to the microscope. Oil Red O stained areas in randomly sampled regions from each slide were quantified by ImageJ (22). The fat content of each sample was expressed by quantification of Oil Red O–stained areas as a percentage of whole area.

#### **Liver diglyceride acyltransferase (DGAT) enzyme assay**

The microsomal fraction of the liver was obtained by the methods of Ko et al. (23) and Coleman (24). Rat liver (approximately 1.5 g) was minced and then homogenized in 15 ml of STE buffer (0.25 M sucrose, 10 mM Tris-HCl, pH 7.4, 1.0 mM EDTA) with a Teflon-glass homogenizer at medium speed. The homogenate was centrifuged at 14,000  $\times g$  for 20 minutes at 4 °C. The supernatant was centrifuged at 100,000  $\times g$  for 1 h at 4 °C to obtain a microsomal pellet. The pellet was suspended in STE buffer without EDTA and centrifuged at 100,000  $\times g$  for 1 h at 4 °C. The final pellet was resuspended in STE buffer without EDTA. Total protein in final solution was quantified by the Bradford Assay. The microsomal fractions were stored in aliquots at -80 °C.

A fluorescent DGAT assay was carried out as described by McFie and Stone (25). Briefly, a master mix was prepared in a test tube containing: 20  $\mu$ l of 1 M Tris-HCl (pH 7.6), 4  $\mu$ l of 1 M MgCl<sub>2</sub>, 10  $\mu$ l of 4 mM dioleoyl-sn-glycerol, 10  $\mu$ l of 12.5 mg/ml bovine

serum albumin, 10  $\mu$ l of 500  $\mu$ M NBD-palmitoyl CoA and 96  $\mu$ l of water per reaction.

Tubes were pre-incubated in a 37 °C water bath for 2 minutes and 50  $\mu$ l of protein sample was added to start the reaction, which was held at 37 °C for 10 minutes with occasional shaking. The reaction was terminated by addition of 4 ml  $\text{CHCl}_3/\text{MeOH}$  (2:1, v/v).

Samples were added 800  $\mu$ l of water and allowed to sit at room temperature for 1 h.

Tubes were centrifuged at  $3000 \times g$  for 5 minutes to separate aqueous and organic phases.

The organic phase was removed via pipette and dried under stream of nitrogen. Lipids were resuspended in 50  $\mu$ L  $\text{CHCl}_3/\text{MeOH}$  (2:1) and spotted on a 20 x 20 cm TLC plate.

TLC plates were developed in the solvent system, hexane/diethyl ether/acetic acid (80:20:1, v/v/v). The plates were air dried for 1 h and scanned by Typhoon Trio+ Laser Imager 7 (GE Healthcare, Waukesha, WI). The following settings were used: Excitation - Blue (488 nm) LED laser light source; Emission – 520 nm BP emission filter.

Fluorescence was quantified by ImageJ (22). The newly synthesized NBD-TG was quantified as units (fluorescence intensity) of NBD-TG formed per minute per mg protein.

### **Statistical analysis**

A one-way ANOVA was performed using SAS software version 9.2 (SAS Institute Inc.) to perform comparisons among groups or using FlexArray 1.6 for gene expression among groups and tissues. Group means were compared using Cyber-T algorithm for gene expression data and Ryan-Einot-Gabriel-Welsch Multiple Range Test for other data. Data are reported as Mean  $\pm$  Standard Error of the Mean (SEM).

## Results

### Fatty acid profile of diets

The most abundant fatty acids of the test diets are shown in Figure 2.1. Both the milk fat based diets have similar fatty acid profiles, and are very different from the CO diet. The milk fat diets both have significant contributions of saturated fatty acids (~65%) whereas in the CO diet the percentage is much lower (~17.5%). All diets have similar levels of monounsaturates, with oleic acid contributing approximately 25%. The other notable difference is in the polyunsaturated fatty acid content (PUFA) content (CO 54%, AMF 4.5% and AMF-MFGM 6%) and n6:n3 ratio (CO 54:1, AMF 6:1, AMF-MFGM 7:1).

### Food intake, body weight, growth rate and body fat composition

There were no significant differences in terms of food intake, final body weight, growth rate or body fat composition (MRI analysis) among groups (Figure 2.2) (10).

### Fatty acids profile of RBCs

The RBC fatty acid profile was measured to compare the CO diet to the milk fat based diets, and to determine if the higher polar lipid content of the AMF-MFGM had an effect compared with the AMF diet. RBC fatty acids that were significantly affected by the diets and present at least one percent of total fatty acids are shown in Figure 2.3. Not surprisingly, the CO cohort had a higher percentage of 18:2n-6, 20:4n-6 and 22:4n-6, all n6 fatty acids, presumably due to the high linoleic acid content of the diet. In addition, these animals had lower percentages of 16:1n-7, 18:1n-9, 18:1n-7, 20:3n-9, 20:5n-3, 22:5n-3 and 22:6n-3 compared with the animals fed the milk fat diets. The RBCs from

animals fed the two milk fat based diets had remarkably similar fatty acid profiles with two statistically relevant differences. Namely, the AMF-MFGM fed animals had a higher percentage of 18:1n-7 and a lower percentage of 20:3n-9.

### **Fatty acids profile of skeletal muscle tissue and visceral adipose tissue**

As with the RBCs, there were large differences between the fatty acid profile in skeletal muscle and visceral adipose tissue of the rats fed the CO diet versus the milk fat diets, which were virtually identical (Figure 2.4 & 2.5). In skeletal muscle, the CO fed animals had significantly less 16:1n-7, 18:1n-9, and 20:3n-9, and more 18:2n-6, 20:4n-6, and 22:4n-6 (Figure 2.4). Unlike skeletal muscle, the contribution of long chain fatty acids to the adipose lipids was low (Figure 2.5). However, among the major fatty acids (> 1% total), the CO animals had less 16:0, 16:1n-7, 18:0, 18:1n-9 and more 18:2n-6. The only fatty acid that differed among the animals fed the milk fat diets was 20:3n-9, which in both tissues was slightly lower in the AMF-MFGM group.

### **Fatty acids profile of liver tissue**

Fatty acids in liver tissue which were significantly affected by the CO, AMF and AMF-MFGM diets and which contribute at least 1% of fatty acids in one tissue are presented in Figure 2.6. Animals from the CO group had less 16:1n-7, 18:1n-9, 20:3n-9, and 22:6n-3 and more 18:2n-6 and 20:4n-6. Unlike the RBCs, skeletal muscle, and adipose tissues, supplementation of the AMF diet with MFGM resulted in several differences in the fatty acid profile of the liver. For example, of the six fatty acids that are significantly affected across the diets and present at least 1%, five are significantly different in livers of the animals fed the AMF and AMF-MFGM diets. Thus, the



increased polar lipid concentration of the AMF-MFGM diet appears to have significant effects in liver lipid metabolism and partitioning. The largest differences are in 18:1n-9, which is higher in the AMF animals, and 20:4n-6 and 22:6n-3, which are higher in the AMF-MFGM cohort.

### **Plasma, visceral adipose and liver lipid classes**

To better understand the differences in lipid partitioning as affected by the CO, AMF and AMF-MFGM diets, plasma, adipose and liver lipid classes were analyzed. Lipid classes with significant differences are shown in Figure 2.7. Interestingly, the animals consuming AMF as the fat source had less total PL in plasma than animals fed the CO and AMF-MFGM diets. Additionally, there was less TG than the animals fed the AMF-MFGM diet. In the visceral adipose, there was more TG in the animals fed CO than those fed the AMF-MFGM. In the liver, there was more FFA in the animals fed the CO diet than in those fed the AMF-MFGM diet, and a similar trend for the AMF animals, although this was not significant. On the other hand, the CO diet resulted in less accumulated TG than the AMF diet, with the AMF-MFGM diet in between. Lastly, both the CO and the AMF-MFGM diets resulted in lower hepatic CE than did the AMF diet.

### **Tissue gene expression**

In total, 293, 1,141, and 831 genes were differentially expressed, respectively, in skeletal muscle, adipose, and liver at  $p < 0.05$ . To identify metabolic pathways that were affected across the three diets all the genes that were differentially regulated according to the ANOVA analysis were analyzed with the program ArrayTrack, a free software tool developed by the National Center for Toxicological Research (NCTR) and the United

States Food and Drug Administration (FDA). All three diets were compared and the data generated from this analysis are summarized in Table 2.2. On a diet comparison basis, the fewest number of pathways affected across the three tissues were between the two milk fat fed animal groups (22 pathways) and the most pathways were affected between the CO and AMF-MFGM groups (40 pathways). In specific tissues, there were 18 pathways differentially affected in skeletal muscle, 31 in adipose and 40 in the liver. In specific diet/tissue comparisons, the fewest number of pathways were affected in skeletal muscle between the CO and the AMF diets (2). There were 16 pathways affected between the AMF and CO diets in the liver and 16 pathways between the AMF-MFGM and CO diets in adipose. In the lower half of Table 2.2 the pathways that were significantly affected across at least two diet combinations are shown. For example, in the muscle tissue, the circadian rhythm pathway (KEGG rno 04710) was significantly affected between all three diets, where as adipocytokine signaling (rno00020) was only affected in the diet combinations in which AMF was compared. Similar to the fatty acid data of the selected tissues, there were fewer pathways affected in the muscle and adipose tissue compared with the liver. A striking feature of the pathway analysis shown in the bottom half of Table 2.2 is that only 3 pathways were different in the liver between the two milk fat diets, whereas > 10 were affected when these diets were compared with the CO diet.

Although the two milk fat diets were nearly identical at the fatty acid level, there were several differences in the liver and plasma lipid profiles of the rats fed the AMF and AMF-MFGM diets. Therefore, the expression of several genes of interest was determined using RT-PCR and the results are shown in Table 2.3. The three genes

selected were chosen from the KEGG (Kyoto Encyclopedia of Genes and Genomes) pathways differentially affected by the milk fat diets in Table 2.2. The results of the RT-PCR in Table 2.3 are expressed relative to actin, beta, and thus a smaller number indicates a higher expression level. Comparing the two milk fat groups, all three genes are more highly expressed in the livers of the AMF-MFGM rats compared with the AMF group.

### **Liver fat analysis by histology and DGAT assay**

In general, both the lipid analysis and the gene expression profiling indicated the diets had the greatest effect on the liver. Although there was not a quantitative difference in the total lipid content of the livers, there were significant differences in distributions across lipid classes (Figure 2.7). For example, there is more triglyceride in the livers of rats fed AMF compared with the CO, yet the total fatty acid was not different. Interestingly, expression of diglyceride O-acyltransferase 2 (DGAT2), was lower in the CO fed animals than in the other two groups. Consequently, the livers were stained with Oil Red O (Figure 2.8) and DGAT activity was measured via enzymatic assay of the microsomal fraction, and the results are shown in Figure 2.9. There was significantly less staining of the hepatic tissue of the CO fed mice (Figure 2.9a), and this corresponded with lower DGAT activity (Figure 2.9b).

### **Discussion**

The main focus of this work was to utilize tissue fatty acid profiling and transcriptomics to determine the effects of changing the lipid source of the AIN-76A diet on lipid metabolism. This work was conducted on key tissues involved in lipid

metabolism, storage and processing (skeletal muscle, visceral adipose and liver) as well as plasma. The fat sources used in formulating the diets (corn oil, anhydrous milk fat and anhydrous milk fat supplemented with milk fat globule membrane) were originally selected for an ACF study previously reported (10). In that study, as in most ACF studies, the CO diet was selected as a control, whereas the AMF-MFGM diet was included to determine potential cancer protective effects of specific lipids associated with this material, such as sphingomyelin and plasmalogens. The AMF diet was included to control for the potential that other lipids in milk fat might affect the development of ACF, such as butyrate and conjugated linoleic acid. While it was expected that fat sources like CO and AMF that vary widely in fatty acid composition would affect both lipid partitioning between tissues as well as gene expression, it was unclear what effect the inclusion of polar lipids would have between the two milk fat based diets as they are so similar at the fatty acid level.

The membrane composition of RBCs reflects dietary fat sources, and several groups have investigated the correlation of RBC fatty acid profiles with disease susceptibility in humans. For example, Harris and Von Schacky have shown that the omega-3 index, the combined percentage of EPA (20:5n-3) and DHA (22:6n-3) in RBCs, correlates in humans with risk of coronary heart disease (CHD) with values above 8% being associated with the most protection and values below 4% with the least (26). A similar metric, the percent contribution of omega-6 fatty acids to highly unsaturated fatty acids (HUFA,  $\geq 20$  carbons and  $\geq 3$  double bonds), %n6 HUFA, was shown by Lands to correlate with CHD mortality in several human populations with levels below 40% being

protective (27). The omega-3 indices were 0.9 for the CO diet, 2.5 for the AMF diet and 2.0 for the AMF-MFGM diet, while the % n-6 HUFA levels were 96%, 79% and 83%, respectively. While these metrics may not be applicable in rodents, it is interesting nonetheless that all three diets result in very low levels of n-3 long chain PUFA in RBCs which likely affect many physiological processes.

One interesting fatty acid which is present at significant levels in the RBCs, muscle, adipose and liver of the milk fat fed animals, but not those consuming CO is 20:3n-9. This fatty acid is an elongation product of oleic acid and has been shown to be a sensitive marker of PUFA intake. According to Lands, 20:3n-9 correlates with low PUFA intakes and a value of approximately 10% in the HUFA indicates PUFA insufficiency (27). To our knowledge, no studies have provided data on the % contribution of 20:3n-9 to tissue HUFA for RBCs, muscle, adipose and liver which are shown in Table 2.4. Animals fed the AMF diet have the highest levels of this fatty acid across all tissues measured, while those consuming the AMF-MFGM diets also had high levels. Interestingly, the HUFA percentage of 20:3n-9 in adipose was high for the CO fed animals, albeit not as high as the other groups. This may be a result of the very low concentration of HUFA in adipose, as the lipids in this tissue are primarily less than 18 carbons in length.

The lipid profiles of the RBCs, muscle, adipose and liver reflect the fat sources of the three diets, and there were few differences between those fed the AMF and AMF-MFGM. However, there were quantitative differences across lipid classes in both plasma and the liver. Pathway analysis of the gene expression data indicated that a fewer number of

pathways was affected in skeletal muscle than in liver. There were no differences in total liver fatty acids between treatments, but there was in the distribution of fatty acid across lipid classes (Figure 2.7). One striking feature is the high FFA and low TG in the livers of the CO fed rats compared with those fed the AMF-MFGM diet. To further investigate this finding we compared oil red O staining in livers across the three treatments, and the results are shown in Figure 2.9a. In the rats fed the CO diets there is less oil red O staining. According to O'Rourke et al., oil red O staining of tissues is well correlated with triglyceride content (28). The inverse relationship between the hepatic TG and FFA suggests the differences may be due to triglyceride synthesis activity. According to the gene expression profiling, DGAT2, the enzyme responsible for the final step in TG synthesis from diglycerides and FFA was 1.25 fold lower in the CO fed rats compared with those fed AMF and 1.46 fold lower compared with those fed AMF-MFGM. These differences are modest, and it was not clear if their expression would translate into physiological differences. Thus, the triglyceride synthetic activity in liver microsomal fractions was measured using a functional assay and the results are shown in Figure 2.9b. In agreement with the oil red O staining, the DG activity measure suggests the differences in FFA, DG and TG levels in the liver may be partially explained by the conversion of FFA and DG into TG.

While excess hepatic TG storage has typically been viewed as a negative physiological response, it may be protective under some metabolic situations. For example, in a mouse model of nonalcoholic steatohepatitis (NASH), Yamaguchi et al. evaluated the effects of hepatic DGAT2 expression on disease development using an

antisense nucleotide treatment (29). While reducing expression of DGAT2 did prevent hepatic steatosis, the increase in FFA was associated with markers of lipid peroxidation/oxidant stress and fibrosis. From this study the authors concluded that accumulation of hepatic TG is actually protective against progressive liver damage in NAFLD. It is unclear why the CO diet resulted in lower DGAT expression and activity in the CO fed rats. However, one distinguishing feature of this diet is the PUFA content primarily in the form of linoleic acid. Interestingly, reviewing the fatty acid composition of diets used to study NASH, Romestaing et al. drew the conclusion that dietary PUFA with a high omega-6 to omega-3 ratio may be a causative factor via effects on lipid peroxidation and proinflammatory cytokine production (30).

There are several differences in the plasma and hepatic lipid profiles of the animals fed the two milk fat diets, which is surprising considering the similarity of these diets at the fatty acid level. According to the KEGG pathway analysis conducted on the hepatic gene expression and shown in Table 2.2, the two milk fat diets affected PPAR signaling (rno03320), C21 steroid hormone metabolism (rno00140) and glycerophospholipid metabolism (rno00564). The affected PPAR signaling in both the liver and skeletal muscle were through PPAR $\alpha$  receptor. The involved genes were associated with lipogenesis, cholesterol metabolism and fatty acid transport in the liver and with lipogenesis in skeletal muscle. Consequently, the expression of three genes from these pathways was validated using RT-PCR. The genes *Cyp8b1*, *Agpat2* and *Angptl4* were selected from the differentially expressed genes in the pathways determined by the gene expression profiling. They were chosen due to their physiological function and potential

to affect tissue lipid partitioning, and the results are shown in Table 2.3. The function of these genes is discussed below including their potential roles in affecting lipid metabolism across the two milk fat groups. Of course these findings are only correlations and positive confirmation of their roles will need to be tested explicitly for confirmation.

*Cyp8b1* is a cytochrome P450 enzyme which is a component of the primary bile acid biosynthesis and PPAR $\alpha$  signaling pathways in the liver. It is involved in the synthesis of cholic acid (31). *Cyp8b1* controls the ratio of cholic acid to chenodeoxycholic acid in bile salts, and as cholic acid is less effective in solubilizing cholesterol it may affect its absorption (32). The AMF-MFGM diet was associated with a lower hepatic cholesteryl ester content (Figure 2.7). Milk polar lipids affect both the absorption and fecal excretion of cholesterol when fed both acutely and chronically. For example, Noh and Koo found that infusion of milk sphingomyelin via a duodenal catheter resulted in decreased cholesterol, fat and vitamin E absorption (33). In a chronic feeding study Kamili et al. fed mice high fat diets for 5 weeks which were supplemented with two different formulation of milk phospholipids at 1.2% by weight (34). Both milk polar lipid preparations resulted in significant decreases in liver cholesterol and triglyceride which was accompanied by an increase in fecal cholesterol excretion. Data from the present study indicates that the decreased cholesterol absorption and increased fecal excretion resulting from luminal milk polar lipids in those previous studies may be mediated, at least in part, by the ratio of bile acids.



*Agpat2* is an enzyme responsible for the conversion of lysophosphatidic acid to phosphatidic acid, a step in PL synthesis and is a component of KEGG pathway glycerophospholipid metabolism. The expression of *Agpat2* was higher in the AMF-MFGM group than the AMF group (Table 2.3) but there was not a significant difference in hepatic PL. There was, on the other hand, a significant increase in plasma PL in the AMF-MFGM. The increased plasma PL may result from increased hepatic synthesis and secretion. Previous studies with milk polar lipids have also shown the ability of these constituents to increase both plasma PL and TG. For example, Wat et al. (35) fed mice both a low fat, non purified diet and a high fat diet formulated with and without a 2.5% PL-rich milk fat extract. In the mice fed the low fat, non purified diet, the milk PL increased the plasma TG by 20% and the plasma PL by 5% over the control mice fed the low fat diet. However, in the mice fed the high fat diets, the PL-rich extract actually reduced both the plasma TG and PL to levels similar to the low fat control. The increased plasma lipid concentration in the rats fed the AMF-MFGM diet, compared with those fed the AMF diet may be a result of either more lipid exported from the liver, or from reduced clearance via peripheral tissues.

Expression of *Angptl4* was also verified by RT-PCR. *Angptl4* is a component of the PPAR $\alpha$  signaling pathway. It is an angiopoietin-like protein which increases plasma TG via suppression of lipoprotein lipase (36). Interestingly, there were significant differences in plasma TG between the two milk fat fed groups (Figure 2.7). Also known as fasting induced adipocyte factor (Fiaf), *Angptl4* is highly expressed in the gut epithelium in germ-free mice and prevents accumulation of fat into adipocytes, whereas

conventionalization with a microflora suppresses this effect (37). Although it is not clear if hepatic expression of *Angptl4* in the AMF-MFGM fed rats contributed to the increase in plasma TG, this finding indicates a potential mechanism via which this effect was mediated.

Despite the fact that it is still commonly used in ACF studies with rodents (7), the high sucrose content of the AIN-76A diet has been long known to cause fatty liver in animals fed the diet for long periods of time (9). Therefore, when reviewing the different effects of the fat sources on tissue lipid composition and gene expression it is necessary to keep in mind these changes are in the context of an overall metabolically stressful diet. From the data presented here, a few hypotheses may be drawn that can be tested in studies designed specifically for their evaluation. For example, compared with the milk fat diets, the CO diet caused a significant increase in hepatic free fatty acids, a potential trigger for the development of NASH from NAFLD. It may be hypothesized that high dietary n6 PUFA facilitates the development of NASH from NAFLD by increasing hepatic free fatty acids. Conversely, compared with the CO and AMF-MFGM diets, the AMF diet resulted in more hepatic TG storage which in itself may be undesirable. It may be hypothesized that dietary saturated fatty acids increases hepatic TG and facilitate the development of hepatic steatosis. Supplementing the AMF diet with polar lipids from milk appears to reduce the accumulation of hepatic TG yet appears to achieve this effect via promotion of lipid export into plasma. The long term physiological significance of this is unknown. It may be hypothesized that dietary polar lipids increase hepatic TG export into the circulation to be stored in adipose tissue and to be utilized by the muscle.

In conclusion, the fat source of the AIN-76A diet affects the tissue profile of key tissues involved in lipid trafficking and storage as well as gene expression networks within these tissues.

## References

1. Reeves PG, Nielsen FH, Fahey GC, Jr. AIN-93 purified diets for laboratory rodents: final report of the American Institute of Nutrition ad hoc writing committee on the reformulation of the AIN-76A rodent diet. *J Nutr* 1993;123:1939-51.
2. Roebuck BD, Wilpone SA, Fifield DS, Yager JD, Jr. Hemorrhagic deaths with AIN-76 diet. *J Nutr* 1979;109:924-5.
3. Nguyen HT, Woodard JC. Intranephronic calculosis in rats: an ultrastructural study. *Am J Pathol* 1980;100:39-56.
4. Medinsky MA, Popp JA, Hamm TE, Dent JG. Development of hepatic lesions in male Fischer-344 rats fed AIN-76A purified diet. *Toxicol Appl Pharmacol* 1982;62:111-20.
5. Nutrition AIO. Second report of the ad hoc committee on standards for nutritional studies. *J Nutr* 1980;110:1726.
6. Council NR. *Nutrient Requirements of Laboratory Animals*, Fourth Revised Edition. National Academy Press: Washington, D.C., 1995.
7. Corpet DE, Tache S. Most effective colon cancer chemopreventive agents in rats: a systematic review of aberrant crypt foci and tumor data, ranked by potency. *Nutr Cancer* 2002;43:1-21.

8. Targher G, Day CP, Bonora E. Risk of cardiovascular disease in patients with nonalcoholic fatty liver disease. *N Engl J Med* 2010;363:1341-50.
9. Bacon BR, Park CH, Fowell EM, McLaren CE. Hepatic steatosis in rats fed diets with varying concentrations of sucrose. *Fundam Appl Toxicol* 1984;4:819-26.
10. Snow DR, Jimenez-Flores R, Ward RE, et al. Dietary milk fat globule membrane reduces the incidence of aberrant crypt foci in Fischer-344 rats. *J Agric Food Chem* 2010;58:2157-63.
11. Jensen RG. *Handbook of Milk Composition*. Academic Press: San Diego, 1995.
12. Mcpherson AV, Dash MC, Kitchen BJ. Isolation of bovine-milk fat globule-membrane material from cream without prior removal of caseins and whey proteins. *J Dairy Res* 1984;51:113-21.
13. MacGibbon A, Taylor M. Composition and structure of bovine milk lipids (p.1-42). In: Fox PF, McSweeney PLH, (eds). *Advanced Dairy Chemistry Lipids*. Springer: New York, NY, USA: 2006.
14. Spitsberg VL. Invited Review: Bovine milk fat globule membrane as a potential nutraceutical. *J Dairy Sci* 2005;88:2289-94.
15. Folch J, Lees M, Sloane Stanley GH. A simple method for the isolation and purification of total lipides from animal tissues. *J Biol Chem* 1957;226:497-509.
16. Curtis JM, Berrigan N, Dauphinee P. The determination of n-3 fatty acid levels in food products containing microencapsulated fish oil using the one-step extraction method. Part 1: Measurement in the raw ingredient and in dry powdered foods. *J Am Oil Chem Soc* 2008;85:297-305.

17. FlexArray: A statistical data analysis software for gene expression microarrays. <http://genomequebec.mcgill.ca/FlexArray> (2012).
18. Long AD, Mangalam HJ, Chan BY, Toller L, Hatfield GW, Baldi P. Improved statistical inference from DNA microarray data using analysis of variance and a Bayesian statistical framework. Analysis of global gene expression in *Escherichia coli* K12. *J Biol Chem* 2001;276:19937-44.
19. Hochberg Y, Benjamini Y. More powerful procedures for multiple significance testing. *Stat Med* 1990;9:811-8.
20. Tong W, Cao X, Harris S, et al. ArrayTrack--supporting toxicogenomic research at the U.S. Food and Drug Administration National Center for Toxicological Research. *Environ Health Perspect* 2003;111:1819-26.
21. Lopez-Parra M, Titos E, Horrillo R, et al. Regulatory effects of arachidonate 5-lipoxygenase on hepatic microsomal TG transfer protein activity and VLDL-triglyceride and apoB secretion in obese mice. *J Lipid Res* 2008;49:2513-23.
22. Abramoff MD, Magalhaes PJ, Ram SJ. Image processing with image j. *Biophotonics International* 2004;11:36-42.
23. Ko JS, Ryu SY, Kim YS, et al. Inhibitory activity of diacylglycerol acyltransferase by tanshinones from the root of *Salvia miltiorrhiza*. *Arch Pharm Res* 2002;25:446-8.
24. Coleman RA. Diacylglycerol acyltransferase and monoacylglycerol acyltransferase from liver and intestine. *Methods Enzymol* 1992;209:98-104.
25. McFie PJ, Stone SJ. A fluorescent assay to quantitatively measure in vitro acyl CoA:diacylglycerol acyltransferase activity. *J Lipid Res* 2011;52:1760-4.

26. Harris WS, Von Schacky C. The Omega-3 Index: a new risk factor for death from coronary heart disease? *Prev Med* 2004;39:212-20.
27. Lands B. A critique of paradoxes in current advice on dietary lipids. *Prog Lipid Res* 2008;47:77-106.
28. O'Rourke EJ, Soukas AA, Carr CE, Ruvkun G. C. elegans major fats are stored in vesicles distinct from lysosome-related organelles. *Cell Metabolism* 2009;10:430-5.
29. Yamaguchi K, Yang L, McCall S, et al. Inhibiting triglyceride synthesis improves hepatic steatosis but exacerbates liver damage and fibrosis in obese mice with nonalcoholic steatohepatitis. *Hepatology* 2007;45:1366-74.
30. Romestaing C, Piquet MA, Bedu E, et al. Long term highly saturated fat diet does not induce NASH in Wistar rats. *Nutr Metab (Lond)* 2007;4:4.
31. Li-Hawkins J, Gafvels M, Olin M, et al. Cholic acid mediates negative feedback regulation of bile acid synthesis in mice. *J Clin Invest* 2002;110:1191-200.
32. Gafvels M, Olin M, Chowdhary BP, et al. Structure and chromosomal assignment of the sterol 12alpha-hydroxylase gene (CYP8B1) in human and mouse: eukaryotic cytochrome P-450 gene devoid of introns. *Genomics* 1999;56:184-96.
33. Noh SK, Koo SI. Milk sphingomyelin is more effective than egg sphingomyelin in inhibiting intestinal absorption of cholesterol and fat in rats. *J Nutr* 2004;134:2611-6.
34. Kamili A, Wat E, Chung RW, et al. Hepatic accumulation of intestinal cholesterol is decreased and fecal cholesterol excretion is increased in mice fed a high-fat diet supplemented with milk phospholipids. *Nutr Metab (Lond)* 2010;7:90.

35. Wat E, Tandy S, Kapera E, et al. Dietary phospholipid-rich dairy milk extract reduces hepatomegaly, hepatic steatosis and hyperlipidemia in mice fed a high-fat diet. *Atherosclerosis* 2009;205:144-50.
36. Kersten S. Regulation of lipid metabolism via angiopoietin-like proteins. *Biochem Soc Trans* 2005;33:1059-62.
37. Backhed F, Ding H, Wang T, et al. The gut microbiota as an environmental factor that regulates fat storage. *Proc Natl Acad Sci U S A* 2004;101:15718-23.

**Table 2.1** Composition of dietary treatments.

	CO <sup>a</sup>	AMF <sup>a</sup>	AMF-MFGM <sup>a</sup>
Protein (g/kg diet)			
casein	183	183	183
whey	17	17	17
$\alpha$ -methionine	3	3	3
Carbohydrate <sup>b</sup> (g/kg diet)			
sucrose	495	495	495
lactose	5	5	5
cornstarch	150	150	150
cellulose	50	50	50
Fat (g/kg diet)			
corn oil (control)	50		
AMF		50	25
MFGM isolate <sup>c</sup>			25
Vitamins and Minerals <sup>d</sup> (mg/kg diet)			
vitamin mix	10000	10000	10000
Zn	30	30	30 (12.6) <sup>e</sup>
Mg	507	507	507 (24.6) <sup>e</sup>
Ca	5000	5000	5000 (88) <sup>e</sup>
P	1561	1561	1561 (14.5) <sup>e</sup>
Cu	6	6	6 (2.5) <sup>e</sup>
choline bitartrate	2000	2000	2000
Sphingolipid Content (% by Weight)			
total phospholipids	0.9%	0.09%	0.53%
sphingomyelin	0.03%	0.03%	0.11%

<sup>a</sup>Diets were prepared by Dyets.com. <sup>b</sup>Four grams of lactose was added to the control and AMF diets to balance lactose in MFGM isolate. <sup>c</sup>MFGM isolate is 68% protein, 20% fat, 4% ash, and 4% lactose. The casein to whey ratio is 80:20. The triglyceride to polar lipid ratio is 3:1. <sup>d</sup>Mineral composition of MFGM isolate was determined by ICP-AAS. Minerals were adjusted in AMF-MFGM diet accordingly. <sup>e</sup>Amount derived from MFGM portion of the diet in parentheses (mg/kg diet).



**Table 2.2** Metabolic pathways significantly affected across all three diet combinations (CO = corn oil; AMF = anhydrous milk fat; AMF-MFGM = anhydrous milk fat-milk fat globule membrane; KEGG = Kyoto Encyclopedia of Genes and Genomes).

Tissue	Diets			All
	<i>AMF vs. CO</i>	<i>AMF-MFGM vs. CO</i>	<i>AMF-MFGM vs. AMF</i>	
Number of pathways affected				
<b>Muscle</b>	2	11	5	<b>18</b>
<b>Adipose</b>	9	16	6	<b>31</b>
<b>Liver</b>	16	13	11	<b>40</b>
<b>All</b>	<b>27</b>	<b>40</b>	<b>22</b>	

KEGG Pathway	<i>AMF</i>	<i>AMF-MFGM</i>	<i>AMF-MFGM</i>
	<i>vs. CO</i>	<i>vs. CO</i>	<i>vs. AMF</i>
<b>Muscle</b> Circadian rhythm (mo04710)	√	√	√
PPAR signaling (mo03320)	√		√
Adipocytokine signaling (mo04920)		√	√
<b>Adipose</b> Circadian rhythm (mo04710)	√	√	√
Endocytosis (mo04710)	√	√	√
Butanoate metabolism (mo00650)	√	√	√
Citrate cycle (TCA cycle) (mo00020)	√	√	
<b>Liver</b> PPAR signaling (mo03320)	√	√	√
C21 Steroid hormone metabolism (mo00140)	√	√	√
Biosynthesis of unsaturated fatty acids (mo01040)	√	√	
Retinol metabolism (mo00830)	√	√	
Starch and sucrose metabolism (mo00500)	√	√	
Pyruvate metabolism (mo00620)	√	√	
Galactose metabolism (mo00052)	√	√	
Insulin signaling pathway (mo04910)	√	√	
Maturity onset diabetes of the young (mo04950)	√	√	
Androgen and estrogen metabolism (mo00150)	√	√	
Glycerophospholipid metabolism (mo00564)		√	√

**Table 2.3** Differentially expressed genes by ANOVA in liver from rats fed with diet containing corn oil (control), anhydrous milk fat (AMF) and milk fat globule membrane (AMF-MFGM) (unit:  $\Delta\Delta Ct$ ).

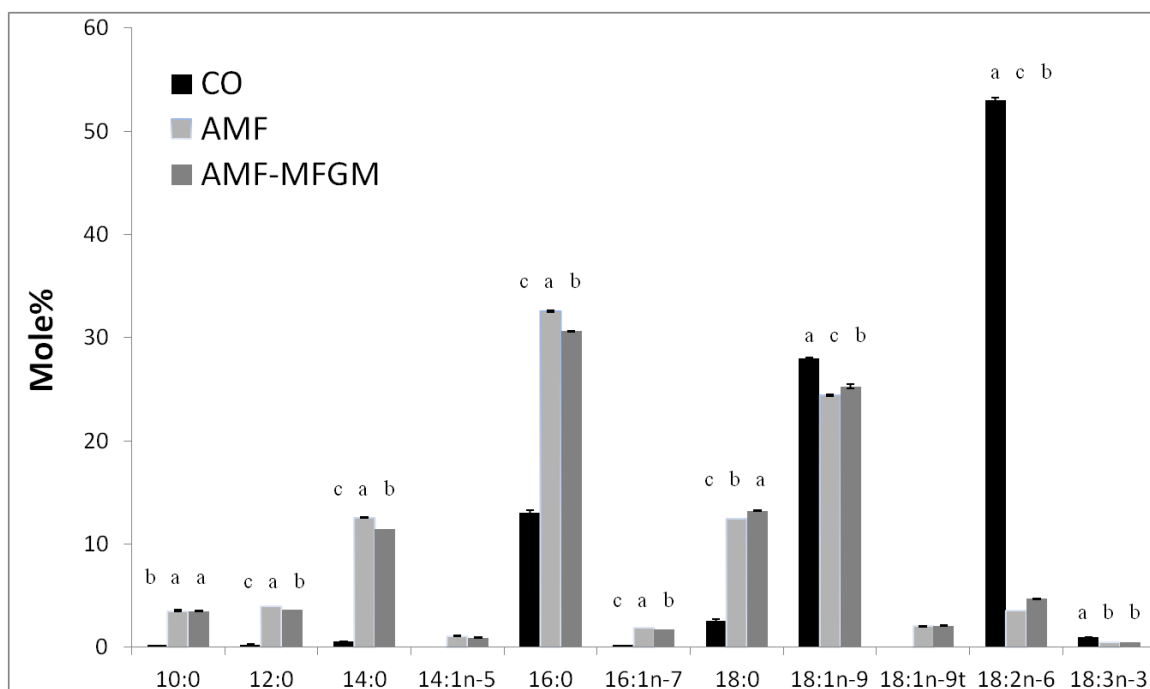
Genes	CO	AMF	MFGM
<i>Cyp8b1</i>	-0.94±0.26 <sup>b</sup>	-0.10±0.16 <sup>a</sup>	-2.49±0.41 <sup>c</sup>
<i>Agpat2</i>	1.93±1.03 <sup>ab</sup>	2.82±0.42 <sup>a</sup>	1.14±0.48 <sup>b</sup>
<i>Angptl4</i>	2.90±0.93 <sup>b</sup>	4.19±0.26 <sup>a</sup>	2.34±0.67 <sup>b</sup>

<sup>a, b, c</sup> Means in a row with different superscripts are significantly different ( $p < 0.05$ ). The data represent mean  $\pm$  SEM (n = 4, 3, 4 for CO, AMF, AMF-MFGM).

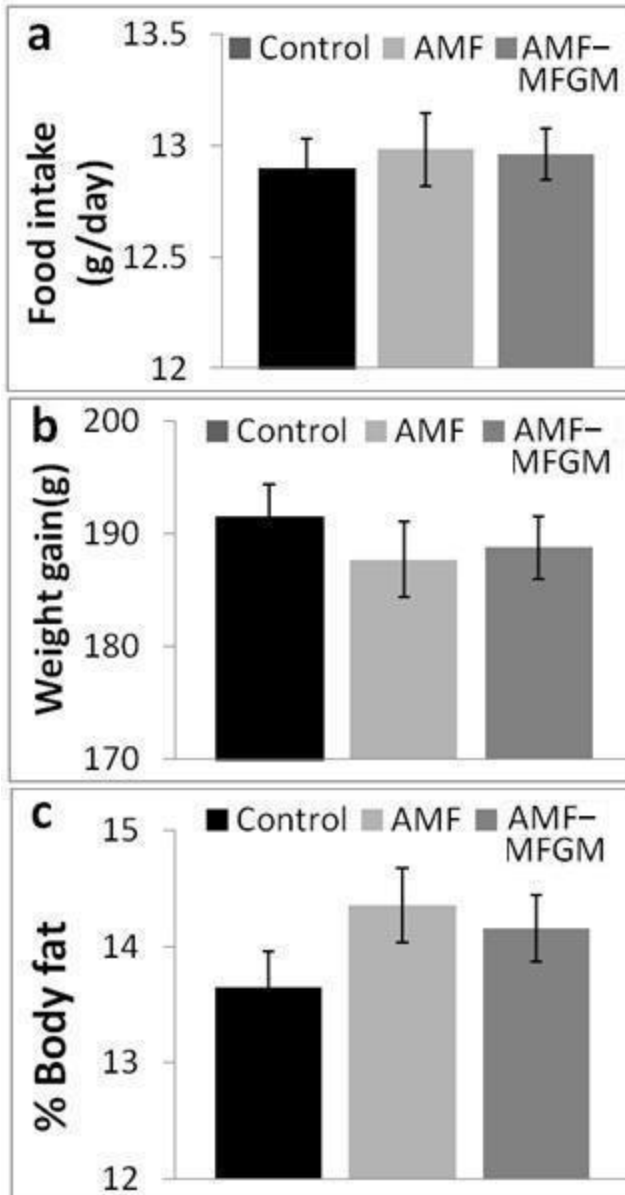
**Table 2.4** %20:3n-9 in highly unsaturated fatty acids (HUFA) in RBCs, skeletal muscle, adipose, and liver as a function of diet.

%20:3n-9 in HUFA	CO	AMF	AMF-MFGM
RBCs	ND <sup>b</sup>	11.05±0.15 <sup>a</sup>	8.60±1.39 <sup>a</sup>
Muscle	0.51±0.05 <sup>c</sup>	20.01±0.26 <sup>a</sup>	12.44±0.16 <sup>b</sup>
Adipose	7.92±0.24 <sup>c</sup>	43.08±1.37 <sup>a</sup>	31.40±0.21 <sup>b</sup>
Liver	0.53±0.02 <sup>c</sup>	15.65±0.84 <sup>a</sup>	8.64±0.49 <sup>b</sup>

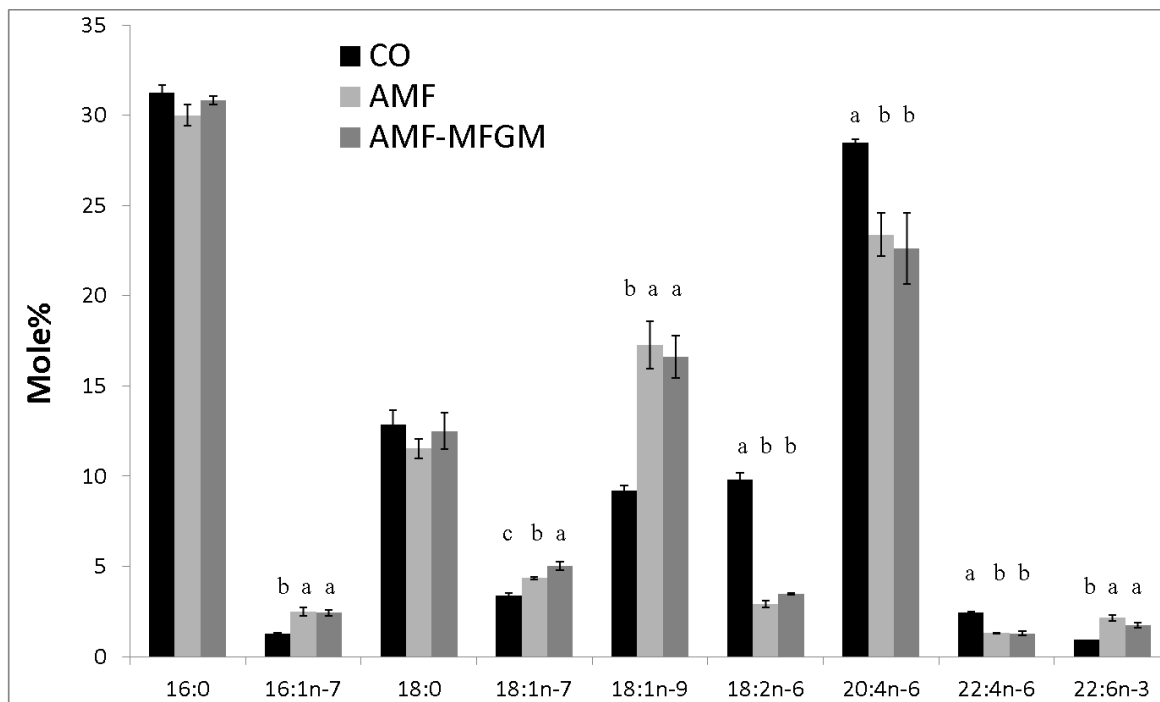
<sup>a, b, c</sup> Means in a row with different superscripts are significantly different ( $p < 0.05$ ), ND = not detected. The data represent mean  $\pm$  SEM (n = 3).



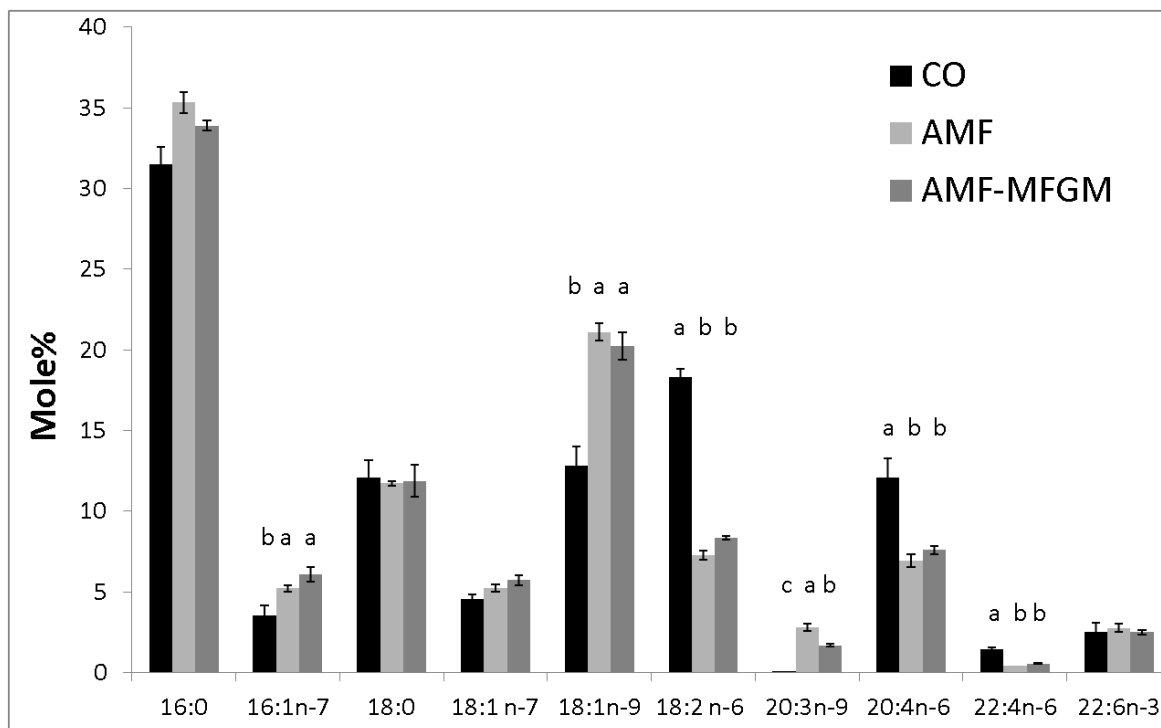
**Figure 2.1** Fatty acid profile of experimental diets. Only fatty acids present at > 1% of total fatty acids are shown. The data represent mean  $\pm$  SEM ( $n = 2$ ). Means in a row with different superscripts are significantly different ( $p < 0.05$ ).



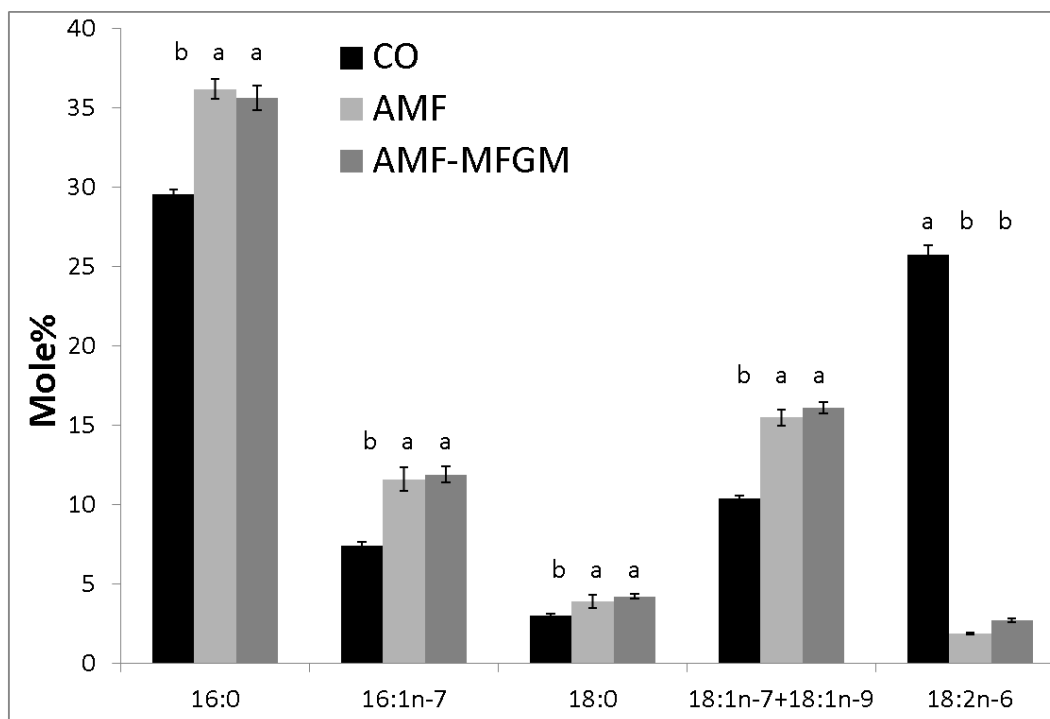
**Figure 2.2** Effect of experimental diets on food intake (a), total weight gain (b) and body fat composition (c). Values are mean  $\pm$  SEM (n = 17, 16, 16 for CO, AMF, AMF-MFGM). Experimental diets did not significantly affect consumption, weight gain or body fat percentage.



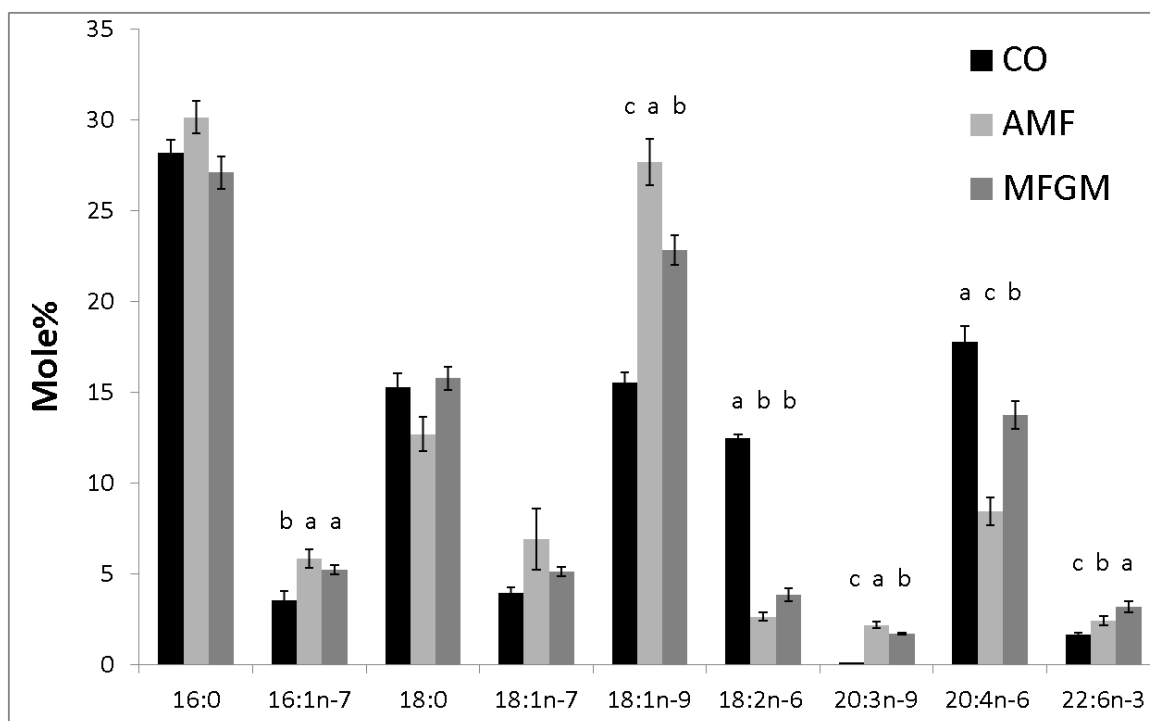
**Figure 2.3** Red blood cell (RBC) fatty acids from rats fed CO (corn oil), AMF (anhydrous milk fat) and AMF-MFGM (anhydrous milk fat-milk fat globule membrane). The data represent mean  $\pm$  SEM ( $n = 3$ ). Only fatty acids present at greater than 1% of total fatty acids are shown. Means in a row with different superscripts are significantly different ( $p < 0.05$ ).



**Figure 2.4** Fatty acid profile of skeletal muscle from rats fed CO (corn oil), AMF (anhydrous milk fat) and AMF-MFGM (anhydrous milk fat-milk fat globule membrane). The data represent mean  $\pm$  SEM ( $n = 3$ ). Only fatty acids present at greater than 1% of total fatty acids are shown. Means in a row with different superscripts are significantly different ( $p < 0.05$ ).

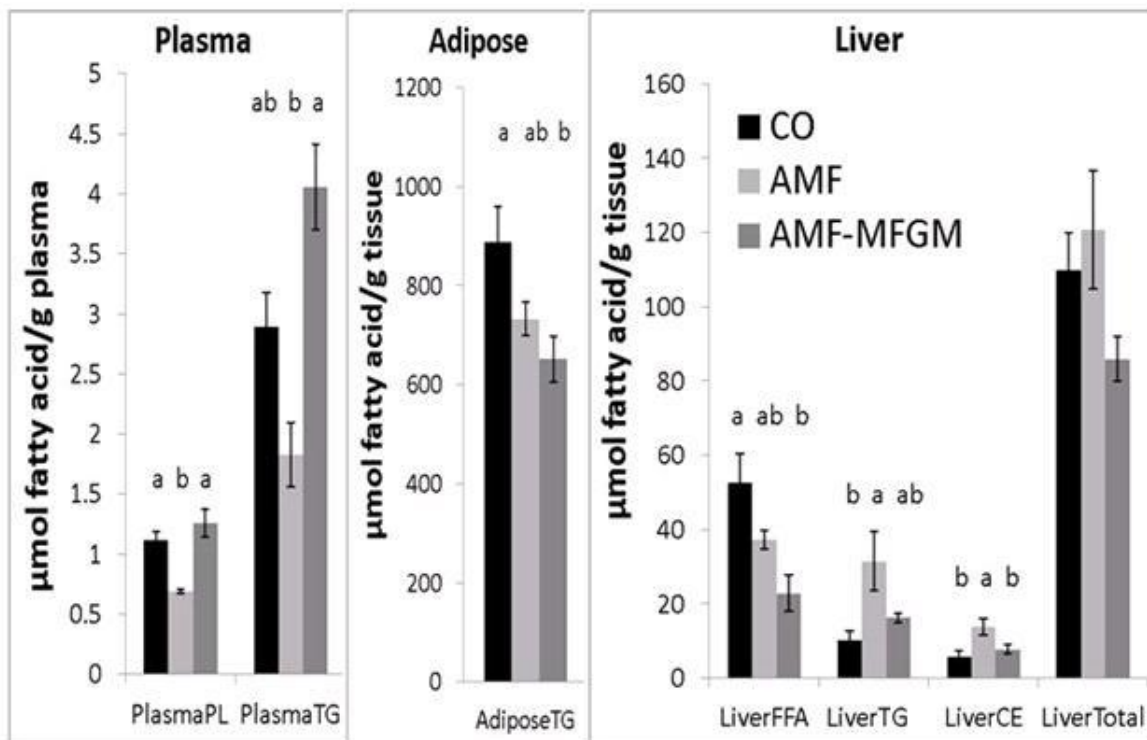


**Figure 2.5** Fatty acid profile of visceral adipose tissue from rats fed CO (corn oil), AMF (anhydrous milk fat) and AMF-MFGM (anhydrous milk fat-milk fat globule membrane). The data represent mean  $\pm$  SEM ( $n = 3$ ). Only fatty acids present at greater than 1% of total fatty acids are shown. Means in a row with different superscripts are significantly different ( $p < 0.05$ ).

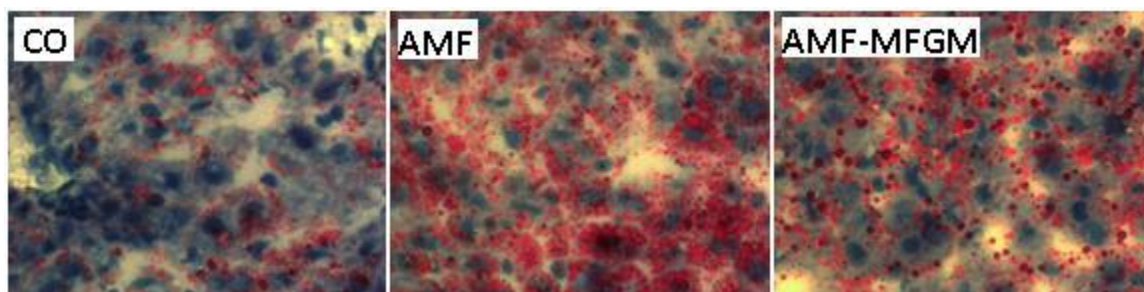


**Figure 2.6** Fatty acid profile of liver tissue from rats fed CO (corn oil), AMF (anhydrous milk fat) and AMF-MFGM (anhydrous milk fat-milk fat globule membrane). The data represent mean  $\pm$  SEM ( $n = 4$ ). Only fatty acids present at greater than 1% of total fatty acids are shown. Means in a row with different superscripts are significantly different ( $p < 0.05$ ).

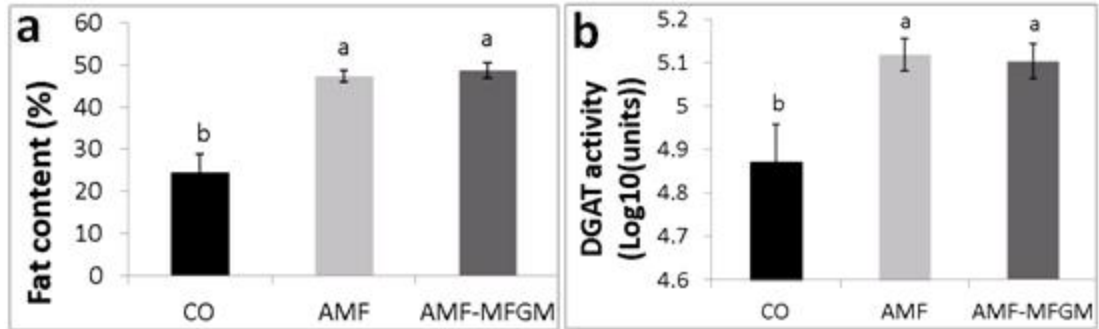




**Figure 2.7** Quantitation of lipid classes from plasma, visceral adipose and liver. PL = phospholipids, TG = triglycerides, FFA = free fatty acids, CE = Cholesteryl esters. The data represent mean  $\pm$  SEM ( $n = 3$  for plasma and adipose,  $n = 4$  for liver). Means in a row with different superscripts are significantly different ( $p < 0.05$ ).



**Figure 2.8** Liver histological slides (light microscope, 18x) by Oil Red O Staining from rats fed CO (corn oil), AMF (anhydrous milk fat) and AMF-MFGM (anhydrous milk fat-milk fat globule membrane).



**Figure 2.9** Hepatic Oil Red O Staining (A) and hepatic DGAT activity (B) in liver tissue from rats fed CO (corn oil), AMF (anhydrous milk fat) and AMF-MFGM (anhydrous milk fat-milk fat globule membrane). The data represent mean  $\pm$  SEM (n = 4, 3, 4 for CO, AMF, AMF-MFGM). Means with different superscripts are significantly different ( $p < 0.05$ ).

**CHAPTER 3**

**DIETARY MILK POLAR LIPIDS AFFECT LIPID METABOLISM, GUT  
PERMEABILITY AND SYSTEMIC INFLAMMATION IN C57BL/6J OB/OB  
MICE**

**Abstract**

Dynamic interactions between lipid metabolism, gut permeability and systemic inflammation remain unclear in the context of obesity. One objective of this study was to explore the dynamic changes of gut permeability, inflammation and lipid metabolism in genetic obesity. Another objective was to test the hypotheses that milk polar lipids will reduce gut permeability, systemic inflammation and liver lipid levels, and affect the expression of genes associated with fatty acid synthesis and cholesterol regulation in the liver in preexisting obesity. Three groups of C57BL/6J ob/ob mice were fed moderately high fat diets for 2 weeks: 1) modified AIN-93G diet (CO) with 34% fat by energy; 2) CO with milk gangliosides (GG); 3) CO with milk phospholipids (PL). The GG and the PL did not affect the total food intake, weight gain or fasting glucose. The PL led to smaller livers and mesenteric fat depots compared with the CO. No difference was found in the gut permeability. Dietary polar lipids did not enrich the polar lipids content in the intestinal mucosa. The GG increased the expression of the tight junction protein occludin in the colon mucosa compared with the CO. The GG and the PL decreased the expression of the tight junction protein ZO-1 in the jejunum mucosa compared with the CO. The moderately high fat diet feeding increased the plasma endotoxin level, which was not affected by the dietary polar lipids. The PL increased the IL-6 level in the plasma and the sphingomyelin levels in the plasma and the liver compared with the CO and the GG. The

increase of the plasma IL-6 level was positively correlated with the sphingomyelin increase in the plasma and the liver. The PL and the GG decreased the PI level in the liver and the skeletal muscle. Hepatic expression of 13 genes involved in lipid metabolism was assessed by RT-qPCR. The GG and the PL differentially regulated the genes associated with fatty acid and cholesterol metabolism. In conclusion, dietary supplementation of milk polar lipids may affect lipid metabolism and have unfavorable effects on systemic inflammation in genetic obesity.

## **Introduction**

Obesity is usually defined as a condition with excessive body fat that has an adverse effect on health (1). The pathological states associated with obesity include many comorbidities, such as type 2 diabetes, cardiovascular disease, leaky gut, dyslipidemia, non-alcoholic fatty liver disease (NAFLD) and systemic inflammation (2-4). The increased intestinal permeability has been observed in obese animals (5) and humans (2). Leptin-deficient C57BL/6J ob/ob (ob/ob) mice have more surface area and mass of their intestinal mucosa for nutrient absorption in proportion to the metabolic mass (6). This increased surface area is caused by the intestinal hyperplasia (7) and the associated inappropriate increase and distribution of the tight junction (TJ) proteins leads to the decrease in the barrier integrity (6). Ob/ob mice also have portal (8) and plasma endotoxemia, the presence of lipopolysaccharide (LPS) in the blood (9). LPS can activate the toll-like receptor 4 (TLR4) and initiate inflammation in various tissues (10). The systemic inflammatory state in obesity is associated with endotoxemia resulting from increased gut barrier permeability in obese animals (5) and humans (2).

In obese subjects, the high levels of inflammatory cytokines may alter structure and localization of the TJ to cause malfunction of the intestinal barrier (11). The adipose tissue contains adipocytes, fibroblasts, leukocytes, and macrophages. These cells may jointly produce proinflammatory cytokines, such as tumor necrosis factor- $\alpha$  (TNF- $\alpha$ ) and interleukin-6 (IL-6) (12). Adipocytes are also targets of the proinflammatory signals such as TNF- $\alpha$  and IL-6 (13). Obesity, systemic inflammation and increased intestinal permeability may generate a self-perpetuating vicious cycle (Figure 1.1) (14). Lipid metabolism is involved with this complex cycle. The plasma long-chain saturated fatty acids (LCSFA, e.g., myristic, palmitic acids) activate the TLR4 in adipocytes and macrophages and initiate the secretion of proinflammatory cytokines such as IL-6 (10). The LCSFA may have synergistic effect with LPS on the activation of the TLR4 (10). Therefore, increased gut barrier permeability, endotoxemia, systemic inflammation, and lipid metabolism are complexly interrelated events during obesity (Figure 1.1).

The current estimates by the Centers for Disease Control is that about 1/3 Americans are obese (body mass index, BMI  $\geq$  30) and 1/3 Americans are overweight ( $25 \leq$  BMI  $<$  30). The burden of the obesity epidemic is well recognized but there are not yet very effective preventive solutions. The main effective therapy is surgery. Dietary intervention might have promising potential in fighting against obesity since the excessive food energy intake (the easily accessible and palatable diet) is one of the main causes of obesity (15, 16). Rich in nutrients, milk provides protection for the gut and enhances the immune system of the newborn (17). One fraction of milk, the polar lipids, may play important roles in biological functions such as maintaining gastrointestinal barrier

integrity and affecting systemic inflammation, and lipid metabolism. The milk polar lipids mainly come from the milk fat globule membrane (MFGM) and include phospholipids (PL) and gangliosides (GG). The most abundant milk polar lipids are phosphatidylcholine (PC), phosphatidylethanolamine (PE), sphingomyelin (SM), phosphatidylinositol (PI) and phosphatidylserine (PS) (36%, 27%, 22%, 11% and 4% respectively of total polar lipids) (18).

A milk isolate, rich in polar lipids, protects against the increase in gut permeability of fluorescein isothiocyanate-dextran (FITC-dextran) in mice stressed by the LPS (19). Dairy GG inhibits the degradation of the gut TJ protein occludin during the LPS-induced acute inflammation (20). Dietary PL reduce liver triglycerides (TG) and cholesterol in rats (21). The PL-rich MFGM extract supplemented diet reduces hepatomegaly, hepatic steatosis and hyperlipidemia and positively regulates genes associated with fatty acid synthesis and cholesterol regulation in mice fed a high-fat diet (22). The effects of the PL on liver lipid metabolism could be partially due to the choline contributed by the PC when the diets were high in sucrose, which promote the development of fatty liver disease (23). The milk sphingolipids, including SM and GG, have been shown to reduce the uptake of cholesterol (24) and the inflammatory response (25, 26). The supplementation of milk polar lipids in a high fat diet in the context of preexisting obesity may facilitate the understanding of the interrelationships among the intestinal barrier integrity, endotoxemia, systemic inflammation, lipid metabolism and obesity.

Ob/ob mice fed a standard chow diet have increased intestinal permeability (8). High fat diets decrease the gut barrier integrity and increase endotoxin absorption, which leads to the systemic inflammation independent of obesity (27). The ob/ob mice can be used as an obesity model in exploring the interrelationships among the intestinal barrier integrity, endotoxemia, systemic inflammation, lipid metabolism and obesity. This study was designed to test the hypotheses that the dietary milk polar lipids will reduce gut permeability and liver lipid levels, affect the expression of genes associated with fatty acid synthesis and cholesterol regulation in the liver, and alleviate the systemic inflammation that resulted from the preexisting obesity and may be sustained and/or exacerbated by the high fat intake.

## **Materials and Methods**

### **Diets formulation**

Diets based on the AIN-93G rodent diet were used in this study. The fat provided 34% energy (16.8% by weight). This amount of fat is considered high compared with the 16% (energy) fat in the regular mouse chow diet (LabDiet 5K52, Table 3.1). The high fat diets with 30% or more fat as energy have successfully induced obesity in the C57BL/6J mice (28). Data from the National Health and Nutrition Examination Survey (NHANES 2007-2008) indicates that the mean amount of fat consumed per individual American was 34% by energy. Thus, using diets with 34% (energy) fat emulates the real dietary practices in America. The current estimates by the Centers for Disease Control is that about 1/3 Americans are obese ( $BMI \geq 30$ ) and 1/3 Americans are overweight ( $25 \leq BMI$

< 30). So it could be common practice to have diets with 34% (energy) fat in the background of obesity.

Three diets based on the AIN-93G rodent diet were formulated (Table 3.1) so that they were identical in the macro and micro nutrient except for the fat source, which were provided by soybean oil + lard (CO diet), soybean oil + lard + milk GG (GG diet), soybean oil + lard + milk PL (PL diet), respectively. The milk polar lipids were provided as a semi-purified milk PL concentrate or a semi-purified milk GG concentrate prepared from the dried milk cream by ethanol extraction (Fonterra (USA), Inc., Rosemont, IL). The GG was supplemented at 0.2 g/kg diet, including 0.17 g of ganglioside GD3 and 0.03 g of ganglioside GM3. The GG diet also contained small amount of PC, PS, PE and SM (0.55, 0.48, 0.21 and 0.2 g/kg diet). The PL was supplemented at 10 g/kg diet, including 2.9 g of SM, 5 g of PC, 1.6 g of PE and 0.6 g of PS. The mineral contents of the diets were verified by the Utah Veterinary Diagnostic Laboratory. The fatty acid composition of the diets was analyzed by Gas Chromatography (GC) as described previously (29).

## **Animals**

Five-week-old male C57BL/6J ob/ob mice (n = 18; Jackson Laboratory) were housed singly in cages at a constant temperature of  $22 \pm 1$  °C with a 12-h light/dark cycle. They were allowed ad libitum access to diet and water. After 2 weeks feeding on chow (for the acclimatization and the baseline data collection), mice were randomly assigned to one of the following treatments: 1) CO diet (n = 6); 2) GG diet (n = 6); 3) PL diet (n = 6). The mice were fed the experimental diets for 2 weeks. The diet intake and body weight were measured every other day. The body composition was assessed at the baseline, day 4 and



day 13 by using the magnetic resonance imaging (MRI) with an EchoMRI-900 Body Composition Analyzer (EchoMRI, Houston, TX). The experiments were conducted in conformity with the Public Health Service Policy on Humane Care and Use of Laboratory Animals and were approved by the Utah State University Institutional Animal Care and Use Committee.

### **Assessments of intestinal barrier integrity**

To assess the intestinal permeability, 4000 Da FITC-dextran (Sigma-Aldrich Co. LLC, St. Louis, MO) suspended in phosphate buffered saline was gavaged and the blood samples were collected through cheek bleeding 5 h after the gavage. The plasma concentrations of FITC-dextran were determined by measuring fluorescence at 530 nm (30).

The gut permeability was also assessed by using the differential sugar absorption test (DST). Three classes of sugar probes are usually used for the DST (31). The Class 1 probes, such as sucrose (molecular weight (MW): 342.3 Da), are metabolized in the stomach and the proximal small intestine. The class 2 probes, such as lactulose (MW: 342.3 Da) and mannitol (MW: 182.2 Da), can stay in the gut before they are degraded by bacteria in the colon. The class 3 probes, such as sucralose (MW: 397.64 Da), remain intact throughout the gut. Sucrose, lactulose and sucralose have similar size and are absorbed exclusively through the paracellular route (31). As a non-metabolizable small molecule, mannitol is absorbed from the gut by passive diffusion and solvent drag and the absorption reflects the background gut permeability (32). By using the aforementioned four sugars together, information regarding site-specific gut permeability

may be obtained. The absorption of sucrose reflects the permeability of the stomach and the proximal intestine. The absorption of lactulose reflects the permeability of the small intestine. The absorption of sucralose reflects the permeability of both the small intestine and the colon. When there is no small intestinal damage as revealed by the lactulose absorption, the sucralose absorption may detect the colonic damage (31). The Sucrose/Lactulose ratio can be used to decide if the intestinal damage is more severe proximally or distally. For example, the Sucrose/Lactulose ratio increases during active celiac disease and severe malaria (33, 34).

The DST was carried out according to the method of Arrieta et al. (35). After a 4 h fast of food and water, the mice were gavaged with 0.2 ml of a sugar probe solution containing 100 mg of sucrose, 12 mg of lactulose, 8 mg of mannitol and 6 mg of sucralose. Immediately after the gavage the mice were housed in the metabolic cages to collect the 24-h urine. During the collection period, the urine sample was preserved by the addition to the collection vessels of 5 mg sodium fluoride. The urinary sugars were quantified by the method of Farhadi using GC (36).

### **Tissue sample collection**

The mice were sacrificed by CO<sub>2</sub> asphyxiation after a 4h fast. After the blood collection, the liver, the quadriceps muscle, the intestinal and colonic mucosa, the feces and the adipose tissue samples were collected. The adipose depots included the gonadal, retroperitoneal, mesenteric, and subcutaneous depots. Each category of tissue was saved separately and the tissue mass was recorded. The tissue samples were flash frozen and stored at -80 °C until further analysis.

### **Biochemical analyses of plasma**

The blood was obtained by cheek bleeding and collected in heparin containing tubes (BD, Franklin Lakes, NJ). The plasma samples were obtained after centrifugation at 12,000 x g for 10 minutes and stored at -80 °C. The plasma levels of insulin, leptin, resistin, monocyte chemoattractant protein-1 (MCP-1), IL-6, TNF- $\alpha$  and plasminogen activator inhibitor-1 (PAI-1) were determined by using the MILLIPLEX mouse adipokine kit (Millipore, Billerica, MA). The plasma glucose level was measured by using the Cholestech L.D.X system (Cholestech Corp, Hayward, CA). The homeostasis model assessment-estimated insulin resistance (HOMA-IR) index was calculated from the fasting glucose and insulin levels (fasting glucose\*fasting insulin/22.5) (37, 38). The plasma endotoxin levels were measured by the fluorescence endotoxin assays kit (Lonza Inc., Allendale, NJ).

### **Western Immunoblotting for zonula occludens (ZO)-1 and occludin proteins**

The small intestine (without the duodenum) and the colon were excised after the mouse was sacrificed. The proximal 1/3 segment of the small intestine (jejunum), the distal 2/3 segment of the small intestine (ileum) and the entire length of the colon were collected and opened longitudinally. The intestine was washed with ice-cold 0.9% saline solution to remove the visible mucus and dietary debris. Then the moisture was carefully removed with tissue paper. The intestine segments were gently scraped twice with a glass microscope slide to obtain the mucosa, which were flash frozen and stored at -80 °C until further analysis. Mucosal samples were homogenized in 500  $\mu$ L ice-cold tissue protein extraction reagent (contains a proprietary detergent in 25 mM bicine, 150 mM sodium chloride; pH 7.6) with 1% protease inhibitor and 1% phosphatase inhibitor

(Pierce Biotechnology, Rockford, IL). The homogenates were centrifuged at 10,000 x g for 5 minutes to collect the supernatants. The protein samples were suspended in the sodium dodecyl sulfate (SDS) sample buffer (Invitrogen, Grand Island, NY) and were boiled at 100 °C for 5 minutes. The proteins were separated by sodium dodecyl sulfate-polyacrylamide gel electrophoresis using 6% (ZO-1) or 8% to 16% (occludin,  $\beta$  actin) Tris-glycine polyacrylamide gradient gels and subsequently transferred to nitrocellulose membranes (Invitrogen, Grand Island, NY). The membranes were blocked with 5% bovine serum albumin (BSA) in Tris-buffered saline (TBS, 0.0242% Tris base, 0.08% NaCl; pH 7.6)/0.1% Tween 20 for 1 h. The primary antibodies specific for ZO-1 (1:500; Zymed, Grand Island, NY), occludin (1:500; Santa Cruz Biotechnology, Santa Cruz, CA), or  $\beta$  actin (1:500; Cell Signaling, Danvers, MA) were incubated with the membranes overnight at 4 °C in 5% BSA with Tris-buffered saline/ Tween 20. The membranes were washed and incubated for 1 h at the room temperature with the secondary antibody horseradish peroxidase-linked antirabbit IgG (1:2000; Cell Signaling, Danvers, MA) prepared in the blocking solution. After thorough washing, the Pierce Supersignal West Pico Chemiluminescent Kit was applied for antibody detection with Kodak 2000R Image Station (Raytest USA Inc., Wilmington, NC). The mean pixel density was estimated using ImageJ (NIH, Bethesda, MD). The data were expressed as the relative band density from the Western blots. The relative band density was calculated by dividing the pixel density of the target protein by the mean pixel density of beta actin.

### **Liver gene expression analysis**

The expression of genes associated with lipid metabolism in the liver was analyzed by the real-time quantitative polymerase chain reaction (RT qPCR) assays. The total

RNA was extracted from the liver tissue by using the TRI reagent (Sigma-Aldrich Co. LLC, St. Louis, MO) and the SurePrep RNA Purification Kit (Thermo Fisher Scientific Inc., Waltham, MA) according to the manufacturer's instructions. The genomic DNA in the RNA samples were eliminated with the RNase-free DNase I solution (Thermo Fisher Scientific Inc., Waltham, MA). The RNA (1  $\mu$ g) was reverse transcribed into the cDNA using the QuantiTect® Reverse Transcription Kit (Qiagen, Valencia, CA) and MJ Mini™ Thermal Cycler (Bio-Rad, Hercules, CA). RT qPCR was then performed with the EvaGreen® method using the Biomark™ 48.48 Dynamic Arrays (Fluidigm, South San Francisco, CA). Primer sequences were as in Table 3.2. These mouse primers were selected from the Primer Bank developed by the Massachusetts General Hospital and Harvard Medical School (39). The primers were verified with the corresponding mRNA sequences from the GenBank maintained by the National Center for Biotechnology Information. The cycle threshold (Ct) values for the genes of interest were normalized with the Ct values for peptidylprolyl isomerase A. The relative gene expression was calculated by using the  $2^{-\Delta\Delta C_t}$  method.

### **Tissue lipid profiling**

The tissue samples were removed from the freezer, an unbiased sample of the tissue was cut into small pieces with a razor and placed in a mortar with liquid nitrogen and ground to obtain a fine homogenous powder. About 50 mg (20 mg for the intestinal mucosa) of the tissue powder from each sample were weighed and put into a glass test tube with a screw cap. The lipids were extracted by the method of Folch et al. (40) with slight modifications. The samples were mixed with 1.5 ml Folch solution (chloroform/methanol, 2:1, v/v). The whole mixture was sonicated and then agitated for

15-20 minutes in an orbital shaker at room temperature. The agitated mixture was vortexed for 30 seconds and washed with 0.2 volumes (0.3 ml for 1.5 ml solvent mixture) 0.9% NaCl solution. The washed mixture was vortexed for 20 seconds and centrifuged at  $1,500\times g$  for 10 minutes to separate the two phases. The lower chloroform phase containing lipids was collected and evaporated under a nitrogen stream. The lipids were reconstituted in a small volume of Folch solution in a 2 ml amber vial, topped with nitrogen and stored at  $-80\text{ }^{\circ}\text{C}$  until further analysis.

The individual lipid classes of the extracted lipid were separated using high performance thin layer chromatography (HPTLC). The extracted lipid from each tissue was diluted by the Folch solution such that  $5\text{ }\mu\text{l}$  of the solution contained 2.5 mg of the lipid. The HPTLC plate ( $10\times 20\text{ cm}$  silica gel,  $3\text{ }\mu\text{m}$  particle,  $100\text{ }\mu\text{m}$  layer) (Scientific Adsorbents Inc., Atlanta, GA) was pre-washed with 100 ml of chloroform/methanol (1:1 v/v) and activated in the  $100\text{ }^{\circ}\text{C}$  oven for 10 minutes. The lipid class standards were spotted for detecting the target bands. The aliquots of  $5\text{ }\mu\text{l}$  lipid sample or plasma sample were spotted 1 cm from the bottom of the plate and the plate was air dried. The plate development was carried out by the method of Kupke (41). The plate was first developed in a solvent system containing chloroform-methanol-water (60:30:5 v/v/v) until the solvents reached the middle of the plate. The plate was dried for 30 minutes before a second development in the same solvent system. Then the plate was dried and developed in another solvent system containing hexane-diethyl ether-acetic acid (80:20:1.5 v/v/v) until the solvents reached 0.5 cm from the top of the plate. After being dried, the plate was sprayed until translucent with a 10% (w/v) cupric sulfate solution in 8% (w/v) orthophosphoric acid (42). The plate was heated in an oven at  $145\text{ }^{\circ}\text{C}$  for 10 minutes (43).

The plate was scanned with a document scanner EPSON Stylus NX400 (Epson America Inc., Long Beach, CA) and the lipid bands were quantified with ImageJ (NIH, Bethesda, MD). The detected lipid classes from the HPTLC plate were: PE, PC, PS, and PI, SM, diglycerides (DG), free fatty acids (FFA), TG, and cholesteryl ester (CE).

### **GG analysis of intestinal mucosa**

The total GG content in the intestinal mucosa was determined by measuring the gangliosides bound sialic acid with Gas Chromatography–Mass Spectrometry (GC-MS). The gangliosides were extracted and purified by using the Sep-Pak C18 reverse-phase cartridges (Waters, Milford, MA) according to the method of Schnabl et al. (44). The gangliosides were derivatized by trimethylsilylation. One hundred microliter ganglioside samples with 5 µg phenyl N-acetyl-alpha-D-glucosaminide as internal standard were dried and treated with 700 µl of 0.05 N fresh methanolic HCl by heating for 1 hr at 80 °C. The mixture was cooled and extracted with 0.5 ml of hexane to remove the liberated fatty acid esters. The methanolic layer was dried under a nitrogen stream. The trimethylsilylation derivatization reagent was formed according to the method of Carter and Gaver (45). Hexamethyldisilazane (2.6 ml) and dry pyridine (2 ml) were mixed. Trimethylchlorosilane (1.6 ml) was then added. The mixture was shaken and the opaque solution was centrifuged to give a clear colorless supernatant solution, which was stored in the dark. The silylation reagent (50 µl) was added to the samples in the small ample vials. The samples were agitated well with a Vortex vibrator and allowed to stand for 15 minutes. The derivatized samples were transferred into the GC inserts and 1 µl was injected per assay into a DB-5 GC Column installed on a Shimadzu GC-2010 coupled with a Mass Spectrometer. The quantification was achieved from the standard curve

generated by concurrent analysis of a series of ganglioside GD3 standards in different concentrations.

### **Statistical analyses**

One-way or mixed models analysis of variance (ANOVA) was performed by SAS 9.2. The group means were compared by the Ryan-Einot-Gabriel-Welsch Multiple Range Test or the Least Squares Means Contrast in SAS. The data were reported as Mean  $\pm$  Standard Error of the Mean (SEM).

### **Results**

Dietary polar lipids supplementation did not affect the daily food intake and weight gain (Figure 3.1a). There were no significant differences in the tissue masses of total, subcutaneous, and visceral adipose depots. The PL and GG groups had less mesenteric adipose depot as percentage of body weight compared with the CO group (GG vs CO:  $p = 0.05$ , PL vs CO:  $p = 0.06$ , Figure 3.1b). The PL group accumulated more body fat as revealed by the MRI scan (Figure 3.2a) compared with the GG and CO groups. Body weight gain was mainly contributed by fat accumulation (Figure 3.2b). The PL and GG groups had higher rate of body fat increase compared with the CO group (Figure 3.2b).

One mouse in the GG group died during the second MRI scan. After staying in the metabolic cage for 24h for the final DST, two mice in the CO group, one mouse in the GG group and one mouse in the PL group died. They consumed less food compared with those that survived ( $0.34 \pm 0.12$  g vs  $1.83 \pm 0.62$  g) in the metabolic cage and they had a similar symptom, diarrhea of not fully digested food. One mouse in the PL group developed an anal ulcer after the final DST and was sacrificed and not included in the



following analyses. The remaining mice were sacrificed 3 days after the final DST. Postmortem pathological examination of the dead mice was done by the Utah Veterinary Diagnostic Laboratory. The pathological examination revealed that there was no evidence of infectious disease in any tissues or organs. The hepatic lipidosis was severe and considered the primary cause of mortality. There was also renal lipidosis. For the final tissue analyses, the mice sacrificed at the end were used (CO (n = 3); GG (n = 4); PL (n = 4)).

### **Tissue lipid profiles and gene expression**

Dietary polar lipids, especially the PL, lowered liver mass and liver weight percentage (normalized by body weight) (diet effect  $p = 0.02$ , Figure 3.3a). PL decreased liver weight percentage by 2.6% compared with CO ( $p = 0.006$ ). Dietary polar lipids, especially the PL, decreased CE and PI in the liver and decreased PI in the skeletal muscle ( $p < 0.05$ , Figure 3.3b). Compared with the CO, the GG and the PL down regulated the hepatic expression of the fatty acid oxidation gene *Acaa2* and the fatty acid synthesis gene *Acacb*. The PL up regulated the hepatic expression of the cholesterol esterifying gene *Acat2* ( $p < 0.05$ , Figure 3.4) compared with the CO and the GG. The polar lipids did not affect the following genes associated with lipid metabolism in the liver: the fatty acid synthesis genes: *Elovl5*, *Slc27a5*, *Me1* and *Scd1*; the fatty acid oxidation genes: *Acox3* and *Cpt2*; the cholesterol regulation genes: *Hmgcr*, *Ldlr*, *Scarb1* and *Cyp7a1*.

The PL group had higher plasma levels of FFA (Figure 3.5a) and DG (Figure 3.5b) compared with the GG and CO groups. The PL group had higher plasma SM (Figure 3.5c) and total phospholipids (Figure 3.5d) levels compared with the GG and CO groups.

### **Gut permeability**

The plasma FITC-dextran level decreased significantly during the feeding period (Figure 3.6a). The polar lipids did not affect the plasma FITC-dextran or the LPS level. There was no change in the urinary ratios of Lactulose/Mannitol, Sucrose/Lactulose and Lactulose/Sucralose but the urinary Sucralose/Mannitol ratio increased (Figure 3.6b). There was no significant dietary treatment effect on the urinary sugar ratios. The plasma LPS level was increased by 3-4 fold during the study (Figure 3.6c).

The PL and the GG decreased ZO-1 in jejunum mucosa compared with the CO (Figure 3.6d). The expression of the TJ protein ZO-1 was not affected in the mucosa of the ileum and the colon (Figure 3.6d). The GG slightly increased the occludin expression in the colon mucosa compared with the PL and the CO (Figure 3.6d). The polar lipids did not affect the expression of occludin in the mucosa of the small intestine (Figure 3.6d).

### **Plasma biochemistry**

The PL increased plasma IL-6 level from 41 to 745 pg/ml ( $p = 0.001$ ). The plasma IL-6 level did not change in the CO group (18 vs 16 pg/ml). The GG increased plasma IL-6 level from 44 to 133 pg/ml. The plasma IL-6 level in the PL group was significantly higher than that in the GG and CO groups (Figure 3.7a,  $p = 0.02, 0.01$ , respectively). The correlation between the plasma IL-6 level and the plasma SM level was strong ( $r = 0.978$ ,

$p < 0.0001$ ) while the correlation between the plasma FFA and IL-6 levels was not significant ( $r = 0.338$ ,  $p = 0.34$ ). The correlation between the plasma LPS and IL-6 levels was negative and not significant ( $r = -0.459$ ,  $p = 0.16$ ).

Compared with baseline value, there was an increase of the plasma levels of PAI-1, resistin and leptin. The plasma PAI-1 level increased 2-5 fold (time effect  $p = 0.0007$ , Figure 3.7b). The plasma resistin level increased 1-2 fold (time effect  $p < 0.0001$ , Figure 3.7c). The plasma leptin level increased slightly (time effect  $p = 0.049$ , Figure 3.7d). No statistically significant dietary treatment effect was observed in the plasma levels of PAI-1 and leptin. The GG increased the plasma resistin level compared with the CO and the PL (diet x time effect  $p = 0.03$ , Figure 3.7c).

The plasma levels of insulin, MCP-1 and TNF- $\alpha$  did not change significantly over time and were not significantly affected by dietary polar lipids supplementation (Table 3.3). There was no treatment effect on the fasting glucose and HOMA-IR at the end of the study (Table 3.3).

### **Symptoms related to diabetes**

One mouse in the GG group (GO3) and one mouse in the PL group (PO4) developed obvious diabetic symptoms during the study. Compared with the rest of the mice, these two mice had wetter beddings, consumed more food, had much higher volume of urine, and had higher fasting glucose, insulin and HOMR-IR (Table 3.4). Compared with the other mice, the level of obesity was lower in the diabetic mice (GO3 and PO4) as indicated by the plots of body fat against fat-free mass (Figure 3.8a-f). When all

measurements at 6 time points (at day -15, -11, -7, -3, 4, 13) are included, there is obvious separation of the diabetic mice (GO3 and PO4) from the rest of the mice (Figure 3.8a). The slope for the obese mice was 0.94. From day -15 to day 4, GO3 and PO4 were gradually separated from the rest of the group (Figure 3.8b-e). The slope decreased to 0.71 at day -3 and returned to 1.17 at day 4. When the slope decreased to 0.57 at day 13, GO3 and PO4 were not separated from the rest of the group (Figure 3.8f).

## **Discussion**

This study was designed to test the hypotheses that milk polar lipids reduce liver lipid levels and affect gene expression associated with liver lipid metabolism, prevent the increase of gut permeability, and reduce plasma inflammatory cytokines in ob/ob mice. The milk phospholipids reduced the liver lipids level and slightly affected gene expression associated with lipid metabolism in the liver. The milk phospholipids increased the colon permeability and the plasma IL-6 level. The milk gangliosides decreased ZO-1 and increased occludin in the colon mucosa; did not affect gut permeability, systemic inflammation, and lipid metabolism.

The MRI scan indicated that the PL group had higher total body fat percentage than the other two groups (diet effect  $p = 0.29$  at day 13, Figure 3.2a). The adipose depot measurements revealed that the PL group did not have more subcutaneous fat and had less visceral fat depots and liver mass compared with the CO group. The PL group had higher lipid levels in the plasma. There was no significant difference in the level of muscle lipids among groups. Taken together, the PL may have caused fat redistribution

from the liver and visceral fat depots into the blood stream. Or the PL could have prevented fat accumulation in the liver and visceral fat depots from the circulation.

The milk polar lipids, especially the PL, lowered the liver mass, liver CE & PI, muscle PI and plasma CE. The decrease of the hepatic CE may have resulted from the reduction of the intestinal cholesterol uptake by the PL (46). The milk PL increased the SM level in the liver and plasma compared with the CO and the GG. The PL group had higher amount of SM in the diet and the SM may accumulate in the plasma and the liver.

The plasma TG, DG and FFA levels decreased over time in the CO and GG groups but not in the PL group. Free fatty acids, especially saturated fatty acids, induce the expression of proinflammatory cytokines in cultured macrophages and adipocytes through the activation of the TLR4 (47). Saturated fatty acids may bind to the TLR4 in the adipose tissue and induce inflammation in the adipose tissue of the C57BL/6/J mice (10). Large amounts of saturated fatty acids are released during the macrophage-induced lipolysis in the hypertrophied adipocytes cocultured with macrophages. The released saturated fatty acids bind the TLR4 and thereby induce inflammation in both adipocytes and macrophages by activating the TLR4/NF-kappaB pathway (48). The higher level of FFA in the plasma may explain the increase of plasma IL-6 level.

Dietary milk polar lipids decrease the hepatic expression of genes associated with fatty acid synthesis in the C57BL/6 mice on a high fat diet as demonstrated by Wat et al. (22). In the present study, the milk polar lipids had complex effects on gene expression

related to lipid metabolism in the liver. The PL upregulated the cholesterol esterifying gene *Acat2* compared with the CO and the GG. The PL and the GG downregulated the fatty acid oxidation gene *Acaa2* and the fatty acid synthesis gene *Acacb* compared with the CO. The beneficial effect of milk polar lipids on hepatosteatosis and lipidemia reported by Wat et al. (22) may result from, at least partially, the PI, which has antiobesity effect through regulating gene expression associated with hepatic lipid metabolism in a mouse model of diet-induced obesity (49). Those beneficial effects of polar lipids could also be partially due to the choline contributed by the PC when the mice were fed high sucrose-hepatosteatosis promoting diets (23). The milk polar lipids concentrates used in the present study did not contain significant amount of PI and the amount of choline was balanced among diets (Table 3.1). The difference in the composition of phospholipids may explain the disparity in the findings. The soybean lecithin and PC downregulate the expression of the cholesterol esterifying gene *Acat2* in the liver (50). In the present study the milk PL upregulated the hepatic *Acat2*. Different sources of phospholipids may have different effects on the *Acat2* expression in the liver.

When the ob/ob mice were fed moderately high fat diets (34% energy), gut permeability to FITC-dextran (4000 Da) decreased. The decrease of gut permeability to large molecules may be due to the gut maturation during development when the mice were 7-9 weeks old. Although the C57BL/6J mice reach sexual maturation by day 35, fast maturational growth continues for most biologic processes and structures from week 5 until week 13 (51). The colon permeability to sucralose (Figure 3.6b) and the gut permeability to the LPS (Figure 3.6c) increased. The rise of urinary Sucralose/Mannitol

ratio without the Lactulose/Mannitol ratio being affected indicated that the permeability of the colon increased (31). This may explain the increase of the plasma LPS through enhanced LPS absorption from the colon. A diet with 34% energy by fat would represent the average American fat intake (34% by energy, NHANES 2007-2008) and be considered high fat diet compared with regular rodent chow diet. The high fat diet may have also contributed to the increase of gut permeability during the digestion (27).

The GG decreased TJ protein ZO-1 in the jejunum mucosa and increased occludin in the colon mucosa compared with the CO. But the GG did not affect the permeability of the small intestine or the colon. The change of TJ protein content in the intestinal mucosa may not necessarily result in the change of gut permeability since the distribution of the TJ proteins also plays an important role in affecting gut permeability (6).

The phospholipids fed group had a higher IL-6 level in the plasma compared with the other two groups at the end of the experiment. During the experimental feeding, the plasma fatty acid levels stayed constant in the PL group. The change of fatty acid profile is yet to be verified. The increased plasma IL-6 level could be due to the activation of the TLR4 (10) by the increased plasma saturated fatty acids level, which may be contributed by the dietary intake since 60% of the fatty acids in the dairy PL are saturated (22). The increased plasma SM level could also cause the increase of IL-6 level through stimulating the adipocytes (52). The correlation between the plasma IL-6 level and the plasma SM level was strong ( $r = 0.978$ ,  $p < 0.0001$ ) while the correlation between the plasma FFA level and the IL-6 level was not significant ( $r = 0.338$ ,  $p = 0.34$ ). Although the plasma

LPS level increased and the LPS has the potential to activate the TLR4 and initiate inflammation, the plasma IL-6 level did not increase in the CO and GG groups in which the LPS level increased similarly as in PL group. The correlation between the plasma LPS level and the IL-6 level was negative and not significant ( $r = -0.459$ ,  $p = 0.16$ ). These results indicate that the plasma SM may have a bigger influence on the systemic inflammation than the plasma FFA and LPS in the ob/ob mouse model. One of the main concerns of the increased gut permeability is the resultant increase of the LPS absorption. The findings of this study support the suggestion that the plasma lipids levels may play more important roles in the inflammatory response than the gut permeability in the ob/ob mouse model. Dietary supplementation of the milk PL may pose negative effects by raising the plasma SM level in the ob/ob mice.

The dietary GG did not significantly affect the GG contents in the intestinal mucosa. The GG fed group had higher tight junction protein occludin level in the colon mucosa. The increase of occludin level was not accompanied by an increase of the colon barrier integrity. The PL and GG groups had less PC per gram tissue in the mucosa of the small intestine although the diets had higher amounts of PC compared with the CO group. There were no differences in other phospholipid classes in the intestinal mucosa among the groups. These data do not support the hypothesis that the dietary GG and PL may increase the intestinal barrier integrity through enriching the GG and PL in the intestinal mucosa.



The dietary addition of GG (0.02% w/w) was determined according to a previous study where the dietary GG were observed to protect the tight junction protein occludin in the intestinal mucosa from degradation during the LPS-induced acute inflammation (20). In the present study, the GG supplemented group also had a higher level of occludin in the colon mucosa compared with the CO group. For practicability in general dietary supplement, the GG was provided as a concentrate that also contains the milk phospholipids. The amount of phospholipids in the GG diet was about one ninth of that in the PL diet. Most of the effects of the GG that were similar to the PL may be due to the phospholipids content in the GG diet. The only unique effect of the GG compared with the PL in the present study was that the GG group had a higher occludin expression in the colon mucosa compared with the CO group. Therefore, the GG at the dose used may not have any significant effect on lipid metabolism, gut permeability and systemic inflammation in the ob/ob mice when they are fed a moderately high fat diet.

Some mice died after staying in the metabolic cage for 24h during the second DST. Before the mice were put on the experimental diets, they were fed the chow diet and a baseline DST was carried out. None of the mice had any abnormal symptoms after the baseline DST. At that time, they were small enough to easily access the food in the metabolic cage. After two weeks, their increased size made it difficult to access the food in the metabolic cages and the dietary intake was reduced significantly ( $5.9 \pm 0.5$  vs  $1.4 \pm 0.5$  g,  $p < 0.0001$ ). Starving has been shown to induce hepatic steatosis (53) in ob/ob mice sacrificed 24h after the food was withheld. The food restriction in the metabolic cages in the present study did not kill the mice immediately.

Mice that died thereafter consumed less food in the metabolic cages and did not resume normal food consumption after they were returned to the regular cages. It is unlikely that the animal deaths were mainly due to the high fat diet feeding. Diets with much higher fat contents, such as 80% (54), 66% (55), and 48% (56) by energy, have been used, respectively, in 3-6, 3.5-6.5, and 6-8 week old ob/ob mice and no animal death was reported. The ob/ob mice develop spontaneous liver steatosis and a “second metabolic hit”, such as a high fat diet, is needed to induce a more severe injury (57). Non-alcoholic steatohepatitis (NASH) develops in the ob/ob mice on a moderately high fat diet (35.7% by energy) for 4 weeks (58). The food restriction in the present study was unintentional and it should have worsened the hepatic lipidosis. Extreme steatosis and stress in the metabolic cages may have resulted in the animal mortality. Although the number of animal per group became small after animal mortality, the data on gut permeability were collected before the animal death.

Two mice developed obvious diabetic symptoms in this study. One of the mice died after the last DST and the other one developed an anal ulceration. Both mice were not included in the final analyses. The ob/ob mouse is widely used as an animal model of type 2 diabetes mellitus (59). Diabetes mellitus is usually defined by the fasting hyperglycemia. The fasting glucose above 250 mg/dl (13.87 mM) is out of the normal range for the mouse and may be used as the threshold for a diagnosis of diabetes mellitus in mice (59). The average fasting glucose level was  $16.58 \pm 2.61$  mM in this study and it is similar to the  $20.2 \pm 1.6$  mM reported in another study by Prasain et al. using the ob/ob mice at a similar age of 10 weeks (60). The diet composition in the Prasain’s study was

not described for the ob/ob mice but was likely the regular rodent chow. The ob/ob mice in Prasain's study had plasma insulin level of  $541.1 \pm 69.6$   $\mu$ IU/ml, which is much higher than the  $89.87 \pm 13.87$   $\mu$ IU/ml observed in the present study. The HOMA-IR index is also much smaller in the present study ( $499.4 \pm 81.5$  vs  $68.99 \pm 11.38$ ). The main difference between these two studies is the diet. Further studies are needed to clarify the reasons for the different levels of plasma insulin observed between the Prasain's study and the current study.

Most of the mice in this study had a fasting glucose level exceeding 250 mg/dl (or 13.87 mM) yet only two mice developed clinical symptoms of overt diabetes. Currently there are no standardized criteria defining type 2 diabetes for the mouse. In future studies, a better diagnosing standard may be developed and the diabetic mice may be excluded for the preexisting obesity model to reduce confounding factors contributed by the diabetes.

Fenton's method for defining obesity (61) was supported by the data from the current study. The level of obesity in the diabetic mice decreased when the diabetic symptoms became more severe (Figure 3.8a-f). Stresses, such as staying in the metabolic cage, decreased the level of obesity. After the first two DSTs, the obesity level decreased at day -3 (Figure 3.8d) and at day 13 (Figure 3.8f).

## **Summary**

The high fat feeding compromised the gut barrier integrity, decreased the plasma lipids level but had little effect on the level of systemic inflammatory cytokines. The GG

increased the expression of the tight junction protein occludin in the colon mucosa and had little effect on lipid metabolism and systemic inflammation. The PL supplementation increased the total body fat percentage and redistributed lipids from the liver and the visceral fat depots into the plasma. The PL increased the plasma SM and the inflammatory cytokine IL-6. The PL increased the gut permeability of the colon. In summary (Figure 3.9), dietary supplementation of the milk phospholipids resulted in unfavorable effects on the intestinal barrier integrity and systemic inflammation in the ob/ob mice. The milk phospholipids reduced the liver mass and lipids in the liver but increased the lipid levels in the plasma. The milk gangliosides at the current dose affected the tight junction proteins expression in the intestinal mucosa but did not have significant effect on the intestinal barrier integrity, lipid metabolism and systemic inflammation in the ob/ob mice. Future studies may explore which components of the milk phospholipids are responsible for the observed effects.

The PL supplementation affected lipid metabolism but had little effect on gut permeability and systemic inflammation. Often times, a few organ systems are assessed during the dietary intervention. The limitation of these kinds of studies is that the dietary treatment may benefit one or a few organ systems but could negatively affect other organ systems. During this study, although as many systems were assessed as conditions permit, there are still many systems that were not assessed, such as the nervous system, cardiovascular system, skeletal system, respiratory system, excretory system, endocrine system, reproductive system and immune system. As a result, only four out of the eleven organ systems were assessed in some detail. Although the milk polar lipids did not show

beneficial effects on gut permeability and systemic inflammation in the ob/ob mice, they may benefit other organ systems that were not tested. The overall effects cannot be concluded until all systems are taken into consideration. Therefore, the effects of dietary milk polar lipids on the whole body in the ob/ob mice needs to be further assessed in a systematic manner.

## References

1. Haslam DW, James WP. Obesity. *Lancet* 2005;366:1197-209.
2. Teixeira TF, Souza NC, Chiarello PG, et al. Intestinal permeability parameters in obese patients are correlated with metabolic syndrome risk factors. *Clin Nutr* 2012.
3. Bullo M, Casas-Agustench P, Amigo-Correig P, Aranceta J, Salas-Salvado J. Inflammation, obesity and comorbidities: the role of diet. *Public Health Nutr* 2007;10:1164-72.
4. Malnick SD, Knobler H. The medical complications of obesity. *QJM* 2006;99:565-79.
5. Cani PD, Bibiloni R, Knauf C, et al. Changes in gut microbiota control metabolic endotoxemia-induced inflammation in high-fat diet-induced obesity and diabetes in mice. *Diabetes* 2008;57:1470-81.
6. Ferraris RP, Vinnakota RR. Intestinal nutrient transport in genetically obese mice. *Am J Clin Nutr* 1995;62:540-6.
7. Morton AP, Hanson PJ. Monosaccharide transport by the small intestine of lean and genetically obese (ob/ob) mice. *Q J Exp Physiol* 1984;69:117-26.

8. Brun P, Castagliuolo I, Di Leo V, et al. Increased intestinal permeability in obese mice: new evidence in the pathogenesis of nonalcoholic steatohepatitis. *Am J Physiol Gastrointest Liver Physiol* 2007;292:G518-25.
9. Naito E, Yoshida Y, Makino K, et al. Beneficial effect of oral administration of *Lactobacillus casei* strain Shirota on insulin resistance in diet-induced obesity mice. *J Appl Microbiol* 2010.
10. Laugerette F, Furet JP, Debard C, et al. Oil composition of high-fat diet affects metabolic inflammation differently in connection with endotoxin receptors in mice. *Am J Physiol Endocrinol Metab* 2012;302:E374-86.
11. Bruewer M, Luegering A, Kucharzik T, et al. Proinflammatory cytokines disrupt epithelial barrier function by apoptosis-independent mechanisms. *J Immunol* 2003;171:6164-72.
12. Iyer A, Fairlie DP, Prins JB, Hammock BD, Brown L. Inflammatory lipid mediators in adipocyte function and obesity. *Nat Rev Endocrinol* 2010;6:71-82.
13. Weisberg SP, McCann D, Desai M, Rosenbaum M, Leibel RL, Ferrante AW. Obesity is associated with macrophage accumulation in adipose tissue. *J Clin Invest* 2003;112:1796-808.
14. Iacono A, Raso GM, Canani RB, Calignano A, Meli R. Probiotics as an emerging therapeutic strategy to treat NAFLD: focus on molecular and biochemical mechanisms. *J Nutr Biochem* 2011.
15. Lau DC, Douketis JD, Morrison KM, Hramiak IM, Sharma AM, Ur E. 2006 Canadian clinical practice guidelines on the management and prevention of obesity in adults and children [summary]. *CMAJ* 2007;176:S1-13.

16. Drewnowski A, Specter SE. Poverty and obesity: the role of energy density and energy costs. *Am J Clin Nutr* 2004;79:6-16.
17. Armogida SA, Yannaras NM, Melton AL, Srivastava MD. Identification and quantification of innate immune system mediators in human breast milk. *Allergy Asthma Proc* 2004;25:297-304.
18. Astaire JC, Ward R, German JB, Jimenez-Flores R. Concentration of polar MFGM lipids from buttermilk by microfiltration and supercritical fluid extraction. *J Dairy Sci* 2003;86:2297-307.
19. Snow DR, Ward RE, Olsen A, Jimenez-Flores R, Hintze KJ. Membrane-rich milk fat diet provides protection against gastrointestinal leakiness in mice treated with lipopolysaccharide. *J Dairy Sci* 2011;94:2201-12.
20. Park EJ, Thomson AB, Clandinin MT. Protection of intestinal occludin tight junction protein by dietary gangliosides in lipopolysaccharide-induced acute inflammation. *J Pediatr Gastroenterol Nutr* 2010;50:321-8.
21. Cohn JS, Wat E, Kamili A, Tandy S. Dietary phospholipids, hepatic lipid metabolism and cardiovascular disease. *Curr Opin Lipidol* 2008;19:257-62.
22. Wat E, Tandy S, Kapera E, et al. Dietary phospholipid-rich dairy milk extract reduces hepatomegaly, hepatic steatosis and hyperlipidemia in mice fed a high-fat diet. *Atherosclerosis* 2009;205:144-50.
23. Bacon BR, Park CH, Fowell EM, McLaren CE. Hepatic steatosis in rats fed diets with varying concentrations of sucrose. *Fundam Appl Toxicol* 1984;4:819-26.

24. Noh SK, Koo SI. Milk sphingomyelin is more effective than egg sphingomyelin in inhibiting intestinal absorption of cholesterol and fat in rats. *J Nutr* 2004;134:2611-6.
25. El Alwani M, Wu BX, Obeid LM, Hannun YA. Bioactive sphingolipids in the modulation of the inflammatory response. *Pharmacol Ther* 2006;112:171-83.
26. Park EJ, Suh M, Thomson B, et al. Dietary ganglioside inhibits acute inflammatory signals in intestinal mucosa and blood induced by systemic inflammation of Escherichia coli lipopolysaccharide. *Shock* 2007;28:112-7.
27. Laugerette F, Vors C, Peretti N, Michalski MC. Complex links between dietary lipids, endogenous endotoxins and metabolic inflammation. *Biochimie* 2010.
28. Takahashi M, Ikemoto S, Ezaki O. Effect of the fat/carbohydrate ratio in the diet on obesity and oral glucose tolerance in C57BL/6J mice. *J Nutr Sci Vitaminol (Tokyo)* 1999;45:583-93.
29. Snow DR, Jimenez-Flores R, Ward RE, et al. Dietary milk fat globule membrane reduces the incidence of aberrant crypt foci in Fischer-344 rats. *J Agric Food Chem* 2010;58:2157-63.
30. Peterson CY, Costantini TW, Loomis WH, et al. Toll-like receptor-4 mediates intestinal barrier breakdown after thermal injury. *Surg Infect (Larchmt)* 2010;11:137-44.
31. Meddings JB, Gibbons I. Discrimination of site-specific alterations in gastrointestinal permeability in the rat. *Gastroenterology* 1998;114:83-92.



32. Krugliak P, Hollander D, Schlaepfer CC, Nguyen H, Ma TY. Mechanisms and sites of mannitol permeability of small and large intestine in the rat. *Digestive Diseases and Sciences* 1994;39:796-801.
33. Smecuol E, Bai JC, Vazquez H, et al. Gastrointestinal permeability in celiac disease. *Gastroenterology* 1997;112:1129-36.
34. Wilairatana P, Meddings JB, Ho M, Vannaphan S, Looareesuwan S. Increased gastrointestinal permeability in patients with Plasmodium falciparum malaria. *Clinical infectious diseases: an official publication of the Infectious Diseases Society of America* 1997;24:430-5.
35. Arrieta MC, Madsen K, Doyle J, Meddings J. Reducing small intestinal permeability attenuates colitis in the IL10 gene-deficient mouse. *Gut* 2009;58:41-8.
36. Farhadi A, Keshavarzian A, Fields JZ, Sheikh M, Banan A. Resolution of common dietary sugars from probe sugars for test of intestinal permeability using capillary column gas chromatography. *J Chromatogr B* 2006;836:63-8.
37. Matthews DR, Hosker JP, Rudenski AS, Naylor BA, Treacher DF, Turner RC. Homeostasis model assessment: insulin resistance and beta-cell function from fasting plasma glucose and insulin concentrations in man. *Diabetologia* 1985;28:412-9.
38. Wallace TM, Levy JC, Matthews DR. Use and abuse of HOMA modeling. *Diabetes Care* 2004;27:1487-95.

39. Wang X, Spandidos A, Wang H, Seed B. PrimerBank: a PCR primer database for quantitative gene expression analysis, 2012 update. *Nucleic Acids Res* 2012;40:D1144-9.
40. Folch J, Lees M, Sloane Stanley GH. A simple method for the isolation and purification of total lipides from animal tissues. *J Biol Chem* 1957;226:497-509.
41. Kupke IR, Zeugner S. Quantitative high-performance thin-layer chromatography of lipids in plasma and liver homogenates after direct application of 0.5-microliter samples to the silica-gel layer. *J Chromatogr* 1978;146:261-71.
42. Baron CB, Coburn RF. Comparison of 2 copper reagents for detection of saturated and unsaturated neutral lipids by charring densitometry. *J Liq Chromatogr* 1984;7:2793-801.
43. Churchward MA, Brandman DM, Rogasevskaia T, Coorsen JR. Copper (II) sulfate charring for high sensitivity on-plate fluorescent detection of lipids and sterols: quantitative analyses of the composition of functional secretory vesicles. *J Chem Biol* 2008;1:79-87.
44. Schnabl KL, Larcelet M, Thomson AB, Clandinin MT. Uptake and fate of ganglioside GD3 in human intestinal Caco-2 cells. *Am J Physiol Gastrointest Liver Physiol* 2009;297:G52-9.
45. Carter HE, Gaver RC. Improved reagent for trimethylsilylation of sphingolipid bases. *J Lipid Res* 1967;8:391-5.
46. Kamili A, Wat E, Chung RW, et al. Hepatic accumulation of intestinal cholesterol is decreased and fecal cholesterol excretion is increased in mice fed a high-fat diet supplemented with milk phospholipids. *Nutr Metab (Lond)* 2010;7:90.

47. Shi H, Kokoeva MV, Inouye K, Tzameli I, Yin H, Flier JS. TLR4 links innate immunity and fatty acid-induced insulin resistance. *J Clin Invest* 2006;116:3015-25.
48. Suganami T, Tanimoto-Koyama K, Nishida J, et al. Role of the Toll-like receptor 4/NF-kappa B pathway in saturated fatty acid-induced inflammatory changes in the interaction between adipocytes and macrophages. *Arterioscl Throm Vas* 2007;27:84-91.
49. Shimizu K, Ida T, Tsutsui H, Asai T, Otsubo K, Oku N. Anti-obesity effect of phosphatidylinositol on diet-induced obesity in mice. *J Agric Food Chem* 2010.
50. LeBlanc MJ, Brunet S, Bouchard G, et al. Effects of dietary soybean lecithin on plasma lipid transport and hepatic cholesterol metabolism in rats. *J Nutr Biochem* 2003;14:40-8.
51. Flurkey K, Curren J, Harrison D. Mouse models in aging research. In: Fox J, Davisson M, Quimby F, Barthold S, Newcomer C, Smith A, (eds). *The Mouse in Biomedical Research*. Academic Press: Massachusetts: 2007. pp 637-72.
52. Samad F, Hester KD, Yang G, Hannun YA, Bielawski J. Altered adipose and plasma sphingolipid metabolism in obesity: a potential mechanism for cardiovascular and metabolic risk. *Diabetes* 2006;55:2579-87.
53. Xu JL, Kulkarni SR, Li LY, Slitt AL. UDP-Glucuronosyltransferase expression in mouse liver is increased in obesity- and fasting-induced steatosis. *Drug Metab Dispos* 2012;40:259-66.

54. Tuig JG, Romsos DR, Leveille GA. Maintenance energy requirements and energy retention of young obese (ob/ob) and lean mice housed at 33 degrees and fed a high-carbohydrate or a high-fat diet. *J Nutr* 1980;110:35-41.
55. Kim HK, Romsos DR. Brown adipose tissue metabolism in ob/ob mice: effects of a high-fat diet and adrenalectomy. *Am J Physiol* 1987;253:E149-57.
56. Mercer SW, Trayhurn P. Effect of high fat diets on energy balance and thermogenesis in brown adipose tissue of lean and genetically obese ob/ob mice. *J Nutr* 1987;117:2147-53.
57. Stefano JT, de Oliveira CP, Correa-Giannella ML, et al. Nonalcoholic steatohepatitis (NASH) in ob/ob mice treated with yo jyo hen shi ko (YHK): effects on peroxisome proliferator-activated receptors (PPARs) and microsomal triglyceride transfer protein (MTP). *Digestive Diseases and Sciences* 2007;52:3448-54.
58. de Lima VM, de Oliveira CP, Sawada LY, et al. Yo jyo hen shi ko, a novel Chinese herbal, prevents nonalcoholic steatohepatitis in ob/ob mice fed a high fat or methionine-choline-deficient diet. *Liver Int* 2007;27:227-34.
59. Clee SM, Attie AD. The genetic landscape of type 2 diabetes in mice. *Endocrine Reviews* 2007;28:48-83.
60. Kim MK, Chae YN, Son MH, et al. PAR-5359, a well-balanced PPARalpha/gamma dual agonist, exhibits equivalent antidiabetic and hypolipidemic activities in vitro and in vivo. *Eur J Pharmacol* 2008;595:119-25.
61. Fenton PF. Growth and fat deposition in the mouse; a definition of obesity. *Am J Physiol* 1956;184:52-4.

**Table 3.1** Diets composition (unit: g/kg; Chow: LabDiet 5K52; CHO = carbohydrates).

Ingredient	CO	GG	PL	Chow
Casein, Vitamin-Free Test	188	188	188	193 (crude protein)
L-Cystine	3	3	3	0
Corn Starch	348	348	348	397.9 (crude CHO)
Maltodextrin	100	100	100	0
Sucrose	100	100	100	6.2
Soybean Oil	73	73	73	72 (crude fat)
Lard	95.30	91.93	83.20	0
Lactose	6.87	0	5.88	0
Cellulose	34.90	34.90	34.90	43 (crude fiber)
Nitrogen-free non-carbohydrate	0	0	0	138.1
Mineral Mix, AIN-93G	35	35	35	65 (crude ash)
Vitamin Mix, AIN-93	10	10	10	Crude vitamin
TBHQ, antioxidant	0.04	0.04	0.04	0
GG concentrate	0	11.24	0	0
PL concentrate	0	0	14.24	0
Water	0.03	0.06	1.45	0
Food Color	0.15	0.15	0.15	0
	Choline adjustment (g/kg)			
Choline Bitartrate	3.95	3.76	2.50	0
	Minerals adjustment (mg/kg)			
Sodium Meta-Silicate, nonahydrate	7.7	0	1.5	0
Sodium Chloride	196.8	20.5	0	0
Potassium Phosphate, monobasic	1259.7	897.3	0	0
Potassium Sulfate	281.4	0	644.7	0
Calcium Carbonate	8	4.8	0	0
Magnesium Oxide	1.1	0	0.1	0
	Energy contribution (Kcal%)			
Protein	16.78	16.78	16.78	22.24
Carbohydrate	49.02	49.02	49.02	61.73
Fat	34.20	34.20	34.20	16.03
Energy density (Kcal/g)	4.3	4.3	4.3	3.5

**Table 3.2** Mouse primers sequences for real-time quantitative polymerase chain reaction (qPCR) assays.

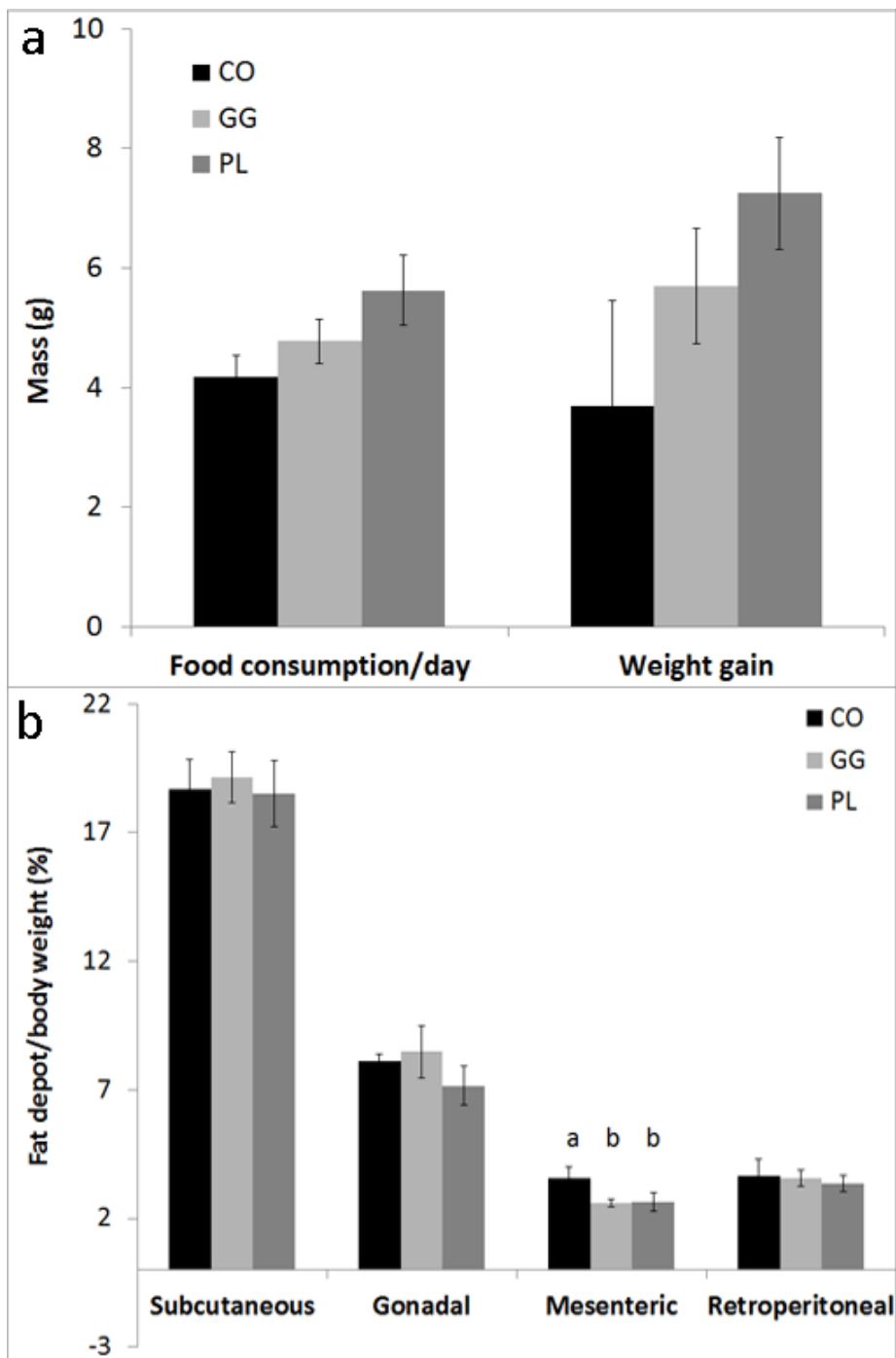
Gene symbol	Gene name	Primers (5'→3': forward; reverse)
Fatty acid synthesis		
<i>Acacb</i>	Acetyl-Coenzyme A carboxylase beta	TTCTGAATGTGGCTATCAAGACTGA; TGCTGGGTGAACTCTCTGAACA
<i>Elovl5</i>	ELOVL family member 5, elongation of long chain fatty	GAACATTTTCGATGCGTCACTCA; GGAGGAACCATCCTTTGACTCTT
<i>Slc27a5</i>	Solute carrier family 27 (fatty acid transporter),	GGAGGTGGTGATAGCCGGTAT; TGGGTAATCCATAGAGCCCAG
<i>Me1</i>	Malic enzyme 1, NADP(+)-dependent, cytosolic	TCTGACTTCGACAGGTATCTCC; CGGAATGCCAACTGTACTGC
<i>Scd1</i>	Stearoyl-Coenzyme A desaturase 1	GATAGAGCAAGTCCCCGCTG; CCTGCATTAACCCCTTCAC
Fatty acid oxidation		
<i>Acaa2</i>	Acetyl-Coenzyme A acyltransferase 2	CTGCTACGAGGTGTGTTTCATC; TCCAAAGGGTGTTCGCTTCG
<i>Acox3</i>	Acyl-Coenzyme A oxidase 3, pristanoyl	CAGAATGGTGTGCTAGAGCGT; AGCCTGTCCGGCTACAGATTTG
<i>Cpt2</i>	Carnitine palmitoyltransferase 2	CCTGCTCGCTCAGGATAAACA; GTGTCTTCAGAAACCGCACTG
Cholesterol regulation		
<i>Acat2</i>	Acetyl-Coenzyme A acetyltransferase 2	CCCGTGGTCATCGTCTCAG; GGACAGGGCACCATTGAAGG
<i>Hmgcr</i>	3-hydroxy-3-methylglutaryl-Coenzyme A reductase	TGTTCCACCGGCAACAACAAGA; CCGCGTTATCGTCAGGATGA
<i>Ldlr</i>	Low density lipoprotein receptor	TGACTCAGACGAACAAGGCTG; ATCTAGGCAATCTCGGTCTCC
<i>Scarb1</i>	Scavenger receptor class B, member 1	TTTGAGTGGTAGTAAAAAGGGC; TGACATCAGGGACTCAGAGTAG
<i>Cyp7a1</i>	Cytochrome P450, family 7, subfamily a, polypeptide 1	CAGGGAGATGCTCTGTGTTCA; AGGCATACATCCCTTCCGTGA
Housekeeping		
<i>Gapdh</i>	Glyceraldehyde-3-phosphate dehydrogenase	AGGTCGGTGTGAACGGATTTG; TGTAGACCATGTAGTTGAGGTCA
<i>Actb</i>	Actin, beta	GGCTGTATTCCCCTCCATCG; CCAGTTGGTAACAATGCCATGT
<i>Ppia</i>	Peptidylprolyl isomerase A	GGACCAAACACAAACGGTTCC; CCAGCCATTCAGTCTTGCA

**Table 3.3** Effects of milk polar lipids on plasma levels of MCP-1, TNF- $\alpha$ , insulin, glucose, and homeostasis model assessment of insulin resistance (HOMA-IR) in ob/ob mice (Mean  $\pm$  SEM; unit: Log10(pg/ml) for cytokines; mM for glucose; arbitrary for HOMA-IR).

<b>Lipids</b>	<b>CO</b>	<b>GG</b>	<b>PL</b>
<b>Baseline</b>			
MCP-1	1.86 $\pm$ 0.09	1.66 $\pm$ 0.14	1.66 $\pm$ 0.05
TNF- $\alpha$	1.43 $\pm$ 0.03	1.45 $\pm$ 0.02	1.33 $\pm$ 0.06
Insulin	3.62 $\pm$ 0.09	3.34 $\pm$ 0.18	3.57 $\pm$ 0.08
<b>Day 16</b>			
MCP-1	1.88 $\pm$ 0.31	2.09 $\pm$ 0.22	2.09 $\pm$ 0.23
TNF- $\alpha$	1.40 $\pm$ 0.04	1.47 $\pm$ 0.12	1.53 $\pm$ 0.21
Insulin	3.50 $\pm$ 0.03	3.48 $\pm$ 0.03	3.57 $\pm$ 0.07
Glucose	15.04 $\pm$ 1.01	18.94 $\pm$ 4.80	14.97 $\pm$ 7.01
HOMA-IR	60.09 $\pm$ 1.39	76.54 $\pm$ 23.37	67.82 $\pm$ 48.02

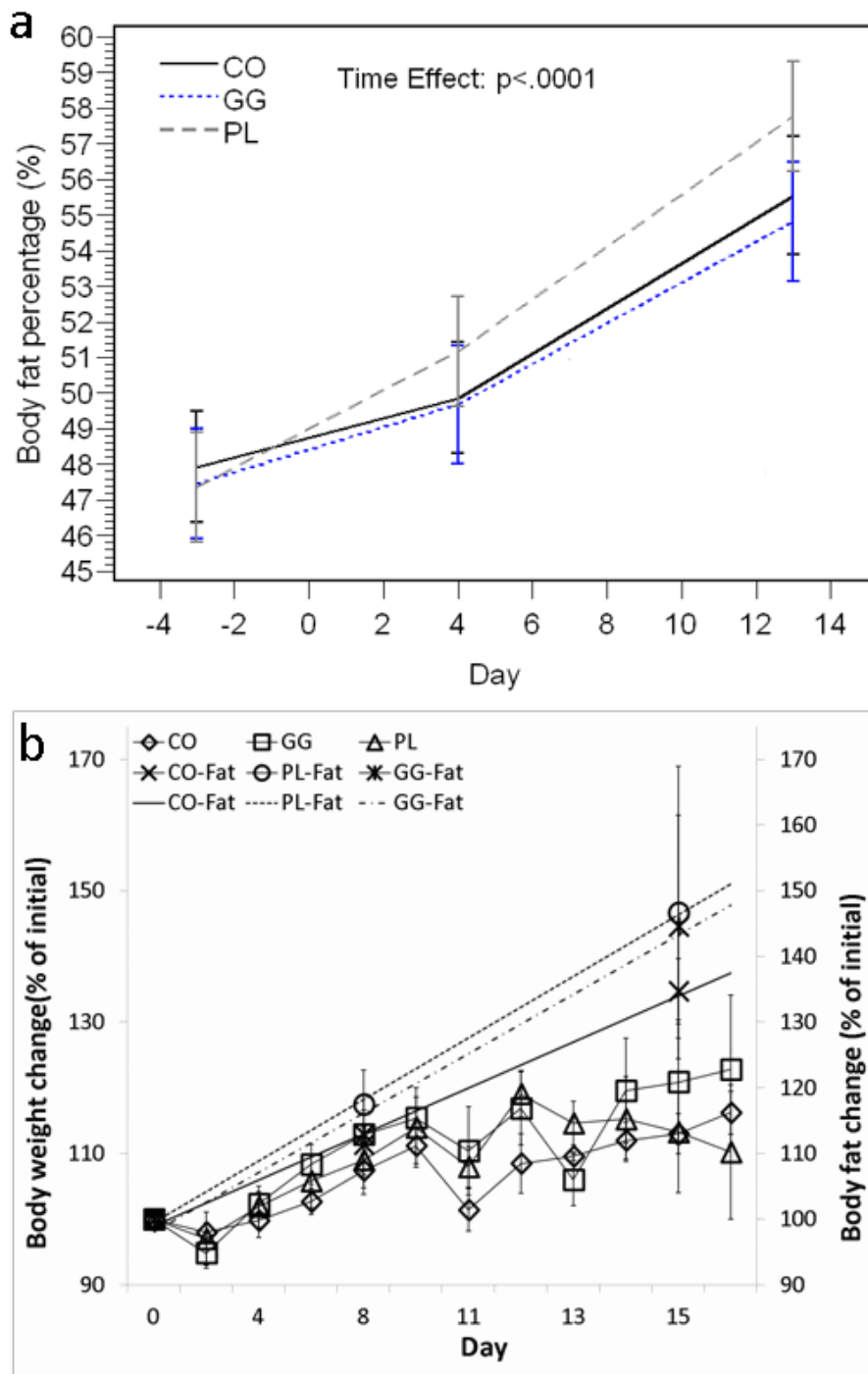
**Table 3.4** Diabetes associated parameters measured in mice GO3 and PO4 (The data represent mean  $\pm$  SEM).

<b>Lipids</b>	<b>Average</b>	<b>GO3 (GG)</b>	<b>PO4 (PL)</b>
Daily food intake (g)	4.93 $\pm$ 0.29	5.50	7.24
Body weight at day 16 (g)	37.22 $\pm$ 1.10	29.00	34.00
24h urine at day 13 (ml)	3.06 $\pm$ 1.50	17.50	17.00
Insulin at day 16 ( $\mu$ IU/ml)	89.87 $\pm$ 13.87	96.94	117.99
Glucose at day 16 (mM)	16.58 $\pm$ 2.61	27.75	27.75
HOMA-IR at day 16	68.99 $\pm$ 11.38	115.60	103.64

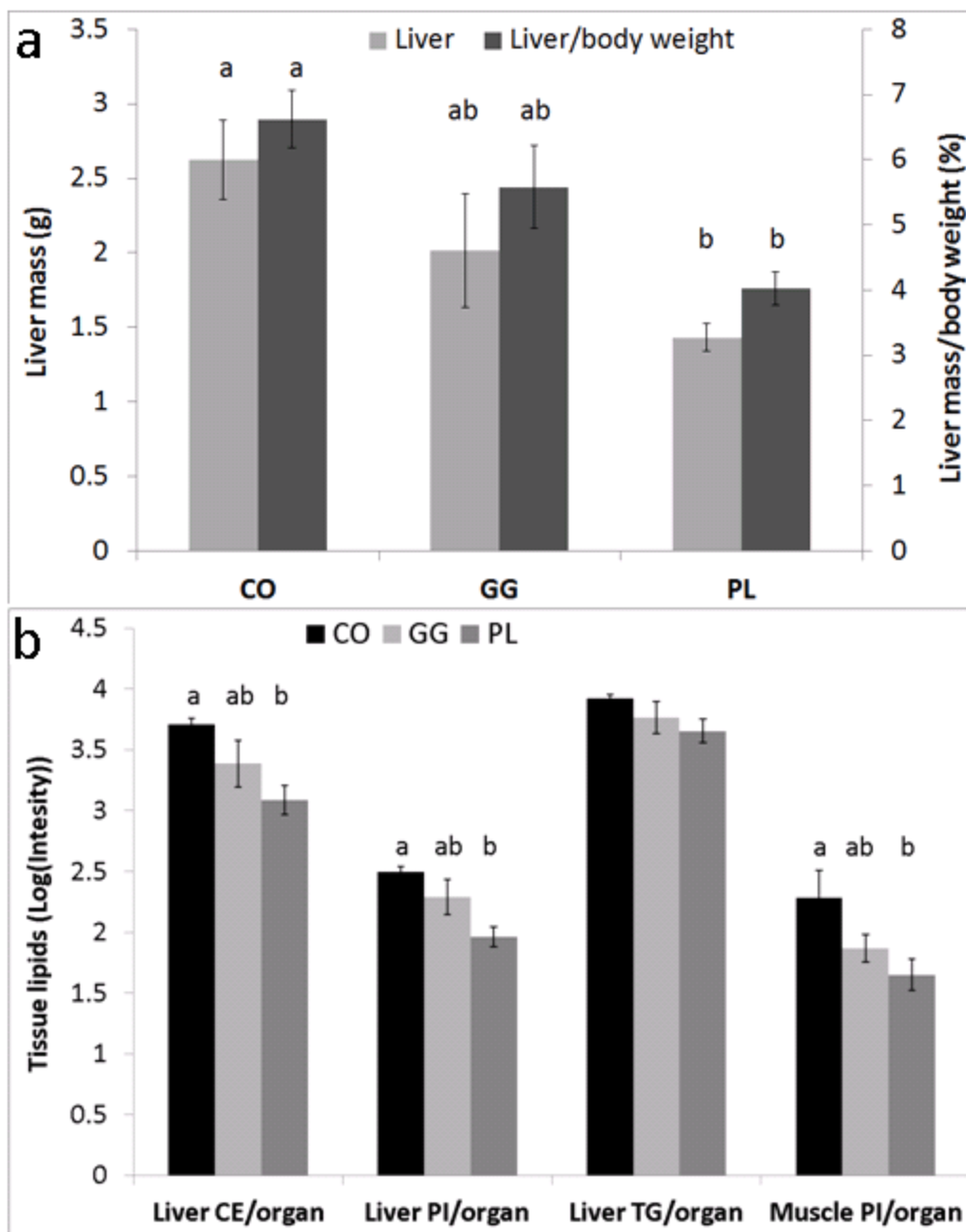


**Figure 3.1** Effects of polar lipids on food intake, weight gain and fat depots. The data represent mean  $\pm$  SEM ( $n = 3, 4, 4$  for CO, GG, PL). (a) GG and PL did not affect food intake and weight gain compared with CO. (b) GG and PL decreased mesenteric fat percentage (by body weight) compared with CO. Means in a row with different superscripts are significantly different ( $p < 0.05$ ).

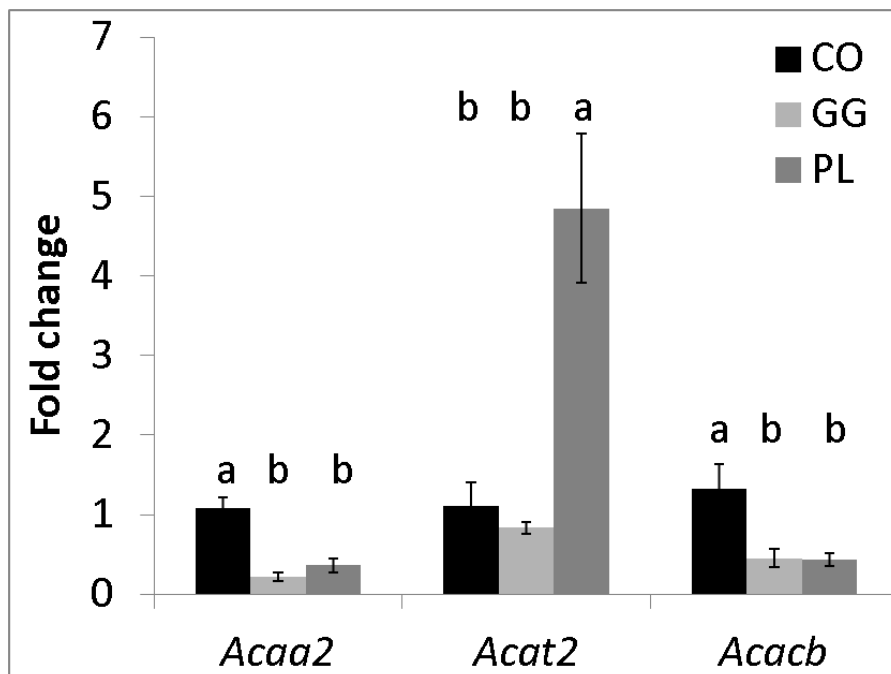




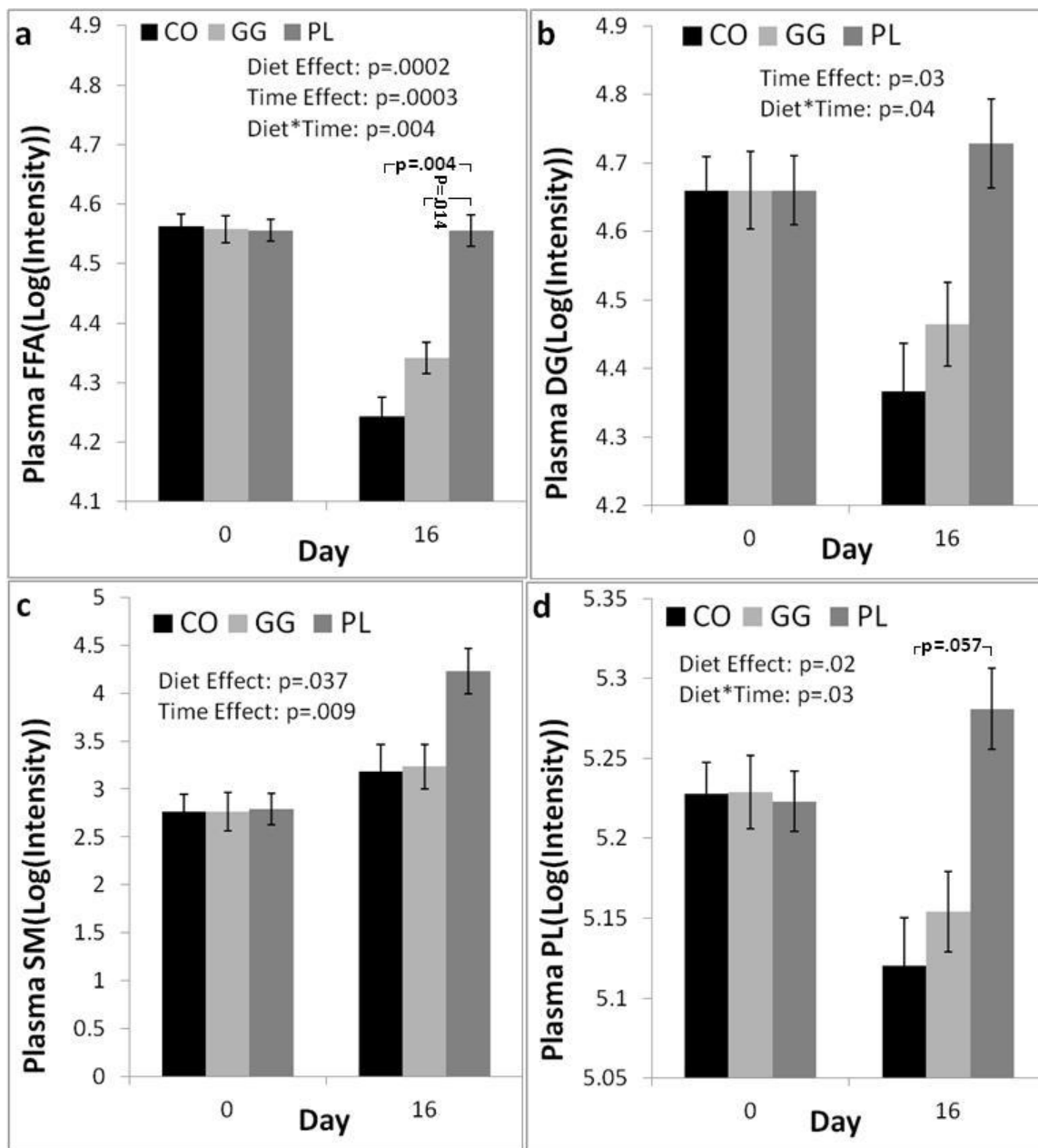
**Figure 3.2** Effects of milk polar lipids on body fat and body weight. The data represent mean  $\pm$  SEM ( $n = 5, 5, 6$  for CO, GG, PL). Initial body weight for CO, GG and PL groups:  $34.2 \pm 0.8, 31.8 \pm 2.8, 35.5 \pm 2.4$  (g). (a) PL facilitated body fat accumulation. (b) Body fat increased at faster rate compared with body weight.



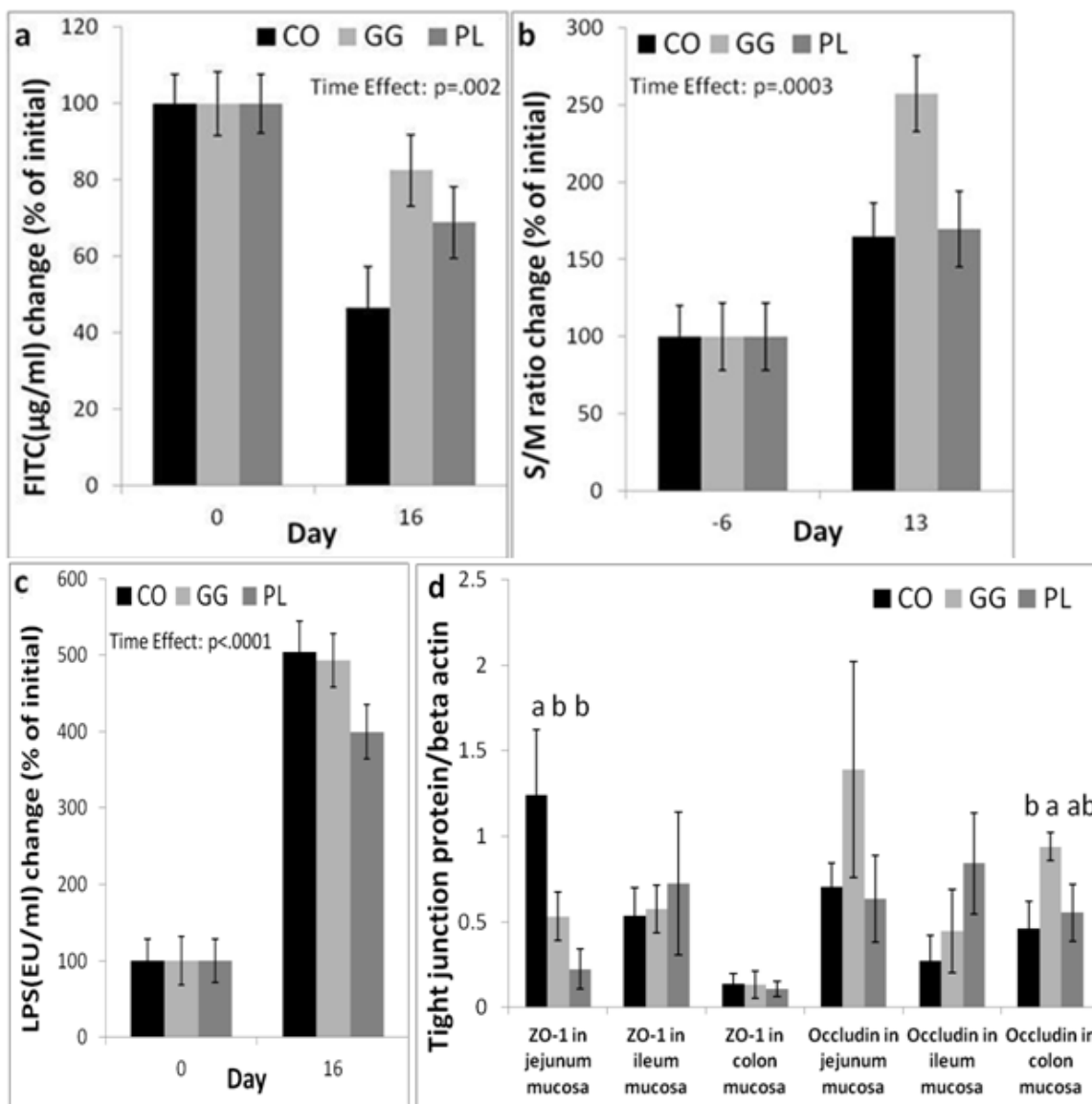
**Figure 3.3** Effects of milk polar lipids on liver mass and tissue lipid profile. The data represent mean  $\pm$  SEM. (a) GG and esp. PL decreased liver mass. (b) GG and esp. PL decreased CE & PI in the liver and decreased PI in skeletal muscle. Means in a row with different superscripts are significantly different ( $p < 0.05$ ).



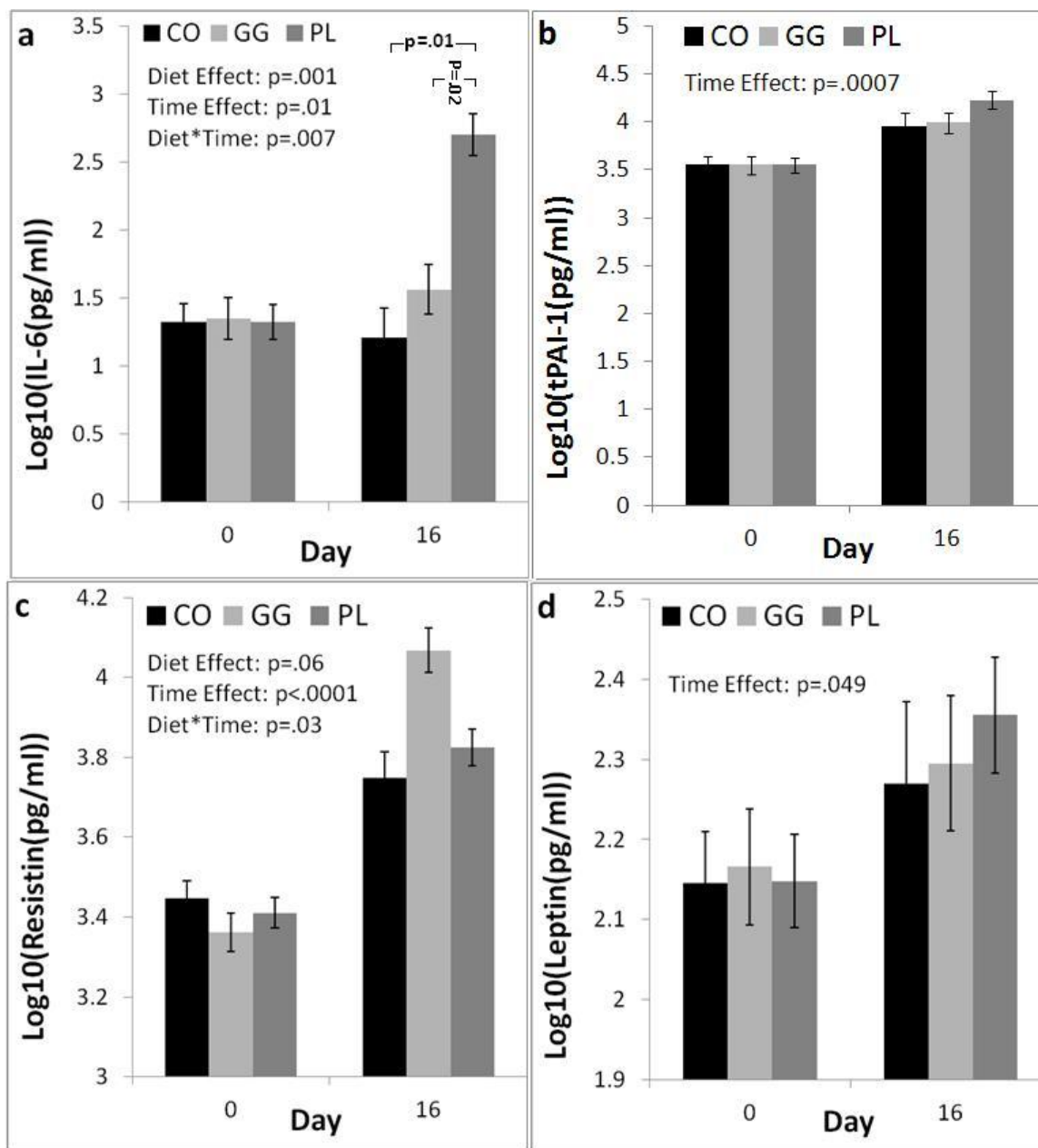
**Figure 3.4** Effects of milk polar lipids on gene expression associated with lipid metabolism in the liver. The data represent mean  $\pm$  SEM. PL and GG down regulated the expression of *Acaa2* and *Acacb* compared with CO. PL up regulated the expression of *Acat2* compared with CO and GG. Means in a row with different superscripts are significantly different ( $p < 0.05$ ).



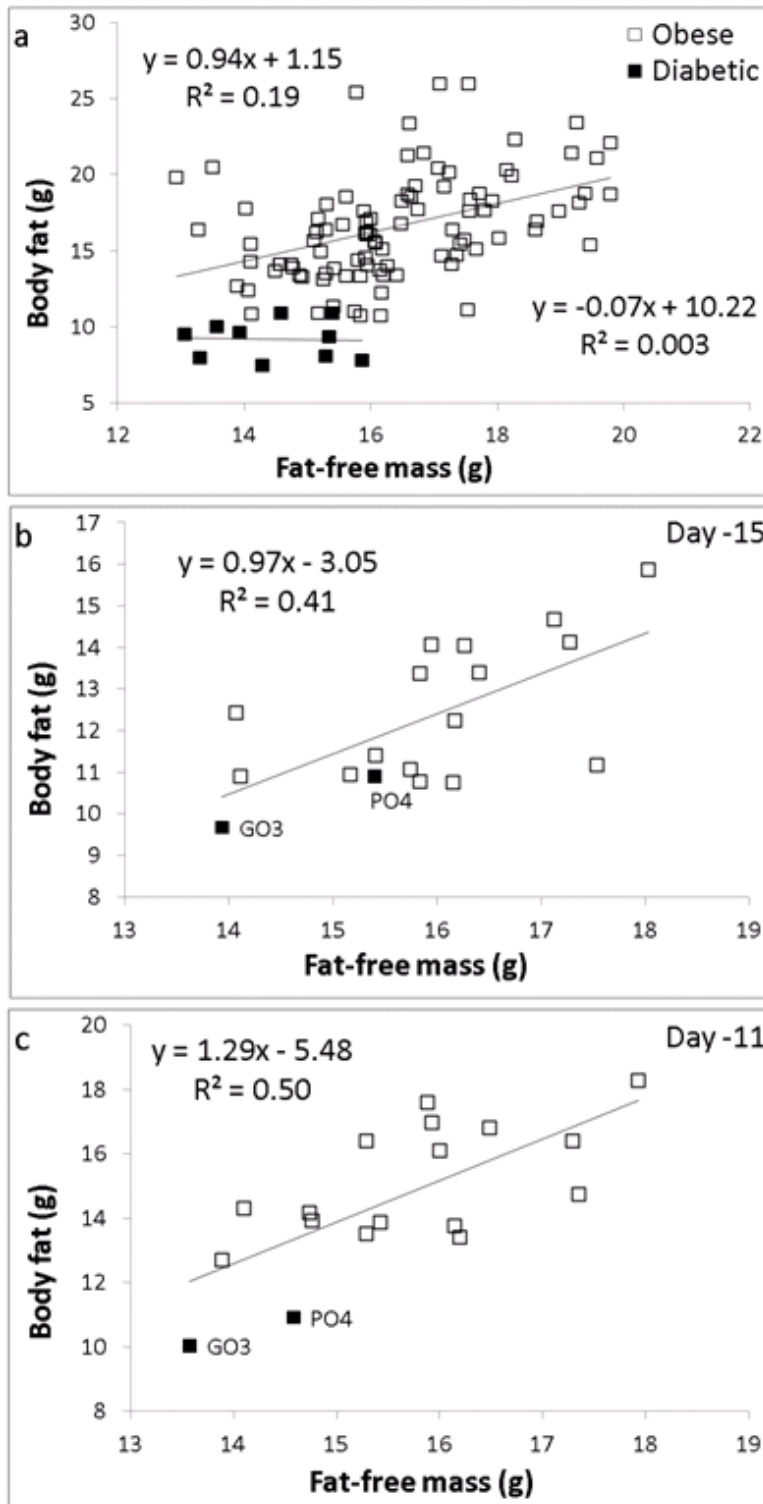
**Figure 3.5** Effects of milk polar lipids on plasma lipid profile. The data represent mean  $\pm$  SEM (n = 6/group at day 0, n = 3, 4, 4 for CO, GG, PL at day 16). (a) PL group had higher plasma FFA level. (b) Plasma DG level decreased. (c) Plasma SM increased. (d) PL group had higher plasma PL level.



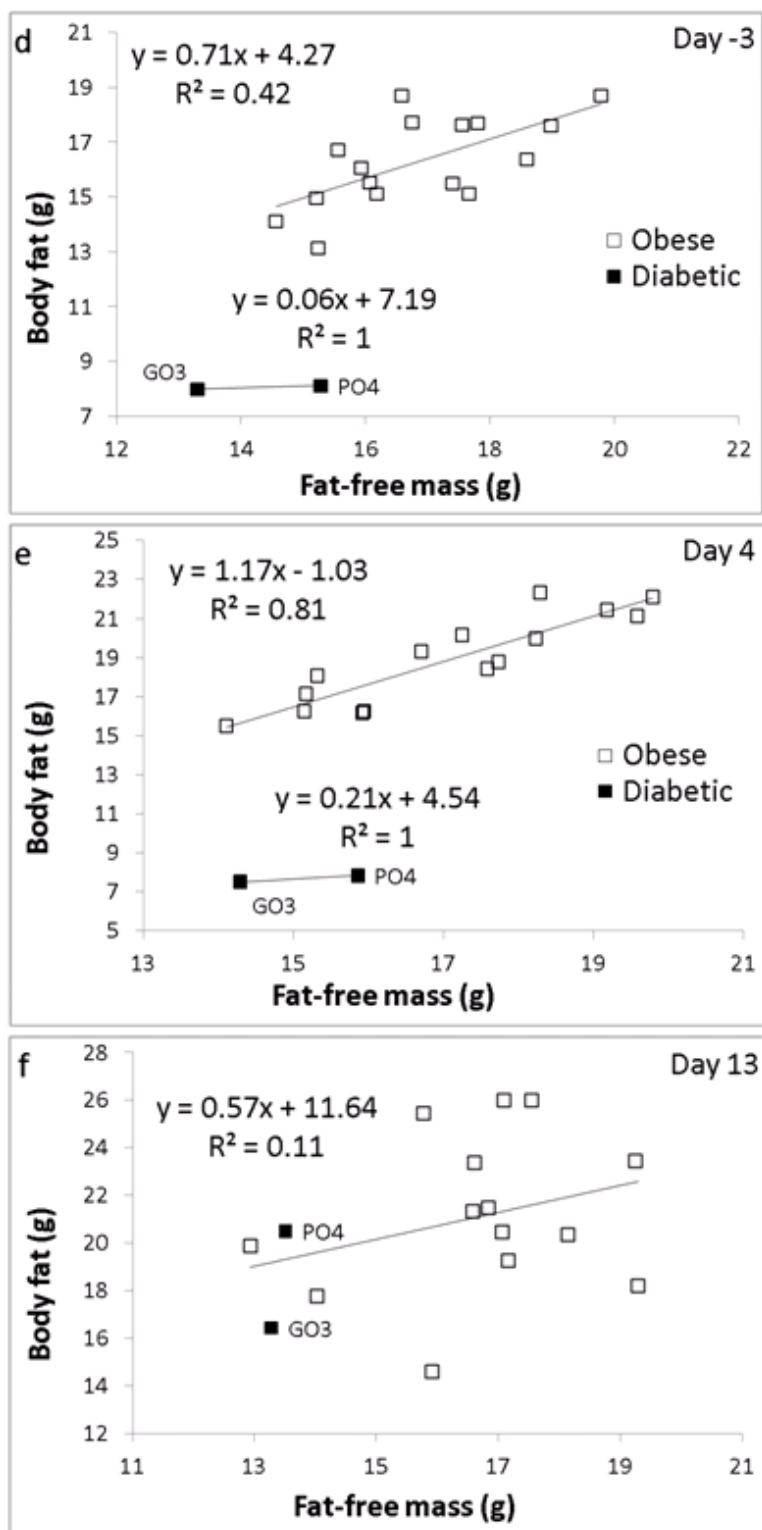
**Figure 3.6** Effects of milk polar lipids on gut permeability. The data represent mean  $\pm$  SEM ( $n = 6$ /group at baseline). (a) Plasma FITC-dextran decreased ( $n = 3, 4, 4$  for CO, GG, PL). (b) Urinary Sucralose/Mannitol (S/M) ratio increased ( $n = 5, 4, 4$  for CO, GG, PL). (c) Plasma LPS level increased ( $n = 3, 4, 4$  for CO, GG, PL). (d) PL and GG decreased ZO-1 expression in jejunum mucosa ( $n = 3, 4, 4$  for CO, GG, PL). Means in a row with different superscripts are significantly different ( $p < 0.05$ ).



**Figure 3.7** Effects of milk polar lipids on plasma cytokines. The data represent mean  $\pm$  SEM. (a) PL increased plasma IL-6 level. (b) Plasma PAI-1 level increased. (c) Plasma resistin level increased. (d) Plasma MCP-1 level increased.

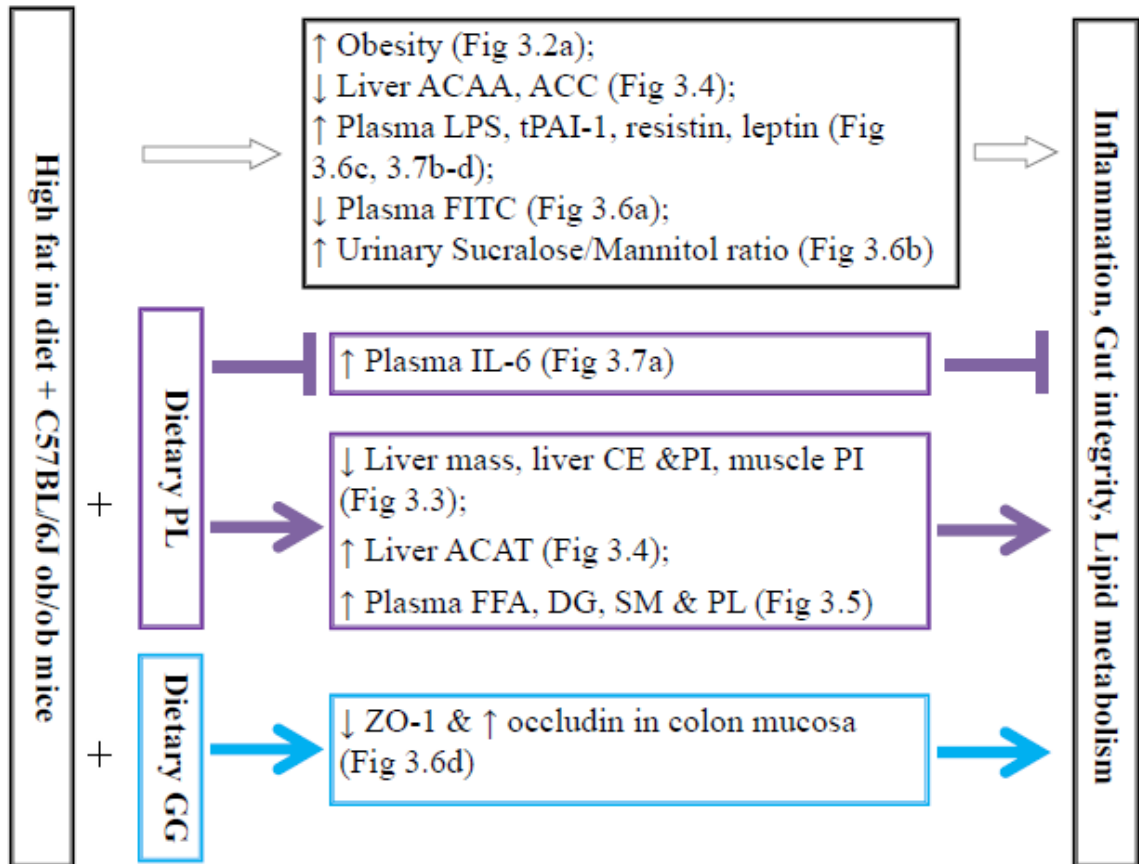


**Figure 3.8a-c** Body fat plotted against fat-free mass for individual animals during (a) day -15 through 13 and at (b) day -15 and (c) day -11.



**Figure 3.8d-f** Body fat plotted against fat-free mass for individual animals at (e) day -3, (f) day 4 and (g) day 13.





**Figure 3.9** Summary of major findings in Chapter 3. Horizontal white arrows indicate the effects of the control diet. Horizontal T-shaped purple arrows indicate undesirable effects. Horizontal solid purple and blue arrows indicate desirable or neutral effects.

**CHAPTER 4**

**DIETARY MILK POLAR LIPIDS AFFECT GUT BARRIER INTEGRITY AND  
LIPID METABOLISM IN C57BL/6J MICE DURING SYSTEMIC  
INFLAMMATION INDUCED BY ESCHERICHIA COLI  
LIPOPOLYSACCHARIDE**

**Abstract**

Adiposity is linked to the complications of obesity by metabolic inflammation. High fat diets can increase gut permeability and lead to endotoxemia and metabolic inflammation. Milk polar lipids protect the gut barrier integrity. One objective of this study was to test the hypotheses that dietary polar lipids may prevent the increase of gut permeability and plasma inflammatory cytokines, reduce liver lipid levels and affect the expression of genes associated with fatty acid synthesis and cholesterol regulation in the liver during the acute and chronic inflammation induced by the subcutaneously injected lipopolysaccharide (LPS). Another objective was to explore the dynamic changes in gut permeability, plasma inflammatory cytokines and lipid metabolism during systemic inflammation. Three groups of C57BL/6J mice were fed for 8 weeks: 1) modified AIN-93G diet (CO); 2) CO with milk gangliosides (GG); 3) CO with milk phospholipids (PL). After 2 weeks' experimental feeding, the mice were injected subcutaneously with LPS to induce acute and chronic inflammation. The animals were fed the experimental diets for another 6 weeks. The gut permeability was assessed by the differential sugar tests at baseline and 24 h, 2 weeks, and 4 weeks after stress. The tight junction protein expression in the intestinal mucosa was evaluated by Western blot at day 57. The plasma cytokines and lipids were measured at the baseline, day 34 and 57. The tissue lipid profiles in the

liver, skeletal muscle, adipose and intestinal mucosa were assessed by high performance thin layer chromatography at day 57. The GG or the PL did not affect the total food intake, weight gain or fasting glucose, plasma cholesteryl ester and plasma triglycerides. The milk polar lipids did not protect the gut barrier integrity at 24 h post LPS injection. There was no dietary treatment effect on systemic inflammation. The experimental feeding increased the plasma levels of leptin and resistin and decreased the plasma insulin level. The increased LPS absorption from the gut was not accompanied by the increase of plasma proinflammatory cytokines while systemic inflammation increased after the LPS injection. In conclusion, the milk GG did not affect the gut permeability and the systemic inflammation, and increased the hepatic gene expression of *Acaa2*. The milk PL had complex effects on the gut permeability, did not affect systemic inflammation, decreased the liver mass, and suppressed the hepatic gene expression of *Acacb* and *Hmgcr*.

## **Introduction**

Obesity is a big health concern in America. In 2009–2010, 16.9% of children and adolescents, and 35.7% of adults in the United States were obese (1). Metabolic inflammation is a link between adiposity and the complications of obesity (2). High fat diets increase intestinal permeability (3). Chronic feeding of high fat diets result in the increased endotoxin absorption and the low-grade metabolic inflammation (4). Gut permeability plays an important role in the metabolic inflammation.

The gastrointestinal surface hydrophobicity decreases under the pathological conditions. Maintenance of the phosphatidylcholine (PC) in the hydrophobic surface may

play an important role in the promotion of health and the prevention of disease (5). The phospholipid (PL) concentration and species composition of the intestinal mucus barrier are significantly altered in the patients with ulcerative colitis (6). The alterations in PL may be important for the pathogenesis of diseases associated with the disruption of intestinal barrier integrity. It may be hypothesized that dietary PL supplementation may help maintain the intestinal barrier integrity and therefore reduce the endotoxin absorption and the metabolic inflammation.

The mouse model of gut leakiness and systemic inflammation induced by lipopolysaccharide (LPS) is well established. LPS at 2 mg/kg (7) and 10 mg/kg (8) body weight injected subcutaneously induces endotoxemia and the intestinal stress in mice. The LPS elevates the serum concentrations of various cytokines in mice, including interleukin-6 (IL-6), monocyte chemotactic protein-1 (MCP-1), and tumor necrosis factor- $\alpha$  (TNF- $\alpha$ ) (9). Approximately 30% of the subcutaneously LPS injection leaves the injection site within an hour and the injected LPS is retained at the injection site for more than a month (10). The LPS retention decreases to 30% of the injected bolus by the post injection day 4 and then decreases at a slower rate to 6% by the post injection day 32 (10). Both acute and chronic inflammation may be achieved by injecting LPS subcutaneously.

A chronic high fat diet could increase endotoxemia during the digestion of dietary lipids and contributes to low-grade metabolic inflammation (4). Endotoxemia caused by periodontal gram-negative pathogens in patients with severe periodontitis facilitate the development of obesity in these people (11). The effects of the nutrient uptake on

metabolism could be used to break the link between the metabolic inflammation and obesity (2). A milk extract, rich in polar lipids, prevents the increase in intestinal permeability of fluorescein isothiocyanate-dextran (FITC-dextran) in mice stressed by intraperitoneal LPS (12). One type of milk polar lipids, sphingolipids, protect against the bacterial infections in the gut (13-15) and reduce the inflammatory response (16-19). Sphingomyelin (SM), one subfraction of the sphingolipids, plays an important role in neonatal gut maturation during the suckling period in rats (20). Another subfraction of the milk sphingolipids, gangliosides (GG), inhibits the degradation of gut occludin tight junction (TJ) protein during the LPS-induced acute inflammation (21). The GG affect the intestinal immune system maturation in mice during weaning (22). Taken together, dietary milk polar lipids may directly reduce systemic inflammation and may decrease inflammation by preventing the increase of gut permeability.

Cellular lipid loading may initiate inflammation through lipid mediators, which are precursors to inflammatory signaling molecules (23). High fat diets could result in nonalcoholic fatty liver disease (NAFLD) (24). According to the “two-hit” hypothesis by Day et al. (25), saturated fatty acids could be a first hit and LPS could be a second hit (26). The second hit leads to hepatic inflammation and non-alcoholic steatohepatitis (NASH) (27). LPS stress in combination with high fat diets may result in NAFLD/NASH (26). NAFLD is associated with low-grade systemic inflammation (28). NAFLD, gut leakiness and systemic inflammation could form a self-perpetuating cycle (Figure 1.1). The milk polar lipids reduce hepatic steatosis in mice fed a high fat diet (29). It would be

interesting to explore how milk polar lipids may affect liver lipid metabolism in mice fed a high fat diet and stressed by LPS.

This study was designed to test the hypotheses that dietary polar lipids may prevent the increase of gut permeability and plasma inflammatory cytokines, reduce liver lipid levels, and affect the expression of genes associated with fatty acid synthesis and cholesterol regulation in the liver during the acute and chronic inflammation induced by the subcutaneously injected lipopolysaccharide (LPS).

## **Materials and Methods**

### **Diets formulation**

Three diets were the same as described in Chapter 3 (Table 3.1): CO diet, GG diet and PL diet.

### **Animals and stresses**

Five-week-old male C57BL/6J mice (n = 18; Jackson Laboratory) were housed in single cages at a constant temperature of  $22 \pm 1$  °C with a 12-h light/dark cycle. They were allowed ad libitum access to diet and water. After one week's feeding on chow (for the acclimatization and the baseline data collection), mice were randomly assigned to one of the following treatments (Table 3.1): 1) CO diet (n = 6); 2) GG diet (n = 6); 3) PL diet (n = 6). The diet intake was monitored daily and the body weight was measured every other day. The body composition was assessed every week by using the magnetic resonance imaging (MRI) with an EchoMRI-900 Body Composition Analyzer (EchoMRI, Houston, TX).

The mice were fed the experimental diets for 2 weeks before they were challenged with the LPS injected subcutaneously (5 mg/kg body weight). The LPS injected intraperitoneally is absorbed at a faster rate compared with the LPS injected subcutaneously (10). To prevent lethal inflammatory response, the LPS was injected subcutaneously. The LPS injected subcutaneously at 2 mg/kg (7) and 10 mg/kg (8) body weight has induced intestinal stress and endotoxemia. Those mice were sacrificed within 24h and no animal death was reported. So a dose of 5 mg/kg body weight was chosen for this study to guarantee intestinal stress and prevent lethal effect. After the LPS injection and the oral gavage of sugar probes, 0.5 ml PBS was injected subcutaneously to facilitate the urine production. The animals were observed periodically during the following week to monitor the gross pathological changes, including the eye discharge. After the LPS challenge, all animals were fed the experimental diets for another 6 weeks. The experiments were conducted in conformity with the Public Health Service Policy on Humane Care and Use of Laboratory Animals and were approved by the Utah State University Institutional Animal Care and Use Committee.

### **Assessments of intestinal barrier integrity**

The intestinal permeability was assessed by using the FITC-dextran absorption test and the DST as described in Chapter 3. The FITC-dextran absorption test was done at the baseline, week 5 and 8. The DST was carried out at the baseline, week 3, 4, and 7.

### **Tissue sample collection**

The mice were sacrificed by CO<sub>2</sub> asphyxiation after a 4h fast. After the blood collection, the liver, the quadriceps muscle, the intestinal and colonic mucosa, the feces

and the adipose tissue samples were collected. The adipose depots included the gonadal, retroperitoneal, mesenteric, and subcutaneous depots. Each category of tissue was saved separately and the tissue mass was recorded. The tissue samples were flash frozen and stored at -80 °C until further analysis.

### **Biochemical analyses of plasma**

The blood samples were collected and the plasma were analyzed as described in Chapter 3 to measure the levels of glucose, insulin, leptin, resistin, MCP-1, IL-6, TNF- $\alpha$ , plasminogen activator inhibitor-1 (PAI-1) and endotoxin. The homeostasis model assessment of insulin resistance (HOMA-IR) index was calculated from the fasting glucose and insulin levels (fasting glucose\*fasting insulin/22.5) (30, 31).

### **Western Immunoblotting for zonula occludens (ZO)-1 and occludin proteins**

The mucosal samples of the small intestine and the colon were collected and the Western immunoblotting for the ZO-1 and occludin proteins were carried out as described in Chapter 3.

### **Liver gene expression analysis**

The expression of 13 genes associated with lipid metabolism in the liver was analyzed as described in Chapter 3.

### **Tissue lipid profiling**

The tissue lipid profiles of the liver, the skeletal muscle and the gonadal adipose were analyzed as described in Chapter 3. The lipid classes included phosphatidylethanolamine (PE), PC, phosphatidylserine (PS), and phosphatidylinositol (PI), SM, diglycerides (DG), free fatty acids (FFA), triglycerides (TG), and cholesteryl ester (CE).



### **GG analysis of intestinal mucosa**

The GG content in the intestinal mucosa was determined as describe in Chapter 3.

### **Statistical analyses**

One-way or mixed models analysis of variance (ANOVA) was performed by SAS 9.2. The group means were compared by Ryan-Einot-Gabriel-Welsch Multiple Range Test or Least Squares Means Contrast in SAS. The data were reported as Mean  $\pm$  Standard Error of the Mean (SEM).

### **Results**

There were no significant differences among the groups regarding the daily diet intake (Figure 4.1) and the total weight gain. The PL group had higher body weight at day 2 compared with the CO group (Figure 4.2a). The GG and PL groups had higher body fat percentage 3 days after the dietary treatments compared with the CO group and the difference was maintained during the rest of the study (diet effect:  $p = 0.03$ , Figure 4.2b).

Two mice from the GG group and two mice from the PL group died after the LPS stress (64-112 h after the LPS injection). For the data analysis after the LPS challenge, the following number of mice was used: CO,  $n = 6$ ; GG,  $n = 4$ ; PL,  $n = 4$ .

### **Tissue and plasma lipid profiles**

The PL group had lower liver mass ( $p = 0.01$ ) and lower liver/body weight percentage ( $p = 0.024$ ) compared with the CO group while the GG group was in the middle (Figure

4.3a). The GG group had less PE and PC in the visceral adipose tissue compared with the CO group. The GG group had less SM in the visceral adipose tissue than the PL group. The PL group had less TG and more PI in the skeletal muscle compared with the CO and GG groups. The GG and PL groups had more FFA and PI in the liver compared with the CO group ( $p < 0.05$ , Figure 4.3b). The GG increased hepatic expression of the beta-oxidation gene *Acaa2* (vs the CO & the PL). The PL suppressed hepatic expressions of the fatty acid synthesis gene *Acacb* and the cholesterol synthesis gene *Hmgcr* (vs the CO & the GG) ( $p < 0.05$ , Figure 4.3c). The PL group had less PE, PC and PL in the jejunum mucosa, less PE and PL in the colon mucosa, and less PE, PC and PL in the mucosa of the small intestine and the whole gut on a per organ basis compared with the other two groups ( $p < 0.05$ , Figure 4.4a). The PL group had lower level of gangliosides in the colon mucosa compared with the other two groups ( $p < 0.05$ , Figure 4.4b).

The plasma CE level was lower in the GG and PL groups at day 34 compared with the CO group ( $p < 0.05$ , Figure 4.5a). The plasma CE level decreased during day 34 and 57 ( $p < 0.05$ , Figure 4.5a). The plasma TG level decreased over time and there was no significant treatment effect (time effect  $p < 0.0001$ , Figure 4.5b). The plasma free fatty acids level decreased over time ( $p < 0.0001$ ) and the PL group had higher level at day 34 compared with the CO and GG groups ( $p = 0.04$ , Figure 4.5c). The plasma DG level increased slightly toward day 34 and decreased significantly from day 34 to 57 ( $p < 0.0001$ , Figure 4.5d). There was no diet effect for the plasma DG level.

### **Gut permeability**

The PL increased the expression of the TJ proteins ZO-1 and occludin in the colon mucosa compared with the CO and the GG (Figure 4.6a). The GG and the PL decreased the occludin expression in the jejunum mucosa compared with the CO (Figure 4.6a). The plasma FITC level decreased in the PL and GG groups during the study (Figure 4.6b). At day 34, the PL group had lower plasma FITC level compared with the CO and GG groups ( $p < 0.05$ ). Five weeks of feeding plus the LPS challenge two weeks after dietary treatment did not increase the plasma LPS level significantly in the CO and GG groups but increased the plasma LPS level in the PL group (Figure 4.6c). The plasma LPS level is strongly correlated with body fat mass in the PL group ( $r = -0.93$ ,  $p = 0.07$ ) but not in the CO ( $r = 0.55$ ,  $p = 0.26$ ) group and GG ( $r = -0.48$ ,  $p = 0.52$ ) group. The difference disappeared after the LPS levels were normalized by the body fat mass (Figure 4.6d). After 3 more weeks of experimental feeding post the LPS stress, the plasma LPS level increased significantly (Figure 4.6c).

The urinary Lactulose/Mannitol ratio increased significantly after the LPS challenge at day 18 and returned to the baseline level by day 44. There was no treatment effect (Figure 4.7a). The urinary Sucrose/Lactulose ratio decreased after the LPS challenge and increased during the rest of the study. The PL increased the urinary Sucrose/Lactulose ratio compared with the CO at day 29 and especially at day 44 (Figure 4.7b). The urinary Lactulose/Sucralose ratio increased after the LPS challenge and then returned to the baseline level. There was a trend of PL and GG increasing the urinary Lactulose/Sucralose ratio after the LPS stress and decreasing the ratio during the recovery

compared with CO (Figure 4.7c). The urinary Sucralose/Mannitol ratio did not change right after the LPS challenge and the Sucralose/Mannitol ratio increased significantly during the recovery. There was no treatment effect (Figure 4.7d).

### **Systemic inflammation and plasma cytokines**

All mice developed severe conjunctivitis 16h after the LPS stress as indicated by the bilateral purulent discharges (32). The plasma insulin level decreased toward day 34 and then stayed stable (Figure 4.8a). The plasma IL-6 level increased (measured at day 34) and then decreased (measured at day 57) but did not return to the baseline level. There was no treatment effect (Figure 4.8b). The plasma PAI-1 level increased slightly during the first 34 days and then increased at a higher rate toward the end of the study (Figure 4.8c). The plasma resistin level stayed stable during the first 34 days and then increased (Figure 4.8d).

Neither high fat feeding nor LPS challenge increased the plasma TNF- $\alpha$  level (Table 4.1). There was neither statistically significant time effect nor diet effect for the plasma levels of leptin and MCP-1 (Table 4.1).

### **Body fat changes**

The plots of body fat against fat-free mass indicated dynamic changes in the body fat mass during the course of the study (Figure 4.9a-j). When all measurements at 9 time points (at day -7, -1, 3, 5, 11, 23, 32, 39, 54) were included, there was no obvious segregation of the mice and the slope was 0.1 (Figure 4.9a). The slope was around 0 during the first MRI scan at day -7 (7 days before dietary intervention, Figure 4.9b). The

slope decreased to -0.5 at day -1 (Figure 4.9c) and then increased to 0.3 at day 3 and 0.4 at day 5 (Figure 4.9d & e). The slope dropped to 0 at day 11 and stayed around 0 at day 23 (Figure 4.9f & g). From day 23 to day 32, the slope increased to 0.08 (Figure 4.9h). The slope kept increasing to 0.62 at day 39 (Figure 4.9i) and 0.65 at day 54 (Figure 4.9j).

## Discussion

This study was designed to test the hypotheses that 1) the milk polar lipids prevent the increase of gut permeability, 2) reduce the plasma inflammatory cytokines, and 3) reduce the liver lipid level and affect the gene expression associated with the liver lipid metabolism in the C57BL/6J mice stressed with the subcutaneous LPS. The first and the second hypotheses were not supported by the data. The milk phospholipids decreased the occludin protein expression in the jejunum mucosa and increased the ZO-1 & occludin protein levels in the colon mucosa. The milk phospholipids increased the permeability of small intestine and the plasma LPS, and did not affect the plasma inflammatory cytokines. The milk gangliosides did not affect gut permeability and systemic inflammation. The data supported the third hypothesis. The milk phospholipids decreased the liver mass but did not affect liver TG. The milk phospholipids decreased hepatic expression of *Acacb* & *Hmgcr* and the plasma CE. Surprisingly the milk phospholipids decreased the PC & PE in the ileum mucosa and the PE & GG in the colon mucosa. The milk gangliosides decreased the adipose PE, PC & SM and the liver FFA & PI. The milk gangliosides increased hepatic expression of *Acaa2*.

The mouse model of LPS-induced inflammation and increased gut permeability was established in the context of moderately high fat diets. The LPS stress in combination

with the high fat diets increased gut permeability and plasma proinflammatory cytokine levels. The LPS stress reduced the plasma insulin level, blocked the accumulation of body fat, and increased the plasma IL-6 level. The experimental feeding increased the plasma LPS but did not raise the plasma cytokine levels.

The mice in the PL group gained more weight compared with the other groups by day 2 (Figure 4.2a). During the first 32 days, the PL and GG groups tended to have higher body weight (Figure 4.2a). The body fat percentage increase was blocked by the LPS challenge except in the PL group where the body fat percentage increased at day 23 (Figure 4.2b). Eventually the body fat percentage dropped in all groups and then started to increase back after day 39. The mean retention of the LPS injected subcutaneously is 73.4% after 6h, 49.1% after 3 days, 23.1% after 14 days, and less than 6% after 32 days in the injection site (10). The retained LPS can continuously stimulate B cells and macrophage lineage cells at the draining lymph node (10). The decrease of body fat percentage might be due to the persistent existence of the LPS and the resultant chronic inflammation.

The LPS stress decreased the plasma insulin level. While the C57BL/6J mice are prone to high fat diet-induced obesity (33) and the mice were fed a high fat diet in the present study, the mice did not gain body fat during the 6 weeks after the LPS stress. The mice gained considerable amount of the body weight during that period of time. Insulin plays an important role in increasing body fat storage (34). It is possible that the plasma insulin level after the LPS stress was sufficient in promoting animal growth but was not

high enough to stimulate body fat accumulation. It might be hypothesized that the decreased plasma insulin level may be responsible for the lack of the body fat accumulation.

The plasma insulin level decreased during the first 34 days and then increased toward the end of the study. The decrease of the plasma insulin may be caused by the injected LPS. The intraperitoneal injection of LPS at 10  $\mu\text{g}$  per mouse induces pancreatic cell damage in 10-week-old BALB/c male mice (35). The LPS injection caused low or a lack of insulin expression in the pancreatic islets as revealed by immunohistochemistry and RT-PCR. The expression of the insulin mRNA in the pancreatic tissues decreased to less than half of the original level during 3h and 6h after the LPS injection (35). The amount of the injected LPS was about 9% of the dose used in this study. Although the LPS was injected subcutaneously in this study, it may induce similar pancreatic damages due to the higher dose used. The intravenous injection of LPS decreased plasma insulin from 0.5 ng/ml at baseline to 0.2 ng/ml at day 11 in C57BL/6 mice fed the chow diet at 4 months of age (36). The proinflammatory cytokine, TNF- $\alpha$ , decreases serum insulin in mice. In C57BL/6 mice at 10–11 weeks of age, serum insulin level decreased from 1.3 ng/ml at 6 hrs to 0.6 ng/ml at 24 hrs after the intraperitoneal injection of TNF- $\alpha$  at a dose of 0.166 mg/kg (37). High fat feeding decreases plasma insulin level in rats. Plasma insulin level peaks at 6 nmol/L (34.8 ng/ml) on day 8 and decreases to 3.5 nmol/L (20.3 ng/ml) in female obese ZDF rats fed a high fat (48% energy) diet while the plasma insulin level stays at around 6 nmol/L (34.8 ng/ml) in the control group fed the rodent chow diet (38). The main cause for the decreased plasma insulin level in this study should have been the

LPS injection. Further studies are needed to clarify if the high-fat feeding itself may decrease the plasma insulin level in mice.

The plasma resistin level increased steadily throughout the course of the study in the GG group. The plasma resistin level decreased during the first 34 days and then increased toward the end of the study in the CO and PL groups. That could mean the resistin level was more influenced by the high fat diet than by the LPS stress and the GG tended to increase the plasma resistin level regardless of the background condition. As an adipocytokine secreted in proportion to obesity level, resistin counteracts the effects of insulin in mice (39). The GG may have negative effect on insulin action by increasing resistin.

Although the GG increased the expression of the beta-oxidation gene *Acaa2* in the liver (vs the CO & the PL, Figure 4.3c), the GG group had similar FFA level in the liver as the PL group and higher FFA level than the CO group. The PL suppressed hepatic expression of the fatty acid synthesis gene *Acacb* and the suppression did not decrease the FFA level in the liver.

The fact that the GG and PL groups had lower level of PE, PC and SM in the visceral adipose tissue than the CO group is surprising since the polar lipids groups had higher dietary content of PE, PC and SM. It was quite surprising that the PL group had lower PE, PC and PL in intestinal mucosa given the fact that the PL diet had much higher level of these polar lipid classes. This may indicate that dietary phospholipids suppress the



incorporation of luminal phospholipids into the mucosa. It is not clear through which mechanism did the dietary polar lipids affect the tissue polar lipids levels.

The plasma lipids stayed stable or increased slightly during the first 34 days and decreased significantly from day 34 to 57. The decrease of plasma lipids level may be associated with the increasing storage of body fat into adipose tissue after the inflammation was relieved.

The PL increased the expression of the TJ proteins ZO-1 and occludin in the colon mucosa compared with the CO and the GG and decreased the occludin expression in the jejunum mucosa compared with the CO. The increased amount of the TJ proteins in the PL group could decrease the permeability of colon but the PL group did not have lower plasma LPS level (Figure 4.6c) or different permeability to the sugar probes (Figure 4.7 a-d). The decrease of the jejunal occludin in the PL group was not associated with the increased gut permeability as indicated by the plasma LPS and FITC levels and the urinary sugar levels. Not only the amount of the TJ proteins but more importantly the distribution of the TJ proteins affects the intestinal permeability (40). The plasma LPS level was negatively correlated with the occludin level in the jejunum mucosa ( $r = -0.84$ ,  $p = 0.038$ ) in the CO group but not in the polar lipid groups. The decreased jejunal occludin level in the PL group may be compensated by other mechanisms provided by the PL that may increase the gut integrity.

The general trend of the decreased gut permeability to FITC in all groups may be explained by the maturing of the gut barrier during development since the mice barely entered adulthood (3 months old) by the end of study (41). The gut permeability to larger molecules was lower in the PL group compared with the other groups as indicated by the lower plasma FITC level. Although the difference was not statistically different, it is consistent with the result from a previous mouse study by Snow et al. where milk polar lipids concentrate prevented the increase in gut permeability to FITC during LPS stress (12). The plasma FITC level at day 35 was lower than the level at baseline. In the study by Snow et al., the gut permeability of FITC was assessed at 24 h and 48 h after the LPS stress. The plasma FITC level in the current study may have increased within 48 h after the LPS stress. To reduce stress level, the plasma FITC was not measured during that time when the mice were kept in the metabolic cages for 24h immediately after the LPS injection. Additional factors may contribute to the difference between the Snow's result and the current result. Firstly, the LPS was administered intraperitoneally and subcutaneously, respectively. Secondly, the milk polar lipids-rich material used in the Snow's study contained milk proteins and nonpolar lipids. That material was more complex than the milk polar lipids concentrate used in the current study. It is not clear how the PL may have decreased gut permeability to FITC. Given the fact that phospholipids are important building blocks of the gut epithelium, it may be hypothesized that the PL facilitate the maturing of the intestinal barrier.

The presence of bilateral purulent discharges in all mice was a good indicator of successful systemic inflammation induced by the bacterial LPS (42). The PL group had

higher level of the plasma LPS at day 34 and the difference disappeared after normalization by the body fat content. This indicates that the plasma LPS may be directly associated with the body fat mass. The plasma LPS level did not increase to a high level 3 weeks after the LPS challenge by day 34. There could be 6% of the injected LPS still retained at the injection site at day 34 (10). The low level of plasma LPS may indicate that the injected LPS did not contribute to the plasma LPS level at this time point. By the end of the study, the plasma LPS level reached a very high level and the injected LPS should have been gone by this time. The increased plasma LPS level at day 57 may not be contributed significantly by the injected LPS. The increase of the gut permeability to LPS was accompanied by the accumulation of body fat from day 40 to day 57.

The increase of the urinary Lactulose/Mannitol ratio is associated with increased small intestinal permeability (43). The LPS challenge increased the urinary Lactulose/Mannitol ratio significantly and the Lactulose/Mannitol ratio returned to the baseline level during the recovery. The urinary Sucrose/Lactulose ratio decreased right after the LPS stress and then increased gradually during the recovery. The decrease of the Sucrose/Lactulose ratio indicated distal damage of the small intestine. The damage became proximal when the Sucrose/Lactulose ratio increased to a high level (43). The LPS stress caused the permeability increase of distal small intestine and the experimental feeding increased the permeability of the proximal small intestine. The increased permeability of the proximal small intestine was coupled with the decreased expression of the TJ protein occludin in the jejunum mucosa. The urinary Lactulose/Sucralose ratio selectively increases upon intestinal damage and decreases upon colonic damage (43).

The Lactulose/Sucralose ratio increased significantly after the LPS stress, indicating the permeability increase for the small intestine. The Lactulose/Sucralose ratio dropped back below the baseline during the recovery for the GG and PL groups, which means the experimental feeding did not affect the small intestine permeability but caused the colonic damage. Combined with the indication of the Sucrose/Lactulose ratio, the permeability of the proximal small intestine may not affect the Lactulose/Sucralose ratio significantly. The colonic damage is coupled with the increase of the urinary Lactulose/Mannitol ratio (43). The LPS stress barely affected the Lactulose/Mannitol ratio and the feeding during the recovery increased the Lactulose/Mannitol ratio significantly. Taken together, the high-fat feeding in the context of systemic inflammation mainly resulted in the colonic damage while the LPS-induced systemic inflammation caused the permeability increase in the small intestine.

The rise of the urinary Sucralose/Mannitol ratio without the Lactulose/Mannitol ratio being affected indicated that the permeability of the colon increased (43). The increased colon permeability may result in an increase of the plasma LPS through the enhanced LPS absorption from the colon. The Sucralose/Mannitol ratio returned to the baseline level while the plasma LPS level increased significantly toward the end of the study. The high level of plasma LPS should have been contributed mainly by the LPS absorbed through the gut.

The PAI-1 level in plasma increased slightly during the first five weeks and increased at a faster rate during the last three weeks of the study. The plasma PAI-1 level became

much higher in the PL group by the end of the study compared with the CO and GG groups. Lysophosphatidylcholine (LPC) in oxidized low-density lipoprotein (OxLDL) enhances the PAI-1 expression in mouse 3T3-L1 adipocytes (44). The extra increase of the plasma PAI-1 level in the PL group may be caused by the metabolites of the dietary PC.

The plasma IL-6 level increased significantly after the LPS stress and receded to the baseline level by the end of the experiment. The increased plasma IL-6 level could be due to the activation of the TLR4 (45) by the increased plasma saturated fatty acids level. But the plasma fatty acids level decreased in all groups during the experimental feeding. Although the change of the fatty acid profile is yet to be determined, the increased IL-6 level at week 3 (day 34) after the LPS stress may be due to the LPS challenge. The plasma IL-6 level was not in parallel with the high plasma LPS level at the end. This could mean that the LPS absorbed from the gut is not as proinflammatory as the injected LPS. The intestinal LPS may have been deactivated. The intestinal alkaline phosphatase (IAP) secreted by the enterocytes detoxifies the intestinal LPS by dephosphorylation of the lipid A moiety (46, 47). The IAPs reduce the serum LPS content in Wistar male rats (48). The IAPs affect both the toxicity and the concentration of the LPS in the plasma. It is not clear whether the IAPs reduced plasma LPS in this study. The LPS is absorbed gradually from the gut into the circulation. The tolerance to the LPS could also help explain the lack of proinflammatory response by the LPS absorbed from the gut. The tolerance to LPS-induced increase of serum colony-stimulating factor develops in C57BL/6J mice after either intravenous or intraperitoneal injection of LPS and the

tolerance occurs after one to two preinjections (49). The inhaled low-dose LPS can induce adaptation to subsequent higher doses for cellular and inflammatory parameters in bronchoalveolar lavage from young and old C57BL/6J mice (50). A third explanation is that the plasma LPS may be deactivated by anti-LPS antibodies (51). It is not clear if the anti-LPS antibodies involved in the process of deactivating the plasma LPS that were absorbed from the gut.

The plots of body fat against fat-free mass suggested that stresses may have considerable effect on body fat content in the C57BL/6J mice. The second MRI scan (at day -1) was carried out right after the first DST (at day -2). The housing in the metabolic cage reduced the adiposity as indicated by the decreased slope (Figure 4.9b & c). Once the stress was removed, the body fat increased back within a week (Figure 4.9d & e). The LPS stress decreased the body fat content as indicated by the decreased slope (Figure 4.9g). The third DST also decreased the body fat content (Figure 4.9h). During the following recovery the body fat content kept increasing (Figure 4.9i & j). Based on these observations, it is important to prevent unnecessary stresses and make sure the animals are handled in the same manner to reduce variances caused by the potential variability in the stresses.

The LPS induced inflammation model in this study had two phases, the acute and chronic stages. Dietary milk polar lipids did not protect the gut integrity during the acute phase, 24 h after LPS injection. The LPS was injected subcutaneously and the LPS can be retained in the body until a month later (10). In the context of chronic inflammatory stress

induced by the LPS in young C57BL/6J mice, gut permeability to large molecules decreased and to small molecules increased. High fat feeding increased the plasma level of resistin and plasma resistin level could also increase over time in C57BL/6J mice (52). The milk GG decreased gut permeability and increased the hepatic gene expression of *Acaa2*. The milk PL had complex effect on gut permeability, decreased the liver mass, and suppressed the hepatic gene expression of *Acacb* and *Hmgcr*. The milk polar lipids were provided as semi-purified concentrates containing multiple compounds. Further studies are needed to explore which components of the polar lipids are responsible for the observed effects. The LPS dosage may be slightly decreased (e.g., at 2.5-3 mg/kg body weight) to prevent animal death for chronic studies.

## Summary

The major effects of the dietary polar lipids during the LPS-induced inflammation are summarized in Figure 4.10. The dietary PL increased the plasma LPS level and the permeability of the small intestine. The PL decreased the liver mass and affected hepatic expression of genes associated with fatty acid and cholesterol synthesis. The PL did not affect the plasma inflammatory cytokines. The GG slightly affected lipid metabolism and did not affect the gut permeability and the systemic inflammation.

Although the results support the hypotheses that the polar lipids may have positive effects on lipid metabolism and negative or no effects on gut permeability and systemic inflammation in the ob/ob mice, the effects of the polar lipids on other biological functions are still unclear. Before systematic investigations of all major biological

endpoints are done on the main organ systems in the ob/ob mice, comprehensive and conclusive statements cannot be generated regarding the effects of dietary polar lipids.

The experimental feeding and the LPS stress together resulted in increased gut permeability to small molecules, increased body weight and decreased body fat content, and increased the plasma LPS and inflammatory cytokines (Figure 4.10). The data from the current study indicated that the acute and chronic inflammation induced by the subcutaneously injected LPS is a great animal model for studying systemic inflammation and gut permeability. The increased LPS absorption from the gut into the plasma was not accompanied by the increase of the plasma proinflammatory cytokines but the injected LPS increased the systemic inflammation. The LPS stress decreased the plasma insulin level. The decrease of the plasma insulin level may have increased the body weight without increasing the body fat content. It may be hypothesized that the insulin level may be intervened for controlling the body fat content.

## References

1. Ogden CL, Carroll MD, Kit BK, Flegal KM. Prevalence of obesity in the United States, 2009-2010. *NCHS Data Brief* 2012;1-8.
2. Johnson AR, Justin Milner J, Makowski L. The inflammation highway: metabolism accelerates inflammatory traffic in obesity. *Immunol Rev* 2012;249:218-38.
3. Suzuki T, Hara H. Dietary fat and bile juice, but not obesity, are responsible for the increase in small intestinal permeability induced through the suppression of



- tight junction protein expression in LETO and OLETF rats. *Nutr Metab (Lond)* 2010;7:19.
4. Laugerette F, Vors C, Peretti N, Michalski MC. Complex links between dietary lipids, endogenous endotoxins and metabolic inflammation. *Biochimie* 2011;93(1):39-45.
  5. Dial EJ, Zayat M, Lopez-Storey M, Tran D, Lichtenberger L. Oral phosphatidylcholine preserves the gastrointestinal mucosal barrier during LPS-induced inflammation. *Shock* 2008;30:729-33.
  6. Braun A, Treede I, Gotthardt D, et al. Alterations of phospholipid concentration and species composition of the intestinal mucus barrier in ulcerative colitis: a clue to pathogenesis. *Inflamm Bowel Dis* 2009;15:1705-20.
  7. Mathan VI, Penny GR, Mathan MM, Rowley D. Bacterial lipopolysaccharide-induced intestinal microvascular lesions leading to acute diarrhea. *J Clin Invest* 1988;82:1714-21.
  8. Wang Q, Wang JJ, Fischer JE, Hasselgren PO. Mucosal production of complement C3 and serum amyloid A is differentially regulated in different parts of the gastrointestinal tract during endotoxemia in mice. *J Gastrointest Surg* 1998;2:537-46.
  9. Nandi D, Mishra MK, Basu A, Bishayi B. Protective effects of interleukin-6 in lipopolysaccharide (LPS)-induced experimental endotoxemia are linked to alteration in hepatic anti-oxidant enzymes and endogenous cytokines. *Immunobiology* 2009.

10. Yokochi T, Inoue Y, Yokoo J, Kimura Y, Kato N. Retention of bacterial lipopolysaccharide at the site of subcutaneous injection. *Infection and Immunity* 1989;57:1786-91.
11. Saito T, Hayashida H, Furugen R. Comment on: Cani et al. (2007) Metabolic endotoxemia initiates obesity and insulin resistance: *Diabetes* 56:1761-1772. *Diabetes* 2007;56:e20; author reply e21.
12. Snow DR, Ward RE, Olsen A, Jimenez-Flores R, Hintze KJ. Membrane-rich milk fat diet provides protection against gastrointestinal leakiness in mice treated with lipopolysaccharide. *J Dairy Sci* 2011;94:2201-12.
13. Pfeuffer M, Schrezenmeir J. Dietary sphingolipids: metabolism and potential health implications. *Kieler Milchw Forsch* 2001;53:31-42.
14. Vesper H, Schmelz EM, Nikolova-Karakashian MN, Dillehay DL, Lynch DV, Merrill AH. Sphingolipids in food and the emerging importance of sphingolipids to nutrition. *J Nutr* 1999;129:1239-50.
15. Clare DA, Zheng Z, Hassan HM, Swaisgood HE, Catignani GL. Antimicrobial properties of milkfat globule membrane fractions. *J Food Prot* 2008;71:126-33.
16. Dalbeth N, Gracey E, Pool B, et al. Identification of dairy fractions with anti-inflammatory properties in models of acute gout. *Ann Rheum Dis* 2010;69:766-9.
17. El Alwani M, Wu BX, Obeid LM, Hannun YA. Bioactive sphingolipids in the modulation of the inflammatory response. *Pharmacol Ther* 2006;112:171-83.
18. Park EJ, Suh M, Thomson B, et al. Dietary ganglioside inhibits acute inflammatory signals in intestinal mucosa and blood induced by systemic inflammation of *Escherichia coli* lipopolysaccharide. *Shock* 2007;28:112-7.

19. Park EJ, Suh M, Thomson B, Thomson AB, Ramanujam KS, Clandinin MT. Dietary ganglioside decreases cholesterol content, caveolin expression and inflammatory mediators in rat intestinal microdomains. *Glycobiology* 2005;15:935-42.
20. Motouri M, Matsuyama H, Yamamura J, et al. Milk sphingomyelin accelerates enzymatic and morphological maturation of the intestine in artificially reared rats. *J Pediatr Gastroenterol Nutr* 2003;36:241-7.
21. Park EJ, Thomson AB, Clandinin MT. Protection of intestinal occludin tight junction protein by dietary gangliosides in lipopolysaccharide-induced acute inflammation. *J Pediatr Gastroenterol Nutr* 2010;50:321-8.
22. Vazquez E, Gil A, Rueda R. Dietary gangliosides positively modulate the percentages of Th1 and Th2 lymphocyte subsets in small intestine of mice at weaning. *Biofactors* 2001;15:1-9.
23. Iyer A, Fairlie DP, Prins JB, Hammock BD, Brown L. Inflammatory lipid mediators in adipocyte function and obesity. *Nat Rev Endocrinol* 2010;6:71-82.
24. Hebbard L, George J. Animal models of nonalcoholic fatty liver disease. *Nature reviews. Gastroenterology & Hepatology* 2011;8:35-44.
25. Day CP, James OF. Steatohepatitis: a tale of two "hits"? *Gastroenterology* 1998;114:842-5.
26. Csak T, Ganz M, Pespisa J, Kodys K, Dolganiuc A, Szabo G. Fatty acid and endotoxin activate inflammasomes in mouse hepatocytes that release danger signals to stimulate immune cells. *Hepatology* 2011;54:133-44.

27. Gentile CL, Pagliassotti MJ. The role of fatty acids in the development and progression of nonalcoholic fatty liver disease. *J Nutr Biochem* 2008;19:567-76.
28. Haukeland JW, Damas JK, Konopski Z, et al. Systemic inflammation in nonalcoholic fatty liver disease is characterized by elevated levels of CCL2. *J Hepatol* 2006;44:1167-74.
29. Wat E, Tandy S, Kapera E, et al. Dietary phospholipid-rich dairy milk extract reduces hepatomegaly, hepatic steatosis and hyperlipidemia in mice fed a high-fat diet. *Atherosclerosis* 2009;205:144-50.
30. Matthews DR, Hosker JP, Rudenski AS, Naylor BA, Treacher DF, Turner RC. Homeostasis model assessment: insulin resistance and beta-cell function from fasting plasma glucose and insulin concentrations in man. *Diabetologia* 1985;28:412-9.
31. Wallace TM, Levy JC, Matthews DR. Use and abuse of HOMA modeling. *Diabetes Care* 2004;27:1487-95.
32. Kardon R, Price RE, Julian J, et al. Bacterial conjunctivitis in Muc1 null mice. *Invest Ophthalmol Vis Sci* 1999;40:1328-35.
33. Takahashi M, Ikemoto S, Ezaki O. Effect of the fat/carbohydrate ratio in the diet on obesity and oral glucose tolerance in C57BL/6J mice. *J Nutr Sci Vitaminol (Tokyo)* 1999;45:583-93.
34. Dimitriadis G, Mitrou P, Lambadiari V, Maratou E, Raptis SA. Insulin effects in muscle and adipose tissue. *Diabetes res and Clinical Practice* 2011;93 Suppl 1:S52-9.

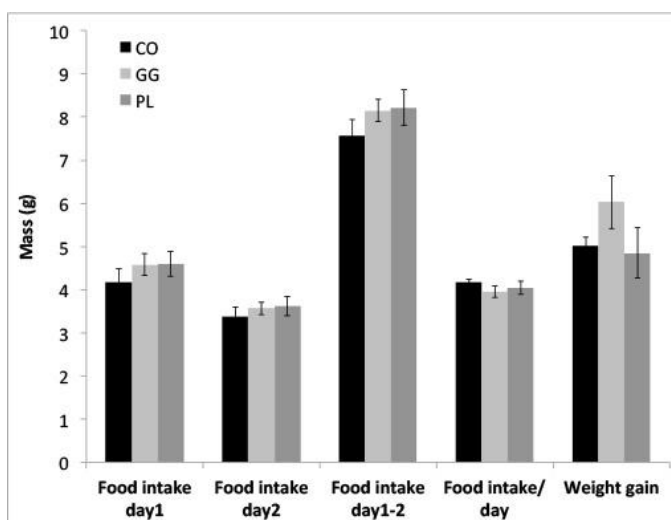
35. Saitoh N, Awaya A, Sakudo A, et al. Serum thymic factor prevents LPS-induced pancreatic cell damage in mice via up-regulation of Bcl-2 expression in pancreas. *Microbiology and Immunology* 2004;48:629-38.
36. Tweedell A, Mulligan KX, Martel JE, Chueh FY, Santomango T, McGuinness OP. Metabolic response to endotoxin in vivo in the conscious mouse: role of interleukin-6. *Metabolism: Clinical and Experimental* 2011;60:92-8.
37. Endo M, Masaki T, Seike M, Yoshimatsu H. TNF-alpha induces hepatic steatosis in mice by enhancing gene expression of sterol regulatory element binding protein-1c (SREBP-1c). *Experimental Biology and Medicine* 2007;232:614-21.
38. Teague J, Gyte A, Peel JE, et al. Reversibility of hyperglycaemia and islet abnormalities in the high fat-fed female ZDF rat model of type 2 diabetes. *J Pharmacological and Toxicological Methods* 2011;63:15-23.
39. Inadera H. The usefulness of circulating adipokine levels for the assessment of obesity-related health problems. *Int J Med Sci* 2008;5:248-62.
40. Ferraris RP, Vinnakota RR. Intestinal nutrient transport in genetically obese mice. *Am J Clin Nutr* 1995;62:540-6.
41. Flurkey K, Curren JM, Harrison DE. The mouse in aging research. In: Fox JG, Davisson MT, Quimby FW, Barthold SW, Newcomer CE, Smith AL, (eds). *The Mouse in Biomedical Research*. Elsevier: Burlington, MA: 2007. pp 637-72.
42. Senaratne T, Gilbert C. Conjunctivitis. *Community Eye Health* 2005;18:73-5.
43. Meddings JB, Gibbons I. Discrimination of site-specific alterations in gastrointestinal permeability in the rat. *Gastroenterology* 1998;114:83-92.

44. Kuniyasu A, Tokunaga M, Yamamoto T, et al. Oxidized LDL and lysophosphatidylcholine stimulate plasminogen activator inhibitor-1 expression through reactive oxygen species generation and ERK1/2 activation in 3T3-L1 adipocytes. *Bba-Mol Cell Biol L* 2011;1811:153-62.
45. Laugerette F, Furet JP, Debard C, et al. Oil composition of high-fat diet affects metabolic inflammation differently in connection with endotoxin receptors in mice. *Am J Physiol Endocrinol Metab* 2012;302:E374-86.
46. Poelstra K, Bakker WW, Klok PA, Hardonk MJ, Meijer DK. A physiologic function for alkaline phosphatase: endotoxin detoxification. *Lab Invest* 1997;76:319-27.
47. Poelstra K, Bakker WW, Klok PA, Kamps JA, Hardonk MJ, Meijer DK. Dephosphorylation of endotoxin by alkaline phosphatase in vivo. *Am J Pathol* 1997;151:1163-9.
48. Koyama I, Matsunaga T, Harada T, Hokari S, Komoda T. Alkaline phosphatases reduce toxicity of lipopolysaccharides in vivo and in vitro through dephosphorylation. *Clinical Biochemistry* 2002;35:455-61.
49. Quesenberry P, Halperin J, Ryan M, Stohlman F, Jr. Tolerance to the granulocyte-releasing and colony-stimulating factor elevating effects of endotoxin. *Blood* 1975;45:789-800.
50. Elder AC, Finkelstein J, Johnston C, Gelein R, Oberdorster G. Induction of adaptation to inhaled lipopolysaccharide in young and old rats and mice. *Inhalation Toxicology* 2000;12:225-43.

51. Poxton IR. Antibodies to lipopolysaccharide. *J Immunological Methods* 1995;186:1-15.
52. Moreira AP, Texeira TF, Ferreira AB, do Carmo Gouveia Peluzio M, de Cassia Goncalves Alfenas R. Influence of a high-fat diet on gut microbiota, intestinal permeability and metabolic endotoxaemia. *Br J Nutr* 2012;108:801-9.

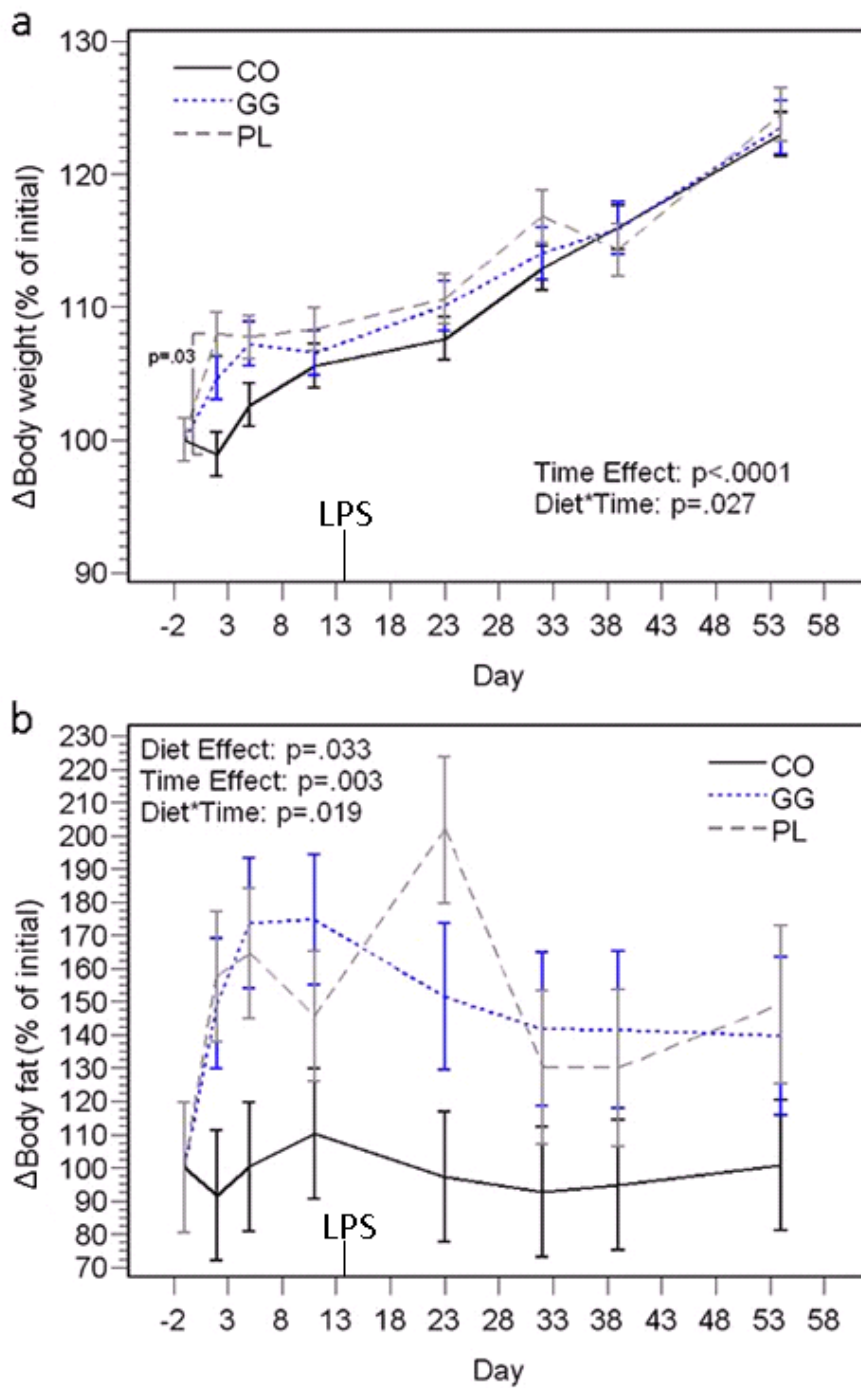
**Table 4.1** Effects of milk polar lipids on plasma levels of leptin, MCP-1 and TNF- $\alpha$  in mice challenged with LPS (Mean  $\pm$  SEM; unit: Log<sub>10</sub>(pg/ml)).

Lipids	CO	GG	PL
<b>Baseline</b>			
Leptin	3.13 $\pm$ 0.05	3.11 $\pm$ 0.11	3.03 $\pm$ 0.14
MCP-1	1.61 $\pm$ 0.03	1.50 $\pm$ 0.08	1.52 $\pm$ 0.05
TNF- $\alpha$	1.49 $\pm$ 0.02	1.45 $\pm$ 0.03	1.46 $\pm$ 0.03
<b>Day 34</b>			
Leptin	3.44 $\pm$ 0.14	3.34 $\pm$ 0.06	3.09 $\pm$ 0.10
MCP-1	1.55 $\pm$ 0.08	1.54 $\pm$ 0.13	1.53 $\pm$ 0.13
TNF- $\alpha$	1.39 $\pm$ 0.02	1.42 $\pm$ 0.02	1.45 $\pm$ 0.05
<b>Day 57</b>			
Leptin	3.76 $\pm$ 0.19	3.50 $\pm$ 0.14	3.46 $\pm$ 0.11
MCP-1	1.60 $\pm$ 0.03	1.55 $\pm$ 0.06	1.54 $\pm$ 0.05
TNF- $\alpha$	1.46 $\pm$ 0.03	1.38 $\pm$ 0.05	1.49 $\pm$ 0.03

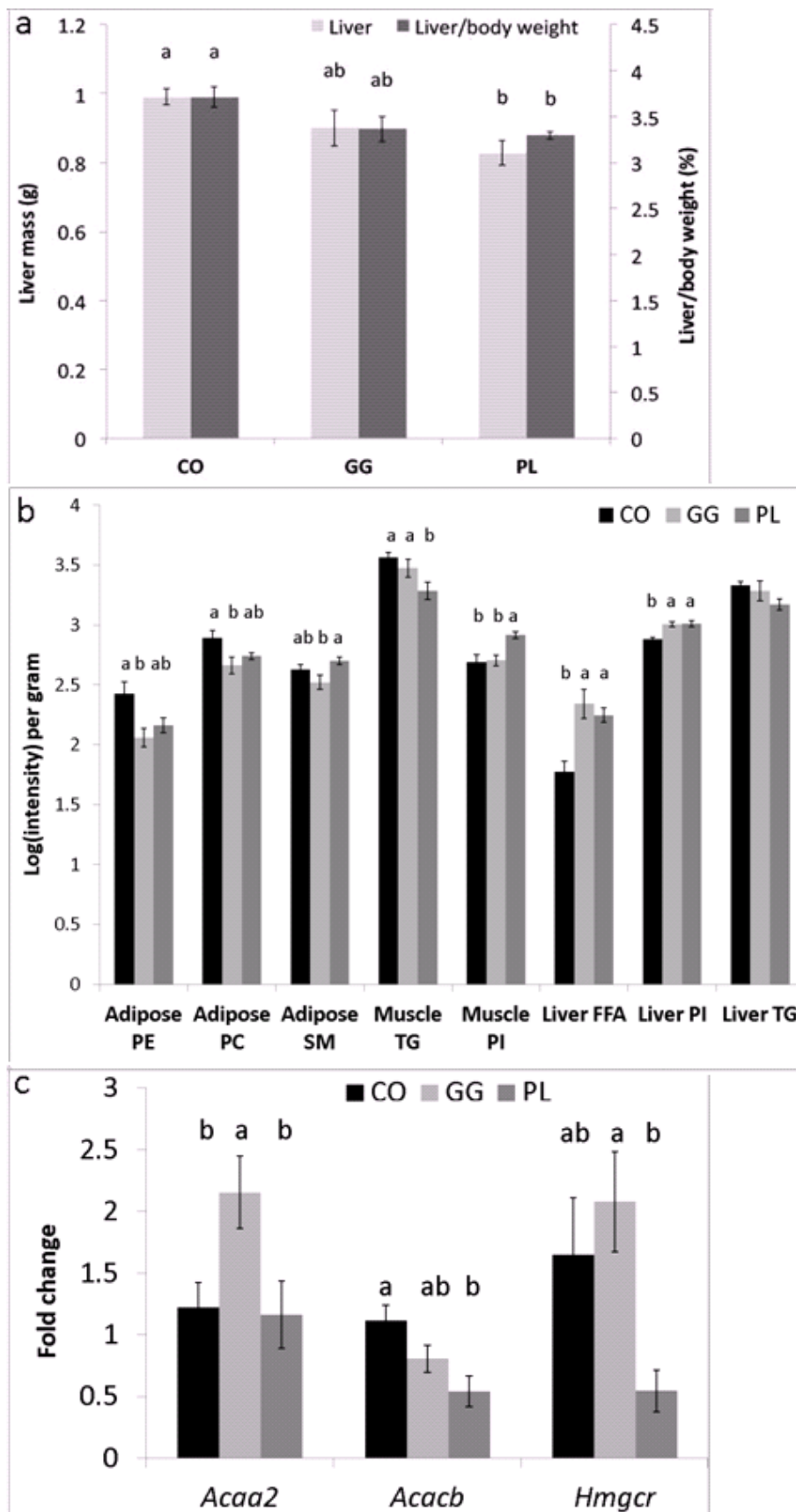


**Figure 4.1** Dietary milk polar lipids did not significantly affect food intake during the first two days, daily food intake during the study, and weight gain. The data represent mean  $\pm$  SEM.

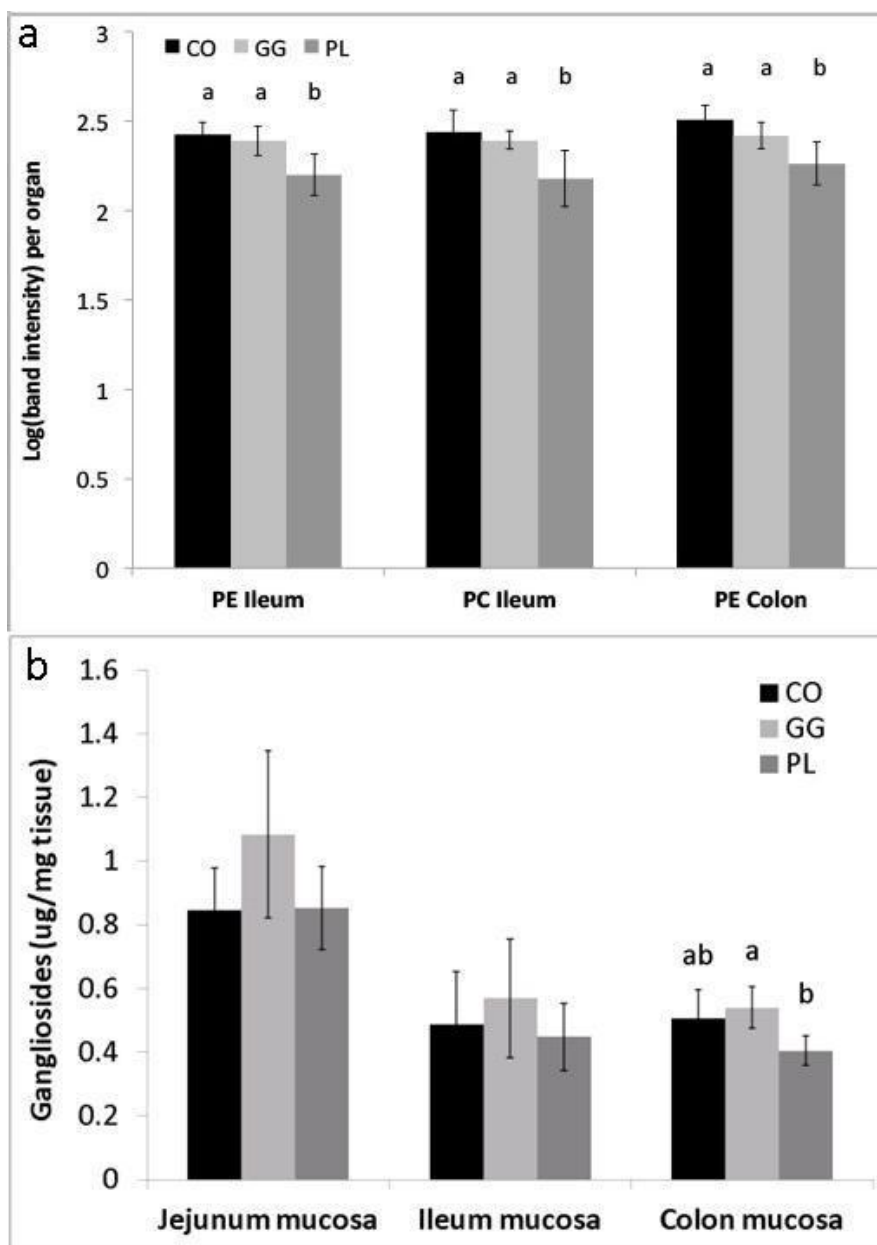




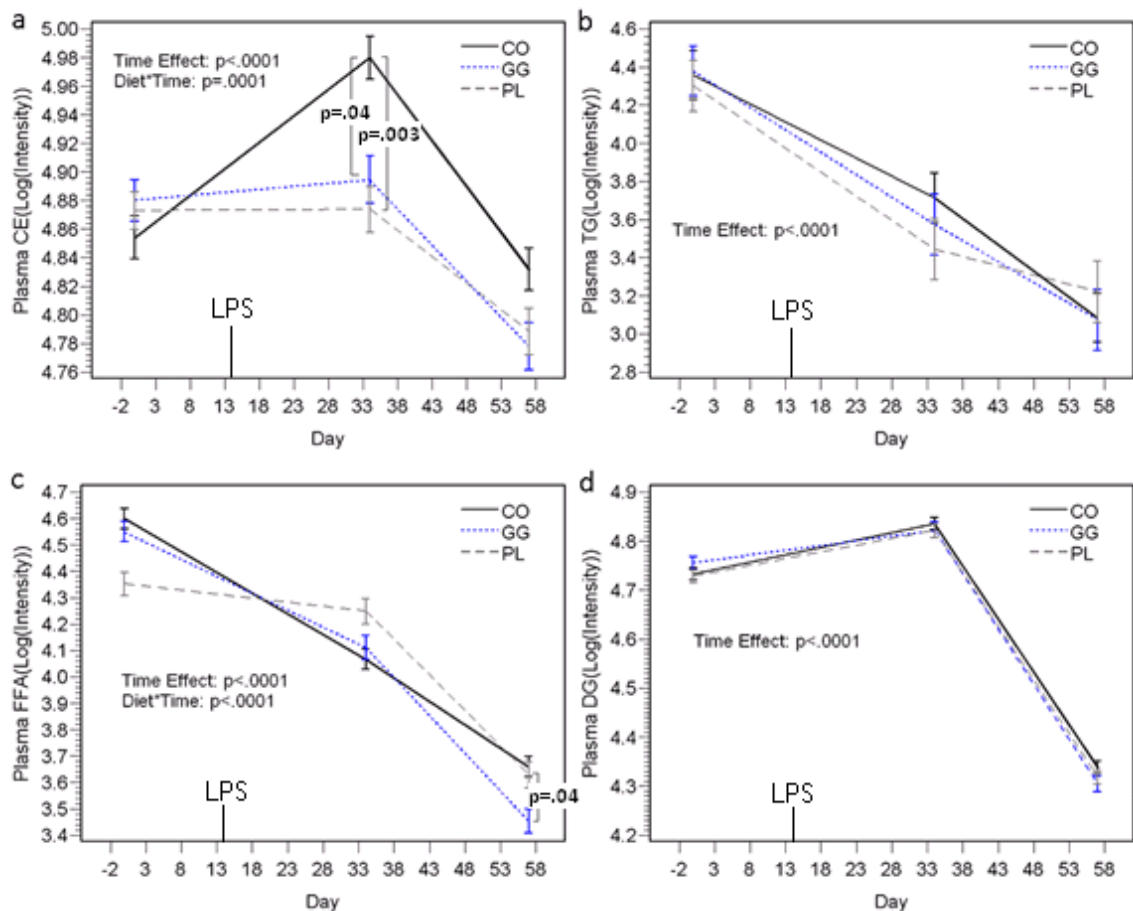
**Figure 4.2** Effects of the polar lipids on body weight and body fat content. Initial body weight for CO, GG and PL groups:  $22.0 \pm 0.2$ ,  $21.9 \pm 1.0$ ,  $21.1 \pm 0.2$  (g). Initial body fat for CO, GG and PL groups:  $2.14 \pm 0.31$ ,  $2.28 \pm 0.14$ ,  $2.14 \pm 0.18$  (g). (a) Body weight changes as percentage of baseline. (b) Body fat changes as percentages of baseline. The data represent mean  $\pm$  SEM.



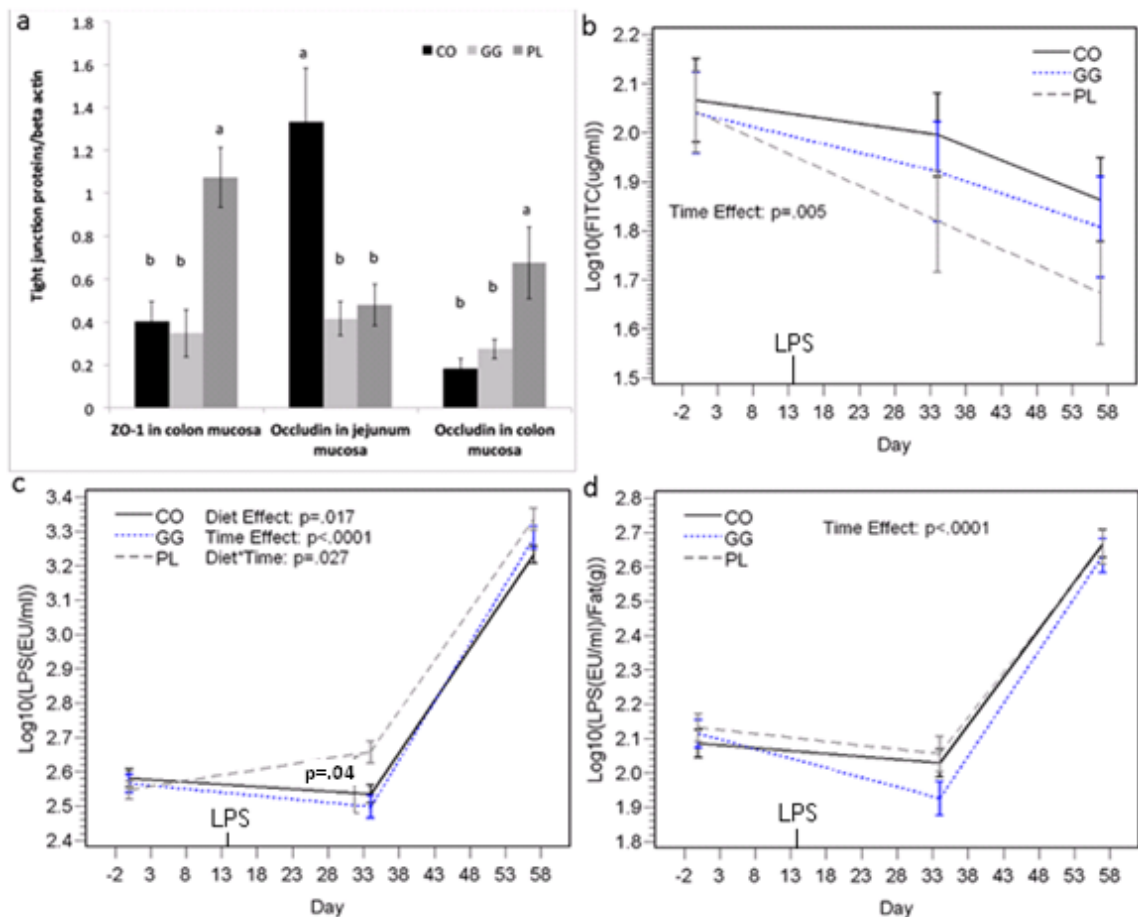
**Figure 4.3** Effects of milk polar lipids on liver mass, tissue lipid profile, and gene expression associated with lipid metabolism in the liver. The data represent mean  $\pm$  SEM. (a) GG and esp. PL decreased liver mass. (b) GG decreased PE, PC & SM in adipose, PL decreased TG and increased PI in muscle, GG and PL increased FFA and PI in the liver. (c) GG up regulated *Acaa2*, *Acacb* and *Hmgcr* compared with PL. Means in a row with different superscripts are significantly different ( $p < 0.05$ ).



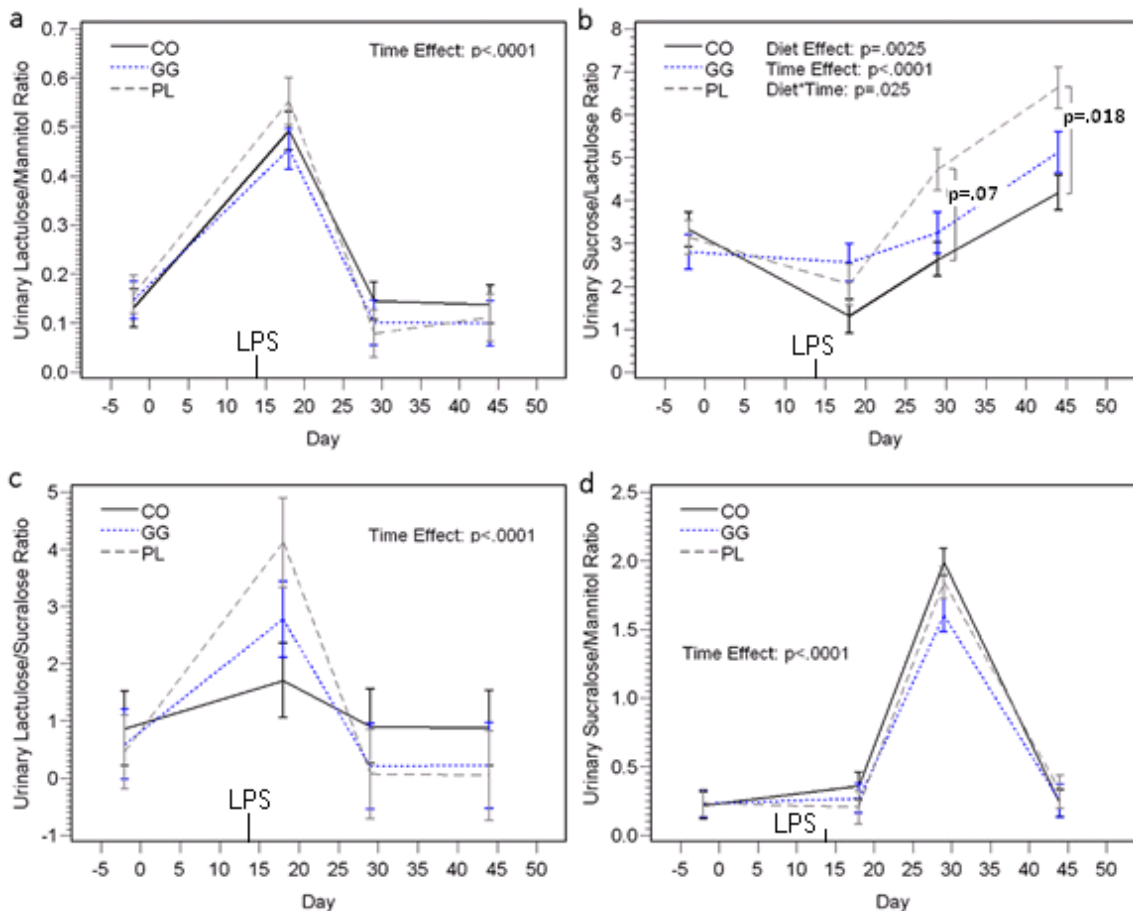
**Figure 4.4** Effects of milk polar lipids on PL and GG content in intestinal mucosa. The data represent mean  $\pm$  SEM. (a) PL decreased PE, PC & PL in ileum mucosa and PE & PL in colon mucosa compared with CO and GG. (b) PL decreased GG level in colon mucosa compared with CO and GG. Means in a row with different superscripts are significantly different ( $p < 0.05$ ).



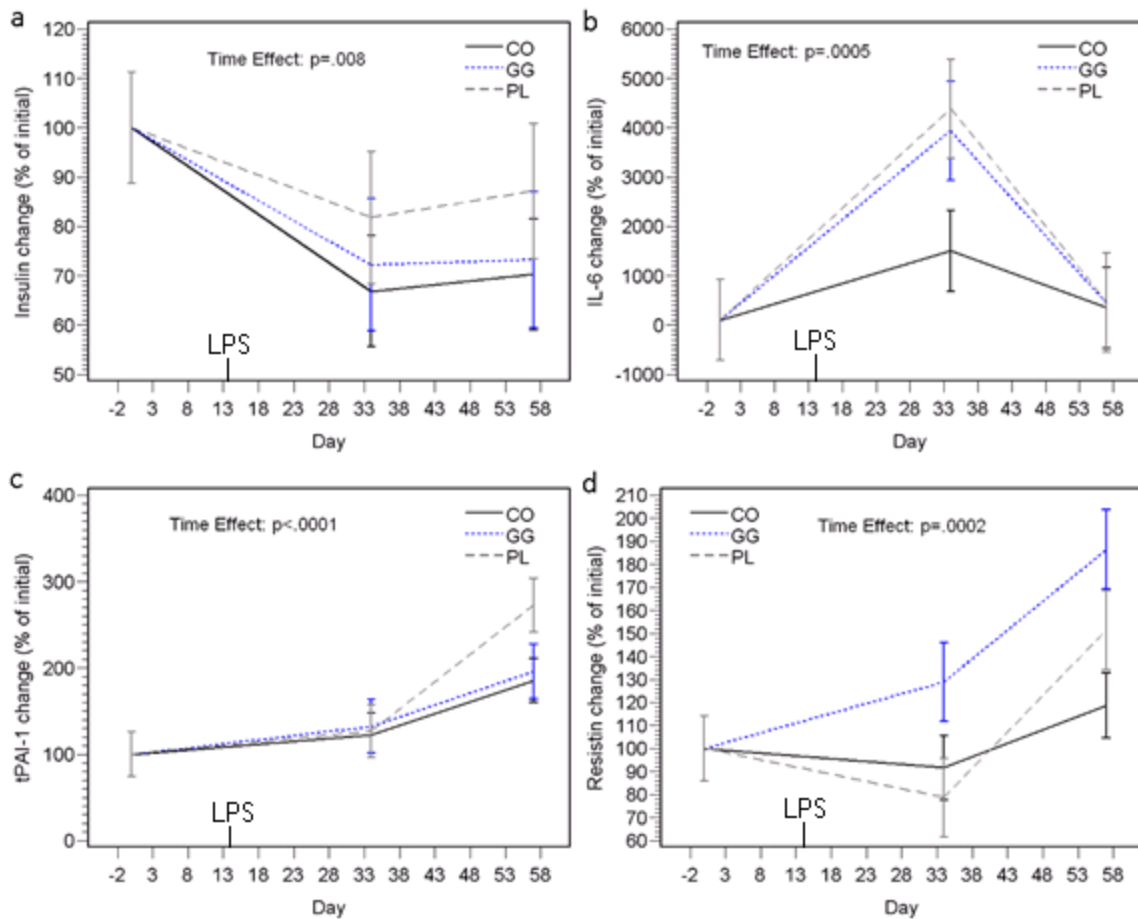
**Figure 4.5** Effects of milk polar lipids on plasma lipid profile. The data represent mean  $\pm$  SEM. (a) GG and PL groups had lower plasma CE level at day 34 compared with CO. (b) Plasma TG level decreased over time. (c) Plasma FFA level decreased over time and PL group had higher plasma FFA at day 34. (d) Plasma DG level increased at day 34 and decreased significantly at day 57.



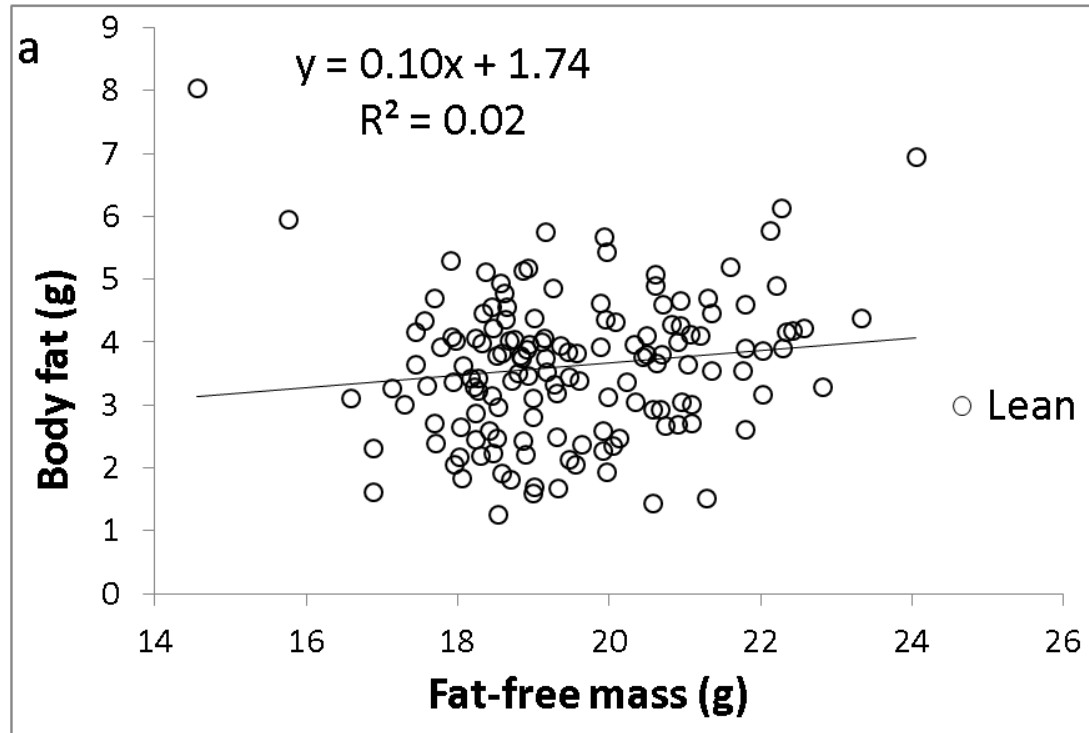
**Figure 4.6** Effects of milk polar lipids on gut permeability. The data represent mean  $\pm$  SEM. (a) PL increased ZO-1 and occludin expression in colon mucosa, PL and GG decreased occludin expression in jejunum mucosa. (b) Plasma FITC decreased over time. (c) PL increased plasma LPS level at day 34 and LPS level increased significantly by the end of the study. (d) The effect of PL on LPS at day 34 disappeared after normalization by body fat mass. Means in a row with different superscripts are significantly different ( $p < 0.05$ ).



**Figure 4.7** Effects of milk polar lipids on gut permeability as revealed by differential sugar probes test. The data represent mean  $\pm$  SEM. (a) Urinary Lactulose/Mannitol ratio increased after LPS stress and returned to baseline level during recovery. (b) Urinary Sucrose/Lactulose ratio decreased after LPS stress and increased gradually during recovery. (c) Urinary Lactulose/Sucralose ratio increased after LPS stress and returned to baseline level during recovery. (d) Urinary Sucralose/Mannitol ratio did not increase after LPS stress, increased during recovery and returned to baseline level by the end of the study.

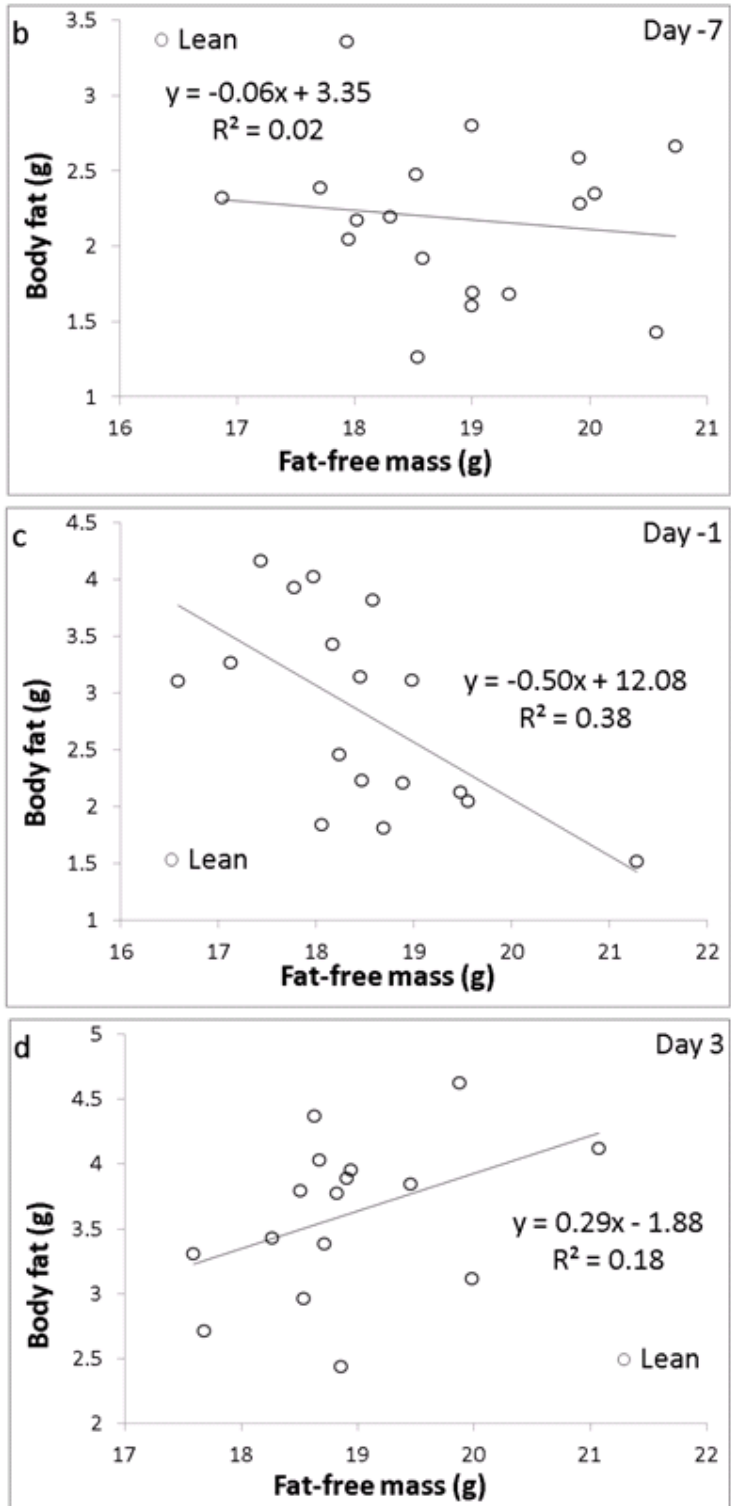


**Figure 4.8** Effects of milk polar lipids on plasma cytokines. The data represent mean  $\pm$  SEM. (a) Plasma insulin level decreased. (b) Plasma IL-6 level increased after LPS stress and returned to baseline level by the end of the study. (c) Plasma PAI-1 level increased. (d) Plasma resistin level increased.

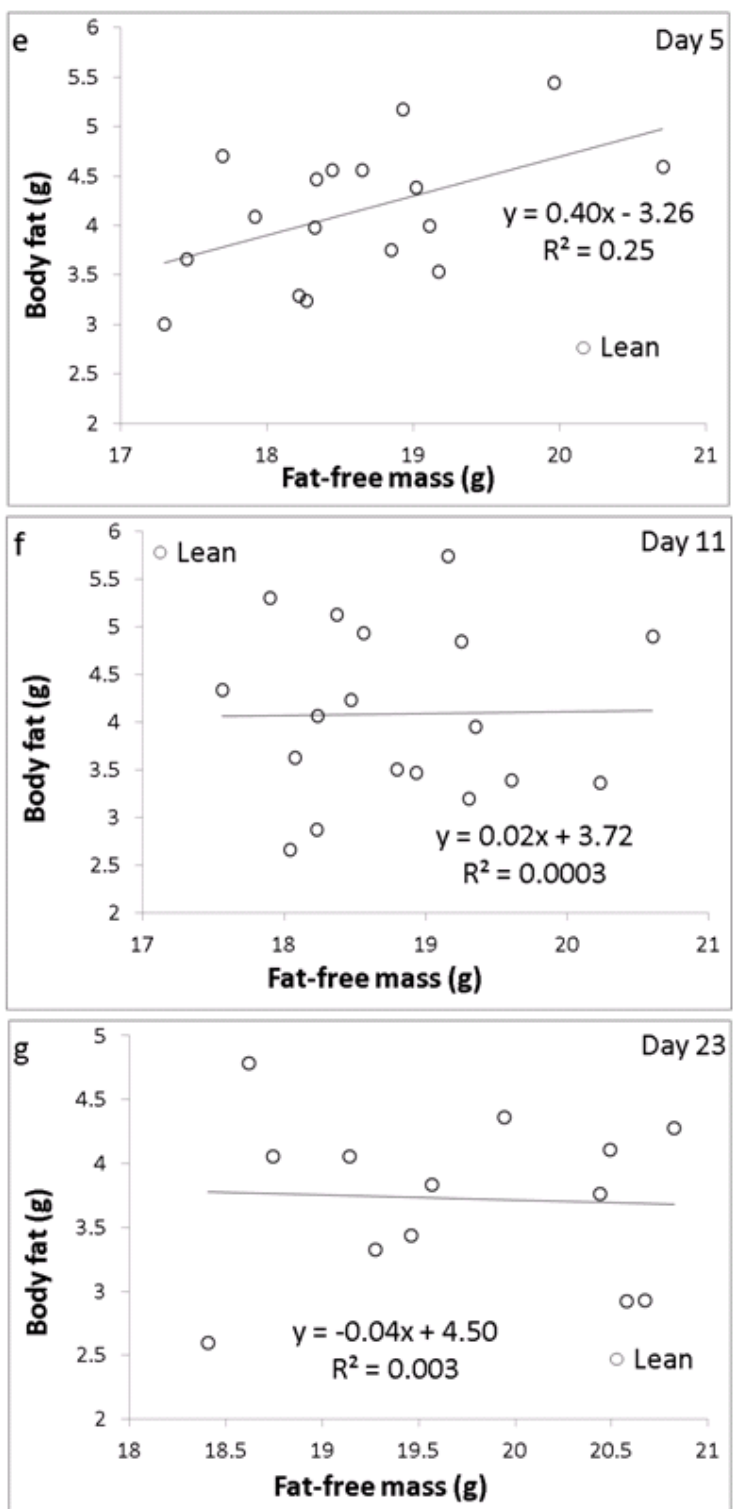


**Figure 4.9a** Body fat plotted against fat-free mass for individual animals during day -7 through day 54.

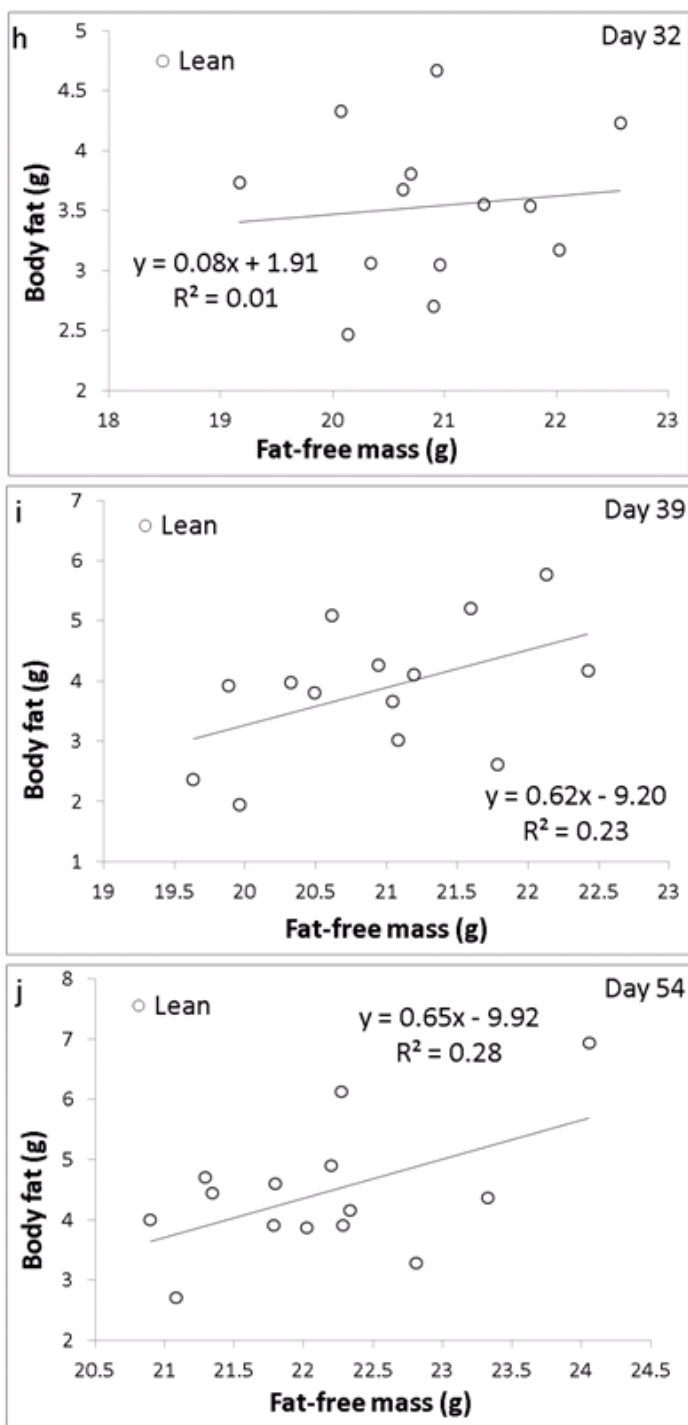




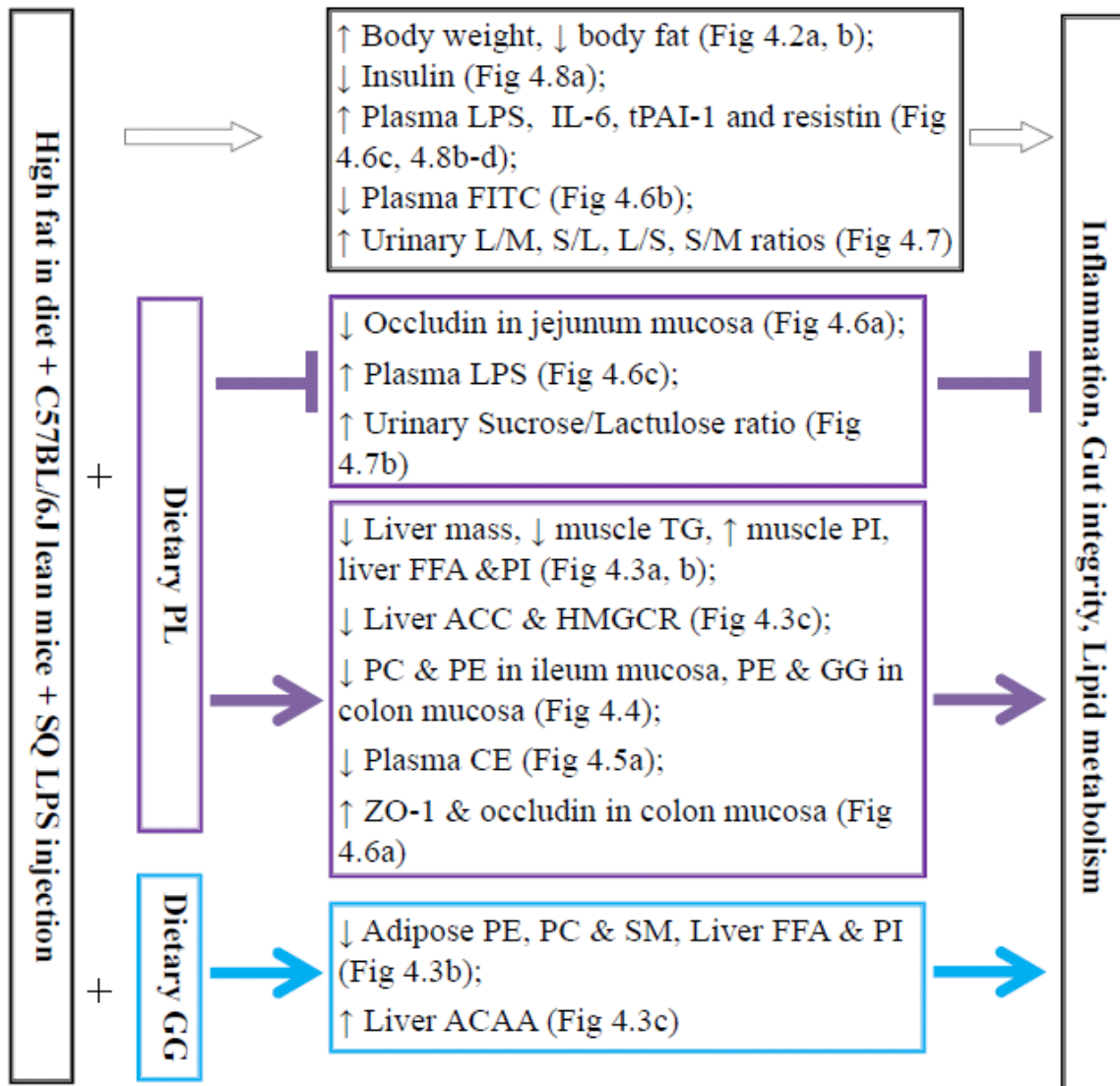
**Figure 4.9b-d** Body fat plotted against fat-free mass for individual animals at (e) day -7, (f) day -1 and (g) day 3.



**Figure 4.9e-g** Body fat plotted against fat-free mass for individual animals at (e) day 5, (f) day 11 and (g) day 23.



**Figure 4.9h-j** Body fat plotted against fat-free mass for individual animals at (e) day 32, (f) day 39 and (g) day 54.



**Figure 4.10** Summary of major findings in Chapter 4. Horizontal white arrows indicate the effects of the control diet. Horizontal T-shaped purple arrows indicate undesirable effects. Horizontal solid purple and blue arrows indicate desirable or neutral effects. SQ: subcutaneous, L/M: Lactulose/Mannitol, S/L: Sucrose/Lactulose, L/S: Lactulose/Sucralose, S/M: Sucralose/Mannitol.

## CHAPTER 5

### **DIETARY MILK POLAR LIPIDS PROMOTE FAT ACCUMULATION AND AFFECT GUT PERMEABILITY, SYSTEMIC INFLAMMATION, AND LIPID METABOLISM IN C57BL/6J MICE FED A MODERATELY HIGH-FAT DIET**

#### **Abstract**

Metabolic inflammation is associated with increased gut permeability, endotoxemia and obesity. High fat diets increase endotoxin absorption from the gut and result in endotoxemia. It is not clear which one occurs first, a compromised gut barrier, endotoxemia, metabolic inflammation or obesity. Studying the effects of different lipid classes on the aforementioned endpoints may facilitate the clarification of their complex interrelationships. This study was designed to test the hypotheses that dietary milk polar lipids will (1) prevent the gut permeability increase, (2) reduce systemic inflammation during the development of DIO and (3) reduce the lipid level in the liver and affect the expression of genes associated with fatty acid synthesis and cholesterol regulation in the liver. An additional objective was to explore the dynamic changes in gut permeability, systemic inflammation, and lipid metabolism during the development of DIO. Three groups of C57BL/6J mice (n = 6) were fed diets with 34% fat as energy for 15 weeks: (1) modified AIN-93G diet (CO); (2) control diet supplemented with a milk gangliosides concentrate (GG); (3) control diet supplemented with a milk phospholipids concentrate (PL). The milk PL increased food consumption, weight gain and body fat accumulation compared with the CO and the GG. Neither the GG nor the PL had a significant effect on the fasting plasma glucose, cholesteryl ester or triglyceride. The PL significantly down regulated hepatic expression of the fatty acid synthesis gene acetyl-Coenzyme A

carboxylase beta compared with the GG and up regulated hepatic expression of the scavenger receptor class B member 1 gene compared with the CO and the GG. As revealed by the differential sugar test, gut permeability showed a significant time effect and diet x time interaction over the course of the study. The small intestinal permeability increased slightly at the beginning and then decreased significantly over the feeding period. There was a gradual increase in colonic damage as indicated by the declining of the urinary Lactulose/Sucralose ratio and the colonic recovery as indicated by the urinary Sucralose/Mannitol ratio. During the early phase, the PL and especially the GG had some protective effect against the increase of small intestinal permeability. As indicated by Western blot, the PL decreased the tight junction protein occludin level in the jejunum but did not affect the occludin level in the ileum and the colon compared with the CO. The tight junction protein zonula occludens-1 level was not affected in the small intestine and the colon. The GG and PL did not affect the plasma endotoxin level, which increased significantly after 14 weeks. The GG and PL did not significantly affect the plasma levels of interleukin-6, insulin, monocyte chemotactic protein-1, leptin, tumor necrosis factor- $\alpha$ , plasminogen activator inhibitor-1, and resistin. The plasma levels of leptin and resistin increased significantly after 14 weeks. In conclusion, the milk polar lipids had little effect on the gut permeability and systemic inflammatory cytokines during the development of DIO. The milk PL increased the polar lipids level in the liver and facilitated the body fat accumulation in the context of DIO.

## **Introduction**

Excess energy can result in body fat accumulation (1, 2) and eventually lead to obesity (3). Excessive fat accumulation in the adipocytes may initiate inflammation since

lipid mediators are precursors to inflammatory signaling molecules (4). The inflamed adipose tissue can produce proinflammatory cytokines, such as tumor necrosis factor- $\alpha$  (TNF- $\alpha$ ), and interleukin-6 (IL-6) (4). These cytokines can initiate local intestinal inflammation, which increase mucosal permeability and bacterial translocation. In obese subjects, the high level of inflammatory cytokines disrupt intestinal barrier (5, 6). Therefore, obesity, adipose inflammation and compromised gut integrity can self-perpetuate (see Figure 1.1) (7).

One of the mechanisms for leaky gut (8, 9) in obese animals is the adaptation for nutrient absorption by intestinal hyperplasia (10), which causes the TJ proteins to malfunction (11). Mice with diet-induced obesity (DIO) develop endotoxemia compared with the lean mice (12). Increased gut barrier permeability can result in endotoxemia and metabolic inflammation (13). High fat diets can independently increase gut permeability and result in metabolic endotoxemia that leads to metabolic inflammation (14). Metabolic inflammation can also promote obesity. Patients with periodontitis develop endotoxemia and tend to become obese (15).

According to current evidence, gut barrier permeability, endotoxemia, systemic inflammation and obesity may be a series of continuous events during the development of DIO. These events could also occur in the order of DIO, adipose/systemic inflammation, leaky gut, and aggravation of obesity. In general, compromised gut barrier integrity, endotoxemia, systemic inflammation and DIO are complexly interrelated (see Figure 1.1).

The interrelatedness of the aforementioned events may be elucidated by investigating them along with lipid metabolism, which is involved in all events.

Various studies have explored the physiological effects of milk polar lipids. Milk sphingolipids reduce the uptake of cholesterol (16, 17), protect against bacterial infections in the gut (18-20), and reduce inflammatory response (21-24). Sphingomyelin (SM) affects neonatal gut maturation in rats (25) and regulates intestinal cholesterol absorption (26). Dairy gangliosides (GG) inhibit degradation of gut occludin tight junction (TJ) protein during lipopolysaccharide (LPS) - induced acute inflammation (27). PL reduce hepatic TG and cholesterol (28) in rats. A PL-rich MFGM extract reduces hepatomegaly, hepatic steatosis and hyperlipidemia in mice (29). A buttermilk MFGM isolate promotes intestinal barrier integrity against LPS stress in mice (30). Based on these findings, it is possible that the milk polar lipids may influence endotoxemia and systemic inflammation through affecting the intestinal barrier integrity. The milk polar lipids could also influence lipid metabolism and the development of DIO. The dietary supplementation of milk polar lipids during the development of DIO may facilitate the understanding of the interrelationships among intestinal barrier integrity, endotoxemia, systemic inflammation and obesity.

This study was designed to test the hypotheses that dietary milk polar lipids will prevent the gut permeability increase and reduce systemic inflammation during the development of DIO in C57BL/6J mice fed a diet with 34% fat by energy. A tertiary hypothesis was that dietary milk polar lipids will reduce liver lipid levels and affect the



expression of genes associated with fatty acid synthesis and cholesterol regulation in the liver.

## **Materials and Methods**

### **Diets formulation**

The three diets were the same as described in Chapter 3 (Table 3.1): CO diet, GG diet and PL diet.

### **Animals**

Five-week-old male C57BL/6J mice (n = 18; Jackson Laboratory) were housed in single cages at a constant temperature of  $22 \pm 1$  °C with a 12-h light/dark cycle. They were allowed ad libitum access to diet and water. After being put on normal chow diet for 2 weeks (for acclimatization and baseline data collection), the mice were randomly assigned to one of the following treatments: 1) CO diet (n = 6); 2) GG diet (n = 6); 3) PL diet (n = 6). The mice were fed the experimental diets for 14 weeks. The diet intake was monitored daily and the body weight was measured every other day. The body compositions were assessed every week by magnetic resonance imaging (MRI) using an EchoMRI-900 Body Composition Analyzer (EchoMRI, Houston, TX). The experiments were conducted in conformity with the Public Health Service Policy on Humane Care and Use of Laboratory Animals and were approved by the Utah State University Institutional Animal Care and Use Committee.

### **Assessments of intestinal barrier integrity**

The intestinal permeability was assessed by the FITC-dextran absorption test and the DST as described in Chapter 3. The FITC-dextran absorption test was done at the baseline, day 35 and 101. The DST was carried out at the baseline, day 15, 30, 45, 73 and 87.

### **Tissue sample collection**

The mice were sacrificed by CO<sub>2</sub> asphyxiation after a 4h fast. After the blood collection, the liver, the quadriceps muscle, the intestinal and colonic mucosa, the feces and the adipose tissue samples were collected. The adipose depots included the gonadal, retroperitoneal, mesenteric, and subcutaneous depots. Each category of tissue was saved separately and the tissue mass was recorded. The tissue samples were flash frozen and stored at -80 °C until further analysis.

### **Biochemical analyses of plasma**

The blood samples were collected and the plasma was analyzed as described in Chapter 3 to measure glucose, insulin, leptin, resistin, monocyte chemoattractant protein-1 (MCP-1), IL-6, TNF- $\alpha$ , plasminogen activator inhibitor-1 (PAI-1) and endotoxin. The homeostasis model assessment of insulin resistance (HOMA-IR) index was calculated from fasting glucose and insulin levels (fasting glucose\*fasting insulin/22.5) (31, 32).

### **Western Immunoblotting for zonula occludens (ZO)-1 and occludin proteins**

Mucosal samples of the small intestine and the colon were collected and Western immunoblotting for the zonula occludens (ZO-1) and occludin proteins were carried out as described in Chapter 3.

### **Liver gene expression analysis**

The expression of 13 genes associated with lipid metabolism in the liver was analyzed as described in Chapter 3.

### **Tissue lipid profiling**

Tissue lipid profiles of the liver, the skeletal muscle and the gonadal adipose were analyzed as described in Chapter 3. The lipid classes included phosphatidylethanolamine (PE), phosphatidylcholine (PC), phosphatidylserine (PS), and phosphatidylinositol (PI), SM, diglycerides (DG), free fatty acids (FFA), triglycerides (TG), and cholesteryl ester (CE).

### **GG analysis of intestinal mucosa**

The GG content in the intestinal mucosa was determined as described in Chapter 3.

### **Statistical analyses**

One-way or mixed models analysis of variance (ANOVA) was performed by SAS 9.2. The group means were compared by Ryan-Einot-Gabriel-Welsch Multiple Range Test or Least Squares Means Contrast in SAS. The data were reported as Mean  $\pm$  Standard Error of the Mean (SEM).

### **Results**

The PL group consumed more diet than the other two groups during the first 3 days and the difference persisted until day 10 (Table 5.1). The PL group consumed 1.3 g more experimental diet during the first day than the CO group and 0.97 g more diet than the GG group. The daily diet intakes for the first 3 days were larger than daily food

consumption during the whole study. That difference in food intake disappeared by day 10. There were no differences among groups regarding diet intake during the rest of the study. There was a significant diet effect for body weight gain ( $p = 0.02$ ) during the first 3-10 days of dietary treatment (Figure 5.1a). The PL group consumed more energy, gained more body fat and converted a higher percentage of consumed energy into body fat from day -3 to day 4 (3 days before to 4 days after dietary intervention, Table 5.2).

The body fat composition data (by MRI) indicated that the body fat percentage plateaued at around 70 days of the experimental feeding (Figure 5.1b). The PL facilitated fat accumulation after day 70 compared with the CO and GG (Figure 5.1b). The body fat percentage of the PL group increased at a faster rate compared with that of the other groups (Figure 5.1c). The accumulating body weight gain of the PL group also increased at a higher rate compared with the other groups but the slope was much smaller (Figure 5.1d) than that of the body fat increase.

### **Tissue and plasma lipid profiles**

Dietary treatment did not affect the final liver mass and the liver weight percentage (Table 5.3). There were no differences in tissue masses for skeletal muscle and adipose depots (Table 5.3). The PL decreased the adipose PC and SM compared with the CO. The PL increased the liver PE, PC and SM (Figure 5.2a) compared with the CO. Dietary treatment did not affect lipid profile in the skeletal muscle.

As shown in Figure 5.2b, the PL suppressed hepatic expression of the fatty acid synthesis gene *Acacb* (vs the GG) and up regulated cholesterol reverse transport gene

*Scarb1* (vs the CO & the GG). Dietary GG did not affect the mucosal gangliosides content. Dietary PL increased the mucosal PC in the small intestine and decreased the mucosal PC, PE and SM in the colon compared with the CO and the GG (Figure 5.2c).

The plasma TG level increased over time and the PL group had higher plasma TG level (Figure 5.3a) compared with the CO and GG groups at the end of the study. The plasma CE level increased over time during the study and there was no treatment effect (Figure 5.3b). The plasma FFA (Figure 5.3c) and PC (Figure 5.3d) levels were lower in the PL and GG groups compared with that in the CO group at day 35. Those differences disappeared toward the end of the study.

### **Gut permeability**

Dietary PL decreased the gut permeability to the FITC-dextran before the DIO and increased it after the DIO was achieved (Figure 5.4a). The differential sugar tests revealed significant time effect and diet x time interactions on the gut permeability. The urinary Lactulose/Mannitol ratio increased slightly and then decreased in the CO group (Figure 5.4b). The PL increased the urinary Lactulose/Mannitol ratio significantly at day 73 and then decreased it toward the end of the study (Figure 5.4b). The urinary Sucrose/Lactulose ratio increased in the CO group and decreased in the GG and PL groups during the first 15 days (Figure 5.4c). Then the urinary Sucrose/Lactulose ratio increased gradually in all groups toward day 30 and dropped down by day 45 before rising again (Figure 5.4c). The PL group had high level of the urinary Sucrose/Lactulose ratio at day 73 compared with the CO and GG groups and the ratio decreased toward the end of the study (Figure 5.4c). The urinary Lactulose/Sucralose ratio decreased

significantly during the first 45 days (Figure 5.4d). The urinary Lactulose/Sucralose ratio stayed stable from day 45 to the end except in the PL group where the ratio increased significantly at day 73 (Figure 5.4d). The urinary Sucralose/Mannitol ratio in the CO group increased slightly during the first 15 days, decreased toward day 30, increased significantly toward day 45, dropped significantly toward day 73 and then increased toward day 87 (Figure 5.4e). The PL group had higher urinary Sucralose/Mannitol ratio at day 45 compared with the other groups (Figure 5.4e). The GG group had lower urinary Sucralose/Mannitol ratio at day 87 compared with the CO group (Figure 5.4e).

As indicated by Western blot (Figure 5.4f), the PL decreased the tight junction protein occludin level in jejunum mucosa but did not affect occludin level in the mucosa of ileum and colon compared with the CO. The GG increased the tight junction protein ZO-1 level in the colon mucosa compared with the CO and the ZO-1 level was not affected in the mucosa of jejunum and ileum.

### **Plasma endotoxin and cytokines**

The plasma LPS level increased slightly in the GG and PL groups compared with the CO group during the first 35 days (Figure 5.5a). The plasma LPS level increased significantly after 101 days (Figure 5.5a). The PL group had higher plasma LPS level compared with the CO group at day 101 (Figure 5.5a).

The GG and PL did not significantly affect the plasma levels of MCP-1, TNF- $\alpha$ , IL-6, leptin, resistin, PAI-1 and insulin (Table 5.4 and Figure 5.5 b-f). The plasma IL-6 level increased during the first 35 days and then returned toward baseline level (Figure 5.5b).

The plasma levels of leptin and resistin increased significantly after 101 days (Figure 5.5c&d).

The PL increased the plasma PAI-1 level during the study compared with the other two groups (Figure 5.5e). The plasma insulin level increased over time (Figure 5.5f).

### **Plasma glucose and HOMA-IR**

Hyperglycemia was observed at day 101 (Figure 5.6a). The HOMA-IR index increased over time (Figure 5.6b). By the end of the study, insulin resistance was developed as indicated by HOMA-IR (33).

### **Body fat changes**

The plots of body fat against fat-free mass revealed the gradual increase and the dynamic changes in the body fat mass during the study (Figure 5.7a-g). When all measurements at 12 time points (at day -15, -11, -7, -3, 4, 20, 27, 34, 55, 68, 83, 96) were included, the data points fell into two groups with different slopes (0.98 and 0.39) (Figure 5.7a). The slope was around 0 during the first MRI scan at day -15 (Figure 5.7b). The slope increased to 0.14 at day -7, 0.2 at day -3 (Figure 5.7c), and 0.33 at day 4 (Figure 5.7d). The slope decreased from 0.35 at day 20 to 0.30 at day 34. The slope then increased back to 0.36 at day 55 (Figure 5.7e). At day 68, the data points started to segregate into two groups with different slopes (1.02 and 0.27) (Figure 5.7f). From day 68 to day 96, the slopes for the two groups increased further to 1.18 and 0.34 at day 96 (Figure 5.7g).

### **Comparison between lean and obese mice**

The lean and obese mice (Figure 5.7g) had differences in many parameters at the end of the study (Figure 5.8) regardless of dietary interventions. The obese mice had higher plasma insulin and leptin compared with the lean mice (Figure 5.8a). The obese mice had higher HOMA-IR compared with the lean mice (Figure 5.8b). The obese mice had higher plasma CE, DG, TG, PC and higher liver TG compared with the lean mice (Figure 5.8c). The obese mice had lower occludin protein expression in jejunum mucosa compared with the lean mice (Figure 5.8d). The obese mice had higher amount of brown adipose tissue, inguinal, gonadal, mesenteric and retroperitoneal fat depots compared with the lean mice (Figure 5.8e). Obese mice had lower amount of cecum content, jejunum, ileum, colon, jejunum mucosa and ileum mucosa compared with lean mice (Figure 5.8e).

### **Discussion**

This study was designed to test the hypotheses that the milk polar lipids (1) reduce liver lipid level and affect the expression of genes associated with fatty acid synthesis and cholesterol regulation in the liver, (2) prevent the increase of gut permeability, and (3) reduce plasma inflammatory cytokines in the C57BL/6J mice during the development of DIO. The first hypothesis was not supported by the data. The milk phospholipids promoted body fat accumulation and increased obesity. The milk phospholipids increased the liver PE, PC, SM & the plasma TG and decreased the plasma FFA & PC. The milk phospholipids decreased the PC & SM in the colon mucosa. The milk gangliosides decreased the adipose SM, the plasma FFA & PC and increased the liver PE & SM.



The data did not support the second and the third hypotheses. The milk phospholipids increased the gut permeability and decreased the occludin in the jejunum mucosa. The milk phospholipids increased the plasma LPS and did not affect the plasma inflammatory cytokines level. The milk gangliosides decreased the ZO-1 in the colon mucosa and did not affect the gut permeability. The milk gangliosides did not affect the plasma level of the inflammatory cytokines.

The mouse model of DIO, increased gut permeability and increased systemic inflammation was established. The high fat feeding increased body fat and the plasma level of CE, leptin, resistin, insulin, and glucose. The high fat feeding decreased the insulin sensitivity as indicated by the increased HOMA-IR index. The high fat feeding decreased the permeability of the small intestine, increased the colon permeability and the plasma levels of LPS, and increased the plasma IL-6 level before the establishment of DIO.

The PL group consumed more diet and gained more weight and body fat compared with the CO group while the GG group was in the middle. The difference was already significant by the first 3 days and should have been contributed mainly by the first 10 days (Table 5.1). The average chow diet intake was 3.69 g/mouse/day. The mice in the PL group consumed 4.15 g high fat diet on average on the first day. The overconsumption of the high fat diet in the PL group during first 3 days may play an important role in the resulting higher body weight and body fat percentage. It was not clear which factor caused the overconsumption. The PL diet was slightly softer and the

GG diet was slightly harder than the CO diet. No measurement of the hardness was done for the diets. If the texture of the diet caused the difference in the diet intake during the first 3 days, the PL group should have consumed similar amount of diet later on. The diet intake decreased in all groups from the beginning and reached the average level by 10 days.

It might be argued that a run-in diet similar to the experimental diets may help optimize the experimental conditions. Although a run-in diet may reduce the variabilities in food intake during the transition from baseline diet to experimental diet, it was obvious that the PL group consumed more food during the first 3-10 days. By the end of the study, the PL group had consumed 20.54 g (8.0%) more diet than the CO group and 27.26 g (10.9%) more diet than the GG group. The PL group gained more weight and body fat than the other two groups. The GG group did not gain more weight and body fat than the CO group although the GG group consumed more diet. The body weight gain was mainly contributed by the body fat accumulation.

The plasma LPS did not increase much during the first 35 days. The main increase occurred from day 35 to 101. For the LPS challenged mice (reported in chapter 4), the plasma LPS did not increase during the first 34 days. It happened during day 35 to 57. It is apparent that gut permeability may change significantly from day 35 to 57. An additional 6 weeks of feeding did not significantly increase the plasma LPS. One week of feeding increased the plasma LPS to similar level observed in the ob mice (reported in

chapter 3). The plasma LPS level increased significantly in all groups once the DIO was established.

There were no significant dietary treatment effects on major plasma inflammatory cytokines and adipokines, including IL-6, TNF- $\alpha$ , PAI-1, MCP-1, resistin and leptin. The plasma resistin and leptin increased over time. Dietary phospholipids increased the plasma insulin level after the DIO (Figure 5.5f). The mechanism for this increase of insulin is not clear. Dietary phospholipids rich in n-3 polyunsaturated fatty acids reduced plasma insulin level under obesogenic conditions and the mechanism may be through modulating the endocannabinoid system activity in the white adipose tissue (34). It could be possible that the opposite effect of dietary phospholipids on the plasma insulin level in this study was due to the saturated fatty acids in the milk phospholipids.

Dietary phospholipids decreased phospholipids in the visceral adipose tissue and the colon mucosa but increased phospholipids in the liver (Figure 5.2a & c). The higher dietary phospholipids level was not always accompanied by higher phospholipids level in the tissue. The dietary phospholipids decreased the SM level in the colon mucosa. Little or no radioactively labeled SM was absorbed intact into the chyle (35). Luminal SM is hydrolyzed to ceramide, and then to sphingosine and free fatty acids (36). The free sphingosine is well absorbed and most of the absorbed sphingosine is rapidly converted to palmitic acid and incorporated into chylomicrons (37, 38). A smaller portion of the sphingosine is incorporated into the mucosa as ceramide and SM (35, 39). It may be hypothesized that the dietary SM may have suppressed the tissue SM level in the

intestinal mucosa through down regulation of the receptors for sphingosine. Similar mechanisms of receptor regulation may account for the effects of dietary phospholipids on tissue phospholipids level in the visceral adipose tissue and the liver.

During the maturation of the gut, gut permeability to FITC decreased (Figure 5.4a). Compared with the CO and the GG, the PL facilitated the decrease of permeability to FITC when the mice were lean and increased the permeability to FITC when the animals were obese. Although the difference between the PL and the other two was not statistically significant at any of the time points, the opposite effect of the PL before DIO and after DIO was quite interesting. It is not clear what the mechanism was for the opposite effect in the PL group. Further studies are needed to explore how the PL may have different effect on gut permeability when the mouse is lean and after DIO.

The permeability of the small intestine decreased during the first 45 days (Figure 5.4b) in all groups as revealed by the urinary Lactulose/Mannitol ratio (40). Taken together, the intestinal integrity was enhanced during the first 45 days. The mice were still developing during that period of time and the gut may be maturing. After the DIO was established, the small intestinal permeability increased significantly in the PL group compared with that in the CO and GG groups. There was a peaking of the body fat percentage around that time point (Figure 5.1b). The decrease of the urinary Sucrose/Lactulose ratio indicated the distal damage of small intestine. The damage became proximal when the urinary Sucrose/Lactulose ratio increased to a high level (40).

The high-fat feeding increased the permeability of the proximal small intestine and the GG and PL supplementations caused a permeability increase of the distal small intestine during the first 15 days (Figure 5.4c). Then the damage became proximal also in the GG and PL groups by day 30. The damage then moved to the distal small intestine and back to the proximal by the end of the study. This is consistent with the Western blot result that the dietary polar lipids (especially phospholipids) suppressed the TJ protein occludin expression in the jejunum mucosa. The urinary Lactulose/Sucralose ratio selectively increases upon the intestinal damage and decreases upon the colonic damage (40). The high fat feeding increased the permeability of the colon (Figure 5.4e). The colon permeability stayed stable from day 45 to the end except in the PL group where small intestine permeability increased during the early phase of the DIO. There was an increase of the colon permeability during the first 15 days and the permeability receded by day 30. Then the colon permeability increased significantly at day 45. The significant increase of the colon permeability at day 45 (Figure 5.4e) may be due to the increased inflammation as indicated by the increase of the plasma IL-6 level (Figure 5.5b) around this time. Taken together, the high-fat feeding increased the permeability of proximal small intestine and the colon at the beginning and there was a recovery after the initial permeability increase. Then the permeability of the distal small intestine and the colon increased when the systemic inflammation increased during the early phase of the DIO.

The dietary fat level was 34% fat as energy, which was lower than most of the fat levels used for the DIO model. The colon permeability increased significantly at the onset of the DIO (Figure 5.4c) and then decreased significantly. The initial increase of the

colon permeability may be caused by the high fat diet, which increases intestinal permeability through the dietary fat and increased luminal bile juice levels (41). The high fat feeding before the DIO increased the colon permeability but did not increase the plasma LPS level significantly. The colon permeability decreased (Figure 5.4e) and the plasma LPS increased (Figure 5.5a) after the establishment of DIO. The increase of the plasma LPS level after the DIO may not be contributed significantly by the decreased colon permeability but may be mediated through the chylomicrons as the postprandial carriers for the LPS (42). The chylomicron secretion process is different in DIO from when the mice are lean (43). The mechanisms remain unclear for the altered intestinal TG metabolism in mouse models of obesity (43). Compared with lean controls, men with visceral obesity may have normal fasting plasma lipids but an abnormal postprandial accumulation of TG-rich remnant lipoproteins due to the greatly decreased clearance of chylomicron remnants (44). Taken together, it may be hypothesized that the absorption of gut LPS in DIO is mainly mediated through the transcellular pathway instead of the paracellular route. If the absorbed gut LPS in the plasma during DIO is mainly carried by chylomicron remnants, this may help explain the lack of a considerable inflammatory response corresponding to the increased plasma LPS since the lipoproteins may inactivate LPS (45).

The plasma LPS level did not increase (Figure 5.5a) at day 35 but the IL-6 level increased manyfold (Figure 5.5b). The plasma IL-6 then decreased toward the end of the study while the LPS level increased dramatically. These results indicate that a diet with 34% fat as energy may not pose a strong inflammatory stress for the C57BL/6J mice. The

PL and GG supplementations enhanced the inflammatory response. On the other hand the DIO was complicated with the high level of plasma LPS but not a strong inflammatory response.

The plasma resistin level increased steadily throughout the course of the study in the CO and GG groups. That could mean the resistin level is influenced more by the high fat diet than by the DIO. As an adipocytokine secreted in proportion to the obesity level, resistin counteracts the effects of insulin in mice (46). The PL did not increase the resistin level during the first 35 days and the resistin level was lower in the PL group compared with the CO and GG groups after the DIO. The PL prevented the increase of the resistin during the high fat feeding and the DIO. It is not clear which component of the milk phospholipids had this effect.

The PL increased the plasma PAI-1 level during the first 35 days and the plasma PAI-1 level flattened in the PL group when the mice became obese (Figure 5.5e). The CO and the GG decreased the plasma PAI-1 level before the DIO and the level regressed after the DIO. PAI-1 is an adipocytokine and the increased PAI-1 level in obesity has been associated with the mediation of obesity, insulin resistance and metabolic syndrome (47, 48). Lysophosphatidylcholine (LPC) in oxidized low-density lipoprotein (OxLDL) enhances the PAI-1 expression in mouse 3T3-L1 adipocytes (49). The increase of the plasma PAI-1 level in the PL group may be caused by the metabolites of dietary PC and may have contributed to the development of the DIO. Suppression of de novo ceramide synthesis significantly reduces the PAI-1 expression in the adipose tissue of obese mouse

(50). It is not clear why the CO and the GG decreased the plasma PAI-1 level before the DIO. Taken together, dietary supplementations of PL may pose risk factors for obesity and metabolic syndrome by increasing the plasma PAI-1.

The plasma leptin level did not increase by the high fat feeding itself and the leptin level was proportional to the body fat content for the PL group (Figure 5.5c). For the plasma leptin level, variances exist in the literature. Levi et al. reported that the plasma leptin of 11-week old C57BL/6J was at 1.5 ng/ml (51) measured by an enzyme-linked immunosorbent assay (Crystal Chem, Downers Grove, IL, USA). Burgueño reported that the plasma leptin of 12-week-old C57BL/6J was at 0.2 ng/ml measured by an enzyme-linked immunoassay kit (Assay Designs, Ann Arbor, MI) (52). In this study, the plasma leptin level (measured by fluorescent immunoassay) increased over time, from 2.3 - 3.4 ng/ml for the 12-week-old to 17 - 28 ng/ml for the 21-week-old. The range is similar to Murphy et al.'s report that the plasma leptin level (measured by radioimmunoassay) was 3.8 ng/ml for the 12-week old, peaked at 4.2 ng/ml for the 14-week-old, and declined to 2.3 ng/ml at week 16 (53). The increase of leptin level may be explained by the increase of body fat accumulation.

The plots of body fat against fat-free mass showed that the slope increased gradually until the data points segregated at day 68 (Figure 5.7f), which indicated the establishment of the DIO. This coincided with the plateauing of the body fat percentage at day 68 (Figure 5.1b). These data support that the plot of body fat against fat-free mass is an effective way for defining obesity (54). By the end of the study, 10 out of the 17 mice



were obese according to the aforementioned definition. The obese and lean mice had significant differences in many parameters (Figure 5.8) regardless of the dietary treatments. Significant body weight increase is usually used to define obesity (55). The use of body weight gain to define obesity is more arbitrary than using the plot of body fat against fat-free mass. The data in the current study and the data from the ob/ob mouse model (Chapter 3) and the LPS-stressed mouse model (Chapter 4) all support that the Fenton's method is an effective and relatively objective way for defining obesity.

The data from the present study also showed that stresses may have considerable effect on body fat content in the C57BL/6J mice. The MRI scan at day 34 was carried out soon after the third DST (at day 30). Residing in the metabolic cage may be responsible for the reduced body fat content as indicated by the decreased slope (0.35 at day 20 to 0.30 at day 34). Once the stress was removed, the body fat increased back (Figure 5.7e). The other 5 DST did not affect the MRI data when those DST were at least 5 days apart from the MRI scans. It may be emphasized that unnecessary stresses should be avoided and the animals should be handled in the same manner to reduce variances from the potential variability in the stresses.

## **Summary**

The major effects of the dietary polar lipids on gut permeability, systemic inflammation, and lipid metabolism during the development of the DIO are summarized in Figure 5.9. During the development of the DIO in the C57BL/6J mice fed high fat diets, gut permeability to sugar probes increased before the DIO and decreased after the DIO.

The plasma LPS level increased after the DIO. Hyperglycemia and insulin resistance developed by the end of the study. Compared with the CO, the PL decreased the TJ protein occludin in the jejunum mucosa and increased the permeability of the small intestine and the colon after the DIO. The PL increased the body fat content and the plasma LPS level compared with the CO. Compared with the CO, the PL increased the polar lipids content in the liver and decreased the polar lipids content in the colon mucosa. Compared with the CO, the PL increased the plasma TG, decreased the plasma FFA and PC, and decreased the adipose PC. The dietary milk GG increased the TJ protein ZO-1 in the colon mucosa and did not affect the gut permeability compared with the CO and the PL. Compared with the CO, the GG decreased the adipose SM, increased the liver PE and SM, and decreased the plasma FFA and PC. The GG did not affect the plasma inflammatory cytokines.

In conclusion, the plasma inflammatory cytokines were not significantly affected by the high fat feeding or the dietary treatments. The dietary phospholipids increased obesity, gut permeability and the plasma LPS. This study revealed important dynamic changes in gut permeability and the body fat content during the development of DIO. The milk phospholipids may have unfavorable effects on obesity and gut permeability in the context of high fat diet induced obesity. Further studies are needed to identify which components of the milk polar lipids concentrates are responsible for the observed effects.

The data from the current study did not support the hypotheses that during the development of DIO dietary milk polar lipids will 1) prevent the gut permeability

increase and subsequent systemic inflammation and 2) reduce liver lipid levels and affect the expression of genes associated with fatty acid synthesis and cholesterol regulation in the liver. The polar lipids are important building blocks for all the organ systems. The dietary polar lipids may affect all of the organ systems in the body. It is still not clear how the polar lipids may affect those organ systems that were not assessed in the present study. The overall effects of the dietary polar lipids cannot be concluded until the effects of the polar lipids are systematically evaluated in all of the major organ systems.

### References

1. Singh R, Kaushik S, Wang Y, et al. Autophagy regulates lipid metabolism. *Nature* 2009;458:1131-5.
2. Duncan RE, Ahmadian M, Jaworski K, Sarkadi-Nagy E, Sul HS. Regulation of lipolysis in adipocytes. *Annu Rev Nutr* 2007;27:79-101.
3. Jaworski K, Ahmadian M, Duncan RE, et al. AdPLA ablation increases lipolysis and prevents obesity induced by high-fat feeding or leptin deficiency. *Nat Med* 2009;15:159-68.
4. Iyer A, Fairlie DP, Prins JB, Hammock BD, Brown L. Inflammatory lipid mediators in adipocyte function and obesity. *Nat Rev Endocrinol* 2010;6:71-82.
5. Bruewer M, Luegering A, Kucharzik T, et al. Proinflammatory cytokines disrupt epithelial barrier function by apoptosis-independent mechanisms. *J Immunol* 2003;171:6164-72.
6. Das UN. Is obesity an inflammatory condition? *Nutrition* 2001;17:953-66.

7. Iacono A, Raso GM, Canani RB, Calignano A, Meli R. Probiotics as an emerging therapeutic strategy to treat NAFLD: focus on molecular and biochemical mechanisms. *J Nutr Biochem* 2011.
8. Cani PD, Amar J, Iglesias MA, et al. Metabolic endotoxemia initiates obesity and insulin resistance. *Diabetes* 2007;56:1761-72.
9. Cani PD, Bibiloni R, Knauf C, et al. Changes in gut microbiota control metabolic endotoxemia-induced inflammation in high-fat diet-induced obesity and diabetes in mice. *Diabetes* 2008;57:1470-81.
10. Morton AP, Hanson PJ. Monosaccharide transport by the small intestine of lean and genetically obese (ob/ob) mice. *Q J Exp Physiol* 1984;69:117-26.
11. Ferraris RP, Vinnakota RR. Intestinal nutrient transport in genetically obese mice. *Am J Clin Nutr* 1995;62:540-6.
12. Naito E, Yoshida Y, Makino K, et al. Beneficial effect of oral administration of *Lactobacillus casei* strain Shirota on insulin resistance in diet-induced obesity mice. *J Appl Microbiol* 2010.
13. Kahn SE, Hull RL, Utzschneider KM. Mechanisms linking obesity to insulin resistance and type 2 diabetes. *Nature* 2006;444:840-6.
14. Laugerette F, Vors C, Peretti N, Michalski MC. Complex links between dietary lipids, endogenous endotoxins and metabolic inflammation. *Biochimie* 2010.
15. Suvan J, D'Aiuto F, Moles DR, Petrie A, Donos N. Association between overweight/obesity and periodontitis in adults. A systematic review. *Obesity Reviews* 2011;12:e381-404.

16. Eckhardt ERM, Wang DQH, Donovan JM, Carey MC. Dietary sphingomyelin suppresses intestinal cholesterol absorption by decreasing thermodynamic activity of cholesterol monomers. *Gastroenterology* 2002;122:948-56.
17. Noh SK, Koo SI. Milk sphingomyelin is more effective than egg sphingomyelin in inhibiting intestinal absorption of cholesterol and fat in rats. *J Nutr* 2004;134:2611-6.
18. Pfeuffer M, Schrezenmeir J. Dietary sphingolipids: metabolism and potential health implications. *Kieler Milchw Forsch* 2001;53:31-42.
19. Vesper H, Schmelz EM, Nikolova-Karakashian MN, Dillehay DL, Lynch DV, Merrill AH. Sphingolipids in food and the emerging importance of sphingolipids to nutrition. *J Nutr* 1999;129:1239-50.
20. Clare DA, Zheng Z, Hassan HM, Swaisgood HE, Catignani GL. Antimicrobial properties of milkfat globule membrane fractions. *J Food Prot* 2008;71:126-33.
21. Dalbeth N, Gracey E, Pool B, et al. Identification of dairy fractions with anti-inflammatory properties in models of acute gout. *Ann Rheum Dis* 2010;69:766-9.
22. El Alwani M, Wu BX, Obeid LM, Hannun YA. Bioactive sphingolipids in the modulation of the inflammatory response. *Pharmacol Ther* 2006;112:171-83.
23. Park EJ, Suh M, Thomson B, et al. Dietary ganglioside inhibits acute inflammatory signals in intestinal mucosa and blood induced by systemic inflammation of *Escherichia coli* lipopolysaccharide. *Shock* 2007;28:112-7.
24. Park EJ, Suh M, Thomson B, Thomson AB, Ramanujam KS, Clandinin MT. Dietary ganglioside decreases cholesterol content, caveolin expression and

- inflammatory mediators in rat intestinal microdomains. *Glycobiology* 2005;15:935-42.
25. Motouri M, Matsuyama H, Yamamura J, et al. Milk sphingomyelin accelerates enzymatic and morphological maturation of the intestine in artificially reared rats. *J Pediatr Gastroenterol Nutr* 2003;36:241-7.
  26. Chen H, Born E, Mathur SN, Johlin FC, Jr., Field FJ. Sphingomyelin content of intestinal cell membranes regulates cholesterol absorption. Evidence for pancreatic and intestinal cell sphingomyelinase activity. *Biochem J* 1992;286 (Pt 3):771-7.
  27. Park EJ, Thomson AB, Clandinin MT. Protection of intestinal occludin tight junction protein by dietary gangliosides in lipopolysaccharide-induced acute inflammation. *J Pediatr Gastroenterol Nutr* 2010;50:321-8.
  28. Cohn JS, Wat E, Kamili A, Tandy S. Dietary phospholipids, hepatic lipid metabolism and cardiovascular disease. *Curr Opin Lipidol* 2008;19:257-62.
  29. Wat E, Tandy S, Kapera E, et al. Dietary phospholipid-rich dairy milk extract reduces hepatomegaly, hepatic steatosis and hyperlipidemia in mice fed a high-fat diet. *Atherosclerosis* 2009;205:144-50.
  30. Snow DR, Ward RE, Olsen A, Jimenez-Flores R, Hintze KJ. Membrane-rich milk fat diet provides protection against gastrointestinal leakiness in mice treated with lipopolysaccharide. *J Dairy Sci* 2011;94:2201-12.
  31. Matthews DR, Hosker JP, Rudenski AS, Naylor BA, Treacher DF, Turner RC. Homeostasis model assessment: insulin resistance and beta-cell function from

- fasting plasma glucose and insulin concentrations in man. *Diabetologia* 1985;28:412-9.
32. Wallace TM, Levy JC, Matthews DR. Use and abuse of HOMA modeling. *Diabetes Care* 2004;27:1487-95.
33. Choi WS, Lee JJ, Kim Y, Kim IS, Zhang WY, Myung CS. Synergistic improvement in insulin resistance with a combination of fenofibrate and rosiglitazone in obese type 2 diabetic mice. *Arch Pharm Res* 2011;34:615-24.
34. Rossmeisl M, Jilkova ZM, Kuda O, et al. Metabolic effects of n-3 pufa as phospholipids are superior to triglycerides in mice fed a high-fat diet: possible role of endocannabinoids. *Plos One* 2012;7.
35. Nilsson A. Metabolism of sphingomyelin in the intestinal tract of the rat. *Biochimica et biophysica acta* 1968;164:575-84.
36. Nilsson A. The presence of spingomyelin- and ceramide-cleaving enzymes in the small intestinal tract. *Biochimica et Biophysica Acta* 1969;176:339-47.
37. Fukuda Y, Kihara A, Igarashi Y. Distribution of sphingosine kinase activity in mouse tissues: contribution of SPHK1. *Biochemical and Biophysical Res Communications* 2003;309:155-60.
38. van Veldhoven PP, Mannaerts GP. Sphingosine-phosphate lyase. *Advances in Lipid Res* 1993;26:69-98.
39. Schmelz EM, Crall KJ, Larocque R, Dillehay DL, Merrill AH, Jr. Uptake and metabolism of sphingolipids in isolated intestinal loops of mice. *J Nutr* 1994;124:702-12.

40. Meddings JB, Gibbons I. Discrimination of site-specific alterations in gastrointestinal permeability in the rat. *Gastroenterology* 1998;114:83-92.
41. Suzuki T, Hara H. Dietary fat and bile juice, but not obesity, are responsible for the increase in small intestinal permeability induced through the suppression of tight junction protein expression in LETO and OLETF rats. *Nutr Metab (Lond)* 2010;7:19.
42. Laugerette F, Vors C, Geloën A, et al. Emulsified lipids increase endotoxemia: possible role in early postprandial low-grade inflammation. *J Nutr Biochem* 2010.
43. Uchida A, Whitsitt MC, Eustaquio T, et al. Reduced triglyceride secretion in response to an acute dietary fat challenge in obese compared to lean mice. *Frontiers in Physiology* 2012;3:26.
44. Martins IJ, Redgrave TG. Obesity and post-prandial lipid metabolism. Feast or famine? *J Nutr Biochem* 2004;15:130-41.
45. Vreugdenhil AC, Rousseau CH, Hartung T, Greve JW, van 't Veer C, Buurman WA. Lipopolysaccharide (LPS)-binding protein mediates LPS detoxification by chylomicrons. *J Immunol* 2003;170:1399-405.
46. Inadera H. The usefulness of circulating adipokine levels for the assessment of obesity-related health problems. *Int J Med Sci* 2008;5:248-62.
47. Alessi MC, Juhan-Vague I. PAI-1 and the metabolic syndrome: links, causes, and consequences. *Arterioscler Thromb Vasc Biol* 2006;26:2200-7.
48. Ma LJ, Mao SL, Taylor KL, et al. Prevention of obesity and insulin resistance in mice lacking plasminogen activator inhibitor 1. *Diabetes* 2004;53:336-46.



49. Kuniyasu A, Tokunaga M, Yamamoto T, et al. Oxidized LDL and lysophosphatidylcholine stimulate plasminogen activator inhibitor-1 expression through reactive oxygen species generation and ERK1/2 activation in 3T3-L1 adipocytes. *Bba-Mol Cell Biol L* 2011;1811:153-62.
50. Yang G, Badeanlou L, Bielawski J, Roberts AJ, Hannun YA, Samad F. Central role of ceramide biosynthesis in body weight regulation, energy metabolism, and the metabolic syndrome. *Am J Physiol Endocrinol Metab* 2009;297:E211-24.
51. Levi J, Huynh FK, Denroche HC, et al. Hepatic leptin signalling and subdiaphragmatic vagal efferents are not required for leptin-induced increases of plasma IGF binding protein-2 (IGFBP-2) in ob/ob mice. *Diabetologia* 2012;55:752-62.
52. Burgueno AL, Landa MS, Schuman ML, et al. Association between diencephalic thyroliberin and arterial blood pressure in agouti-yellow and ob/ob mice may be mediated by leptin. *Metabolism-Clinical and Experimental* 2007;56:1439-43.
53. Murphy JE, Zhou S, Giese K, Williams LT, Escobedo JA, Dwarki VJ. Long-term correction of obesity and diabetes in genetically obese mice by a single intramuscular injection of recombinant adeno-associated virus encoding mouse leptin. *Proc Natl Acad Sci U S A* 1997;94:13921-6.
54. Fenton PF. Growth and fat deposition in the mouse; a definition of obesity. *Am J Physiol* 1956;184:52-4.
55. de Wilde J, Smit E, Mohren R, et al. An 8-week high-fat diet induces obesity and insulin resistance with small changes in the muscle transcriptome of C57BL/6J mice. *J Nutrigenetics and Nutrigenomics* 2009;2:280-91.

**Table 5.1** Food intake (Mean  $\pm$  SEM; unit: g).

	CO	GG	PL
1	3.18 $\pm$ 0.27	2.85 $\pm$ 0.65	4.15 $\pm$ 0.17
2	3.03 $\pm$ 0.23	2.83 $\pm$ 0.25	3.40 $\pm$ 0.25
3	2.30 $\pm$ 0.14	2.80 $\pm$ 0.30	2.97 $\pm$ 0.17
4	2.25 $\pm$ 0.11	2.35 $\pm$ 0.21	2.68 $\pm$ 0.30
5	2.85 $\pm$ 0.27	2.38 $\pm$ 0.24	2.60 $\pm$ 0.27
6	2.45 $\pm$ 0.12	2.22 $\pm$ 0.26	2.72 $\pm$ 0.16
7	2.32 $\pm$ 0.18	2.73 $\pm$ 0.20	2.47 $\pm$ 0.16
8	2.28 $\pm$ 0.12 <sup>ab</sup>	1.92 $\pm$ 0.26 <sup>b</sup>	2.80 $\pm$ 0.14 <sup>a</sup>
9	2.85 $\pm$ 0.18	2.33 $\pm$ 0.17	2.38 $\pm$ 0.19
10	2.25 $\pm$ 0.11 <sup>b</sup>	2.47 $\pm$ 0.18 <sup>b</sup>	3.05 $\pm$ 0.22 <sup>a</sup>
days 1-3 sum	8.52 $\pm$ 0.18 <sup>b</sup>	8.48 $\pm$ 0.69 <sup>b</sup>	10.52 $\pm$ 0.52 <sup>a</sup>
days 1-3 mean	2.84 $\pm$ 0.06 <sup>b</sup>	2.83 $\pm$ 0.23 <sup>b</sup>	3.51 $\pm$ 0.17 <sup>a</sup>
days 1-10 sum	25.77 $\pm$ 0.52 <sup>b</sup>	24.88 $\pm$ 1.08 <sup>b</sup>	29.22 $\pm$ 1.16 <sup>a</sup>
days 1-10 mean	2.58 $\pm$ 0.05 <sup>ab</sup>	2.49 $\pm$ 0.11 <sup>b</sup>	2.92 $\pm$ 0.12 <sup>a</sup>
General sum	257.72 $\pm$ 8.34	251.00 $\pm$ 8.57	278.26 $\pm$ 11.53
General mean	2.58 $\pm$ 0.08	2.51 $\pm$ 0.09	2.78 $\pm$ 0.12

<sup>a,b</sup> Means in a row with different superscripts are significantly different ( $p < 0.05$ ).

**Table 5.2** Food intake and energy stored as body fat from day -3 to day 4 (Mean  $\pm$  SEM).

	CO	GG	PL
Food intake as energy (Kcal)	84.74 $\pm$ 2.05 <sup>b</sup>	86.60 $\pm$ 4.21 <sup>b</sup>	98.35 $\pm$ 3.61 <sup>a</sup>
Body fat gain as energy (Kcal)	0.64 $\pm$ 1.58 <sup>b</sup>	7.82 $\pm$ 3.50 <sup>ab</sup>	12.79 $\pm$ 2.16 <sup>a</sup>
%Energy of fat gain/food intake (%)	0.62 $\pm$ 1.87 <sup>b</sup>	8.26 $\pm$ 3.49 <sup>ab</sup>	12.89 $\pm$ 2.08 <sup>a</sup>

<sup>a,b</sup> Means in a row with different superscripts are significantly different ( $p < 0.05$ ).

**Table 5.3** Effects of milk polar lipids on liver and adipose tissue mass (Mean  $\pm$  SEM).

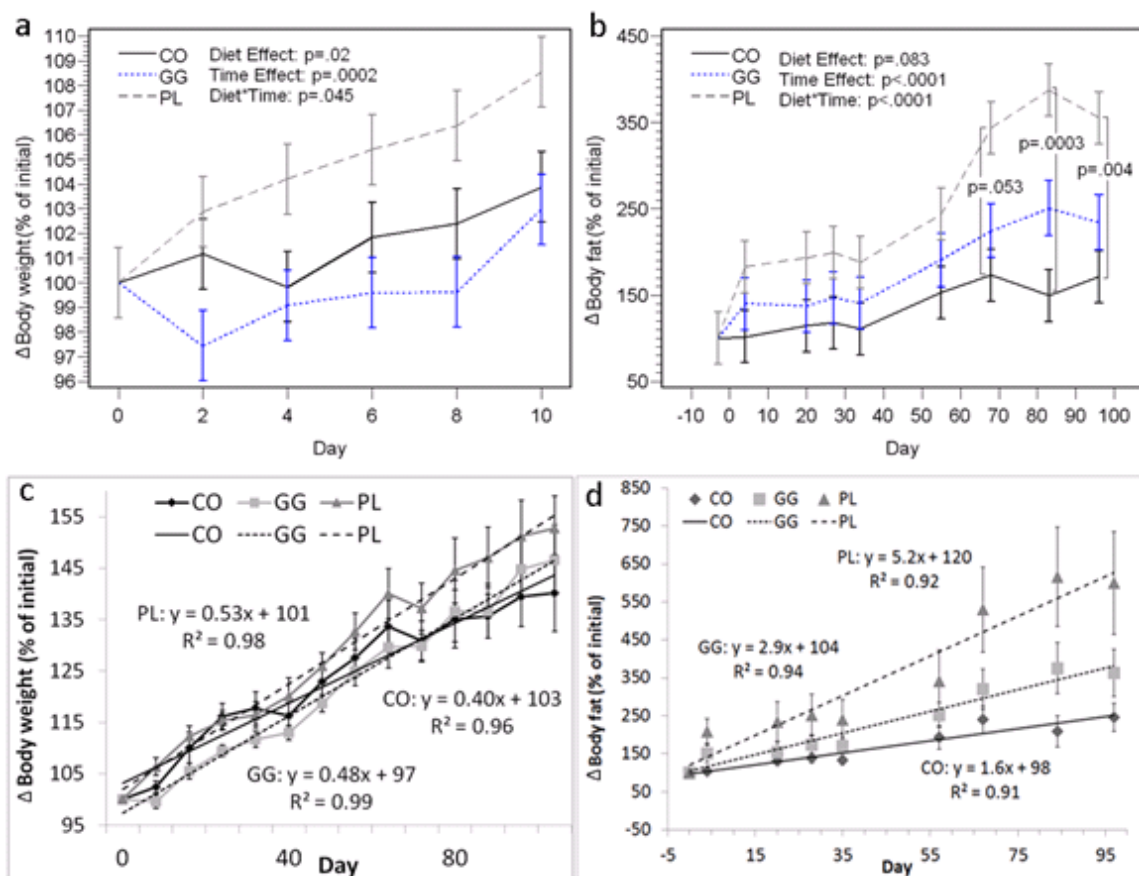
<b>Tissue mass/body weight (%)</b>	<b>CO</b>	<b>GG</b>	<b>PL</b>
Liver%	3.32 $\pm$ 0.25	3.50 $\pm$ 0.13	3.26 $\pm$ 0.05
Brown adipose tissue depot%	0.42 $\pm$ 0.04	0.52 $\pm$ 0.08	0.52 $\pm$ 0.06
Inguinal fat depot%	2.82 $\pm$ 0.49	3.34 $\pm$ 0.52	3.69 $\pm$ 0.38
Gonadal fat depot%	3.34 $\pm$ 0.58	4.37 $\pm$ 0.63	4.81 $\pm$ 0.36
Mesenteric fat depot%	1.39 $\pm$ 0.26	1.75 $\pm$ 0.22	2.19 $\pm$ 0.25
Retroperitoneal fat depot%	1.19 $\pm$ 0.28	1.47 $\pm$ 0.26	1.72 $\pm$ 0.18
Visceral fat depots%	5.92 $\pm$ 1.10	7.59 $\pm$ 1.09	8.72 $\pm$ 0.71
Subcutaneous fat depot%	5.30 $\pm$ 1.08	5.90 $\pm$ 0.98	6.56 $\pm$ 0.52
Total fat depots%	11.64 $\pm$ 2.20	14.01 $\pm$ 2.11	15.80 $\pm$ 1.27

<sup>a,b</sup> Means in a row with different superscripts are significantly different ( $p < 0.05$ ).

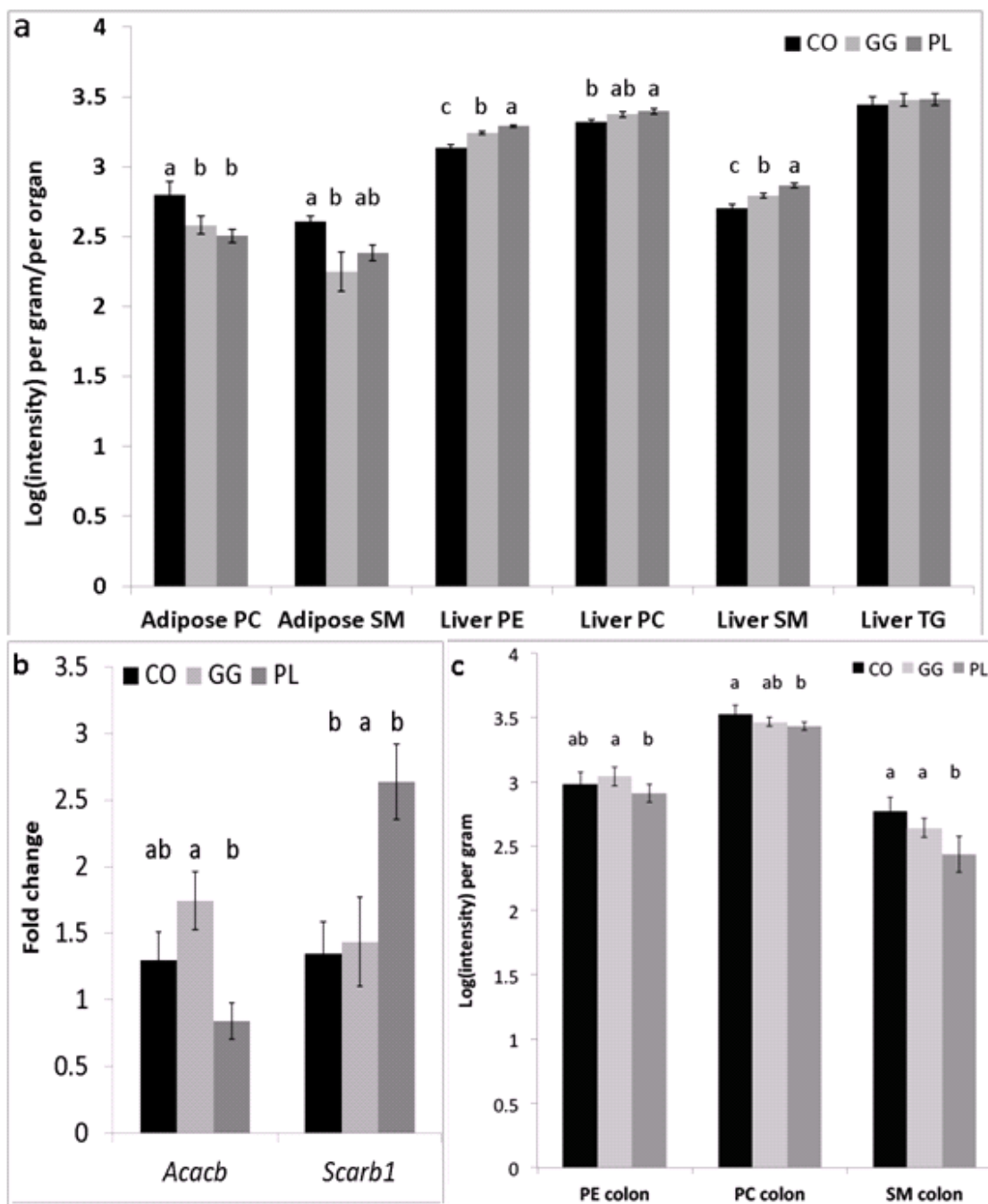
**Table 5.4** Effects of milk polar lipids on plasma levels of MCP-1 and TNF- $\alpha$  in C57BL/6J mice during the development of diet-induced obesity (Mean  $\pm$  SEM; unit: Log<sub>10</sub>(pg/ml)).

<b>Lipids</b>	<b>CO</b>	<b>GG</b>	<b>PL</b>
<b>Baseline</b>			
MCP-1	1.42 $\pm$ 0.07	1.51 $\pm$ 0.10	1.14 $\pm$ 0.15
TNF- $\alpha$	1.38 $\pm$ 0.06	1.36 $\pm$ 0.06	1.16 $\pm$ 0.14
<b>Day 35</b>			
MCP-1	1.50 $\pm$ 0.04 <sup>a</sup>	1.46 $\pm$ 0.03 <sup>a</sup>	1.32 $\pm$ 0.06 <sup>b</sup>
TNF- $\alpha$	1.37 $\pm$ 0.05	1.25 $\pm$ 0.11	1.33 $\pm$ 0.15
<b>Day 101</b>			
MCP-1	1.48 $\pm$ 0.04	1.54 $\pm$ 0.05	1.38 $\pm$ 0.07
TNF- $\alpha$	1.35 $\pm$ 0.08	1.39 $\pm$ 0.08	1.28 $\pm$ 0.11

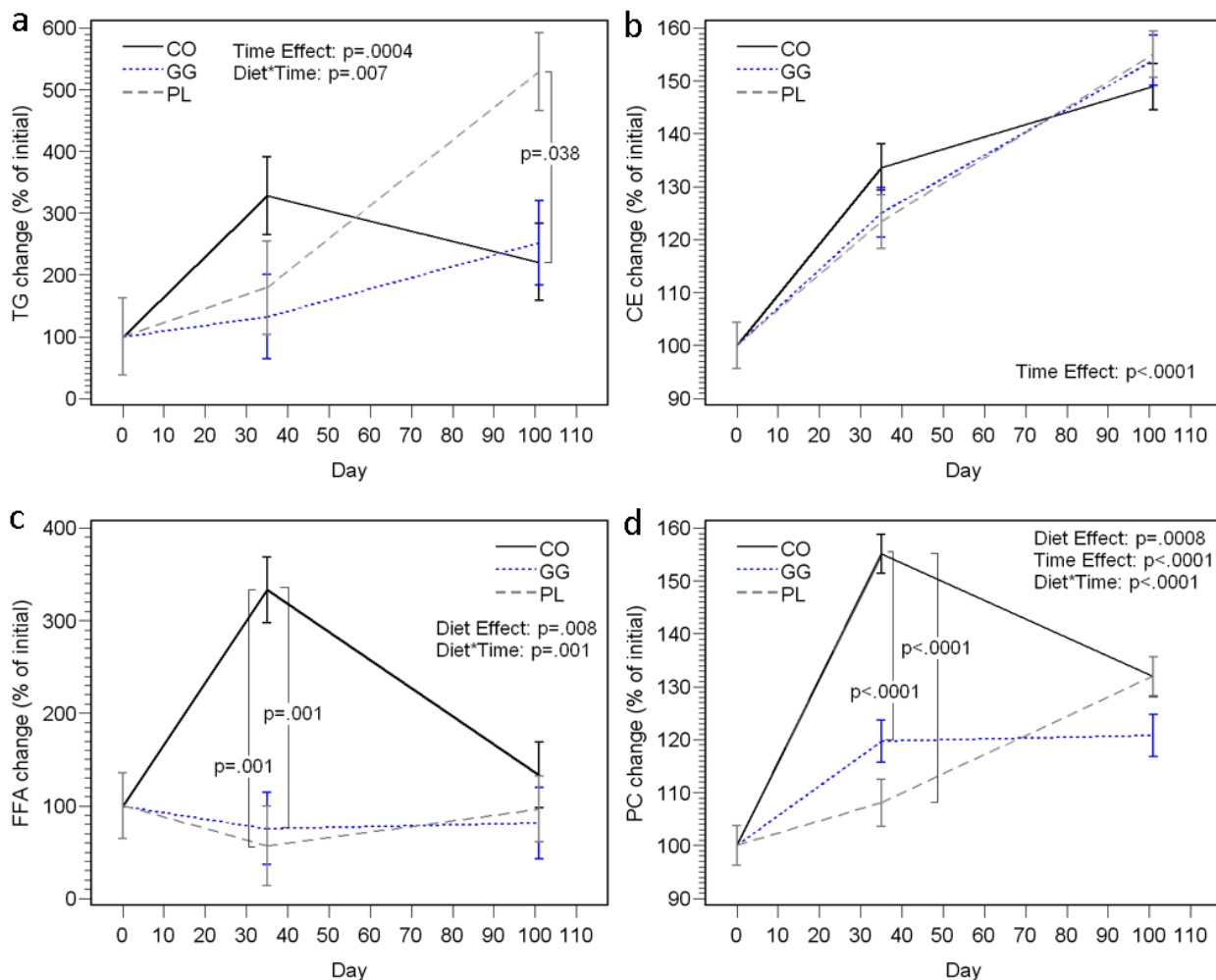
<sup>a,b</sup> Means in a row with different superscripts are significantly different ( $p < 0.05$ ).



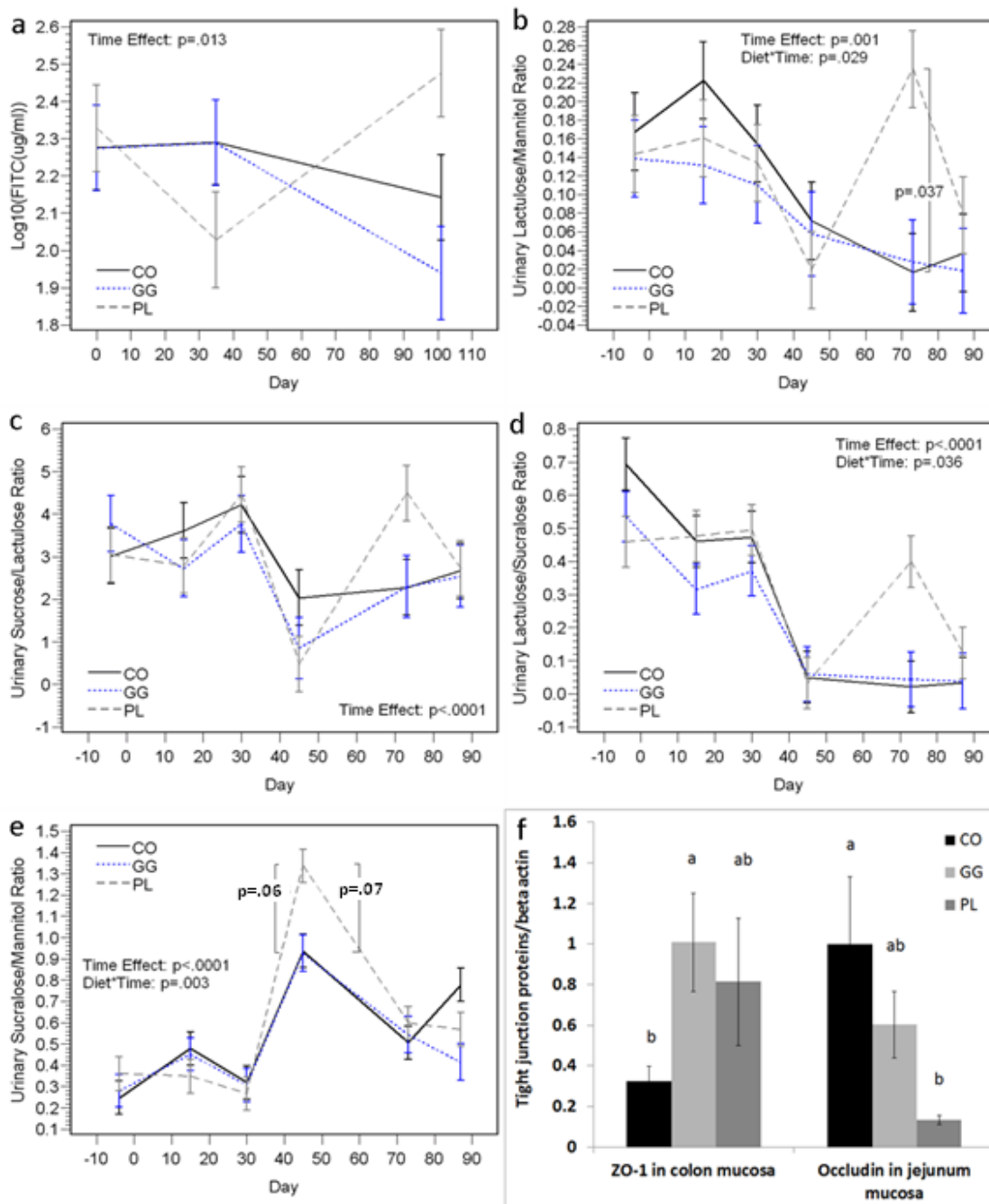
**Figure 5.1** Effects of the polar lipids on body weight and body fat content. Initial body weight for CO, GG and PL groups:  $20.9 \pm 0.5$ ,  $21.2 \pm 0.3$ ,  $21.7 \pm 0.7$  (g). Initial body fat for CO, GG and PL groups:  $2.17 \pm 0.09$ ,  $2.06 \pm 0.08$ ,  $2.18 \pm 0.14$  (g). (a) PL group gained more body weight during the first 10 days. (b) PL group accumulated more body fat compared with CO and GG groups. (c) PL group gained more body weight compared with CO and GG groups. (d) PL increased body fat at a faster rate compared with CO and GG. The data represent mean  $\pm$  SEM ( $n = 6$ ).



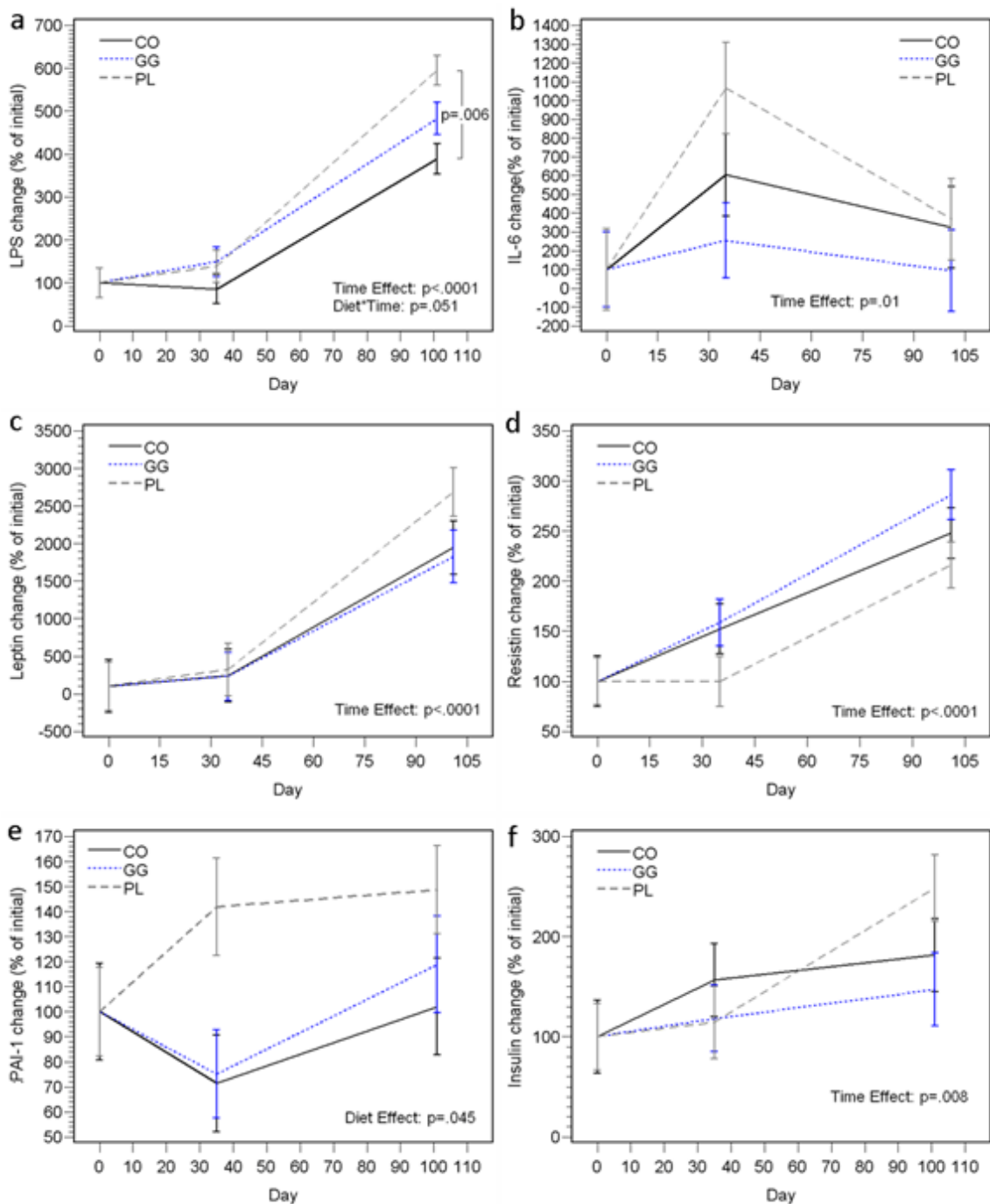
**Figure 5.2** Effects of milk polar lipids on tissue lipid profile. The data represent mean  $\pm$  SEM (n = 6, 5, 6 for CO, GG, PL). (a) GG and PL decreased PC and SM in visceral adipose and increased PE, PC and SM in the liver compared with CO. (b) GG up regulated the expression of *Acacb* in liver compared with PL; PL up regulated expression of *Scarb1* compared with CO and GG. (c) PL decreased PE, PC and SM in colon mucosa compared with CO and GG. Means in a row with different superscripts are significantly different ( $p < 0.05$ ).



**Figure 5.3** Effects of milk polar lipids on plasma lipid profile. The data represent mean  $\pm$  SEM ( $n = 6, 5, 6$  for CO, GG, PL). (a) Plasma TG increased over time in GG and PL groups; PL group had higher TG at the end compared with CO. (b) Plasma CE increased over time. (c) Plasma FFA increased in CO group and the level returned to baseline level by the end of the study. (d) Plasma PC level increased in CO group compared with that in GG and PL groups and the level decreased by the end of the study.

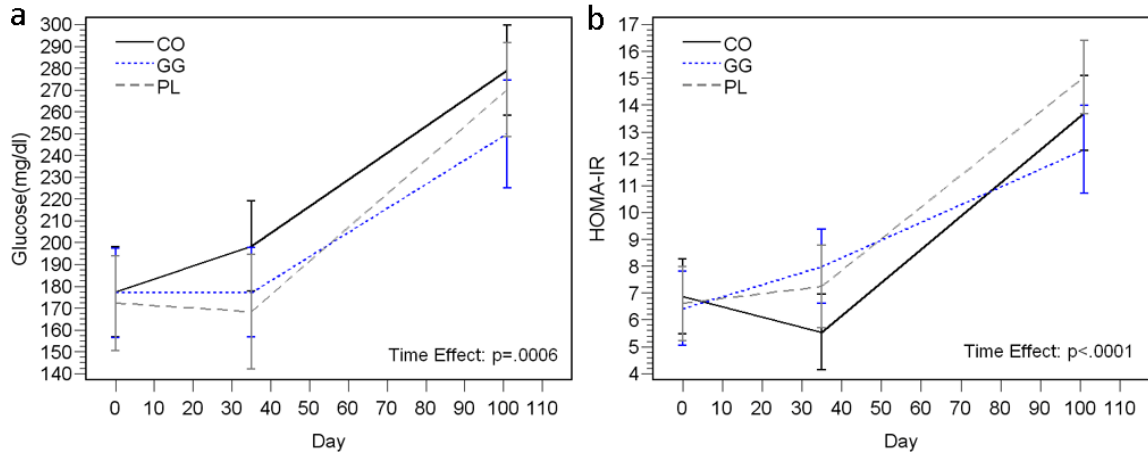


**Figure 5.4** Effects of milk polar lipids on gut permeability. The data represent mean  $\pm$  SEM ( $n = 6, 5, 6$  for CO, GG, PL). (a) The polar lipids did not affect the plasma FITC. (b) The urinary Lactulose/Mannitol ratio decreased over time. (c) The urinary Sucrose/Lactulose ratio decreased over time. (d) The urinary Lactulose/Sucralose ratio decreased over time. (e) The urinary Sucralose/Mannitol ratio increased gradually until day 45 and then decreased. (f) GG and PL increased ZO-1 expression in colon mucosa; PL and GG decreased occludin expression in jejunum mucosa. Means in a row with different superscripts are significantly different ( $p < 0.05$ ).

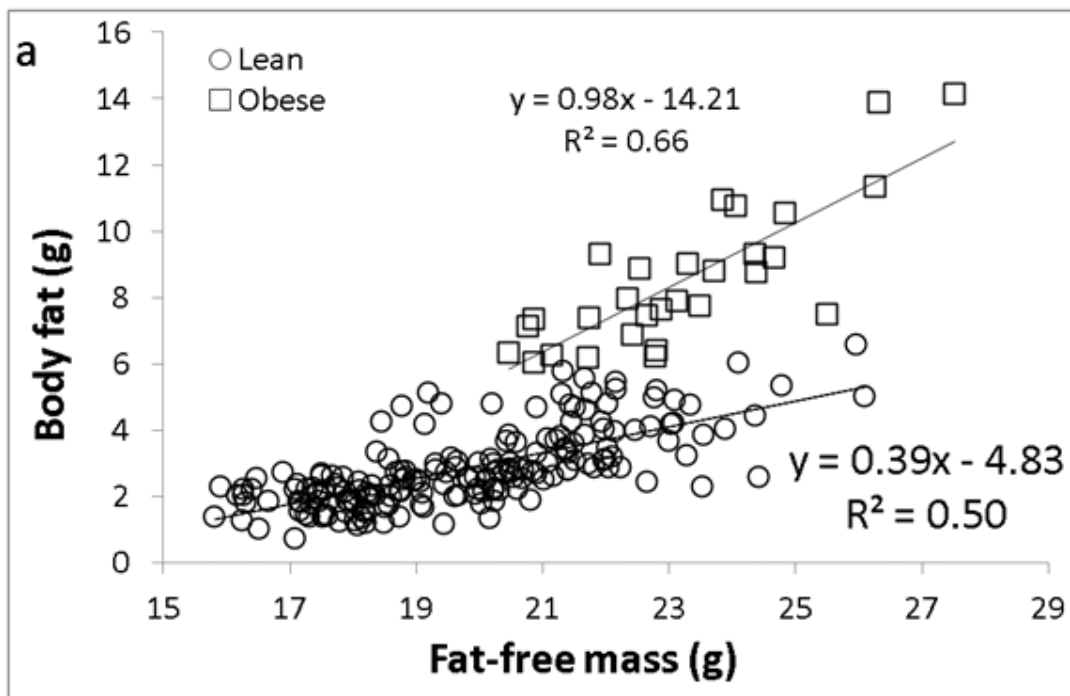


**Figure 5.5** Effects of the polar lipids on plasma LPS and cytokines. The data represent mean  $\pm$  SEM ( $n = 6, 5, 6$  for CO, GG, PL). (a) Plasma LPS level increased over time and the PL increase the plasma LPS at day 101. (b) Plasma IL-6 level increased by day 35 and then decreased. (c) Plasma leptin level increased over time. (d) Plasma resistin level increased over time. (e) Plasma PAI-1 level increased in PL group, decreased in CO and GG groups during the first 35 days and then increased back toward the end of the study. (f) Plasma insulin level increased over time.

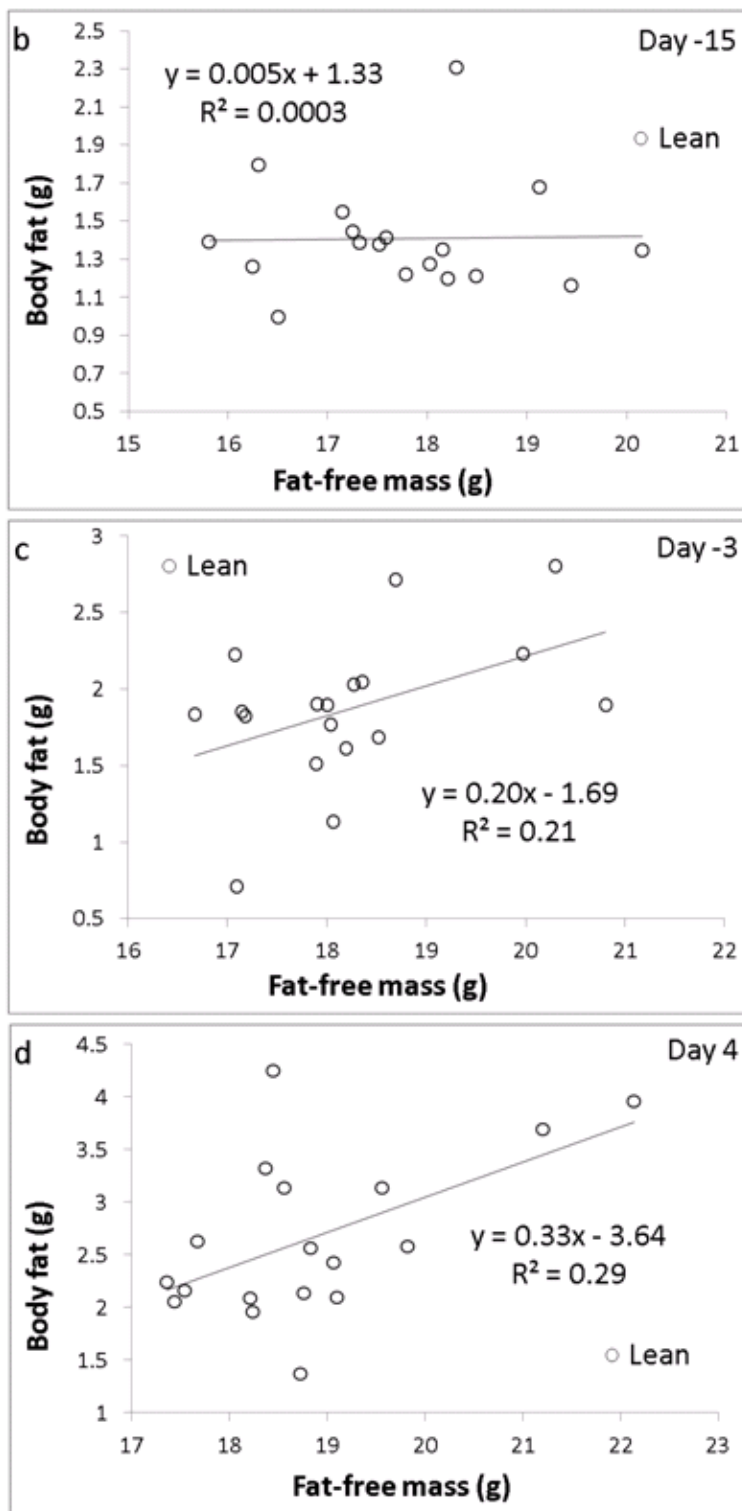




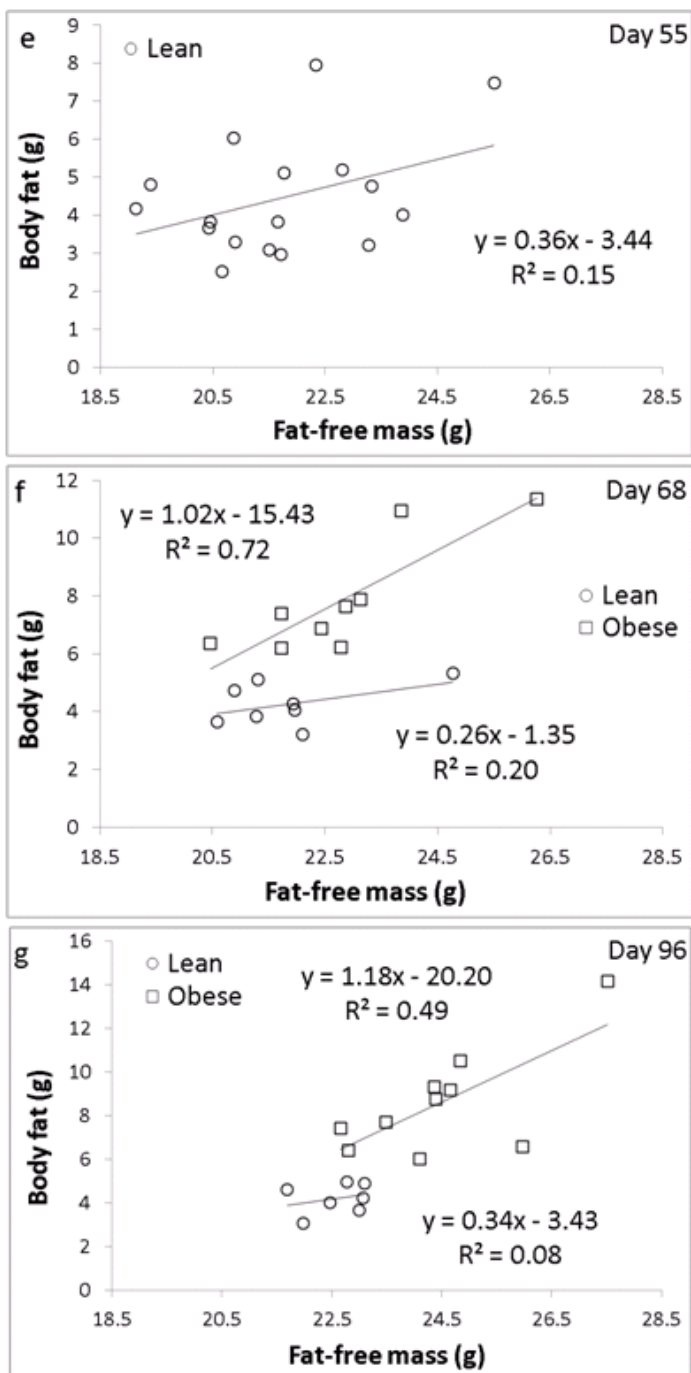
**Figure 5.6** Effects of milk polar lipids on fasting glucose and HOMA-IR. The data represent mean  $\pm$  SEM ( $n = 6, 5, 6$  for CO, GG, PL). (a) The urinary Lactulose/Mannitol ratio increased after LPS stress and returned to baseline level during recovery. (b) The urinary Sucrose/Lactulose ratio decreased after the LPS stress and increased gradually during the recovery.



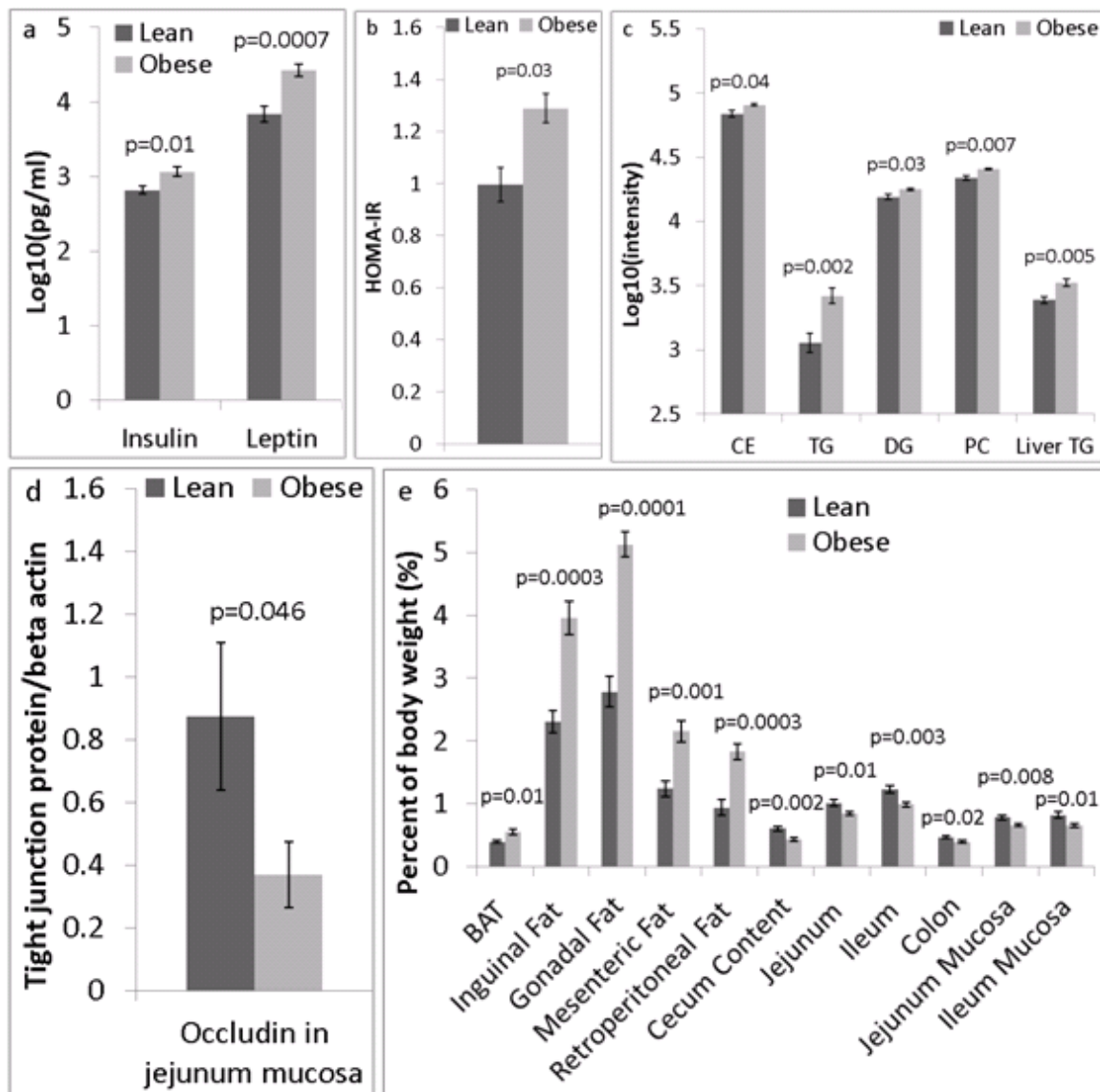
**Figure 5.7a** Body fat plotted against fat-free mass for individual animals during day 1 through day 96.



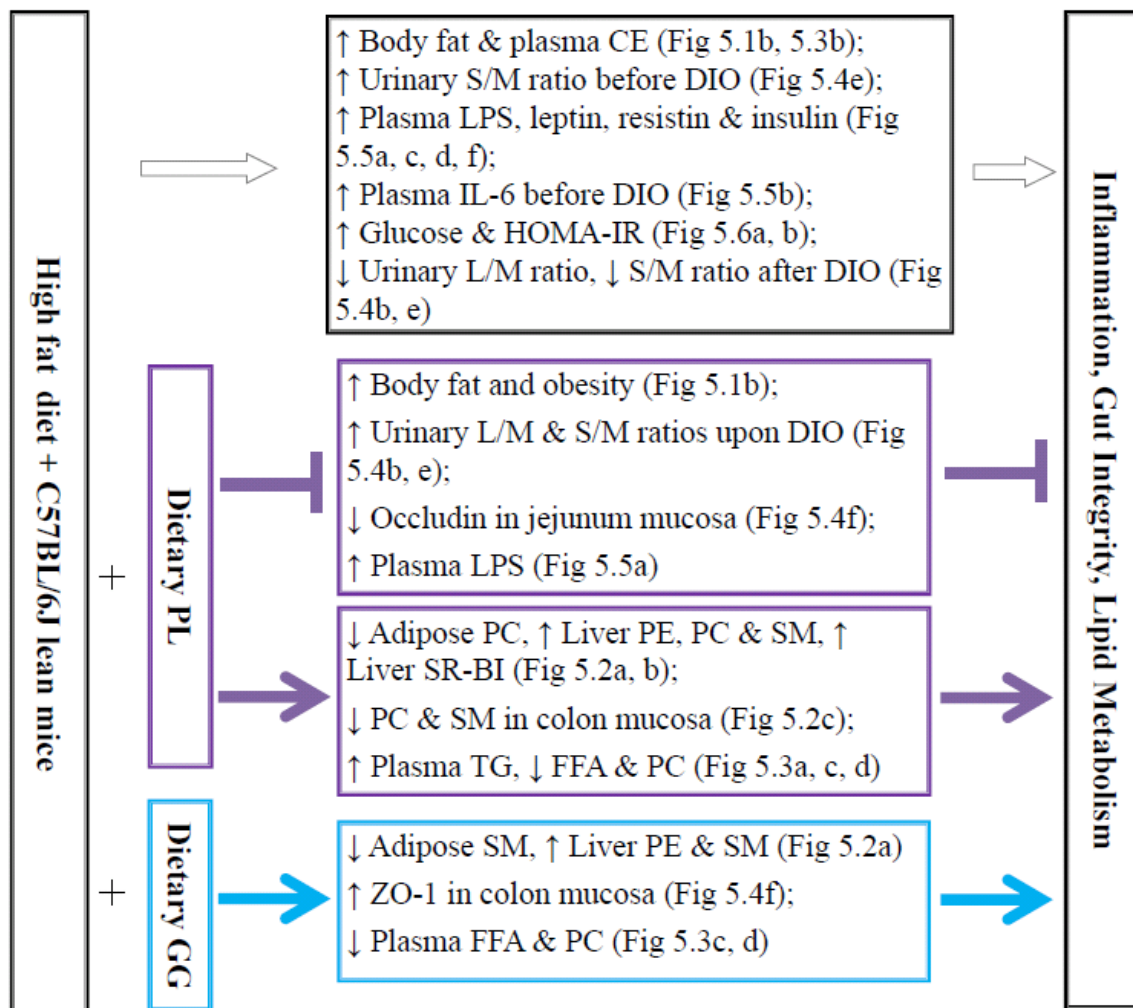
**Figure 5.7b-d** Body fat plotted against fat-free mass for individual animals at (b) day -15, (c) day -3 and (d) day 4.



**Figure 5.7e-g** Body fat plotted against fat-free mass for individual animals at (e) day 55, (f) day 68 and (g) day 96.



**Figure 5.8** Comparison between lean and obese mice. The data represent mean  $\pm$  SEM ( $n = 7$  and  $10$  for Lean and Obese). (a) Obese mice had higher plasma insulin and leptin compared with lean mice. (b) Obese mice had higher homeostasis model assessment of insulin resistance (HOMA-IR). (c) Obese mice had higher plasma cholesteryl ester (CE), triglycerides (TG), diglycerides (DG), phosphatidylcholine (PC) and higher liver TG compared with lean mice. (d) Obese mice had lower occludin protein expression in jejunum mucosa compared with lean mice. (e) Obese mice had higher amount of brown adipose tissue (BAT), inguinal, gonadal, mesenteric and retroperitoneal fat depots compared with lean mice. Obese mice had lower amount of cecum content, jejunum, ileum, colon, jejunum mucosa and ileum mucosa compared with lean mice. Means in a row with different superscripts are significantly different ( $p < 0.05$ ).



**Figure 5.9** Summary of major findings in Chapter 5. Horizontal white arrows indicate the effects of the control diet. Horizontal T-shaped purple arrows indicate undesirable effects. Horizontal solid purple and blue arrows indicate desirable or neutral effects. L/M: Lactulose/Mannitol, S/M: Sucralose/Mannitol.

## CHAPTER 6

### SUMMARY AND FUTURE DIRECTIONS

In this dissertation, I explored the effects of the dietary milk polar lipids on gut permeability, systemic inflammation, and lipid metabolism in several rodent models. The major hypotheses were that the dietary polar lipids would increase the gut barrier integrity, reduce systemic inflammation, and reduce liver lipid levels and affect the expression of genes associated with fatty acid synthesis and cholesterol regulation in the liver. The hypotheses were tested in the context of stressful diets, systemic inflammation, and obesity. The results did not support the majority of the hypothesized effects (Figure 6.1). The milk phospholipids as dietary supplements may increase gut permeability and systemic inflammation and promote body fat accumulation during obesity and inflammatory responses. The milk gangliosides as dietary supplements may have little effect on gut permeability, systemic inflammation, and lipid metabolism during obesity and inflammatory responses. Based on the data from this dissertation, the dietary supplementation of milk polar lipids should not be recommended in the context of obesity and systemic inflammation. Although the milk-derived concentrates used in this dissertation were semi-purified, there were several active compounds in each of the concentrates. The PL concentrate contained sphingomyelin (SM), phosphatidylcholine (PC), phosphatidylethanolamine (PE) and phosphatidylserine (PS). The GG concentrate contained gangliosides, PC and PS. The bioactivities of the individual compounds in the milk polar lipids concentrates need to be explored by systematic investigations. Here I will summarize the major findings in four models separately first and then look

comprehensively at the major endpoints, namely gut permeability, systemic inflammation, and lipid metabolism.

### **Rat Model with High Sucrose Diet**

The AIN-76A diet is still commonly used in the aberrant crypt foci (ACF) studies with rodents (1) and the high sucrose content of the AIN-76A diet causes fatty liver in animals fed the diet for long periods of time (2). Since the diets were quite stressful metabolically, the findings in this study may not be extrapolated to other circumstances. Compared with the milk fat diets, the corn oil diet caused a significant increase in hepatic free fatty acids, a potential trigger for the development of nonalcoholic steatohepatitis (NASH) from non-alcoholic fatty liver disease (NAFLD). The anhydrous milk fat diet resulted in more hepatic TG storage compared with corn oil and MFGM supplemented diets. Saturated fat may facilitate TG accumulated in the liver. Unsaturated fatty acids and polar lipids may alleviate the accumulation of TG in the liver. The mechanism of polar lipids on reducing the accumulation of hepatic TG may be through promoting lipid export into plasma. In conclusion, the fat source of the AIN-76A diet affects the lipid profile of key tissues involved in lipid trafficking and storage as well as gene expression networks within these tissues.

Since the AIN-76A diet has an unreasonably high amount of sucrose and is metabolically stressful, it may confound the findings in gut permeability, lipid metabolism and systemic inflammation. Future studies may use diets with lower sucrose (such as AIN-93G diet) to explore which components of the MFGM have the observed effect.



Rats and mice have different metabolic responses to dietary intervention. For example, after a 48h fast, the hepatic TG increased significantly in 6-8 weeks old Swiss albino mice but declined in Sprague-Dawley derived rats at similar age (3). When 5 weeks old male Wistar CpbIWU rats and NMRI mice were fed a cholesterol-free diet containing corn oil for 20 days, serum TG were reduced and fecal excretion of neutral steroids were increased in the rats but not affected in the mice. The rats and mice had similar responses to corn oil when the diet was supplemented with 1 % (w/w) of cholesterol (4). There are significant differences in postprandial TG patterns between Wistar rats and C57BL/6J mice at the age of 8 weeks fed regular rodent chow diet. C57BL/6J mice have similar postprandial lipid profile in the serum as healthy men (5). So it is reasonable to expect the effects of MFGM to be different in mouse models from rat models. Given the fact that rat models still serve as important platforms for exploring metabolism and nutrition, it may still be worthwhile to test the effects of the individual components of MFGM in rat models.

### **Genetic Obesity Model with High Fat Diet**

In the ob/ob mouse model, the gut barrier integrity was compromised, the plasma lipids level was decreased, and most of the systemic inflammatory cytokine levels did not change from baseline. The food restriction aggravated the hepatic lipidosis and may have caused death in some of the animals. The dietary GG increased the tight junction (TJ) protein occludin expression in the colon mucosa and had little effect on lipid metabolism and systemic inflammation. The dietary PL supplementation increased the total body fat percentage and redistributed lipids from liver and visceral fat depots into the plasma. The dietary PL increased the plasma SM, which was strongly associated with the increase of

the plasma inflammatory cytokine IL-6. Taken together, the supplementation of high fat diets with phospholipids and sphingomyelin could result in unfavorable effects on lipid metabolism and systemic inflammation in the ob/ob mice. The dietary milk gangliosides at the current dietary level may not have significant effect on the intestinal barrier integrity, lipid metabolism and systemic inflammation in the ob/ob mice fed moderately high fat diets. Future studies may further explore which components of the milk phospholipids concentrate are responsible for the observed effects.

The PL supplementation reduced lipid levels in the liver but did not have any effect on the gut permeability to FITC-dextran and sugar probes. The dietary PL also increased systemic inflammation. Often times, a few organ systems are assessed during dietary interventions. The limitation of this kind of study is that the dietary treatment may benefit one or a few organ systems but could be detrimental to the other systems. During this study, only four out of the eleven major organ systems were assessed in some detail. There are still many systems that were not assessed, such as the nervous system, cardiovascular system, skeletal system, respiratory system, excretory system, reproductive system and immune system. The general effects cannot be concluded until all systems are taken into consideration. Therefore, the effects of dietary milk polar lipids on the whole body in the ob/ob mice needs to be further assessed in a systematic manner.

The obese mouse model with a moderately high fat diet is an excellent representation of the dietary practice in America, where over one third of the people are obese and consuming a diet with 34% of fat by energy on average. The evidence from human

studies suggests that leptin mainly affects the human energy balance through regulating appetite instead of energy expenditure (6). The ob/ob mouse model may not provide much information regarding the development of obesity but could offer important insights for the development of the comorbidities associated with obesity. The ob/ob mouse is a great model for studying preexisting obesity if the diabetic mice are excluded. Stresses should be kept at a very low level for this model. Caution should be taken since the ob/ob mouse is leptin deficient and the possibility cannot be excluded that the negative results may be leptin dependent.

The differential sugar test (DST) is an effective method to evaluate the site-specific gut permeability. But the currently available metabolic cages are not suitable for carrying out the DST in the ob/ob mice. A specific metabolic cage system designed for the ob/ob mice is needed to prevent the food restriction. The regular metabolic cage for the lean mice is too small and the ones for the rats are too big for the ob/ob mice.

Since the ob/ob mice have a higher feed efficiency and significantly different energy metabolism at the early age compared with the lean mice (7), adult ob/ob mice may be used in the high fat diet model to prevent extreme fat accumulation and to achieve a healthier development when the mice are young. By using the adult ob/ob mice, diets with 34% fat by energy may pose less stress on the animals comparing with using the younger ob/ob mice. Caution should always be kept in mind since the ob/ob mouse model is leptin deficient and findings from animal models may not be directly applicable in the humans.

There is an association between the self-reported lifetime stress and an increased risk of obesity in adult Canadians (8). Psychological stress is negatively correlated with healthy dietary behaviors and positively correlated with body weight (9). Human and animal studies have shown that the chronic psychological stress tends to affect the dietary pattern and increase craving for the nutrient-dense “comfort foods.” The stress associated with visceral obesity may be linked to the hyperactivity of the sympathetic branch of the autonomic nervous system (ANS) and the hypothalamic-pituitary-adrenal (HPA) axis (10). The depression and anxiety commonly observed in obese people (11-14) can activate the HPA axis (15). The increase of depression and/or anxiety is associated with an increase of waist-to-hip circumference ratio (16, 17). Repeated stresses increase visceral adiposity independent of changes in body weight and the stress-induced visceral obesity may be mediated by the stress-induced IL-1 $\beta$  in non-visceral white adipose tissue (Figure 6.2) (18). In healthy and non-obese rats, the acute stress increases IL-1 $\beta$  more in the subcutaneous white adipose tissue than in the visceral white adipose tissue (18). IL-1 $\beta$  may function through autocrine and/or paracrine signaling in the white adipose tissue (19). The acute rise of IL-1 $\beta$  can have beneficial functions such as increasing lipolysis, increasing leptin secretion and potentiating glucocorticoid signaling. But sustained IL-1 $\beta$  signaling through repeated stress can increase visceral adiposity, which may be achieved by adipose hypertrophy and/or adipocytes hyperplasia in the subcutaneous adipose tissue during energy overflow (18).

The data from this ob/ob mouse study indicate that acute stress during obesity may affect the comorbidities of obesity. The postmortem pathology revealed severe hepatic

lipidosis and renal lipidosis in the ob/ob mouse. One of the possible reasons for the animal death was the stress induced during the second 24-hour stay in the metabolic cage and the last MRI scan one day after the metabolic cage stay. Two days' staying in the metabolic cage results in transient hypertension and sustained tachycardia in the C57BL/6J lean mice (20). It takes 3–4 days for the plasma and urinary biochemistry to reach stable values when the C57BL/6J mice are housed in metabolic cages (21). The serotonin (5-HT)<sub>2C</sub> receptor knockout mice (C57BL/6J background) develop hyperphagia and midlife obesity and they are hyperresponsive to repeated stress (22).

It is possible that the stresses from the second 24-hour stay in the metabolic cage and the MRI scan caused acute hepatic failure on top of the chronic renal and hepatic lipidosis. With the fatty liver in place, the hepatocytes are more vulnerable to damages. There are more apoptotic events in the livers from patients with NAFLD (23). The injection of anti-Fas antibody results in animal death within 12 hrs in 90% of the obese ob/ob mice while all lean control animals survive (24). The animal death is due to the hemorrhagic liver failure mediated by the apoptotic cell death. The ob/ob mice represent a model of NAFLD complicated with type 2 diabetes mellitus and hypertriglyceridemia (24). The hepatic failure in this study could have resulted from the food restriction and the sustained activation and subsequent exhaustion of the ANS and the HPA axis. The ob/ob mice develop spontaneous liver steatosis and the high fat diet can induce a more severe liver injury (25). The activation of the HPA axis could release a large amount of corticoids, which worsens the condition of the acute hepatic failure (26). Further studies are needed to clarify the mechanisms behind the mortality occurred in those ob/ob mice.

The ob/ob mouse is widely used as an animal model of type 2 diabetes. Diabetes mellitus is sometimes defined by fasting hyperglycemia (27). Diabetes mellitus may be more appropriately defined as a group of metabolic disorders featuring hyperglycemia due to defects in insulin secretion and/or insulin action (28). Although most of the ob/ob mice had hyperglycemia toward the end of the study, only two mice developed obvious symptoms of diabetes. The ob/ob mice on a diet with 6% fat (by mass) or on a rodent chow only develops transient hyperglycemia, which partially remits between 10 and 14 weeks of age (29). Therefore, the fasting hyperglycemia may not be an ideal criterion for defining diabetes in the ob/ob mice. Clinical symptoms in combination with hyperglycemia may be used for defining diabetes in these mice. When the ob/ob mouse is used as an animal model of obesity or type 2 diabetes, the mice should be screened to differentiate diabetic and nondiabetic animals. The nondiabetic mouse may be used as a model of obesity and the diabetic mouse may be used as a model of type 2 diabetes to reduce confounding factors.

### **LPS-induced Systemic Inflammation Model**

The LPS induced inflammation model used in this dissertation had two phases, the acute and chronic stages. Dietary milk polar lipids did not protect the gut barrier integrity during the acute phase, within 24 h after the LPS injection. The LPS was injected subcutaneously and the LPS can be retained in the body until a month later (30). In the context of the chronic inflammatory stress induced by the LPS in young C57BL/6J mice, the gut permeability to extra large molecules increased (Figure 4.6c, LPS: 100-1000 kD), to large molecules decreased (Figure 4.6b, FITC-dextran: 4000 Da) and to small molecules increased (Figure 4.7a-d, lactulose and sucrose: 342.3 Da, sucralose: 397.64

Da). The decreased permeability to the large molecules could be due to the maturation of the gut barrier during development in the weaning mice (31). The increased permeability to the smaller molecules could be due to the compromise of the gut barrier integrity by the high fat diet and the LPS-induced inflammation. The absorption of the intestinal LPS can be mediated both through the paracellular diffusion and during the chylomicron secretion (32). So the increase of the plasma LPS may not be explained by the increase of gut permeability to large molecules but should be mediated mainly through chylomicron secretion.

The plasma level of resistin increased overtime in the C57BL/6J mice challenged with the LPS. The increase of plasma levels of resistin may be explained by the high fat feeding and the time of the feeding period (32). The diet with 45% fat by energy increases plasma resistin level compared with the diet with 13% fat by energy (32). The plasma resistin level is higher in the 29-week-old C57BL/6J mice than in the 15-week-old mice regardless of the dietary fat level (32).

The plasma insulin level decreased in the C57BL/6J mice stressed by the subcutaneous LPS injection. The decrease of plasma insulin may be caused by the injected LPS. The intraperitoneal injection of LPS (at 10 µg per mouse) results in a more than half decrease of the insulin mRNA expression in the pancreatic islets in the 10-week-old BALB/c male mice by 6h after the LPS injection (33). About 85% of the LPS injected intraperitoneally and 26% of the LPS injected subcutaneously should have been absorbed by 6h after the injection (34). The amount of the absorbed LPS by 6h post

injection in this study would be higher than the absorbed LPS in the BALB/c mice study (32.5  $\mu\text{g}$  vs 8.5  $\mu\text{g}$ ). Although there could be species difference, the damage to the pancreas should have been much more severe in this study compared with that in the BALB/c mice study. The intravenous injection of LPS and the intraperitoneal injection of TNF- $\alpha$  can also decrease the plasma level of insulin in the C57BL/6 mice (34, 35). The high fat feeding decreases the plasma insulin level in the rats (36). It is not clear if high fat feeding contributed to the decrease of plasma insulin or not in this study. The decrease of the plasma insulin level was accompanied by the lack of body fat increase and the lack of the plasma leptin increase. There were significant increases of the body fat and the plasma leptin in the C57BL/6J mice fed the identical diets but were not stressed by the LPS injection (Figure 5.1b and 5.5c, Chapter 5). The LPS challenge may have prevented the accumulation of body fat by suppressing the secretion of insulin during the high fat diet feeding. It may be hypothesized that the suppression of insulin expression in the pancreas may prevent the body fat accumulation.

Two mice died in each of the GG and PL groups. The cause of the animal death was the LPS challenge. The LPS dosage may be slightly decreased (e.g., at 2.5-3 mg/kg body weight) to prevent animal death for chronic studies. The interesting effect of the decreased insulin level on the body fat content can be further explored by using an ideal dose of the LPS. The amount of LPS may be optimized to induce enough pancreas damage but not result in considerable damages to the other organs.



In this study, the injected LPS resulted in a strong inflammatory response while the high level of plasma LPS (absorbed through the gut) was not accompanied by increased proinflammatory cytokine levels in the plasma. There is strong evidence from animal and human studies indicating that high fat diets result in absorption of the intestinal LPS into the blood (endotoxemia). The majority of the aforementioned studies did not evaluate how the amount, the quality and the structure of the dietary fat may affect the endotoxemia (32). The factors other than the plasma LPS may be changed by the high fat diets, which could affect the systemic inflammation. The dietary fat may serve as detergent and affect the absorption of antigens other than the LPS. The dietary triglycerides increase the intestinal absorption of a protein antigen, ovalbumin, into adipose tissue in a chylomicron-dependent manner (37). The dietary fat absorption increases the ovalbumin absorption into the adipose tissues and the absorbed ovalbumin promotes the T-lymphocyte responses and inflammation (38). Given the fact that the intestinal lumen contains such a mosaic of foreign materials, there could potentially be other antigenic substances that may be absorbed and therefore facilitate systemic inflammation. The possibility of other potential gut-derived antigens is important to keep in mind. Data from the DIO mouse model (chapter 5) shed some light on the potential mechanism for the lack of a considerable inflammatory response corresponding to the increased plasma LPS absorbed from the gut. Chylomicron secretion may play an important role in the mechanism. The exact mechanisms for how the gut-derived LPS may affect systemic inflammation need further study.

The finding that the foreign LPS may play a bigger role in promoting inflammation compared with the LPS absorbed from the gut could have important implications in this metagenomic era. Currently big expectations are given to the study of microbiota. The composition of the gut microbiota is closely associated with adiposity in mice and humans (39). The body should also have flexibility in adapting to the changes in the microbiota composition. The organism may be able to adapt to the antigens released from the gut bacteria. Further studies are warranted to explore how the gut-derived LPS may not induce a strong systemic inflammation.

### **Diet-induced Obesity Model**

In the DIO model, the differences in diet intake during the first few days may have made a difference in the fat accumulation process. This may have important implications in the dietary practice for human beings. People would not be concerned about the overconsumption of food for a short period of time. The data from this study suggest that the short-term overfeeding may have long-term consequences. Compared with mice in the CO and GG groups, the mice in the PL group consumed more diet during the first 3 days and the difference was still significant by 10 days (Table 5.1). The body fat percentage was higher in the PL group compared with that in the CO and GG groups (Figure 5.1b). The differences in the body fat percentage between three groups were maintained until about day 55 when the body fat percentage started to increase at a faster rate in the PL group compared with the other two groups (Figure 5.1b). Obesity was established in half of the mice by day 68 (Figure 5.7f). There was no corresponding increase of food intake in the PL group starting from day 55.

Two hypotheses may be proposed to explain the faster increase of the body fat percentage in the PL group from day 55. One hypothesis is that phospholipids promote the preadipocyte differentiation and result in the adipocytes hyperplasia in the PL group. Another hypothesis is that the phospholipids increase lipid incorporation into the adipocytes and result in the adipocytes hypertrophy in the PL group. Lecithin promotes the preadipocyte differentiation, upregulates differentiation-specific gene expression, and increases lipid levels in the adipocytes (40). The L- $\alpha$ -lysophosphatidylinositol is positively associated with obesity in humans (41). During the early phase of obesity in humans, the adipose expansion is mainly due to adipocyte hypertrophy. In the later stage of obesity after the body weight exceeds 170 per cent of the ideal, the adipocytes hyperplasia starts to play a role and the degree of the hyperplasia is well correlated with the obesity severity (42). At the time when the fat accumulation started to occur at a faster rate in the PL group (day 55, Figure 5.7e), the mice were not obese yet. So the first hypothesis may be better supported. The body fat percentage of the CO group reached a plateau at day 65. At around day 85, the body fat percentage plateaued in the GG and PL groups. The further increase of the body fat after day 65 in the GG and PL groups could have been caused by the phospholipids in the diets. It is possible that the phospholipids induced the preadipocytes differentiation from the beginning of the dietary treatment. It may be further hypothesized that the phospholipids-induced adipocytes hyperplasia did not contribute significantly to the body fat content and the later hypertrophy of the newly differentiated adipocytes were responsible for the higher body fat content observed in the PL group.

This study revealed important dynamic changes in gut permeability and interesting interactions between dietary lipids and gut permeability during the development of the DIO. During the development of the DIO in the C57BL/6J mice fed high fat diets, gut permeability to FITC-dextran decreased (Figure 5.4a) in the CO and GG groups and in the PL group during the first 5 weeks. The decreased permeability to large molecules (FITC-dextran: 4000 Da) could be due to the maturation of the gut barrier during development in weaning mice. The same pattern has been observed in the mice challenged by the LPS (Figure 4.6b). Gut permeability to lactulose decreased over time in all groups except at week 11 in the PL group where the permeability to lactulose increased (Figure 5.4b). Gut permeability to sucralose fluctuated over time, increased to the highest level at week 6 and then decreased toward the end (Figure 5.4e). In general, the gut permeability to sugar probes decreased over time. That means the gut permeability to small molecules decreased and the mechanism could be the maturing process during development in young mice. So gut permeability to both small and large molecules decreased. That could mean the gut permeability through the paracellular diffusion decreased since the aforementioned molecules are absorbed primarily through the paracellular route (43).

The gut permeability to the intestinal LPS increased (Figure 5.5a) in all groups. The absorption of the intestinal LPS can be mediated through paracellular diffusion and chylomicron secretion (32). Given the fact that gut permeability was decreased to both the small molecules (sugar probes) and the large molecules (FITC-dextran), it is unlikely that the LPS was mainly absorbed through the paracellular diffusion since the LPS's

molecular weight is much bigger (100-1000 kD). The increased permeability to the LPS may be mediated mainly through the chylomicron secretion (44). The chylomicron secretion is altered in both obese mice compared with lean animals and obese humans compared with lean controls (45, 46). Data from the LPS-stressed mouse model (chapter 4) indicated that the plasma LPS increased considerably once the mice started to gain body fat but there was no corresponding increase in systemic inflammation. Taken together, it may be hypothesized that the absorption of gut LPS is mainly mediated through the transcellular pathway instead of the paracellular route. More attention should be paid to the nonparacellular pathways for exploring the absorption of the intestinal LPS. If the absorption of bacterial LPS into the plasma is mainly carried by chylomicron remnants, the lack of a considerable inflammatory response corresponding to the increased plasma LPS may be explained by the LPS-neutralizing activity of the lipoproteins (47).

The milk PL increased the permeability of small intestine and colon and decreased the expression of TJ protein occludin in the jejunum mucosa compared with the CO after the DIO. The milk GG increased the expression of the intestinal TJ protein ZO-1 compared with the CO after the DIO but did not affect the gut permeability as measured by the FITC-absorption test and the DST. The change of the TJ proteins level in the intestinal mucosa was not always accompanied by the corresponding change in the gut permeability. The functional endpoints such as the DST and the FITC-absorption test may provide better estimation of the gut permeability than the measurement of TJ proteins. The change of the TJ proteins may help reveal the relevant mechanisms.

The plasma inflammatory cytokines were not significantly affected by the high fat feeding or the dietary treatments. There was significant increase of the plasma LPS by the end of the study. The PL increased the plasma LPS compared with the CO but the PL did not increase the plasma inflammatory cytokines. These data support the finding from the LPS-stressed mouse model that the intestinal LPS may not pose a strong inflammatory response. Further studies are needed to explore the mechanisms for how the intestinal LPS may not induce a potent inflammatory response.

The dietary phospholipids increased obesity. A few days of higher food intake resulted in a significant higher body weight gain in the mice fed the PL-supplemented diet during the first 10 days of the feeding period. A similar trend was observed in the LPS-stressed model. In this study, the mice in the PL group eventually accumulated significantly more body fat after the establishment of the DIO even when they did not consume significantly more food. These observations indicate that the acute nutrient overconsumption or energy overflow may result in an important long-term impact on metabolism. The mechanisms for how dietary milk polar lipids may promote the body fat accumulation may shed light on the etiology of the diet-induced obesity.

Although the C57BL/6J mice are known to be an obesity-prone strain (48), not all of the C57BL/6J mice developed the DIO in this study. For a model of the DIO, the ideal situation may be achieved by using only the obese mice. Once the majority of the mice develop the DIO, the Fenton's method may be used to identify the obese mice. By using only the obese mice, the confounding factors can be reduced to the minimum.

The high-fat diets are usually used to induce the DIO in the C57BL/6J mice while they are weaned on the rodent chow. A run-in diet will help optimize the model by smoothing the diet transition from the rodent chow to the high fat diet. The mice consumed more food in the PL group in this study compared with the other two groups. There are a couple of possible reasons for the higher amount of the diet intake in the PL group. The PL diet was slightly softer than the other diets. Efforts may be taken to equalize the texture of the diets. The addition of the milk polar lipids into the PL and GG diets may have contributed the milk flavors, which could confound the results. At the beginning of the study, the mice had been weaned for 3 weeks and they may still have a strong preference for the milk flavors. If possible, the flavor of the diets should also be controlled. For example, a strong flavor may be added to all diets to mask other flavors.

The dynamic and static phases of obesity in the rats were reported in 1987 by Fukushima (49). More recently, Smith described the two phases during the development of obesity, the dynamic phase and the static phase (50). The dynamic phase is the phase of rapid weight gain. The static phase is when weight gain slowed significantly or stopped and the meal size returned to normal. The dynamic phase is associated with the hyperphagia while the static phase is associated with the endocrine and metabolic abnormalities. Both the DIO obesity model and the hypothalamic obesity model show these two phases of body weight gain (51). Most of the information about human obesity was obtained by studying people in the static phase. The studies on childhood obesity also usually did not monitor the dynamic processes leading to the obesity. While there is a lot of information about the static state of obesity, the data on the dynamic state of

obesity is just beginning to emerge. Little attention has been paid to the initial dynamic phase during the obesity development and the resurgence of the dynamic phase during the weight gain rebound after the weight loss. The dynamic phase is a better situation than the static phase for studying the relevant mechanisms when they are more active and available (50). A recent study revealed that the short-term overeating compromises the insulin sensitivity in the adipocytes (52). Four weeks of high energy diet results in a 10% body weight gain and a 19% body fat increase in the lean young adults. Those volunteers did not become overweight (BMI = 24.3 kg/m<sup>2</sup>) and developed moderate systemic insulin resistance. Insulin signaling in adipocytes was impaired in those volunteers (52). The data from the current mouse study also indicated that the overeating during the dynamic phase may significantly affect the static phase.

## **Effects of Dietary Polar Lipids across Different Rodent Models**

### **Effects of dietary polar lipids on gut permeability**

The dietary gangliosides did not affect gut permeability and the dietary phospholipids increased the permeability of the colon when the ob/ob mice were fed a moderately high fat diet (Figure 6.1a). The ob/ob mouse model is a leptin-deficient model. The lack of the hypothesized effect of the dietary polar lipids on the gut permeability could be due to the absence of the active leptin. In the DIO model, the dietary gangliosides did not affect the gut permeability and the dietary phospholipids increased the permeability of the small intestine and the colon after the DIO. The lack of the expected effect of the polar lipids on the gut permeability in the lean C57BL/6J mice during the DIO indicated that the lack of the effect may not be leptin dependent. Taken together, the polar lipids did not reduce



gut permeability when the mice were obese no matter if they were leptin-deficient or not. The effects of dietary polar lipids on gut permeability may not be leptin-dependent in the context of obesity. In the LPS-stressed mouse model, the gangliosides did not affect the gut permeability and the phospholipids increased the permeability of the small intestine (Figure 4.7). The data from the three mouse models consistently revealed that the gangliosides may not have significant effect on the gut permeability while the phospholipids tend to increase the gut permeability.

### **Effects of dietary polar lipids on systemic inflammation**

When the ob/ob mice were severely obese and fed a stressful diet, the dietary phospholipids increased systemic inflammation as indicated by the increase of the plasma IL-6 level. The dietary gangliosides did not significantly affect systemic inflammation. In the DIO model, the dietary phospholipids increased the plasma LPS level by the end of the study (Figure 6.1a) and had little effect on the plasma inflammatory cytokines. The dietary phospholipids tended to increase the plasma IL-6 level after 5 weeks of dietary treatment. Since no cytokine data were available between 5 and 15 weeks, it is highly possible that the dietary phospholipids may significantly increase the plasma IL-6 level during that period of time. The dietary polar lipids did not affect systemic inflammation when the C57BL/6J lean mice were having acute inflammation after the subcutaneous injection of the LPS. Neither did the dietary polar lipids affect systemic inflammation in the chronic inflammatory process during recovery nor when the LPS-induced inflammation dissipated. The phospholipids increased the plasma LPS level (Figure 6.1b) without affecting the systemic inflammation. It is not clear if the increased endotoxemia was a direct effect of the phospholipids or was due to the increased gut permeability

(Figure 6.1). In conclusion, the dietary phospholipids may increase the plasma IL-6 level in the context of obesity in the C57BL/6J mice and the dietary gangliosides may not have significant effect on systemic inflammation in the C57BL/6J lean and obese mice.

### **Effects of dietary polar lipids on lipid metabolism**

The dietary phospholipids lowered the liver mass in the ob/ob mice and the LPS-stressed C57BL/6J mice (Figure 3.3a & 4.3a). The dietary polar lipids did not have any effect on the liver mass in the C57BL/6J mice with the DIO. The effect of the dietary polar lipids on liver mass may not be leptin-dependent. The dietary polar lipids may have a stronger effect on the liver mass in the context of inflammation as in the ob/ob mice and the LPS-stressed C57BL/6J mice.

The dietary phospholipids decreased the cholesteryl ester and the PI in the liver and decreased the PI in the skeletal muscle of the ob/ob mice. The dietary phospholipids decreased the PI in the skeletal muscle and the dietary phospholipids and gangliosides increased the PI in the liver of the C57BL/6J lean mice stressed with LPS. The PI in the skeletal muscle and the liver was not significantly affected by the dietary polar lipids in the C57BL/6J mice with the DIO. Taken together, the phospholipids decreased the PI in the skeletal muscle in both the ob/ob mice and the LPS-stress mice. It is possible that the effect of the phospholipids on the PI in the skeletal muscle may be affected by the systemic inflammation. The PI can be phosphorylated into phosphoinositides, which play important roles in lipid signaling, cell signaling and membrane trafficking.

Phosphoinositides are essential components of the insulin secretory system (53). The

dietary polar lipids had a bigger effect on the tissue PI level when the organism was in less homeostatic conditions such as severe obesity and systemic inflammation.

The dietary PL down regulated the fatty acid synthesis gene *Acacb* in the liver of all three mouse models. For the fatty acid oxidation gene *Acaa2*, it was down regulated by the dietary PL and GG compared with the CO in the ob/ob mice. The *Acaa2* was down regulated by the dietary PL compared with the GG in the C57BL/6J mice stressed with LPS and was not significantly affected in the C57BL/6J mice with the DIO. The dietary PL suppressed the cholesterol synthesis gene *Hmgcr* in the liver of the C57BL/6J mice stressed with LPS and up regulated the cholesterol reverse transport gene *Scarb1* in the C57BL/6J mice with the DIO. The dietary polar lipids did not significantly affect the gene expression associated with the cholesterol regulation in the liver of the ob/ob mice. Taken together, the dietary polar lipids had different effects on lipid metabolism in the liver in three mouse models. The decrease of the liver lipids level by the phospholipids may be mediated through the down regulation of the fatty acid synthesis gene *Acacb*. The phospholipids tend to decrease the cholesterol level in the liver by either suppressing synthesis or increasing excretion in the C57BL/6J lean mice models.

The dietary polar lipids also had slightly different effects on the plasma lipid levels in the three models. The plasma lipid profile was not significantly affected by the dietary polar lipids in ob/ob mice. The dietary GG and PL reduced the plasma CE level after the LPS stress in the C57BL/6J mice and did not significantly affect the plasma CE level in the C57BL/6J mice with the DIO. The dietary GG and PL reduced the plasma FFA level

before DIO in the C57BL/6J mice and the dietary GG reduce the plasma FFA level in the C57BL/6J mice stressed with the LPS. The gangliosides tend to reduce the plasma FFA level in the C57BL/6J mice regardless of the inflammatory status.

The dietary polar lipids did not significantly affect the polar lipids levels in the intestinal mucosa of the ob/ob mice. Compared with the CO and the GG, the dietary PL decreased PE in the colon mucosa of the C57BL/6J mice stressed by the LPS and the C57BL/6J mice with the DIO. The dietary PL decreased PC in the small intestinal mucosa of the LPS stressed C57BL/6J mice but increased the PC in small intestinal mucosa of the C57BL/6J mice with the DIO. The effects of the dietary polar lipids on PC level in the intestinal mucosa were different during the LPS-induced systemic inflammation and the DIO. The phospholipids tend to decrease the polar lipids in the intestinal mucosa and the skeletal muscle. It is not clear how the dietary phospholipids may reduce the polar lipids level in the tissues. It may be hypothesized that the high dietary phospholipids level may have down regulated the receptors for the absorption of the polar lipids.

### **Future Directions**

Although the milk polar lipids exist in almost all dairy products, the absolute amount of the polar lipids in the dairy products is quite low, ranging from 9 mg per 100 g skim milk to 1250 mg per 100 g butter serum (54). It is quite expensive to purify and collect the individual class of the milk polar lipids. The milk polar lipids may be enriched as a complex compound or a semi purified isolate. So in this dissertation the milk polar lipids were supplemented in the diets either as a complex isolate or a semi-purified isolate to

increase the applicability of the results. In order to pinpoint which specific component of the polar lipids resulted in the increase of gut permeability and plasma LPS, the dietary supplementation of the purified polar lipid classes one at a time is needed to explore the relevant mechanisms. Both the *in vitro* cell model and the animal models may be used to study the mechanisms. For gut permeability, the Caco-2 cell monolayer could be a great model. The well-established animal models of colitis could also be used. For systemic inflammation, the LPS induced acute and chronic animal models could be a good place to start. For lipid metabolism, the animal models of NAFLD and/or NASH can be used. The metabolomic and lipidomic approaches can also be adopted for studying the effects of the dietary polar lipids.

The undesirable effects of the dietary phospholipids on gut permeability and systemic inflammation in this dissertation may be due to the high dietary level of the phospholipids. The phospholipids were supplemented at the level of 1% (w/w) of the diet. Future studies may target a level less than 1% (w/w) of the diet. There may be a dose effect. Different dietary levels may be compared to find a level that may generate more desirable effects.

Large amounts of the milk polar lipids rich material may be produced as a byproduct from buttermilk or cheese whey during the butter or cheese making processes. While it is worthwhile to try a lower dietary level of purified milk polar lipids in the dietary supplementation studies, it is also interesting to look at the effects of the direct dietary incorporation of the polar lipids rich dairy byproducts such as the whey powder and

buttermilk powder. A systematic approach would be ideal to assess the effects of the milk polar lipids rich dairy products on the major organ systems in animal models.

## References

1. Corpet DE, Tache S. Most effective colon cancer chemopreventive agents in rats: a systematic review of aberrant crypt foci and tumor data, ranked by potency. *Nutr Cancer* 2002;43:1-21.
2. Bacon BR, Park CH, Fowell EM, McLaren CE. Hepatic steatosis in rats fed diets with varying concentrations of sucrose. *Fundam Appl Toxicol* 1984;4:819-26.
3. Barbosa CR, Albuquerque EM, Faria EC, Oliveira HC, Castilho LN. Opposite lipemic response of Wistar rats and C57BL/6 mice to dietary glucose or fructose supplementation. *Braz J Med Biol Res* 2007;40:323-31.
4. Beynen AC, Meijer GW, Van der Meer R. Comparison of rats with mice concerning the response of lipid metabolism to dietary fats. *Z Ernahrungswiss* 1988;27:143-9.
5. Panzoldo NB, Urban A, Parra ES, et al. Differences and similarities of postprandial lipemia in rodents and humans. *Lipids Health Dis* 2011;10:86.
6. Hukshorn CJ, Saris WH. Leptin and energy expenditure. *Curr Opin Clin Nutr Metab Care* 2004;7:629-33.
7. Lin PY, Romsos DR, Leveille GA. Food intake, body weight gain, and body composition of the young obese (ob/ob) mouse. *J Nutr* 1977;107:1715-23.
8. Chen Y, Qian L. Association between lifetime stress and obesity in Canadians. *Prev Med* 2012.

9. Moore CJ, Cunningham SA. Social position, psychological stress, and obesity: a systematic review. *J Acad Nutr Diet* 2012;112:518-26.
10. Scott KA, Melhorn SJ, Sakai RR. Effects of chronic social stress on obesity. *Curr Obes Rep* 2012;1:16-25.
11. Rosmond R, Lapidus L, Bjorntorp P. The influence of occupational and social factors on obesity and body fat distribution in middle-aged men. *Int J Obes Relat Metab Disord* 1996;20:599-607.
12. Rosmond R, Lapidus L, Marin P, Bjorntorp P. Mental distress, obesity and body fat distribution in middle-aged men. *Obesity Res* 1996;4:245-52.
13. Lapidus L, Bengtsson C, Hallstrom T, Bjorntorp P. Obesity, adipose tissue distribution and health in women--results from a population study in Gothenburg, Sweden. *Appetite* 1989;13:25-35.
14. Rosmond R, Bjorntorp P. Psychiatric ill-health of women and its relationship to obesity and body fat distribution. *Obesity Res* 1998;6:338-45.
15. Linkowski P, Mendlewicz J, Leclercq R, et al. The 24-hour profile of adrenocorticotropin and cortisol in major depressive illness. *J Clinical Endocrinology and Metabolism* 1985;61:429-38.
16. Bjorntorp P. Do stress reactions cause abdominal obesity and comorbidities? *Obesity Reviews* 2001;2:73-86.
17. Rosmond R, Bjorntorp P. Psychosocial and socio-economic factors in women and their relationship to obesity and regional body fat distribution. *Int J Obes Relat Metab Disord* 1999;23:138-45.

18. Speaker KJ, Fleshner M. Interleukin-1 beta: a potential link between stress and the development of visceral obesity. *BMC Physiol* 2012;12:8.
19. Waki H, Tontonoz P. Endocrine functions of adipose tissue. *Annu Rev Pathol* 2007;2:31-56.
20. Hoppe CC, Moritz KM, Fitzgerald SM, Bertram JF, Evans RG. Transient hypertension and sustained tachycardia in mice housed individually in metabolism cages. *Physiological Res / Academia Scientiarum Bohemoslovaca* 2009;58:69-75.
21. Stechman MJ, Ahmad BN, Loh NY, et al. Establishing normal plasma and 24-hour urinary biochemistry ranges in C3H, BALB/c and C57BL/6J mice following acclimatization in metabolic cages. *Laboratory Animals* 2010;44:218-25.
22. Chou-Green JM, Holscher TD, Dallman MF, Akana SF. Repeated stress in young and old 5-HT(2C) receptor knockout mice. *Physiology & Behavior* 2003;79:217-26.
23. Feldstein AE, Canbay A, Angulo P, et al. Hepatocyte apoptosis and fas expression are prominent features of human nonalcoholic steatohepatitis. *Gastroenterology* 2003;125:437-43.
24. Siebler J, Schuchmann M, Strand S, Lehr HA, Neurath MF, Galle PR. Enhanced sensitivity to CD95-induced apoptosis in ob/ob mice. *Digestive Diseases and Sciences* 2007;52:2396-402.
25. Stefano JT, de Oliveira CP, Correa-Giannella ML, et al. Nonalcoholic steatohepatitis (NASH) in ob/ob mice treated with yo jyo hen shi ko (YHK): effects on peroxisome proliferator-activated receptors (PPARs) and microsomal

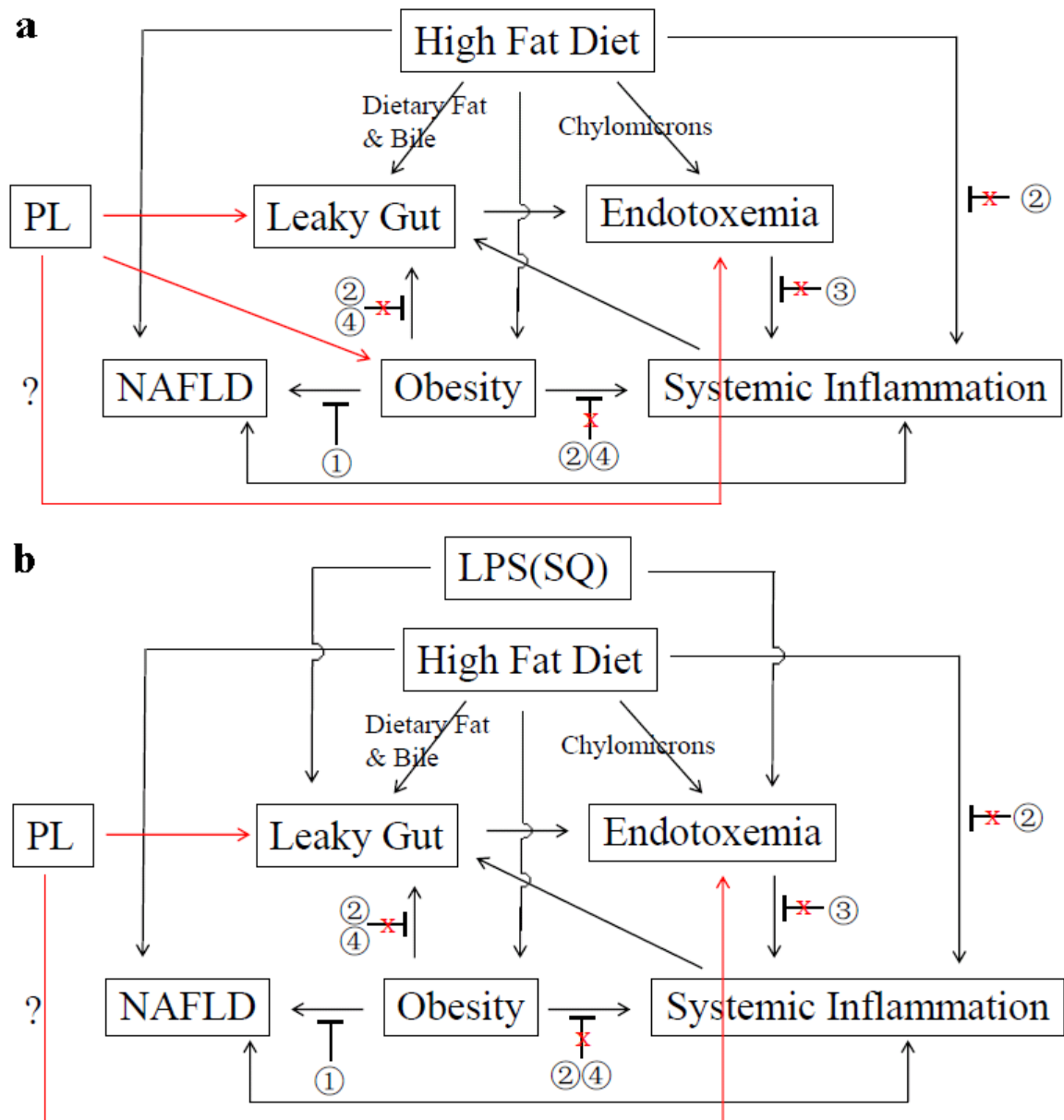


- triglyceride transfer protein (MTP). *Digestive Diseases and Sciences* 2007;52:3448-54.
26. Rakela J, Mosley JW, Edwards VM, Govindarajan S, Alpert E. A double-blinded, randomized trial of hydrocortisone in acute hepatic failure. The Acute Hepatic Failure Study Group. *Digestive Diseases and Sciences* 1991;36:1223-8.
  27. Clee SM, Attie AD. The genetic landscape of type 2 diabetes in mice. *Endocrine Reviews* 2007;28:48-83.
  28. American Diabetes A. Diagnosis and classification of diabetes mellitus. *Diabetes Care* 2012;35 Suppl 1:S64-71.
  29. Stoehr JP, Nadler ST, Schueler KL, et al. Genetic obesity unmasks nonlinear interactions between murine type 2 diabetes susceptibility loci. *Diabetes* 2000;49:1946-54.
  30. Yokochi T, Inoue Y, Yokoo J, Kimura Y, Kato N. Retention of Bacterial Lipopolysaccharide at the Site of Subcutaneous Injection. *Infection and Immunity* 1989;57:1786-91.
  31. Flurkey K, Curren J, Harrison D. Mouse models in aging research. In: Fox J, Davisson M, Quimby F, Barthold S, Newcomer C, Smith A, (eds). *The Mouse in Biomedical Research*. Academic Press: Massachusetts: 2007. pp 637-72.
  32. Moreira AP, Texeira TF, Ferreira AB, do Carmo Gouveia Peluzio M, de Cassia Goncalves Alfenas R. Influence of a high-fat diet on gut microbiota, intestinal permeability and metabolic endotoxaemia. *Br J Nutr* 2012;108:801-9.

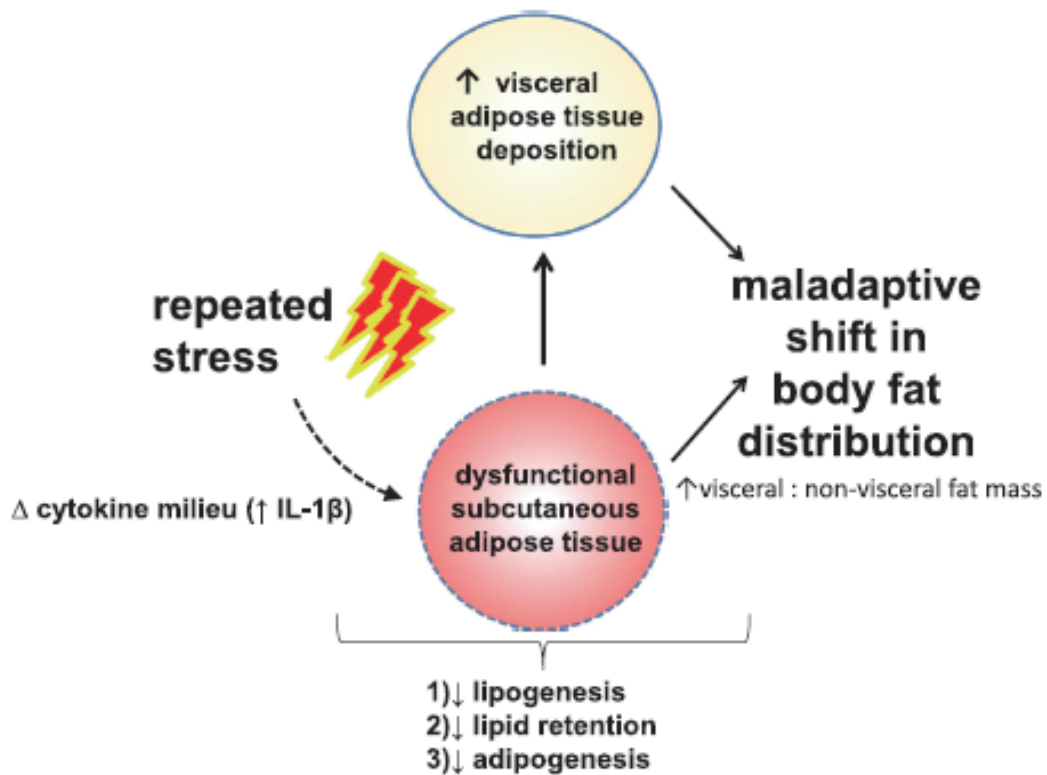
33. Saitoh N, Awaya A, Sakudo A, et al. Serum thymic factor prevents LPS-induced pancreatic cell damage in mice via up-regulation of Bcl-2 expression in pancreas. *Microbiology and Immunology* 2004;48:629-38.
34. Endo M, Masaki T, Seike M, Yoshimatsu H. TNF-alpha induces hepatic steatosis in mice by enhancing gene expression of sterol regulatory element binding protein-1c (SREBP-1c). *Experimental Biology and Medicine* 2007;232:614-21.
35. Tweedell A, Mulligan KX, Martel JE, Chueh FY, Santomango T, McGuinness OP. Metabolic response to endotoxin in vivo in the conscious mouse: role of interleukin-6. *Metabolism: Clinical and Experimental* 2011;60:92-8.
36. Teague J, Gyte A, Peel JE, et al. Reversibility of hyperglycaemia and islet abnormalities in the high fat-fed female ZDF rat model of type 2 diabetes. *J Pharmacological and Toxicological Methods* 2011;63:15-23.
37. Ghoshal S, Witta J, Zhong J, de Villiers W, Eckhardt E. Chylomicrons promote intestinal absorption of lipopolysaccharides. *J Lipid Res* 2009;50:90-7.
38. Wang YH, Li JN, Tang LH, et al. T-Lymphocyte responses to intestinally absorbed antigens can contribute to adipose tissue inflammation and glucose intolerance during high fat feeding. *Plos One* 2010;5.
39. Turnbaugh PJ, Baeckhed F, Fulton L, Gordon JI. Diet-induced obesity is linked to marked but reversible alterations in the mouse distal gut microbiome. *Cell Host Microbe* 2008;3:213-23.
40. Zhang Y, Huang C, Sheng X, Gong Z, Zang YQ. Lecithin promotes adipocyte differentiation and hepatic lipid accumulation. *Int J Mol Med* 2009;23:449-54.

41. Moreno-Navarrete JM, Catalan V, Whyte L, et al. The L-alpha-lysophosphatidylinositol/GPR55 system and its potential role in human obesity. *Diabetes* 2012;61:281-91.
42. Hirsch J, Batchelor B. Adipose tissue cellularity in human obesity. *Clin Endocrinol Metab* 1976;5:299-311.
43. Meddings JB, Gibbons I. Discrimination of site-specific alterations in gastrointestinal permeability in the rat. *Gastroenterology* 1998;114:83-92.
44. Laugerette F, Vors C, Geloën A, et al. Emulsified lipids increase endotoxemia: possible role in early postprandial low-grade inflammation. *J Nutr Biochem* 2010.
45. Uchida A, Whitsitt MC, Eustaquio T, et al. Reduced triglyceride secretion in response to an acute dietary fat challenge in obese compared to lean mice. *Frontiers in Physiology* 2012;3:26.
46. Martins IJ, Redgrave TG. Obesity and post-prandial lipid metabolism. Feast or famine? *J Nutr Biochem* 2004;15:130-41.
47. Vreugdenhil AC, Rousseau CH, Hartung T, Greve JW, van 't Veer C, Buurman WA. Lipopolysaccharide (LPS)-binding protein mediates LPS detoxification by chylomicrons. *J Immunol* 2003;170:1399-405.
48. Surwit RS, Wang S, Petro AE, et al. Diet-induced changes in uncoupling proteins in obesity-prone and obesity-resistant strains of mice. *Proc Natl Acad Sci U S A* 1998;95:4061-5.
49. Fukushima M, Tokunaga K, Lupien J, Kemnitz JW, Bray GA. Dynamic and static phases of obesity following lesions in PVN and VMH. *Am J Physiol* 1987;253:R523-9.

50. Smith GP. Critical Introduction to obesity. In: Blass EM, (ed). *Obesity: causes, mechanisms, prevention, and treatment*. Sinauer Associates: Sunderland: 2008. pp 1-18.
51. Brobeck JR, Tepperman J, Long CN. Experimental hypothalamic hyperphagia in the albino rat. *Yale J Biol Med* 1943;15:831-53.
52. Danielsson A, Fagerholm S, Ost A, et al. Short-term overeating induces insulin resistance in fat cells in lean human subjects. *Mol Med* 2009;15:228-34.
53. Yamazaki H, Zawulich KC, Zawulich WS. Physiologic implications of phosphoinositides and phospholipase C in the regulation of insulin secretion. *J Nutr Sci Vitaminol (Tokyo)* 2010;56:1-8.
54. Rombaut R, Dewettinck K. Properties, analysis and purification of milk polar lipids. *Int Dairy J* 2006;16:1362-73.



**Figure 6.1** Most of the hypothesized effects of the polar lipids were not supported by the data. The phospholipids did not reduce gut permeability but increased obesity and the plasma LPS in the ob/ob mouse model and the DIO model (a). The phospholipids did not reduce gut permeability but increase the plasma LPS in the LPS-stressed mouse model (b). Red X indicates that the data did not support the hypothesis. Red arrow indicates the undesirable effect.



**Figure 6.2** Stress-induced dysfunction of the subcutaneous white adipose tissue contributes to the development of visceral adiposity (18).

**APPENDIX**

## CORRELATION COEFFICIENT NETWORK ANALYSIS

Dietary supplementation of bioactive compounds should affect the eleven organ systems in the body. Claims about the effects of bioactive compounds cannot be appropriately and responsibly made until the main organ systems are assessed. When multiple organ systems are assessed, it is common to observe contradictory effects on different endpoints. A method is needed to assess the overall effect of dietary supplements on multiple endpoints. The network analysis could be a potential method for evaluating the overall effect of dietary supplements. Limited literature indicates that correlation network analysis may help reveal the overall pattern of biological endpoints (1). A lot of parameters were evaluated in the mouse studies of this dissertation. Dietary polar lipids had mixed effects on different endpoints. It is helpful to explore the overall effect of dietary milk polar lipids on the parameters related to the major hypotheses through correlation network analysis. The correlation network analysis was carried out for the LPS-stressed mouse model and the diet-induced obesity model. The network analysis was not done for the ob/ob mouse model since the number of animals per group was low (smallest  $n = 3$ ).

The Pearson correlation coefficients of all final parameters were generated by SAS 9.2. Data from the same number of animals were used among groups. The correlation coefficient matrices were subjected to network analysis. The matrices were imported as Excel workbooks into network analysis software Cytoscape desktop application 2.8.3. Correlation coefficients and associated p values were used as edge attributes. Parameter



names were used as node names and they were categorized into types. Networks were generated and edges were filtered by setting cutoffs for p values, which was 0.05. Nodes connected by the filtered edges were included in the filtered child networks. The Girvan-Newman fast greedy algorithm (by GLay Cytoscape plugin), operating exclusively on connectivity, was carried out to generate community clusters for correlation networks. Nodes for parameters related to the major hypotheses and their first neighbors were selected to generate child networks. The following parameters were selected to reflect the major hypotheses: colon permeability, small intestine permeability, plasma interleukin-6 (IL-6) and tumor necrosis factor- $\alpha$  (TNF- $\alpha$ ), and liver triglycerides (TG). Only edges connecting those selected parameters were retained and the other edges were discarded. Then force-directed network layouts were generated from the retained nodes and edges.

#### **Correlation Network Analysis for Chapter 4**

The correlation network analysis assessed all of the parameters measured at the end of the study (day 57, n=4). The legends for the network analysis are shown in Figures A1a-c. The community cluster analyses indicated less connectivity in the PL group compared with the CO and GG groups (9 vs 7 communities). The PL group had less significant negative and positive correlations compared with the CO and GG groups (Table A1). Less correlations in the PL group is accompanied by less desirable biological functions (Figure 4.10). The deduction in positive correlations is associated with a metabolic disorder in the disease model animals (1). The undesirable effect of PL may be mainly associated with the decrease of positive correlations. Decrease of positive correlations may indicate the compromise of biological functions by dietary polar lipids in the context of systemic inflammation induced by lipopolysaccharide (LPS).

For correlations involve parameters related to the major hypotheses, the force-directed network layout is shown in Figure A2. In the CO group, small intestine permeability is negatively correlated with liver mass and cecum content mass. Small intestine permeability is positively correlated with plasma insulin, retroperitoneal fat mass and body weight. Colon permeability is positively correlated with phosphatidylcholine (PC) content in jejunum mucosa, liver sphingomyelin (SM), muscle free fatty acids (FFA), and jejunum mass. Colon permeability is negatively correlated with liver phosphatidylinositol (PI), plasma diglycerides (DG), TG and cholesteryl ester (CE). Plasma TNF- $\alpha$  is positively correlated with liver DG and muscle CE. Plasma IL-6 is positively correlated with jejunum mucosa mass, colon mucosa mass, adipose PE, and gangliosides content in colon mucosa. Plasma IL-6 is negatively correlated with body fat mass and ileum mucosa mass.

In the GG group (Figure A2), small intestine permeability is positively correlated with plasma PC and is negatively correlated with muscle phosphatidylethanolamine (PE) and phosphatidylserine (PS), and GG content in colon mucosa. Plasma IL-6 is negatively correlated with plasma monocyte chemoattractant protein-1 (MCP-1) and is positively correlated with mesenteric fat mass and occludin protein expression in jejunum mucosa. Liver TG is positively correlated with PC in ileum mucosa and is negatively correlated with colon mucosa mass.

In the PL group (Figure A2), small intestine permeability is positively correlated with adipose TG. Colon permeability is positively correlated with liver PI and is negatively

correlated with subcutaneous fat in upper body. Plasma TNF- $\alpha$  is positively correlated with cecum mass and muscle FFA. Plasma IL-6 is negatively correlated with liver PS and is positively correlated with plasma leptin and LPS, PE in colon mucosa, and gangliosides in ileum mucosa. Liver TG is positively correlated with retroperitoneal fat mass.

It is unexpected that plasma IL-6 is negatively correlated with subcutaneous fat mass, visceral fat mass, brown adipose tissue mass and total fat depots in the CO group. This unexpected observation is not observed in the GG and PL groups. Plasma IL-6 is positively correlated with mesenteric fat mass in the GG group and is not correlated with fat mass in the PL group. There is no good explanation for those unexpected correlations in the CO group.

It is interesting to notice that the small intestine permeability is positively correlated with plasma insulin and body weight in the CO group. These correlations were not observed in the GG and PL groups. It might be speculated that the increase of small intestine permeability may increase plasma insulin. The increase of small intestine permeability may result in endotoxemia and systemic inflammation, which may decrease insulin sensitivity. The body may compensate the decreased insulin sensitivity by increasing plasma insulin. It is unexpected that there were no correlations between tight junction proteins in gut mucosa and gut permeability. This lack of correlation may indicate that the amount of tight junction proteins is not critical in determining gut permeability during inflammatory stress.

The CO group had more correlations involving plasma IL-6 and colon permeability compared with GG and PL groups (Figure A2). The more correlations in the CO group may indicate more desirable biological functions. It might be hypothesized that GG and PL have undesirable effect on biological functions associated with plasma IL-6 and colon permeability.

### **Correlation Network Analysis for Chapter 5**

The correlation network analysis assessed all of the parameters measured at the end of the study (day 101, n=5). The CO group had more total correlations compared with the GG and PL groups (Table A2). The GG group had less negative correlations compared with the CO group (Table A2). The community cluster analyses indicated little difference in connectivity among three groups (Table A2).

The GG and PL groups had less positive correlations compared with the CO group (Table A2). The decrease of positive correlations is associated with a metabolic disorder in the disease model animals (1). If the reduction in positive correlations is an indicator of compromised biological functions, the overall effect of GG and PL may have been undesirable. The GG and PL decreased the negative correlations compared with the CO group (Table A2). Although there is little difference in connectivity of the network layouts among three groups, the GG and PL groups had less total correlations. The overall effect of CO on all endpoints was less desirable compared with that of GG (Figure 5.9). The overall effect of PL on all endpoints is mixed compared with that of CO (Figure 5.9). The decrease of positive correlations in the PL group may indicate the overall effect of PL is undesirable compared with CO. The decrease of negative

correlations in the GG group is accompanied by the lack of undesirable effect compared with the PL group. It may be hypothesized that the decrease of negative correlations is associated with reduction in negative effect.

For correlations involve parameters related to major hypotheses, the force-directed network layout is shown in Figure A3. In the CO group, small intestine permeability is positively correlated with muscle CE and is negatively correlated with plasma insulin. Colon permeability is negatively correlated with occludin protein expression in jejunum mucosa. Plasma IL-6 is positively correlated with plasma PC and is negatively correlated with liver SM and adipose TG. Plasma TNF- $\alpha$  is positively correlated with liver expression of beta-actin and body lean mass. Plasma TNF- $\alpha$  is negatively correlated with subcutaneously fat mass, visceral fat mass, body fat mass, liver TG, and colon mucosa mass. Liver TG is negatively correlated with plasma TNF- $\alpha$  and is positively correlated with plasma FITC and FFA.

In the GG group (Figure A3), small intestine permeability is positively correlated with homeostasis model assessment of insulin resistance (HOMA-IR) and is negatively correlated with muscle PS and liver mass. Colon permeability is positively correlated with PE in jejunum mucosa and PC in colon mucosa. Colon permeability is negatively correlated with colon mass and colon mucosa mass, liver PI and CE, and muscle PC and TG. Plasma IL-6 is negatively correlated with occludin protein expression in colon mucosa, homeostasis model assessment of insulin resistance (HOMA-IR), and liver PE. Plasma TNF- $\alpha$  is positively correlated with liver PE and muscle TG. Liver TG is

positively correlated with body fat mass, subcutaneous fat mass, and mesenteric fat mass. Liver TG is negatively correlated with plasma LPS, PC content in ileum mucosa and body lean mass.

In the PL group (Figure A3), colon permeability is negatively correlated with occludin protein expression in jejunum mucosa, plasma TNF- $\alpha$ , and liver expression of acetyl-Coenzyme A acyltransferase 2. Small intestine permeability is positively correlated with cecum mass, cecum content mass, PE in ileum mucosa, and beta actin expression in liver. Small intestine permeability is negatively correlated with adipose DG, liver expression of acetyl-Coenzyme A acyltransferase 2, retroperitoneal fat mass and inguinal fat mass. Plasma IL-6 is positively correlated with liver FFA and cecum mass. Plasma IL-6 is negatively correlated with body fat mass, plasma TG, muscle TG and liver TG. Plasma TNF- $\alpha$  is positively correlated with PI content in colon mucosa and occludin protein expression in jejunum mucosa. Plasma TNF- $\alpha$  is negatively correlated with colon permeability and ileum mucosa mass. Liver TG is positively correlated with plasma FFA, body fat mass, plasma TG, body weight, and liver expression of scavenger receptor class B, member 1. Liver TG is negatively correlated with body lean mass, liver FFA, plasma IL-6, and muscle mass.

It is unexpected that plasma TNF- $\alpha$  is negatively correlated with subcutaneous fat mass, visceral fat mass, brown adipose tissue mass and total fat depots in the CO group. These unexpected correlations were not observed in the GG and PL groups. Plasma TNF- $\alpha$  is not correlated with fat mass in the GG and PL groups. This observation is consistent

with the unexpected negative correlation between plasma IL-6 and fat mass in the CO group of the LPS model (Figure A2 – CO, Chapter 4). Most of the mice in the CO group were not obese according to Fenton's definition for obesity. It may be hypothesized that the increase of adipose tissue in lean mice decreases plasma proinflammatory cytokines such as IL-6 and TNF- $\alpha$ ; GG and PL may compromise this negative correlation.

It is surprising that no correlations were observed between tight junction proteins in gut mucosa and gut permeability. This lack of correlation may indicate that the amount of tight junction proteins does not play an essential role in determining gut permeability during diet-induced obesity. The CO group had more correlations involving plasma TNF- $\alpha$  compared with GG and PL groups. The small intestine permeability is negatively correlated with plasma insulin in the CO group and positively correlated with insulin sensitivity (HOMA-IR). Positive correlation was observed between small intestine permeability and plasma insulin in the CO group of the LPS model (Figure A2 – CO, Chapter 4). Taken together, the increase of small intestine permeability may decrease insulin sensitivity through increasing systemic inflammation and the body may compensate the decreased insulin sensitivity by increasing plasma insulin.

Liver TG is positively correlated with body fat and negatively correlated with body lean mass in GG and PL groups. Liver TG is not correlated with body fat in the CO group. It may be hypothesized that GG and PL potentiate the effect that body fat accumulation increases liver TG. The GG and PL groups had more correlations involving liver TG compared with the CO group. The GG group had more correlations involving colon

permeability compared with CO and PL groups. The PL group had more correlations involving plasma IL-6 and small intestine permeability. It may be hypothesized that GG and PL have a bigger influence on liver TG and a smaller influence on plasma TNF- $\alpha$  compared with CO; GG has a bigger influence on colon permeability compared with CO and PL; PL has a bigger influence on plasma IL-6 and small intestine permeability compared with CO and GG.

### **Summary**

The results of correlation network analyses in three mouse studies consistently support the hypotheses that decreased network connectivity is associated with less integrative and cohesive connections of biological functions; decrease in positive correlations is associated with compromised biological functions while decrease in negative correlations is associated with less undesirable effects; increased correlations of a parameter is associated with a bigger influence of the treatment on that parameter. Since very little literature is available regarding correlation network analysis of functional biological endpoints, correlation network analysis should be advocated to further test the hypotheses.

### **Reference**

1. van der Greef J, Martin S, Juhasz P, et al. The art and practice of systems biology in medicine: mapping patterns of relationships. *Journal of proteome research* 2007;6:1540-59.



**Table A1** Number of Pearson correlation coefficients ( $p < 0.05$ ) among parameters measured at day 57 in the LPS-stress mouse model.


















<b>Diet</b>	<b>CO</b>	<b>GG</b>	<b>PL</b>
Negative correlations	105	97	72
Positive correlations	109	106	82
Total correlations	214	203	154
Community clusters	7	7	9

**Table A2** Number of Pearson correlation coefficients ( $p < 0.05$ ) among parameters measured at day 101 in the DIO mouse model.

<b>Diet</b>	<b>CO</b>	<b>GG</b>	<b>PL</b>
Negative correlations	162	136	152
Positive correlations	168	160	154
Total correlations	330	296	306
Community clusters	7	8	7

Visual Legend



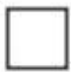







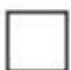






### Node Color Mapping

Node Color	Type	Node Color	Type	Node Color	Type	Node Color	Type
	ALIG		GE		LLIG		TJP
	BC		GGs		LPS		TM
	CK		GIM		MLIG		
	DST		GLU		MuLIG		
	FITC		HOMA		PLI		

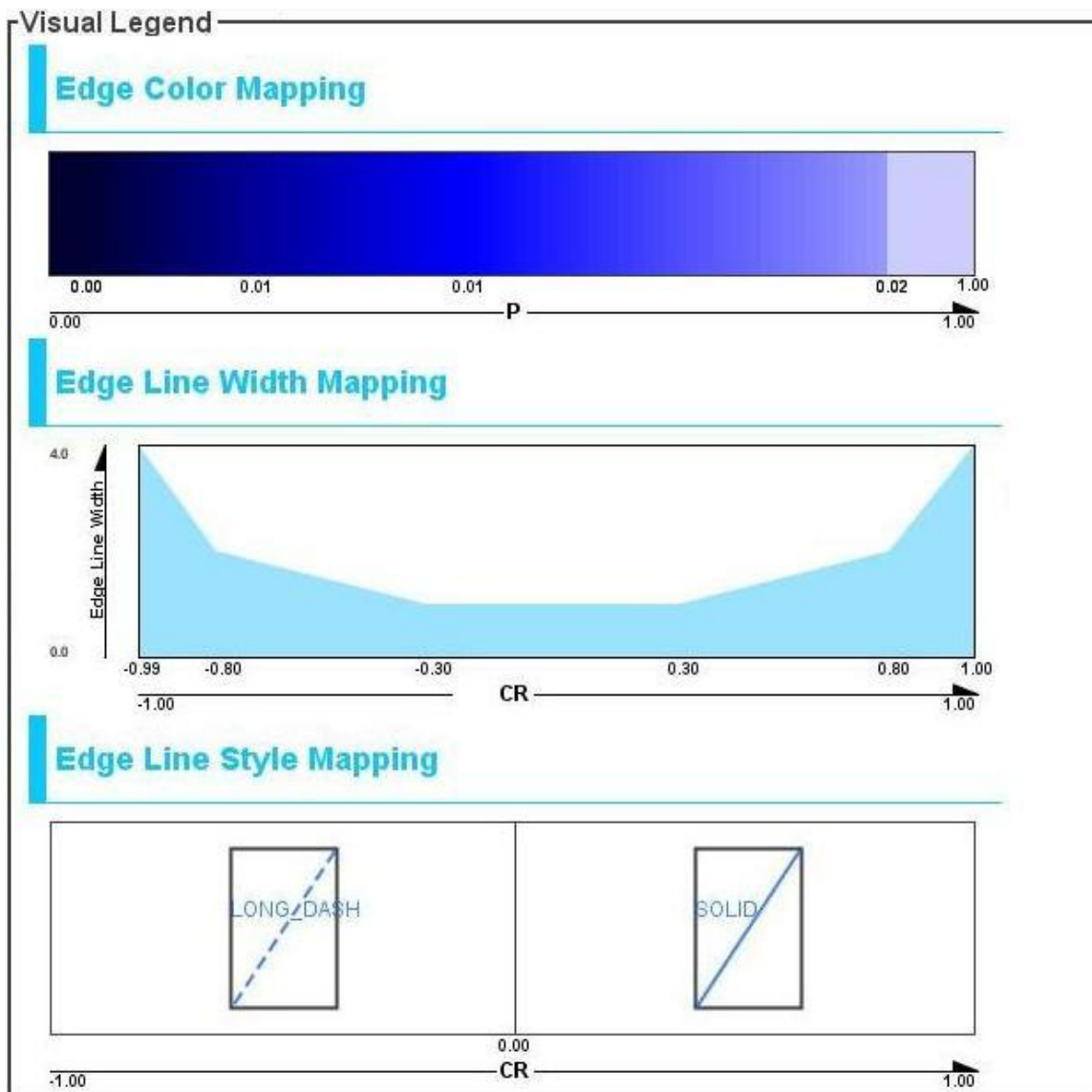
**Figure A1a** Visual legend – node color mapping. ALIG: adipose lipid per gram tissue; BC: body composition; CK: cytokine; DST: differential sugar-absorption test; FITC: fluorescein isothiocyanate; GE: gene expression; GGs: gangliosides; GIM: gastrointestinal mass; GLU: glucose; LLIG: liver lipid per gram tissue; MLIG: muscle lipid per gram tissue; MuLIG: mucosa lipid per gram tissue; PLI: plasma lipid; TJP: tight junction protein; TM: tissue mass.

Visual Legend

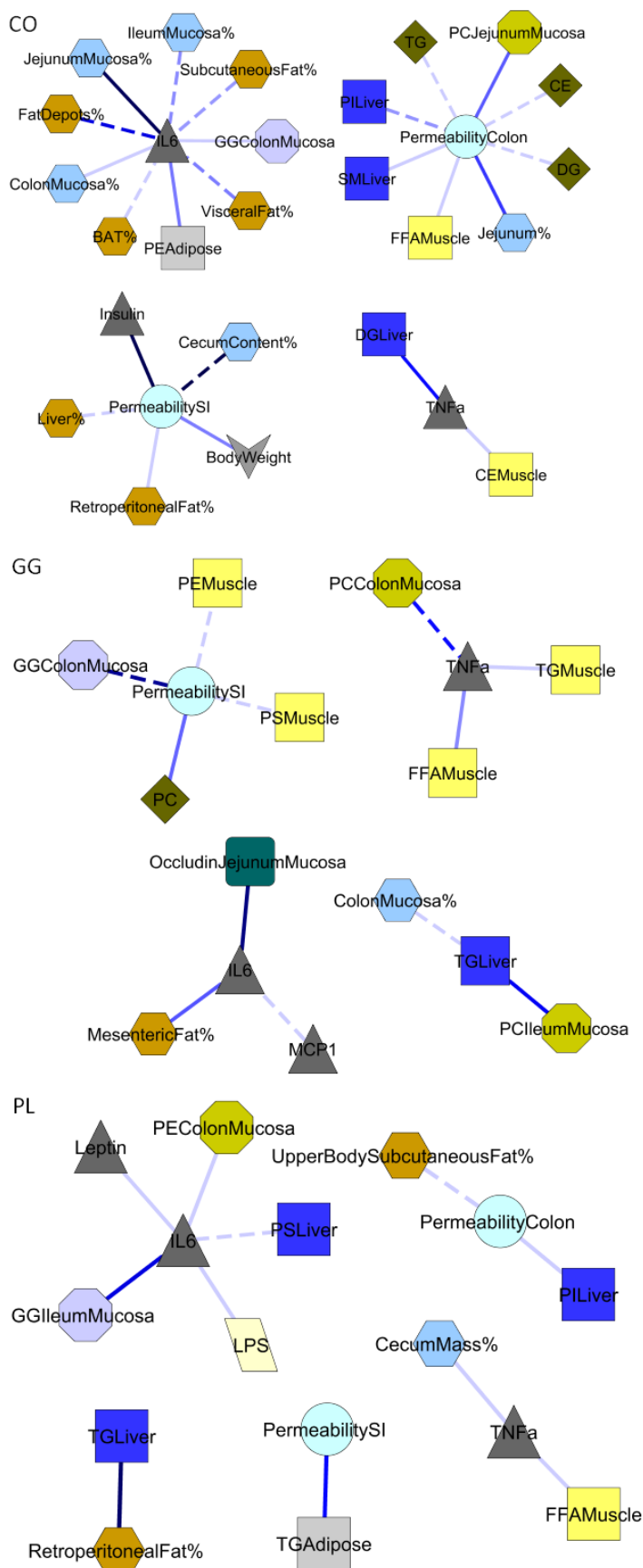
### Node Shape Mapping

Node Shape Type		Node Shape Type		Node Shape Type		Node Shape Type	
	ALIG		GE		LLIG		TJP
	BC		GGs		LPS		TM
	CK		GIM		MLIG		
	DST		GLU		MuLIG		
	FITC		HOMA		PLI		

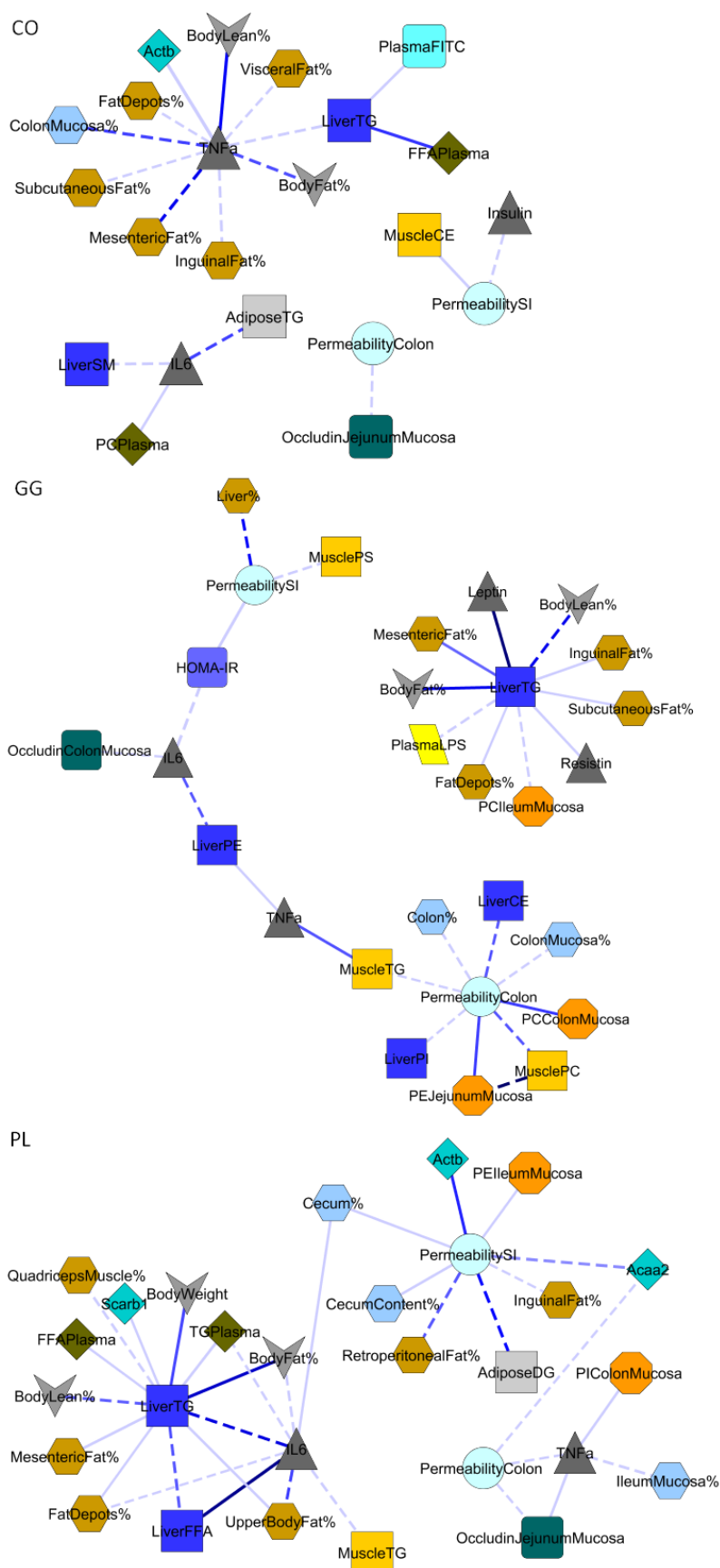
**Figure A1b** Visual legend – node shape mapping. ALIG: adipose lipid per gram tissue; BC: body composition; CK: cytokine; DST: differential sugar-absorption test; FITC: fluorescein isothiocyanate; GE: gene expression; GGs: gangliosides; GIM: gastrointestinal mass; GLU: glucose; LLIG: liver lipid per gram tissue; MLIG: muscle lipid per gram tissue; MuLIG: mucosa lipid per gram tissue; PLI: plasma lipid; TJP: tight junction protein; TM: tissue mass.



**Figure A1c** Visual legend – color, line width and line style of edge mapping. Edge is colored by  $p$  value. Edge line width and style are coded by correlation coefficient (CR).



**Figure A2** Correlations ( $p < 0.05$ ) involve the following parameters measured at the end of the LPS study: liver triglycerides level, small intestine permeability, colon permeability, and plasma IL-6 and TNF- $\alpha$ . %: percentage of body weight. Adipose: gonadal adipose tissue. BAT: brown adipose tissue. LPS: lipopolysaccharide. SI: small intestine.



**Figure A3** Correlations ( $p < 0.05$ ) involve the following parameters measured at the end of the DIO study: liver triglycerides level, small intestine permeability, colon permeability, and plasma IL-6 and TNF- $\alpha$ . %: percentage of body weight. Acaa2: acetyl-Coenzyme A acyltransferase 2. Actb: beta-actin. Scarb1: scavenger receptor class B, member 1. Adipose: gonadal adipose tissue. FITC: fluorescein isothiocyanate. HOMA-IR: homeostasis model assessment of insulin resistance. LPS: lipopolysaccharide. SI: small intestine.

## REPRINT PERMISSIONS

### SPRINGER LICENSE TERMS AND CONDITIONS Oct 25, 2012

This is a License Agreement between Albert Zhou ("You") and Springer ("Springer") provided by Copyright Clearance Center ("CCC"). The license consists of your order details, the terms and conditions provided by Springer, and the payment terms and conditions.

All payments must be made in full to CCC. For payment instructions, please see information listed at the bottom of this form.

License Number	3016121093268
License date	Oct 25, 2012
Licensed content publisher	Springer
Licensed content publication	Lipids
Licensed content title	Dietary Fat Composition Influences Tissue Lipid Profile and Gene Expression in Fischer-344 Rats
Licensed content author	Albert L. Zhou
Licensed content date	Jan 1, 2012
Type of Use	Thesis/Dissertation
Portion	Full text
Number of copies	10
Author of this Springer article	Yes and you are a contributor of the new work
Order reference number	None
Title of your thesis / dissertation	Bioactivities of milk polar lipids in influencing intestinal barrier integrity, systemic inflammation, and lipid metabolism
Expected completion date	Dec 2012
Estimated size(pages)	250
<b>Total</b>	0.00 USD

Terms and Conditions  
Introduction

The publisher for this copyrighted material is Springer Science + Business Media. By clicking "accept" in connection with completing this licensing transaction, you agree that the following terms and conditions apply to this transaction (along with the Billing and Payment terms and conditions established by Copyright Clearance Center, Inc. ("CCC"), at the time that you opened your Rightslink account and that are available at any time at <http://myaccount.copyright.com>).

#### Limited License

With reference to your request to reprint in your thesis material on which Springer Science and Business Media control the copyright, permission is granted, free of charge, for the use indicated in your enquiry.

Licenses are for one-time use only with a maximum distribution equal to the number that you identified in the licensing process.

This License includes use in an electronic form, provided its password protected or on the university's intranet or repository, including UMI (according to the definition at the Sherpa website: <http://www.sherpa.ac.uk/romeo/>). For any other electronic use, please contact Springer at ([permissions.dordrecht@springer.com](mailto:permissions.dordrecht@springer.com) or [permissions.heidelberg@springer.com](mailto:permissions.heidelberg@springer.com)).

The material can only be used for the purpose of defending your thesis, and with a maximum of 100 extra copies in paper.

Although Springer controls copyright to the material and is entitled to negotiate on rights, this license is only valid, provided permission is also obtained from the (co) author (address is given with the article/chapter) and provided it concerns original material which does not carry references to other sources (if material in question appears with credit to another source, authorization from that source is required as well).

Permission free of charge on this occasion does not prejudice any rights we might have to charge for reproduction of our copyrighted material in the future.

#### Altering/Modifying Material: Not Permitted

You may not alter or modify the material in any manner. Abbreviations, additions, deletions and/or any other alterations shall be made only with prior written authorization of the author(s) and/or Springer Science + Business Media. (Please contact Springer at ([permissions.dordrecht@springer.com](mailto:permissions.dordrecht@springer.com) or [permissions.heidelberg@springer.com](mailto:permissions.heidelberg@springer.com)))

#### Reservation of Rights

Springer Science + Business Media reserves all rights not specifically granted in the combination of (i) the license details provided by you and accepted in the course of this licensing transaction, (ii) these terms and conditions and (iii) CCC's Billing and Payment terms and conditions.

#### Copyright Notice: Disclaimer



You must include the following copyright and permission notice in connection with any reproduction of the licensed material: "Springer and the original publisher /journal title, volume, year of publication, page, chapter/article title, name(s) of author(s), figure number(s), original copyright notice) is given to the publication in which the material was originally published, by adding; with kind permission from Springer Science and Business Media"

Warranties: None

Example 1: Springer Science + Business Media makes no representations or warranties with respect to the licensed material.

Example 2: Springer Science + Business Media makes no representations or warranties with respect to the licensed material and adopts on its own behalf the limitations and disclaimers established by CCC on its behalf in its Billing and Payment terms and conditions for this licensing transaction.

Indemnity

You hereby indemnify and agree to hold harmless Springer Science + Business Media and CCC, and their respective officers, directors, employees and agents, from and against any and all claims arising out of your use of the licensed material other than as specifically authorized pursuant to this license.

No Transfer of License

This license is personal to you and may not be sublicensed, assigned, or transferred by you to any other person without Springer Science + Business Media's written permission.

No Amendment Except in Writing

This license may not be amended except in a writing signed by both parties (or, in the case of Springer Science + Business Media, by CCC on Springer Science + Business Media's behalf).

Objection to Contrary Terms

Springer Science + Business Media hereby objects to any terms contained in any purchase order, acknowledgment, check endorsement or other writing prepared by you, which terms are inconsistent with these terms and conditions or CCC's Billing and Payment terms and conditions. These terms and conditions, together with CCC's Billing and Payment terms and conditions (which are incorporated herein), comprise the entire agreement between you and Springer Science + Business Media (and CCC) concerning this licensing transaction. In the event of any conflict between your obligations established by these terms and conditions and those established by CCC's Billing and Payment terms and conditions, these terms and conditions shall control.

Jurisdiction

All disputes that may arise in connection with this present License, or the breach thereof, shall be settled exclusively by arbitration, to be held in The Netherlands, in

accordance with Dutch law, and to be conducted under the Rules of the 'Netherlands Arbitrage Institute'  
(Netherlands Institute of Arbitration).*OR:*

All disputes that may arise in connection with this present License, or the breach thereof, shall be settled exclusively by arbitration, to be held in the Federal Republic of Germany, in accordance with German law.

Other terms and conditions:

v1.3

If you would like to pay for this license now, please remit this license along with your payment made payable to "COPYRIGHT CLEARANCE CENTER" otherwise you will be invoiced within 48 hours of the license date. Payment should be in the form of a check or money order referencing your account number and this invoice number RLNK500884683.

Once you receive your invoice for this order, you may pay your invoice by credit card. Please follow instructions provided at that time.

Make Payment To:  
Copyright Clearance Center  
Dept 001  
P.O. Box 843006  
Boston, MA 02284-3006

For suggestions or comments regarding this order, contact RightsLink Customer Support: [customer@copyright.com](mailto:customer@copyright.com) or +1-877-622-5543 (toll free in the US) or +1-978-646-2777.

Gratis licenses (referencing \$0 in the Total field) are free. Please retain this printable license for your reference. No payment is required.

## COAUTHORS PERMISSION FORM FOR CHAPTER 2

Date 10-25-2012  
 Name Albert Lihong Zhou  
 Address 8700 Old Main Hill  
 Nutrition, Dietetics & Food Sciences  
 Utah State University  
 Logan, UT 84322-8700  
 Phone/e-mail address 435-363-5523/albert.zhou@aggiemail.usu.edu

Journal Name Lipids  
 Journal Article Dietary Fat Composition Influences Tissue Lipid Profile and Gene Expression in Fischer-344 Rats.

Dear Dr. Rafael Jimenez-Flores:

I am preparing my Dissertation in the Nutrition, Dietetics & Food Sciences Department at Utah State University. I hope to complete my degree in the Fall of 2012. The above mentioned article is an essential part of my Dissertation research. I would like your permission to reprint it as a chapter in my Dissertation (Reprinting the chapter may necessitate some revision).

I will include an acknowledgment to the article on the first page of the chapter, as shown below. Copyright and permission information will be included in a special appendix. If you would like a different acknowledgment, please so indicate.

Please indicate your approval of this request by signing in the space provided. If you have any questions, please call me at the number above or send me an e-mail message at the above address.

Thank you for your assistance.

Albert Lihong Zhou

---

I hereby give permission to Albert Lihong Zhou to reprint the requested article in his Dissertation, with the following acknowledgment:

Reprinted with modifications from Zhou AL, Hintze KJ, Jimenez-Flores R, and Ward RE. 2012. Dietary Fat Composition Influences Tissue Lipid Profile and Gene Expression in Fischer-344 Rats. Lipids, DOI: 10.1007/s11745-012-3729-3.

## CURRICULUM VITAE

**Albert Lihong Zhou, M.D., M.S., Ph.D.**

### **Professional Address**

Department of Nutrition, Dietetics and Food Sciences  
Utah State University  
8700 Old Main Hill  
Logan, UT 84322-8700  
Email: albert.zhou@aggiemail.usu.edu

### **Degrees & Education**

**Utah State University**, Logan, Utah

*Ph.D. in Nutrition and Food Sciences*, August 2009 – May 2013

Advisor: Robert E. Ward

Thesis: “Bioactivities of **milk polar lipids** in influencing **intestinal barrier integrity, systemic inflammation, and lipid metabolism**”

**Utah State University**, Logan, Utah

*Pre Doctor of Audiology Student*, January 2009 – May 2009

**Utah State University**, Logan, Utah

*Ph.D. Student in Auditory Neurophysiology*, August 2006 – December 2008

Advisor/Research Mentor: Timothy A. Gilbertson/Donal G. Sinex

**Beijing Institute of Geriatrics**, Beijing, China

*M.S. in Cell Biology*, August 2003 – July 2006

Advisor: Tiemei Zhang

Thesis: “Establishment of **3T3-L1 adipocytes models** with different **insulin sensitivity** by **caloric restriction** & analysis of protein kinase B expression”

**Hubei University of Medicine**, Shiyan, Hubei Province, China

*M.B.B.S. (M.D.), September 1996 – July 2001*

### **Career Objectives**

To work as a research scientist and to teach at university level

### **Professional Experience**

✧ **Research Assistant**, Utah State University, August 2006 – present

- Collected and analyzed electrophysiological data in animal model using interactive graphic user interface
- Established Caco-2 cell monolayer model for studying the effect of polar lipids on intestinal barrier integrity
- Analyzed large bioinformatic and lipidomic data sets and carried out comprehensive statistical analyses
- Carried out experimental design and statistical analyses planning for animal studies
- Received Institutional Review Board training
- Established mouse models of obesity and inflammation for studying the development of diet-induced obesity (DIO) and explored the effects of dietary polar lipids in influencing intestinal barrier integrity, systemic inflammation, and lipid metabolism during DIO and in the context of inflammation
- Attended Getting Started as a Successful Proposal Writer and Academician workshop
- Supervised four undergraduate student researchers

✧ **Teaching Assistant**, Utah State University, August 2006 – May 2009

- Prepared and taught General Biology (BIOL 1610) lab, Fall 2006
- Prepared and taught Human Anatomy (BIOL 2320) lab, Spring 2007, Spring 2008, Summer 2008 and Spring 2009
- Prepared and taught Elementary Microbiology (BIOL 2060) lab, Fall 2007 and Fall 2008

- ✧ **Research Assistant**, Beijing Institute of Geriatrics, August 2003 – July 2006
  - Established cell models of different insulin sensitivity using 3T3-L1 adipocytes
  - Assessed insulin sensitivity by stable isotope labeled glucose uptake test
  - Studied the effect of caloric restriction on insulin sensitivity in cell model
  
- ✧ **Resident/Neurologist**, Hubei University of Medicine affiliated Dongfeng General Hospital, July 2001 – July 2003
  - Worked in inpatient wards and outpatient clinics
  - Carried out patient assessment, diagnosis and therapeutic planning
  - Provided psychological counseling and psychotherapy for patients
  
- ✧ **Instructor**, Hubei University of Medicine, July 2001 – July 2003
  - Supervised senior medical students in doing internship

### **Publications**

- ✧ **Albert Lihong Zhou**, Korry J. Hintze, Rafael Jimenez-Flores and Robert E. Ward. Dietary Fat Composition Influences Tissue Lipid Profile and Gene Expression in Fischer-344 Rats. *Lipids* 2012 (In press)
  
- ✧ Review: **Lihong Zhou** and Tiemei Zhang. Recent research advancements in biological functions of adipose tissue. *Foreign Medical Sciences Geriatrics* 2006; 27(2): 83-86

### **Manuscripts in Preparation**

- ✧ **Albert Lihong Zhou** and Robert E. Ward. Dietary Milk Polar Lipids Affect Lipid Metabolism, Gut Permeability and Systemic Inflammation in ob/ob Mice (In manuscript for *Nutrition Research*)
  
- ✧ **Albert Lihong Zhou** and Robert E. Ward. Dietary Milk Polar Lipids Benefit Gut Barrier and Lipid Metabolism in C57BL/6J Mice during Systemic Inflammation Induced by Escherichia Coli Lipopolysaccharide (In manuscript for *Journal of Nutrition*)

- ✧ **Albert Lihong Zhou** and Robert E. Ward. Dietary Milk Polar Lipids Supplementation Promotes Body Fat Accumulation and Affects Gut Permeability, Systemic inflammation, and lipid Metabolism in C57BL/6J Mice Fed a Moderately High-fat Diet (In manuscript for Obesity)

#### **Invited Presentations/Seminars**

1. Oral Presentation: Effects of Dietary Milk Polar Lipids on Lipid Metabolism in Genetically Obese Mice Fed a Moderately High-Fat Diet. **Albert Lihong Zhou** and Robert E. Ward. Food, Health & Nutrition Student Professional Development Oral Session, Institute of Food Technologists Annual Meeting & Food Expo. Las Vegas, June 25-28, 2012
2. Poster Presentation: Effects of Dietary Milk Polar Lipids on Lipid Metabolism in Genetically Obese Mice Fed a Moderately High-Fat Diet. **Albert Lihong Zhou** and Robert E. Ward. Dairy Division Food, Health & Nutrition Posters, Institute of Food Technologists Annual Meeting & Food Expo. Las Vegas, June 25 – 28, 2012
3. Oral Presentation: Dietary Milk Polar Lipids Benefit Lipid Metabolism and Gut Barrier in Obese Mice Fed Moderately High-fat Diet. **Albert Lihong Zhou**, R. Ward. American Oil Chemists' Society, 103<sup>rd</sup> Annual Meeting & Expo. Long Beach, April 29 – May 3, 2012
4. Oral Presentation: Dietary Milk Polar Lipids Benefit Gut Barrier Integrity and Lipid Metabolism in C57BL/6J Mice during Systemic Inflammation Induced By Escherichia Coli Lipopolysaccharide. **Albert Lihong Zhou**, Robert E. Ward and Korry J. Hintze. American Society for Nutrition Annual Meeting, Experimental Biology. San Diego, April 21 – 25, 2012
5. Poster Presentation: Dietary Milk Polar Lipids Benefit Gut Barrier Integrity and Systemic Inflammation in Mice during Inflammatory Stress Induced by Lipopolysaccharide. **Albert Lihong Zhou**, Robert E. Ward and Korry J. Hintze. American Society for Nutrition Dietary Bioactive Components Research Interest Section poster competition, Experimental Biology. San Diego, April 21 – 25, 2012
6. Poster Presentation: Dietary Milk Polar Lipids Benefit Gut Barrier Integrity and Lipid Metabolism in Mice during Inflammatory Stress Induced by

- Lipopolysaccharide. **Albert Lihong Zhou**, Robert E. Ward and Korry J. Hintze. American Society for Nutrition Energy and Macronutrient Metabolism Research Interest Section poster competition, Experimental Biology. San Diego, April 21 – 25, 2012
7. Oral Presentation: Effects of Dietary Milk Polar Lipids on Gut Permeability and Systemic Inflammation in Genetically Obese Mice Fed a Moderately High-fat Diet. **Albert Lihong Zhou** and Robert E. Ward. Intermountain Graduate Research Symposium, Utah State University. Logan, April 5 – 6, 2012
  8. Poster Presentation: Effects of Dietary Milk Polar Lipids on Gut Integrity and Systemic Inflammation in Mice during Development of Diet-Induced Obesity. **Albert Lihong Zhou** and Robert E. Ward. Intermountain Graduate Research Symposium, Utah State University. Logan, April 5 – 6, 2012
  9. Poster presentation: Effects of Dietary Milk Polar Lipids on Gut Permeability, Systemic inflammation, and lipid Metabolism in C57BL/6J Mice during Inflammatory Stress Induced by Escherichia Coli Lipopolysaccharide. **Albert Lihong Zhou** and Robert E. Ward. IFT/AACT Utah Food & Candy Expo, Institute for Food Technologists Bonneville Section and American Association of Candy Technologists Rocky Mountain Section. Sandy, April 10, 2012
  10. Oral Presentation: Effects of Dietary Milk Fat Globule Membrane on Tissue Lipid Metabolism and Related Gene Expression in Fischer-344 Rats. **Albert Lihong Zhou**, R. Ward, K. Hintze. American Oil Chemists' Society, 102<sup>nd</sup> Annual Meeting & Expo. Cincinnati, May 1 – 4, 2011
  11. Oral Presentation: Effects of Dietary Milk Fat Globule Membrane on Brain Lipid Metabolism and Gene Expression. **Albert Lihong Zhou**, R. Ward. American Oil Chemists' Society, 102<sup>nd</sup> Annual Meeting & Expo. Cincinnati, May 1 – 4, 2011
  12. Poster Presentation: The Effects of Whey Milk Fat Globule Membrane Lipids on Barrier Function of Caco-2 Cell Monolayer against LPS Stress. **Albert Lihong Zhou**, R. Ward, K. Hintze. American Oil Chemists' Society, 102<sup>nd</sup> Annual Meeting & Expo. Cincinnati, May 1 – 4, 2011
  13. Oral Presentation: Effects of Dietary Milk Fat Globule Membrane on Lipid Metabolism and Gene Expression in Fischer-344 rats. **Albert Lihong Zhou**, Robert



- E. Ward, Rafael Jimenez-Flores and Korry J. Hintze. Intermountain Graduate Research Symposium, Utah State University. Logan, April 15, 2011
14. Poster presentation: Effects of Dietary Milk Fat Globule Membrane on Tissue Lipid Metabolism and Gene Expression in Fischer-344 rats. **Albert Lihong Zhou**, Robert E. Ward, Rafael Jimenez-Flores and Korry J. Hintze. IFT/AACT Utah Food & Candy Expo, Institute for Food Technologists Bonneville Section and American Association of Candy Technologists Rocky Mountain Section. Sandy, April 5, 2011
  15. Poster presentation: Effect of dietary fat source on tissue lipids distribution and gene expression associated with lipid metabolism in Fishcer-344 rats. **Albert Lihong Zhou**, Robert E. Ward and Korry J. Hintze. 7th International Symposium on Milk Genomics & Human Health, International Milk Genomics Consortium. Davis, October 20 – 22, 2010
  16. Poster presentation: Effect of dietary fat source on tissue lipid profiles in Fishcer-344 rats. **Albert Lihong Zhou**, Robert E. Ward and Korry J. Hintze. IFT/AACT Utah Food & Candy Expo, Institute for Food Technologists Bonneville Section and American Association of Candy Technologists Rocky Mountain Section. Sandy, April 6, 2010
  17. Oral Presentation: Effect of adding Milk Fat Globule Membrane (MFGM) to anhydrous milk fat on lipid metabolomics in Fischer 344 rats compared to corn oil control. Robert E. Ward\*, Korry Hintze, **Albert Lihong Zhou** and Dallin Snow. American Oil Chemists' Society, 101st Annual Meeting & Expo. Phoenix, May 16 – 19, 2010
  18. Poster and Oral Presentation: Effect of dietary fat source on tissue lipid profiles in Fishcer-344 rats. **Albert Lihong Zhou**, Robert Ward and Korry Hintze. Intermountain Graduate Research Symposium, Utah State University. Logan, March 31, 2010
  19. Poster Presentation: Responses of cochlear nucleus neurons to harmonic and mistuned complex tones. Donal Sinex and **Albert Lihong Zhou**. Association for Research in Otolaryngology, Midwinter Research Meeting. Phoenix, February 16 – 21, 2008

20. Seminar: Adipose tissue as an endocrine organ. **Albert Lihong Zhou**. Seminar at Beijing Institute of Geriatrics. Beijing, May 2005
21. Presentation: Introduction to systems biology. **Albert Lihong Zhou**. Graduate Salon at Beijing Institute of Geriatrics. Beijing, September 2004

### **Institutional Review Board Training**

- ✧ Human Research Curriculum: Board Members; Group 1.Social & Behavioral Research Investigators and Key Personnel
- ✧ CITI Health Information Privacy and Security (HIPS) Curriculum: CITI Health Information Privacy and Security (HIPS)

### **Grants**

- ✧ Graduate Student Senate Research and Projects Grant, \$1000, Utah State University, 2010
- ✧ College of Agriculture Travel Grant, \$600, Utah State University, 2010
- ✧ Graduate Student Senate Travel Grant, \$900, Utah State University, 2011-2012

### **Professional Society Memberships**

- ✧ The Obesity Society, 2012 – present
- ✧ American Oil Chemists' Society, 2010 – present
- ✧ American Society for Nutrition, 2011 – present
- ✧ Institute of Food Technologists, 2011 – present
- ✧ National Lipid Association, 2010-present
- ✧ Association for Research in Otolaryngology, 2007 – 2009
- ✧ American Association for the Advancement of Science, 2007 – 2009
- ✧ Society for Neuroscience, 2008 – 2009

### **Students Mentored**

- ✧ Philip Bassett, Under Undergraduate Research & Creative Opportunities Project: The effects of dietary ganglioside supplementation on ganglioside content of intestinal mucosa in C57BL/6J wild type mice. Utah State University, 2010 – 2011

- ✧ Thiel Lehman, Under Undergraduate Research & Creative Opportunities Project: The Effects of Dietary Phospholipids and Gangliosides on Gene Expression in the Liver of Obese mice. Utah State University, 2010 – 2011
- ✧ Brent Pickett, Under Undergraduate Research & Creative Opportunities Project: Effects of Dietary Gangliosides and Phospholipids on Occludin Expression in Intestinal Mucosa of C57BL/6J ob/ob Mice. Utah State University, 2010 – 2011
- ✧ Allen Chen, high school student, Biomedical Program in Alhambra High School, Alhambra, CA. 2012 – present

### **Awards and Special Recognition**

- ✧ American Oil Chemists' Society Peter & Clare Kalustian award, 2012
- ✧ American Oil Chemists' Society Honored Student Award, 2012
- ✧ American Oil Chemists' Society Health & Nutrition Division Student Award, 2012
- ✧ American Society of Nutrition Energy & Macronutrient Research Interest Section Student-Postdoc Abstract Competition Award, 2012
- ✧ 2<sup>nd</sup> place poster session, IFT/AACT Utah Food & Candy Expo, Sandy, Utah, 2012
- ✧ Graduate Student Senate Enhancement Award, Utah State University, 2011
- ✧ 3<sup>rd</sup> place poster session in Health and Nutrition Division, American Oil Chemists' Society 102<sup>nd</sup> Annual Meeting & Expo, 2011
- ✧ 2<sup>nd</sup> place poster session, IFT/AACT Utah Food & Candy Expo, Sandy, Utah, 2011
- ✧ 2<sup>nd</sup> place lecture session, IGRS, Utah State University, 2011
- ✧ 1<sup>st</sup> place poster session, IFT/AACT Utah Food & Candy Expo, Sandy, Utah, 2010
- ✧ 1<sup>st</sup> place poster session and 3<sup>rd</sup> place lecture session, IGRS, Utah State University, 2010
- ✧ 1<sup>st</sup> Award, Campus Public Speaking Contests, Hubei University of Medicine, 2000
- ✧ Second Award, National College Students English Speaking Contests, Hubei University of Medicine, 1999
- ✧ Heng'an Group Stipend for College Students, Hubei University of Medicine, 1998
- ✧ First Class Scholarship, Hubei University of Medicine, 1996 – 1999
- ✧ Excellent Student Award, Hubei University of Medicine, 1996 – 1999

**Leadership Experience**

- ✧ American Society for Nutrition Student Interest Group Awards Chair, 2012 – present
- ✧ AOCS Health and Nutrition Division Newsletter Coeditor, 2012 – present
- ✧ AOCS Student Common Interest Group Leadership Committee, 2011 – present
- ✧ Founder and the first appointed chairman of Psychological Health Promotion Association, Hubei University of Medicine, 1998 – 2000
- ✧ Executive VP of student government, Hubei University of Medicine, 1996 – 1998

**Services**

- ✧ Food, Health & Nutrition Subpanel member for IFT's 2013 Annual Meeting Scientific Program Development, 2012 – present
- ✧ IFT Career Center eCareer Mentor, 2012 – present
- ✧ Conrad Foundation's Spirit of Innovation Challenge Mentor, 2012 – present
- ✧ Official judge, Health and Nutrition category of Conrad Foundation's Spirit of Innovation Challenge partnered by American Society for Nutrition, 2011 – present
- ✧ Chair for General Nutrition Session at 102<sup>nd</sup> AOCS Annual Meeting & Expo, 2011
- ✧ Volunteer tutor for Chinese classes at USU, 2009
- ✧ Volunteer head chef for the International Banquet at USU, 2007
- ✧ Volunteer barber for Chinese Students & Scholars Association, 2006
- ✧ Volunteer service in the welfare house and orphanage of Shiyan City, 2001 – 2003
- ✧ Volunteer psychological consultant for college students and patients in neurological department, 2000 – 2003
- ✧ Volunteer English course instructor for children, Shiyan City, 2001 – 2002
- ✧ Volunteer guide of Great Three Gorges Travel Service, May 2000

**Language Abilities**

- ✧ Native in Mandarin, professionally fluent in English, good at public speaking
- ✧ Written and spontaneous translation between English and Chinese

## Computer Skills

- ✧ Fluent in SAS, R, STATA, Cytoscape, Windows, Mac, Microsoft Office, Photoshop, ImageJ, Fluidigm and FlexArray
- ✧ Experienced in computer hardware

## Main Coursework

### Utah State University (2006 – present)

Nutrition GPA 4.0

Endocrine Aspect of Nutrition (A)	International Nutrition (A)
Nutrient Gene Interactions (A)	Molecular Nutrition Lab (A)
Statistical Bioinformatics (A)	Scientific Paper Critics Seminar (A)

Biology GPA 3.94

Advanced Topics in Psychophysics (A)	Animal Physiology Lab (A)
Cell Biology (A)	Medical Physiology (A-)
Neurobiology(A)	Graduate Topic in Biology (A)
Graduate College Teaching Seminar (P)	Linear regression/time series (CI)(QI) (A)

COMD GPA 4.0

Psychoacoustics and Instrumentation (A)	Language/Speech/Hearing Development (A)
Speech Science (A)	Language Assessment and Intervention (A)
Pediatric Aural Rehabilitation (A)	Basic Audiology (A)
Independent Study: Observation/ Graduate Preparation (A)	

### Peking Union Medical College (2003 – 2006)

Philosophy of Science (A)	Molecular Biology of the Gene (D)
Experimental Physiology (A)	Basic and Clinical of Endocrinology (A)
Lecture on Cell Biology (B)	Computer Sciences (B+)
Histochemistry (B+)	Tissue Culture (B+)

### Hubei University of Medicine (1996 – 2001)

Higher Mathematics (A)	Biochemistry (B)
Physics (B)	Physiology (A)
Inorganic Chemistry (A)	Human Parasitology (A)
Organic Chemistry (A)	Pathoanatomy (A)
Human Anatomy (A)	Regional Anatomy (A)
Histology & Embryology (A)	Microbiology & Immunology (B)